THE ROLE OF RNAs AND EXTRACELLULAR VESICLES IN THE RADIATION RESPONSE

A thesis submitted in partial
fulfilment of the requirements of
Oxford Brookes University for the degree of
Doctor of Philosophy

LAURA ANN JACOBS

Department of Biological and Medical Sciences

Oxford, United Kingdom

April 2015

Abstract

The bystander effect (BE) occurs when cells that have not been directly traversed by ionizing radiation exhibit DNA damage effects as though they had been. It is established that signalling molecules such as cytokines and reactive oxygen species (ROS) signal to surrounding cells to mediate BE, however more recently it has been demonstrated that extracellular vesicles (EVs) might be involved. In addition, following RNase treatment, the EVs are no longer able to cause DNA damage in unirradiated recipient cells, suggesting that an RNA molecule in association with the EVs is involved with BE.

As the literature documenting differential regulation of RNA in EVs released from irradiated cells is scarce, the work described in this thesis has aimed to better understand the role of RNA in the radiation response. Firstly the miRStress database was developed and used to identify novel miRNA candidates involved in response to radiation by meta-analysis of the published literature. Characterisation of the EVs released was also performed using transmission electron microscopy (TEM), sucrose gradient centrifugation, sizing and the determination of EV concentration released from cells. Next-generation sequencing was performed to identify the mRNA, non-coding RNA and microRNA candidates involved. General characterisation of EVs derived from unirradiated and 2 Gy irradiated MCF7 cells was also performed to gain a better understanding of the populations of vesicles released following irradiation.

The results herein suggest that EVs from irradiated cells have specific characteristics when compared to those from unirradiated cells. An increase in the number and a decrease in the size of EVs released from 2 Gy irradiated cells were observed compared to unirradiated cell EVs. In addition to the changes in size and release of EVs from 2 Gy cells, EVs released from irradiated MCF7 cells contained specific mRNAs, non-coding RNAs and miRNAs. Furthermore the miRStress database identified microRNA candidates predicted to be involved in the radiation response. Following RNA Seq analysis a functional study of the genes *ANP32B*, *MALAT1*, *NET1*, *HSP90AA1* and NCL was performed based upon their upregulation in 2 Gy EVs. Knockdown of some of these genes resulted in changes in the DNA damage response observed in directly irradiated and bystander cells, suggesting that the RNAs carried in irradiated cell EVs do indeed have a functional role in transmission of BE.

In summary, this study has identified diverse RNA species in EVs released from irradiated cells that appear to play functional roles in the mediation of the bystander effect. Further investigation would help to elucidate the mechanisms by which these RNAs function in recipient cells in order to better understand the BE mechanism.

Acknowledgements

I would firstly like to take this opportunity to thank everybody involved in contributing to the research presented in this thesis. It has been a remarkable journey and I am definitely emerging from the experience with a wiser head on my shoulders. I have met some wonderful and inspirational people that I certainly won't forget.

I would like to express my deepest gratitude to my supervisors Dr David Carter and Professor Munira Kadhim for their unwavering support during my project. Your advice and guidance has shaped me as a scientist and inspired me to pursue a career in research. I would also like to extend my thanks to Dr Ryan Pink for always being there to help, and to listen, especially when the going got tough and also to Dr Alistair McGregor for many therapeutic pub sessions.

Furthermore I'd like to add a huge thank you to the members of both labs, past and present, for being a group of wonderful people that I enjoy going to work to see every day. Debbie I cannot thank you enough for helping me walk with all of those boxes to the radiation facility.

I thank my parents for always encouraging me to do my best and equipping me with the work ethic that got me to where I am today. Also thanks to my amazing friends in Oxford and back at home - you fill me with positivity and remind me to relax every once in a while.

Finally I want to thank Immanuel for always encouraging me to have confidence in myself. You have been there for me through the ups and downs and I know that our new life in Munich will be just as exciting as our life in Oxford has been.

Abbreviations

%	Percentage
µg	Micrograms
µl	Microlitres
µM	Micromolar
3'	Three prime
5'	Five prime
AUC	Area under the curve
BCA	Bicinchoninic acid assay
BE	Bystander effect
bp	Base pairs
BSA	Bovine serum albumin
DE	Differentially expressed
dH_2O	Distilled water
DNA	Deoxyribonucleic acid
DSB	Double stand break
EDTA	Ethylenediaminetetraacetic acid
esRNA	Exosome shuttle RNA
EV	Extracellular vesicle
FBS	Foetal bovine serum
FCS	Foetal calf serum
g/ml	Grams per millilitre
G2	Pre-mitotic phase (of the cell cycle)
GI	Genomic instability
GO	Gene Ontology
Gy	Gray
h.p.i	Hours post irradiation
H_2O_2	Hydrogen peroxide
HDL	High density lipoprotein
HR	Homologous recombination
ILV	Intraluminal vesicle
kV	Kilovolts
L	Litre
LMPA	Low melting point agarose
M	Molar
mA	Milliamps
mg	Milligrams
miR	MicroRNA prefix

ml	Millilitres
mM	Millimolar
mRNA	Messenger RNA
MVB	Multivesicular body
NCI-60	National Cancer Institute 60 anticancer drug screen
NFH_20	Nuclease-free water
NHEJ	Non-homologous end joining
nm	Nanometers
NMPA	Normal melting point agarose
NO	Nitric oxide
ISEV	International Society for Extracellular Vesicles
ncRNA	Non-coding RNA
NR	Not recorded
NTA	Nanoparticle tracking analysis
OCDLs	Oxidative clustered DNA lesions
PBS	Phosphate buffered saline
PFA	Paraformaldehyde
piRNA	Piwi-interacting RNA
PMID	PubMed ID
qPCR	Quantitative PCR
RIBE	Radiation induced bystander effect
RIN	RNA integrity number
RNA	Ribonucleic acid
RNAi	RNA interference
RNase	RNA degradation enzyme
ROC	Receiver operator characteristic
ROS	Reactive oxygen species
rpm	Revolutions per minute
rRNA	Ribosomal RNA
S phase	Stationary phase (of the cell cycle)
R^2	R value (coefficient of determination)
SD	Standard deviation of the mean
SEM	Standard error of the mean
snoRNA	Small nucleolar RNA
TEM	Transmission electron microscopy
UTR	Untranslated region (referring to mRNA 3')
V	Voltage
(v/v)	Volume per volume
(w/v)	Weight per volume

g	Relative centrifugal force
yl	Yemtolitres
α-particle	Alpha particle
γ-ray	Gamma ray

Table of Contents

List of Figures

List of Tables

Chapter 1

Introduction

Chapter 1 Introduction

1.1. The importance of ionizing radiation

The biological effects of radiation are an area of great research interest owing to their implications in worldwide health. Exposure to radiation can arise from a variety of sources, both natural and man-made, including environmental exposure (Shahbazi-Gahrouei et al., 2013), occupational exposure (Buitenhuis et al., 2013) and accidental exposure (Sakly et al., 2012). Patients are also exposed to ionizing radiation during diagnostic procedures and during radiotherapy treatments where the balance between radiation exposure and effective cancer treatment - the therapeutic window - is of great importance (Jen & Cheung, 2003). Adverse radiation effects can be observed in patients receiving radiotherapy to treat breast cancers, for example whereby secondary tumours can occur in the lungs following irradiation in tissues such as the breast (Darby et al., 2005; Deutsch et al., 2003). Consequently understanding the causative factors of such secondary malignancies following irradiation or non-targeted effects of radiation such as the bystander effect could help to eliminate such risks in patients undergoing radiotherapy.

1.1.1. Direct and indirect effects of ionizing radiation

Following ionizing irradiation of a population of cells or whole tissue, both direct and indirect effects can be observed. Direct damage generally occurs when the DNA of a cell is directly traversed by radiation, causing DNA damage in the form of double strand breaks (DSBs) considered to be one of the most consequential effects of radiation (Lliakis, 1991) and has been demonstrated by α-particles directed at specific parts of the cell (Hall & Giaccia, 2012). Indirect effects occur where radiation causes the catalytic cleavage of molecules within cells, in particular water, to produce free radical species that cause DNA damage within the cell (Rao et al., 2008). It is postulated that around two-thirds of the damage caused by X-rays occur due to the indirect effects of radiation (Hall & Giaccia, 2012).

1.1.2. The targeted effects of ionizing radiation

The target theory assumes that one particular part of the cell must be directly hit by a track of radiation to cause damage or kill the cell (Marshall et al., 1970). Single-stands breaks may ensue but are rapidly repaired using the template strand (Bryant, 2004; Bailey & Bedford, 2006). DSBs can occur (Mozdarani & Bryant, 1987; Bryant & Iliakis, 1984) and, as these can lead to chromosomal and chromatid aberration, are regarded as the 'critical lesion' caused by ionizing radiation. Other effects include DNA base damage and DNA-DNA or DNA-protein crosslinks (Ward, 1988). In the case of ionizing radiation, a combination of the aforementioned damages described as oxidative clustered DNA lesions (OCDLs) are usually observed due to the track-like

deposition of energy (Goodhead, 1994). Up to 3000 base damages and around 30-40 DSBs are postulated to be induced by a 1 Gy radiation dose (Goodhead, 1994).

These OCDLs and DSBs are usually repaired by DNA repair mechanisms, primarily non-homologous end joining (NHEJ) where no template is required (Hamada et al., 2007). Homologous recombination (HR) may also be employed to repair the damage in the S and G2 phases (Burdak-Rothkamm & Prise, 2009) and the aforementioned ODCLs can be converted into DSBs if they are encountered by a replication fork in the S phase (Aziz et al., 2012; Dickey et al., 2009; Hei et al., 2008; Prise & Sullivan, 2010). DSBs are the most severe form of DNA damage as they can ultimately lead to genomic instability (GI) (Halazonetis et al., 2008; Khanna & Jackson, 2001).

1.1.3. The non-targeted effects of radiation – the paradigm shift

The shift from the classic DNA paradigm of radiation biology followed a number of key studies demonstrating the possibility that a cell did not need to be directly traversed by radiation in order to exhibit radiation-related damage. Such effects included radiation-induced genomic instability seen in the progeny of irradiated cells and the radiation-induced bystander effect (RIBE) as the induction of DNA damage effects in neighbouring cells not hit by radiation (Kadhim et al., 2013). In 1986 the appearance of *de novo* mutations in the progeny of irradiated cells, later proving lethal to the daughter cells, was reported (Seymour et al., 1986). It was furthermore demonstrated that bone marrow cells grown from irradiated stem cells developed *de novo* chromosomal aberrations at a later date (Kadhim et al., 1992). Further to these findings and reflecting the key role of targeted α-particle irradiation in bystander effect studies, it was shown that following α-particle irradiation a higher level of sister chromatid exchanges occurred in cells than α-particles could possibly have traversed, suggesting that communication between irradiated and unirradiated cells was taking place (Nagasawa & Little, 1992). Finally, media transfer from irradiated to non-irradiated cells resulted in DNA damage levels comparable to those in irradiated cells (Seymour & Mothersill, 1997). The culmination of the aforementioned studies, amongst others, led to the hypothesis that bystander effect (BE) might be due to the release of an unknown signalling molecule from irradiated cells conferring GI upon cells in surrounding tissues (Figure 1.1) (Kadhim et al, 1992; Lorimore et al, 1998). The term bystander effect is currently used to describe all biological manifestations in bystander cells receiving extracellular components from directly irradiated cells or via gap junctions (Mothersill & Seymour, 2001; Azzam et al., 2004).

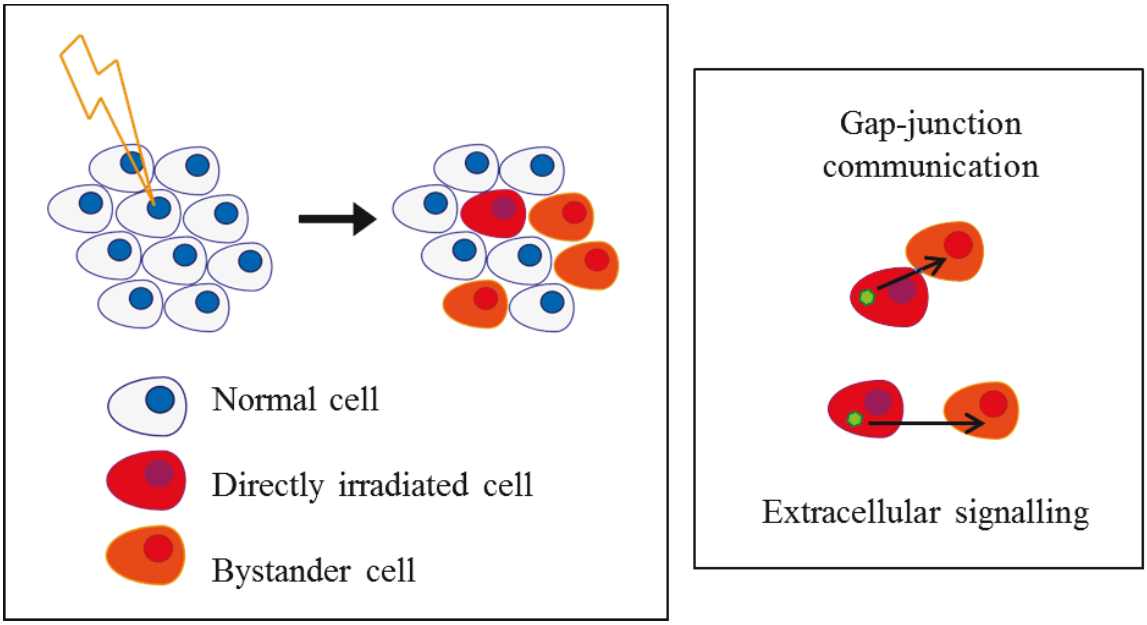

Figure 1.1. Schematic of the radiation-induced bystander effect. *In an irradiated population of cells those directly hit by X-rays (red) demonstrate DNA damage as expected, however some bystander cells (orange) not directly hit by radiation exhibit DNA damage effects as though they had been. This is termed the bystander effect and is known to be mediated by gap junctions or via soluble factors released from the cell.*

1.1.4. DNA damage in bystander cells

DNA damage in bystander cells is characterised by rapid DSB induction as in directly irradiated cells (Sokolov et al., 2007; Smilenov et al., 2006). Proliferative cells in the S phase are also shown to be more susceptible to DSB formation following bystander signalling (Dickey et al., 2012). Both direct and bystander cells utilise ATR/ATM DNA damage pathways, however ATR deficiency of cells has been shown to result in immunity to bystander killing. DNA damage in bystander cells has also been shown to persist for a longer time than the DNA damage in directly irradiated cells (Burdak-Rothkamm et al., 2007; Burdak-Rothkamm et al., 2008).

1.2. Signalling molecules involved in the bystander effect

1.2.1. Reactive oxygen species and nitric oxide

Evidence suggests that in bystander cells DNA damage may be accompanied by rapid influxes of calcium accompanied by widespread reactive oxygen species (ROS) production (Shao et al., 2006; Azzam et al., 2002). ROS already associated with DNA damage and cancer (Lehnert & Goodwin, 1997) have been widely studied in the context of BE and may be transported between cells via gap junctions (Azzam et al., 2003). Most ROS have a short half-life only acting locally, however H_2O_2 produced in irradiated cells has been shown to actively diffuse across membranes with the ability to cause DNA damage at more distant sites potentially mediating BE (Sokolov et al., 2007). The tumour suppressor p53 has also been shown to upregulate the transcription factor NF-Kß that can play roles in attracting macrophages and steadily increasing an inflammatory milieu (Gorgoulis et al., 2003).

A sustained production of ROS via lipid peroxidation can also be observed in directly irradiated and bystander cells and is primarily due to the presence of NADPH oxidase in the membrane of cells (Morel et al., 1991; Narayanan et al., 1997). In addition the actions of the COX-2 gene can lead to ROS production in bystander cells that are then released into the extracellular environment (Hei et al., 2008). Nitric oxide (NO) is also known to be a mediator of media transmitted bystander effects, with the ability to freely diffuse through membranes and affect mitochondrial function (Matsumoto et al., 2001).

1.2.2. Cytokines

In addition to the above effects of oxidative stress caused by direct irradiation, inflammatory cytokines have been shown to play an extensive role in BE by causing additional cellular effects and propagation of these signals. Irradiated cells release such cytokines as TNF-α, Il-1β and Il-33 that bind receptors on bystander cells and cause NO and ROS production by activating the transcription factor NF-κB (Zhou et al., 2008). NO and ROS cause leakage of the mitochondrial membranes, releasing superoxide anions and causing more damage (Hei et al., 2008). As NF-κB also regulates expression of iNOS in the nucleus (Hei et al., 2008), it may be argued that a cyclical production of ROS in the cell is prompted as iNOS controls NO synthesis. Moreover TNF-α released by directly irradiated cells has the ability to bind membrane receptors on bystander cells, causing the release of NF-κB and therefore ROS production via COX-2 modulation (Zhou et al., 2008). TNF-α has also been shown to activate the MAPK super family of kinases, ERK, JNK and p38 protein that also up regulate iNOS and COX-2 (Zhou et al., 2008). Therefore, many of these radiation response signals act to amplify the inflammatory response of the cell.

1.2.3. Involvement of mitochondria in the oxidative stress response of irradiated and bystander cells

Mitochondria also appear to play a role in the manifestation of BE, with mitochondrial DNA depletion of cells, mitochondrial calcium uptake and NOS inhibition resulting in lower BE levels (Chen et al., 2008; Tartier et al., 2007). Damaged, leaky mitochondrial membranes increase the ROS level of cells further (Hei et al., 2008; Zhou et al., 2005) leading to an accumulating stress status. To this end they have been shown to play a role in exacerbating BE by propagating the stress response in the cell.

1.3. The transcriptional response to cellular irradiation and the bystander effect

1.3.1. Deregulation of mRNAs in the radiation response and bystander effect

In a study of 10,000 genes analysed via microarray, 24% of genes assayed were differentially regulated in response to ionizing radiation (Rieger & Chu, 2004). The replication and transcriptional status of cells may also play a role in the response of a cell to radiation assault, due to the highly proliferative nature of cancer cells (Dickey et al., 2012). Core sets of genes have been shown to be in involved in the p53 response to DNA damage in directly irradiated cells and were shown to be conserved between the cell lines studied (Rashi-Elkeles et al., 2011). Upregulated genes included the cell cycle gene *CDKN1A*, the apoptotic genes *FAS* and *DRAM* and the DNA damage genes *DDB2* and *REV3L*. Downregulated core genes included *AURKA* and *PLK1* involved in the G2/M transition (Rashi-Elkeles et al., 2011). Studies have characterised some of the gene changes in bystander cells and have demonstrated some differences in their transcriptional response. Using a genome-wide microarray approach, bystander fibroblasts displayed enrichment of genes involved in ribosomal pathways and oxidative metabolism, whereas directly irradiated cells demonstrated apoptotic gene deregulation and development of immune response (Kalanxhi & Dahle, 2011).

1.3.2. Non-coding RNAs

It is approximated that 98% of the human genome is non-protein coding (Harrow et al., 2012). Consequently the discovery, annotation and acknowledgement of the importance of non-coding RNAs in gene regulation is increasing and are currently split into two broad categories - small non-coding RNAs such as microRNA, piRNAs and small nucleolar RNAs (snoRNAs) that have a limit of 200 nucleotides in length and the long non-coding RNAs that exceed 200 nucleotides (Ma et al., 2013).

Long non-coding RNAs have been shown to play roles in a variety of important biological functions including apoptosis (Reeves et al., 2007), splicing (Rintala-Maki & Sutherland, 2009) and cell cycle regulation (Ginger et al., 2006). The mode of action of long non-coding RNAs

includes recruitment of complexes, for example in the case of chromatin remodelling whereby the *HOTAIR* long non-coding RNA recruits the polycomb repressive complex 2, causing heterochromatin formation leading to reduced gene expression (Rinn et al., 2007). The long non-coding RNA *MALAT1* is upregulated in a variety of cancers (Zheng et al., 2014) and has been shown to increase proliferation of cells (Wang et al., 2014). Other functions of lncRNAs include post-transcriptional processing (Beltran et al., 2008) and transcriptional control (Wang et al., 2010; Feng et al., 2006). SnoRNAs are small nucleolar RNAs of around 60-300 nucleotides that have been shown to pay roles in rRNA processing and RNA splicing (Kawaji et al., 2008).

1.3.3. Non-coding RNAs in radiation response and bystander effect

Some studies have demonstrated that non-coding RNAs, including snoRNAs may be deregulated in radiation response. Direct exposure of cell lines to X-rays resulted in upregulation of the snoRNAs *SNHG1*, *SNHG6*, *SNHG11, MALAT1* and *SOX2OT* (Chaudhry, 2013). In a second study it was confirmed that *SNHG1* and *SNHG4* were upregulated in directly irradiated TK6 wild type cells, but were however repressed in bystander cells (Chaudhry, 2014). In addition the long non-coding RNAs *MALAT1*, *SOX2OT*, *MATR3* and *SRA1* were induced in directly irradiated cells and repressed in bystander cells. Taken together these data suggest that directly irradiated and bystander cells may display different deregulation profiles of snoRNA and non-coding RNAs.

1.3.4. MicroRNAs

MicroRNAs are short non-coding RNAs involved in gene regulation, of which approximately 1000 have been identified to date and are anticipated to regulate around 60% of all human genes (Bentwich et al., 2005). MicroRNAs work to regulate the expression of genes either by translational repression or degradation of target mRNAs and the upregulation of a single microRNA is able to repress hundreds of target genes post-transcriptionally (reviewed in Yates et al., 2013). MicroRNAs were first documented in *C.elegans* larval development (Lee et al., 1993) and have since been widely studied and identified as key players in tumorigenesis. Many microRNAs, known as oncomiRs or oncogenic microRNAs, are associated with cancer progression (Calin et al., 2004) and their deregulation has been demonstrated in a variety of cancers including colorectal cancer (Yang et al., 2013) and breast cancer (Song et al., 2013).

1.3.5. MicroRNA biogenesis

The biogenesis of microRNAs is a tightly regulated process in the cell (Figure 1.2). Firstly transcription of the microRNA from a microRNA gene or an intron to a long primary microRNA (pri-microRNA) is performed. The pri-microRNA is then processed into a hairpin precursor microRNA (pre-microRNA) by the RNase family enzyme Drosha and the RNA binding protein DGCR8 (Bartel, 2009). Exportin-5 then transports the ~70 nucleotide pre-microRNA hairpins from the nucleus to the cytoplasm where they are cleaved by the enzyme Dicer into microRNA duplexes. These microRNA duplexes then separate into their 5' and 3' strand. More commonly the 5' strand

is taken into the RISC complex and if complementary to its mRNA target will degrade it. Conversely, if the sequences are not sufficiently complementary, transcriptional repression of the target mRNA occurs via binding of the microRNA to its 3'UTR (Bartel, 2004).

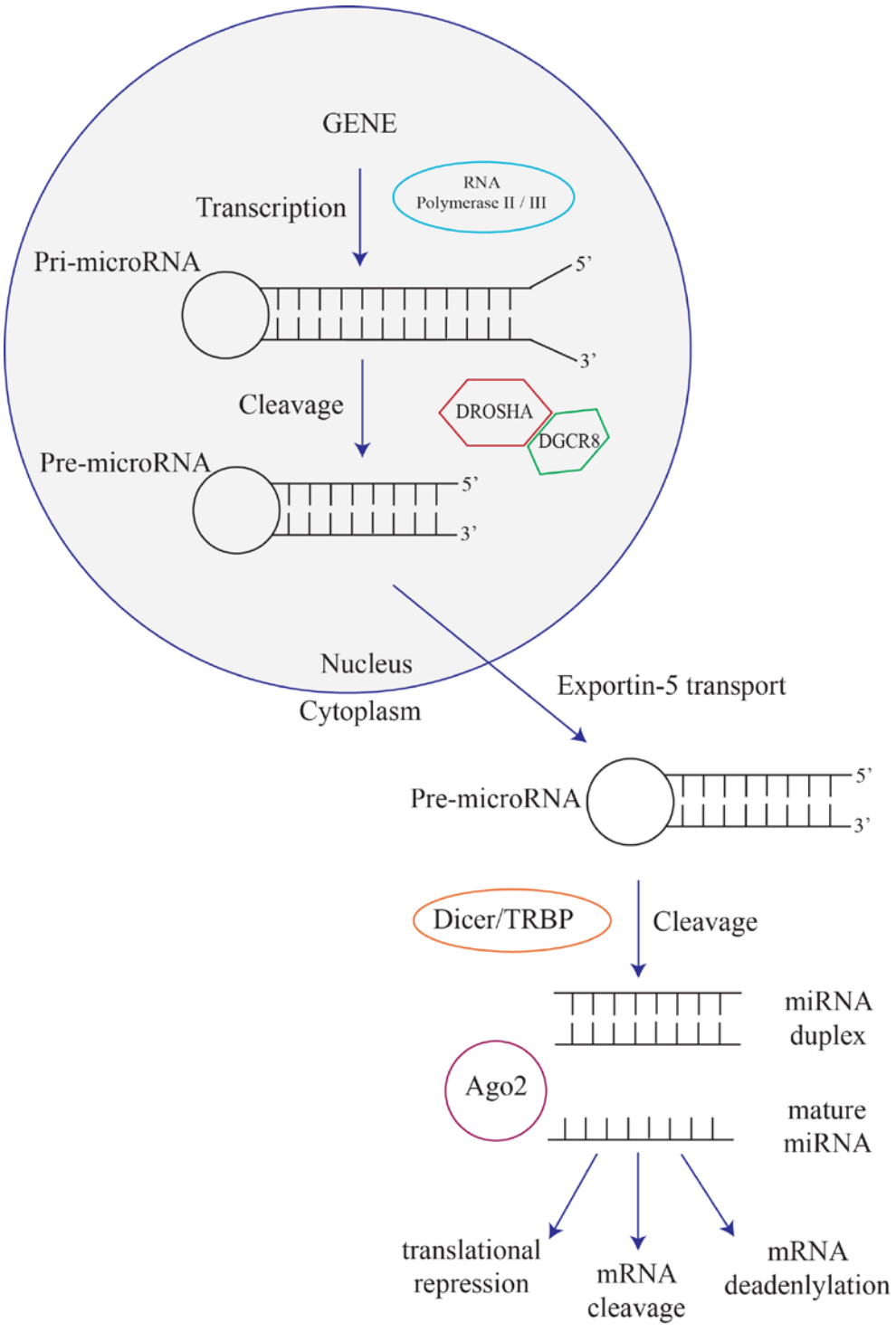

Figure 1.2. MicroRNA biogenesis schematic. *MicroRNAs are transcribed in the nucleus from a microRNA gene or intron and then proceed through a number of steps that cleaves them and moves them from the nucleus of the cell into the cytoplasm. The pre-miRNAs are then cleaved into their mature form and loaded into the RISC complex to then act upon their mRNA target as shown.*

1.3.6. MicroRNAs in the radiation response and bystander effect

MicroRNAs have previously been shown to be differentially modulated following oxidative stress including radiation (Simone et al., 2009) and microRNAs are believed to be both directly and indirectly involved in the radiation response (Dickey et al., 2011). Evidence has however suggested that microRNAs are not likely to be the primary signalling molecule in bystander effect as bystander recipient Dicer knockdown cells, created by disrupting Dicer at exon 5, still exhibited bystander effect damage in response to media transfer from irradiated cells (Dickey et al., 2011). Some microRNAs have however been shown not to require Dicer for maturation, with some microRNAs cleaved within the Ago2 catalytic complex (Cheloufi et al., 2010). Next-generation sequencing of directly irradiated cells has identified the differential regulation of microRNAs in a time-dependent manner in response to radiation, indicating a specific and tailored microRNA response in irradiated cells (Chaudhry et al., 2013).

The microRNA profile of cells can change in cells distant to those at the site of irradiation and cranially irradiated mice showed local microRNA changes in their spleens that had been shielded from irradiation (Koturbash et al., 2007). It has also been shown that ionizing radiation induced BE damage is expressed differently in specific tissues and is reflected by differences in the microRNA profile of those cells and tissues (Ilnytskyy et al., 2009). MicroRNAs are also believed to be involved in late bystander effects causing apoptosis by changing the expression of *BCL-2* and causing DNA hypomethylation by affecting DNMT3A/B (Kovalchuk et al., 2010; Fabbri et al., 2007). Some microRNAs have been shown to affect pathways known to be involved in radiation response, for example the action of miR-21 via the ROS pathway may also play a role in BE (Jiang et al., 2014).

In vivo considerations are also important in the study of the bystander effect. Bystander microRNA responses may be sex-specific in mice, accompanied by changes in Dicer and RISC complex expression (Koturbash et al., 2008). Three dimensional tissue studies have also been undertaken to better represent *in vivo* irradiation (Kovalchuk et al., 2010). In the study miR-17 upregulation led to increased proliferation of bystander cells and miR-16 upregulation affected apoptosis via altered *BCL-2* expression levels. It has also been demonstrated that total radiation dosimetry can be estimated in mice by measuring microRNA expression levels in the plasma (Cui et al., 2011) further supporting that a better understanding of the bystander effect will be of value to the clinical setting.

One approach to better understanding gene deregulation events is to perform bioinformatical analyses to collate data from diverse datasets and to use this to predict novel pathways and identify key players in a given biological response. A large number of studies document microRNA deregulation following radiation at a variety of doses and under different conditions in different cell

lines and models. To this end, bioinformatical analyses have been performed that have identified novel microRNA candidates and analysed the pathways that they are implicated in (Lhakhang & Chaudhry, 2012). For example some specific microRNAs including miR-34a are well characterised in the radiation response (He et al., 2007) but such changes may indeed be cell line specific (Mert et al., 2012) and different modes and doses of radiation may be responsible for the different observations in the literature. MicroRNA profiles have however been shown to be different in directly irradiated compared to bystander cells (Chaudhry et al., 2013). Consequently bioinformatical analyses are required to bring to together data to be able to study it effectively and guide functional experiments in a rational way.

1.4. Extracellular vesicles

1.4.1. Extracellular vesicle nomenclature and classification

Extracellular vesicles (EVs) are lipid vesicles released by a variety of cell types (Raposo & Stoorvogel, 2013). A subset of these EVs, termed exosomes, are small vesicles of around 30-120 nm in size that carry proteins and small RNA molecules that are believed to play roles in intercellular communication (Vlassov et al., 2012). These EVs have been observed as exfoliating vesicles with ectoenzymal activity (Trams et al., 1981) and were later observed in the recycling of transferrin receptors in rat reticulocytes (Harding et al., 1983). Later they were identified as derived from endosomes (Johnstone et al., 1987). Larger EVs, also known as microvesicles, have been shown to bud directly off of the plasma membrane (Deregibus et al., 2008). Both EVs have been shown to carry functional molecules, including mRNAs and microRNAs and have become an area of intense research particularly in intercellular communication (Valadi et al., 2007; Ratajczak et al., 2006). The nomenclature regarding EVs is currently an area of debate as the field grows and establishes a better understanding of the function of vesicles released from cells (Gould and Raposo, 2013). It has been more recently accepted that cells release heterogeneous populations of EVs and that further study is required to fully characterise such vesicles released from different cells types under different conditions (Gardiner et al., 2014).

For the purposes of this thesis the term EV will be used to describe the aforementioned vesicles released from cells and for the vesicles extracted and characterised in the experiments herein.

1.4.2. Composition and biogenesis of EVs

The unique protein and lipid composition of EVs aids in their distinction from other vesicles. As some EVs are derived from multivesicular bodies (MVBs), their membranes can contain transport proteins and fusion proteins. These include for example GTPases and annexins, also tetraspannins including CD9, CD81 and CD63 and other proteins involved in the biogenesis of these EVs including TSG101 (Conde-vancells et al., 2009; Subra et al., 2010). Around 4400 different proteins have been associated with EVs (Mathivanan & Simpson, 2009); indeed databases exist compiling

all known extracellular vesicle composition data, including Exocarta (Simpson et al., 2012), EVpedia (Kim et al., 2013) and Vesiclepedia (Kalra et al., 2012). As well as distinctive protein profiles, EVs also harbour characteristic lipids and sterols in their membranes including ceramide and cholesterol (Wubbolts et al., 2003; Staubach et al., 2009).

EVs can be derived from the endocytic pathway that comprises membrane compartments and internalizes extracellular ligands then recycled into the plasma membrane or degraded in lysosomes (Figure 1.3) (Gould & Lippincott-Schwartz, 2013; Raposo et al., 1996). Some vesicles are derived from MVBs within the cell that contain numerous intra-luminal vesicles (ILVs) that are created during the maturation of the endosomes (Stoorvogel et al., 1991). These MVBs can be directed to the lysosome for degradation; however, if the MVB fuses with the cell membrane it releases the vesicles contained inside as EVs into the extracellular space (Stoorvogel et al., 2002; Raposo et al., 1996).

Recent work has shown that tetraspannins may play an important role in the loading of proteins into the EV membrane (Perez-Hernandez et al., 2013). Using mass spectrometry it was shown that insertion of proteins into the tetraspannins-enriched microdomain may be important for protein incorporation into the EVs. ESCRT proteins have also been suggested to be important in EV biogenesis (Théry et al., 2001) and EVs released from cells in which HRS, STAM1 or TSG101 had been silenced using RNAi resulted in changes in the size and protein content of EVs released from those cells (Bobrie et al., 2012). Consequently, EV biogenesis is a complex and versatile process that may be altered under different biological conditions.

1.4.3. Isolation of EVs and characterisation

Smaller EVs are currently distinguished from other vesicles based upon density, morphology and size and have been reported to have a buoyant density of between 1.1-1.21 g/ml (Mathivanan et al., 2012), differentiating them from Golgi bodies and vesicles from the endoplasmic reticulum (Raposo et al., 1996; van Niel et al., 2006). EVs can be visualised using negative staining techniques and imaged using transmission electron microscopy where they can appear as round dark spheres of below 200 nm, also sometimes appearing cup-shaped due to the fixing process used prior to staining (Raposo et al., 1996). Based on the assumption that the width of the lumen of the extracellular vesicle is 20-90 nm across, the volume of an extracellular vesicle is calculated to be 4.2-380 yl, consequently the potential load of an extracellular vesicle may be up to 100 proteins or 10,000 nucleotides in total (Vlassov et al., 2012). EV surface markers may also be used as identifiers in western blotting. As previously mentioned, EVs carry tetraspannins found in the endosomal pathway such as CD63 and CD81 (Escola et al., 1998) and also some EVs have been demonstrated as enriched in particular proteins following, for example, heat stress (Clayton et al., 2005; Lancaster & Febbraio, 2005).

Isolation of pure vesicle samples is key in avoiding contamination with soluble components that cannot be identified using transmission electron microscopy (TEM) and western blotting alone (Webber & Clayton, 2013). A variety of methods exist for extracellular vesicle extraction including ultracentrifugation approaches (Théry et al., 2006), ultrafiltration (Cheruvanky et al., 2008), reagents such as ExoQuick (Systems Biosciences) and affinity purification of EVs (Valadi et al., 2007). Clearing of foetal calf serum (FCS) used to supplement cell media is also an important consideration in the extraction of EVs (Webber & Clayton, 2013) to remove contaminating bovine EVs. The concentration and size of vesicles can be measured using NanoSight technology and this has become a common way of quantifying vesicles in preparations where the heterogeneity of vesicles can be confirmed by measurement of their refractive index (Gardiner et al., 2013; Gardiner et al., 2014).

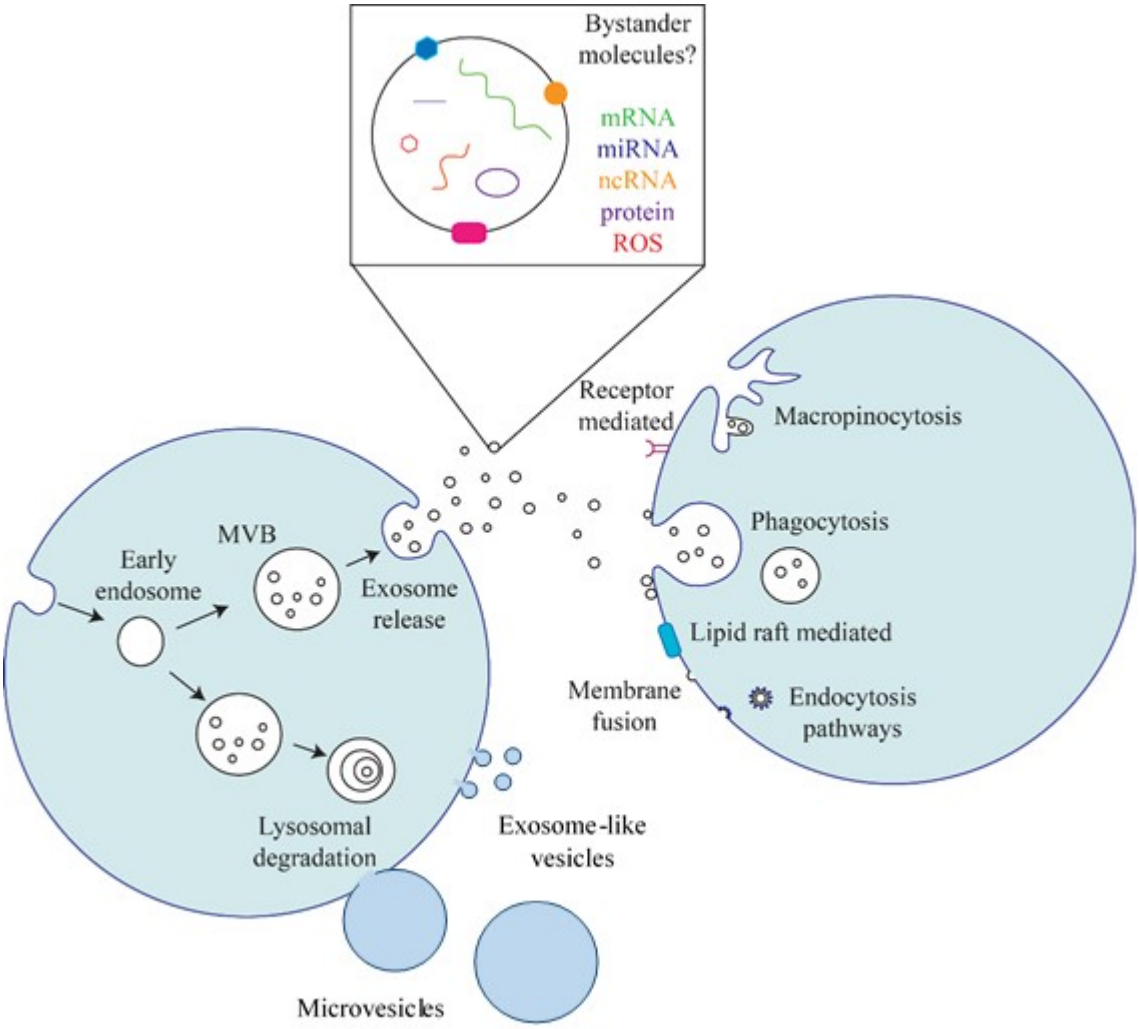

Figure 1.3. Extracellular vesicle biogenesis and uptake mechanisms. *EVs are released from the cell by a variety of mechanisms. ´Éxosomes´are created via the endocytic pathway and are formed when MVBs bud*

inwards to form ILVs. The MVBs may be degraded or fuse with the plasma membrane releasing the vesicles into the extracellular space. Exosomes may be taken up into a recipient cell by one of the uptake mechanisms shown above. Microvesicles (MVs) are released as a result of direct budding from the plasma membrane and exosome-like vesicles also bud directly from the plasma membrane but are smaller in size than MVS.

1.4.4. Biological functions of EVs and intercellular communication

Intercellular communication has traditionally been described as endocrine, exocrine, juxtacrine, paracrine or synaptic (Janowska-Wieczorek et al., 2005) and numerous cell types have been shown to release EVs in a constitutive fashion *in vitro* (Raposo & Stoorvogel, 2013). Due to their presence in cell media and release in a wide variety of biological fluids including blood, urine, saliva and pleural effusions (Bobrie et al., 2011), EVs are a new candidate for mediators of intercellular communication.

EVs were initially believed to remove unwanted components, membrane proteins and receptors from cells (Johnstone et al., 1987) but have been extensively studied in the area of the immune system (Théry et al., 2009), transfer of oncogenic genes (Al-Nedawi et al., 2008) and also in angiogenesis and coagulation (Janowska-Wieczorek et al., 2005) amongst numerous other functions. Specific expression profiles of EV microRNAs in breast milk have been shown to have the potential to modulate immune development in infants during the first six months of lactation with levels then falling, suggesting selective loading of microRNAs into EVs (Kosaka et al., 2010). EVs have also been implicated in the transfer of viruses and prions (Pegtel et al., 2011) and microRNAs being carried by vesicles have also been shown to play a role in the accumulation of age-associated diseases and the accumulation of senescent cells in ageing organisms (Weilner et al., 2012). EVs also have the advantage of being able to robustly deliver their contents to multiple specific locations (Klibi et al., 2015; Keller et al., 2011). It is also believed that EVs act independently of, but also in association with, soluble molecules such as interleukin-1, TNF-α or TGF-ß that play key roles in intercellular communication (Clayton et al., 2007; Qu et al., 2007; Zhang et al., 2006).

1.4.5. Extracellular vesicle uptake

A variety of direct and indirect evidence supports the theory that EVs are internalised by recipient cells and uptake is postulated to occur through a variety of mechanisms (Figure 1.3). Evidence for the uptake of EVs directly into cells includes internalisation of biologically functional microRNA and messenger RNAs (Valadi et al., 2007) and effective siRNA delivery (Alvarez-Erviti et al., 2011). Protein interactions are key for EV uptake and proteinase K has been shown to abrogate internalisation of EVs (Escrevente et al., 2011) as have a number of other chemical treatments (Mulcahy et al., 2014). Key EV uptake mechanisms have been shown to include endocytosis (Montecalvo et al., 2013), phagocytosis (Rudt & Müller, 1993) and membrane fusion (Parolini et

al., 2009). Cell receptor binding of EVs without internalization may be sufficient to cause changes in the phenotype of immune cells (Segura et al., 2007).

It is also possible however that EVs could fuse directly with the plasma membrane as their membranes are abundant with the fusogenic protein CD9 (Théry et al., 1999). Uptake has been more recently documented as lipid-raft dependent in the case of glioblastoma cells and also to be negatively regulated by caveolin-1 (Svensson et al., 2013). EVs have also been shown to move differently depending upon their stage of uptake, for example slowly during the attachment phase and more rapidly along the cytoskeleton once taken up into the cell (Tian et al., 2010) and their contents are also believed to be protected from the host immune system as they are recognised as 'self' molecules (Vlassov et al., 2012). Further work is therefore required to better understand the uptake of EVs under different conditions.

1.4.6. EVs and RNA

The first studies documenting the presence of functional microRNA and mRNA in EVs attracted attention owing to their potential as mediators of intercellular communication (Valadi et al., 2007; Ratajczak et al., 2006). It was demonstrated that human and mouse cell lines released EVs carrying functional RNAs and, furthermore, that mouse proteins were translated in human mast cells upon receipt of mouse EVs (Valadi et al., 2007). Studies subsequently demonstrated the transport of functional RNA between other cell lines including glioblastoma cells and in blood (Skog et al., 2008; Hunter et al., 2008). The transport and selective loading of microRNAs into EVs targeted to recipient cells has also been reported (Mittelbrunn et al., 2011; Montecalvo et al., 2013).

As a consequence of the aforementioned studies, the term 'exosome shuttle RNA' was introduced to describe RNA that is transported between cells in EVs specifically (Lotvall & Valadi, 2007). Next-generation sequencing of EV RNA is revealing the RNA content of EVs as it becomes a more readily available and affordable technology. The first studies published using this technology revealed the presence of mRNAs, microRNAs and various other non-coding RNAs (Bellingham et al., 2012; Jenjaroenpun et al., 2013; Nolte-'t Hoen et al., 2012). The selective loading, or enrichment, of RNAs into EVs is supported by many studies (Nolte-'t Hoen et al., 2012; Valadi et al., 2007; Bellingham et al., 2012; Skog et al., 2008; Zhou et al., 2012) indicating a functional role for them in the recipient cell. Bioinformatical analysis has suggested RNA export sequences that might play a role in the destination of selected cellular mRNAs into EVs (Batagov et al., 2011) and specific sorting of microRNAs into EVs has been reported experimentally (Villarroya-Beltri et al., 2013). Enrichment of particular microRNA sequences have also been identified as flags for export (Montecalvo et al., 2012) and different RNA loading mechanisms may exist, supported by the fact that different microRNA sequences are transported by vesicles with different characteristics and in different centrifugation fractions (Palma et al., 2012; Wang et al., 2010).

1.4.7. EVs, radiation and the bystander effect

Limited research to date exists documenting effects of ionizing radiation on the molecular contents and function of EVs released from irradiated cells. The importance of EVs has emerged, with most cancer phenotypes resulting in increased rates of extracellular vesicle release (Kharaziha et al., 2012) and also specific molecular profiles leading to their use as potential biomarkers (Rak, 2013). The release of EVs from cells has previously been shown to be stimulated by ionizing radiation (Lehmann et al., 2008) suggesting their release in a stress responsive manner. The first study to implicate EVs in the bystander effect demonstrated a role for EVs and RNAs and propagation of GI to progeny of bystander cells (Al-Mayah et al., 2012). DNA damage induced by irradiation has also been shown to induce extracellular vesicle release via a p53 response through the TSAP6 protein (Yu et al., 2006; Lespagnol et al., 2008) supporting that EVs may play a role in the radiation response. Despite the aforementioned evidence for the role of EVs in bystander effect the exact molecular profile and mechanisms of uptake and internalisation of the apparent damaging cargo have yet to be elucidated.

1.4.8. Radiation, EVs and RNA

Evidence further suggests that RNA in association with EVs is involved in BE. When media from irradiated cells was treated with RNase a significant reduction in damage in bystander cells was observed compared to controls (Al-Mayah et al., 2012). Furthermore, it was shown that the extracellular vesicle fraction of the cell media induced a statistically significant increase in DNA damage in recipient cells compared to controls, however when treated with RNase the DNA damage induction was abrogated (Al-Mayah et al., 2012). These preliminary data suggests that BE may be mediated by EVs in association with RNA; however the exact RNAs involved are not known. Moreover, how the RNA acts to mediate BE in recipient cells needs to be addressed. The work in this thesis aims to answer these questions and better characterise EVs for irradiated cells.

1.5. Aims and objectives of the thesis

The key aims of this thesis are to better characterise EVs released from irradiated MCF7 cells and to profile their RNA contents in comparison to unirradiated cells in an attempt to identify novel candidates responsible for RIBE. BE can be observed both *in vitro* and *in vivo* and patients receiving radiotherapy may sustain damage to their surrounding tissues following irradiation of a tumour. This may in turn lead to mutation and malignancy in other parts of the body, therefore further work is required to identify candidate BE molecules. Consequently functional studies of the genes identified will test the plausibility of their role in the bystander effect.

The following aims are addressed in this thesis;

1. To identify novel microRNA candidates involved in the radiation response by miRNA sequencing and construction of the miRStress database to perform meta-analysis of the literature.

2. To characterise EVs released from irradiated MCF7 cells, including their size, density and release from cells.

3. To establish differences in the RNA content between parent cells and the EVs derived from them following exposure to X-rays.

4. To identify and quantify mRNA and non-coding RNAs deregulated in response to radiation using RNA Seq and miRNAs using miRNA Seq.

5. To perform knockdown of the selected candidate RNAs to test their role in mediation of DNA damage and apoptosis in cells.

Chapter 2

Materials and methods

Chapter 2 Materials and methods

2.1. Cell culture

2.1.1. Cell culture of MCF7 breast cancer cells

MCF7 cells were kindly donated by Dr Joestin Dahle (University of Oslo, Norway). MCF7 cells were cultured in DMEM F-12 basal media (Gibco, 21331) supplemented with 10% (v/v) FCS (Sigma, F7524), 5% (v/v) L-glutamine (Fisher, VX15140122) and 5% (v/v) penicillin streptomycin solution (Fisher, VX15140122). Media was changed every three days for growing cells.

2.1.2. Subculture of MCF7 cells

Cells were trypsinised at 70–80% confluence. Cells were washed once with PBS (Fisher, 10214733) and 5 ml 0.005% trypsin (v/v) (Fisher, VX15400054) in PBS added to the flask and placed back into the incubator. Once cells had detached, 5 ml of whole cell media was added to the trypsin-cell PBS solution and centrifuged at 400 x g for 5 minutes to pellet cells. Cells were resuspended in whole warm media and seeded into flasks at the required density. Cells were cultured at 37°C and 5% CO_2 in a humidified environment.

2.2. Clearing Foetal Calf Serum (FCS) for use in cleared media

Media depleted of bovine EVs was used to supplement cell culture media during experiments as indicated in individual chapters to avoid extracellular vesicle sample contamination with bovine EVs. 'Normal' FCS refers to standard, unprocessed FCS (Sigma, F7524). 'Cleared' FCS was FCS that had been cleared once as below. 'Double cleared' FCS underwent the clearing process twice. 'SBI FCS' refers to Exo-FBS EV-depleted FCS (SBI, EXO-FBS-50A-1) that is advertised as free from contaminating bovine EVs. For clearing FCS was carefully injected into heat sealable tubes (Beckman, 342414) and the tubes sealed. FCS was ultracentrifuged at 120,000 x g (Beckman Coulter Optima LE-80K) for 18 hours overnight at 4˚C. The supernatant was then carefully removed, filter sterilised using 0.22 μm filters and aliquotted into sterile falcon tubes and frozen at -20˚C for future use at a concentration of 5% (v/v) in media.

2.3. Extracellular vesicle extraction from MCF7 cell media

Extracellular vesicle extraction via ultracentrifugation was used as previously described (Al-Mayah et al., 2012). Media was harvested from irradiated or unirradiated cells at the time point indicated. Following removal of cellular debris at 400 x g and 0.22 μM filtration, the supernatant was centrifuged at 20,000 x g for 20 minutes at 4˚C to remove further debris and to exclude larger vesicles. The supernatant was then centrifuged at 120,000 x g in a 70 Ti fixed angle rotor (Beckman, 337922) in a Beckman Coulter Optima LE-80K ultracentrifuge for 90 minutes at 4˚C.

The soft deceleration setting was used to reduce pellet resuspension. Supernatants were carefully removed and in some cases retained at 4˚C for further analysis in the bystander experiments. The remaining extracellular vesicle pellets were resuspended thoroughly in sterile PBS and the 120,000 x g spin repeated to wash the extracellular vesicle pellet of contaminants. The supernatant was then carefully removed and the pellet placed onto ice for five minutes to ease pellet resuspension. Pellets were resuspended in sterile PBS (typically 50 µl) and immediately stored at -80˚C until further analysis.

2.4. Alkaline comet assay

The alkaline comet assay is a method used to quantify DNA damage in individual cells (Tice et al., 2000). The 1% normal melting point agarose (NMPA) (Sigma, A9539) coated slides were prepared by dipping clean microscope slides in molten 1% NMPA, wiping one side clean and allowing them to dry at room temperature overnight. Prepared slides were stored in a slide box with desiccant.

In brief, two aliquots of 20,000 cells from each experimental group were taken and placed on ice, with an additional two aliquots taken from one of the control groups as a positive control (treated with 1% (v/v) H_2O_2, (Sigma, H1009), five minutes). Cell aliquots were resuspended in 200 µl molten 1% (w/v) low melting point agarose (LMPA) (Sigma, A9414) and spread using coverslips onto 1% (w/v) NMPA coated microscope slides laid flat on a chilled tray. After 10 minutes the coverslips were carefully removed and the slides placed into Coplin jars containing 4˚C alkaline lysis buffer (2.5 M NaCl, 100 mM Na_2EDTA, pH 8.0, 1% Triton X-100, 1% DMSO, pH 10). Slides were lysed overnight and then placed in a horizontal gel tank in a cold room and left for 40 minutes. Slides were then electrophoresed at 19 V, 300 mA for 30 minutes. Slides were carefully removed taking care not to lose gels and neutralised using comet neutralising buffer (0.5 M Tris-HCl, pH 7.5) for five minutes. Slides were then washed for a further 10 minutes with the neutralising buffer and a further 10 minutes with ultrapure water. The slides were immediately stained using 200 µl 1:10,000 Sybr Gold (Invitrogen, S11494) in TE buffer (10 mM Tris HCL, 1 mM Na_2EDTA, pH 8.0). Coverslips were removed after 10 minutes and the slides left to dry at room temperature then stored in a slide box in a cool, dark place for analysis. Analysis was performed by recording percentage tail DNA measurements using Komet v5.5 (Kinetic Imaging) software with 200 comets assayed per slide. Statistics were performed using SPSS Statistics v19 (IBM) and the Mann-Whitney test to establish significance.

2.5. Quantitative PCR

Quantitative PCR of RNA samples was used to validate RNA Seq candidates and siRNA knockdown levels. Prior to qPCR, cDNA was prepared from cell and extracellular vesicle RNA samples that had been quantified using the Nanodrop or Agilent 2100 Bioanalyzer. For each cellular RNA sample 2 µg of RNA was DNaseI treated (Sigma, AMPD1) as per manufacturer's

instructions with 2 units of DNase in a total reaction volume of 10 µl. Following DNaseI treatment the RNA was re-quantified using the Nanodrop. For each individual sample 1 µg RNA was converted into cDNA using the high-capacity cDNA reverse transcription kit (Applied Biosystems, 4368814) in a total reaction volume of 20 µl, cDNA was also developed for controls. Samples were stored at -20°C for future use.

For extracellular vesicle samples DNaseI treatments were performed on the whole EV RNA sample. Upon confirmation of the absence of genomic DNA contamination by qPCR, cDNA was then produced as above, but for smaller quantities of RNA (~200 ng per sample) alongside the relevant controls.

For qPCR SYBR green mastermix (Biorad, 172-5124) was used 1:1 with a mastermix comprised of cDNA and primers. Results were analysed using the ΔΔCt method and plotted as fold change relative to one of the two housekeeping genes.

2.6. RNA methods

2.6.1. RNA extraction from EVs

For RNA extractions, cells were harvested from flasks by scraping, spun down and snap frozen in liquid nitrogen and stored at -80°C for future RNA extraction. For EV RNA extractions freshly washed EV pellets were always used.

All RNA extractions were carried out using the miRcury RNA isolation kit - cell and plant (Exiqon, 300110). Care was taken at all steps to avoid RNase contamination and to use RNase free reagents and plasticware. EVs were extracted as per the extracellular vesicle extraction protocol, cell pellets were resuspended directly in lysis buffer and the RNA extracted as per the manufacturer's instructions. Extracellular vesicle pellets were resuspended in 350 µl lysis solution and vortex mixed for 15 seconds. Then 200 µl 95% ethanol was then added and the sample vortex mixed for 10 seconds. A new column was placed into a new collection tube and the lysed extracellular vesicle solution added to the column, then centrifuged at 14,000 x g for one minute. The flow-through was retained for protein analysis and the column washed three times with 400 µl wash solution for one minute at 14,000 x g and the flow through discarded. The column containing the washed RNA was centrifuged for two minutes at 14,000 x g to ensure that the column was dry and was then placed into a 1 ml RNase free Eppendorf tube. For elution from the column 50 µl nuclease-free water (Ambion, AM9937) was added directly to the column and centrifuged at 200 x g for two minutes followed by a spin for one minute at 14,000 x g. The RNA was then split into 5 µl aliquots for quality checks on the Agilent 2100 bioanalyzer (Agilent, Santa Clara, CA) using the RNA 6000 pico kit (Agilent, 5067-1513), a 45 µl aliquot was stored at -80˚C for future use. For cellular RNA extractions the same protocol was used, however DNase I (Sigma, AMPD1) treatments were performed on the RNA whilst on the column as per manufacturer's instructions.

2.6.2. RNase A treatment of EVs

RNase A (Promega, A7973) was used at a concentration of 30 µg/ml on extracellular vesicle pellets resuspended in PBS. Samples were incubated at 37°C for one hour. For RNase treatment of EVs that had not been lysed, five volumes of RNA*later* solution was added (Ambion, AM7020). For extracted EV RNA samples no inhibitor was added post RNase treatment and cell controls were always performed to confirm non-RNase treatment RNA integrity (RIN value).

Chapter 3

Identification of novel radiation microRNA candidates using the miRStress database

Adapted from:

Jacobs, L.A., Bewicke-Copley, F., Poolman, M.G., Pink, R.C., Mulcahy, L.A., Baker, I., Beaman, E.-M., Brooks, T., Caley, D.P., Cowling, W., Currie, J.M.S., Horsburgh, J., Kenehan, L., Keyes, E., Leite, D., Massa, D., McDermott-Rouse, A., Samuel, P., Wood, H., Kadhim, M. A. & Carter, D.R.F. (2013). Meta-analysis using a novel database, miRStress, reveals miRNAs that are frequently associated with the radiation and hypoxia stress-responses. *PloS One*, 8(**11**), p.e80844 doi: 10.1371/journal.pone.0080844.

A copy of the above mentioned publication is bound into the back of the accompanying hard copy of this thesis

Chapter 3 Identification of novel radiation microRNA candidates using the miRStress database

3.1. Introduction

The cellular stress response is key in protecting cells from cytotoxic changes in the environment caused by a variety of stressors such as heat, chemical, hypoxia or radiation. Upon employing one of a number of specialised biological responses, the cell will either adapt, repair the DNA damage, or undergo apoptosis to protect the organism in which it resides (Fulda et al., 2010). Radiation is considered a potent stressor of cells with the ability to cause deleterious DNA damage such as mutation and carcinogenesis that are attributed to damage to a cellular target, usually nuclear DNA via direct absorption of radiation energy (Kadhim et al., 2013). Non-targeted mechanisms including the BE have been more recently reported (Lorimore et al., 1998; Kadhim et al., 1992) but the exact candidate signalling molecule or combination of molecules responsible for non-targeted effects have yet to be fully elucidated, however one viable group of candidate molecules are microRNAs (Chaudhry & Omaruddin, 2012).

As described in section 1.3.4, microRNAs are small non-coding RNAs of around 20-24 nucleotides that are potent regulators of gene expression and have been shown to be involved in a variety of biological functions (Yates et al., 2013). MicroRNA levels have been shown to be deregulated in cells in response to stressful stimuli (Figure 3.1), for example heat shock, hypoxia and radiation assault (Saleh et al., 2011; Wang & Cui, 2012; Leung & Sharp, 2010). The data detailing microRNA deregulation following stress to cells are, however, spread across a large number of disparate publications documenting different conditions. The literature published to date demonstrates that microRNAs play an important role in radiation response (Chaudhry et al., 2010; Kovalchuk et al., 2010; Dickey et al., 2011). Additionally it was recently demonstrated that EVs released from MCF7 cells exposed to X-rays were able to cause bystander effect in unirradiated recipient cells and that this mechanism was RNA dependent (Al-Mayah et al., 2012).

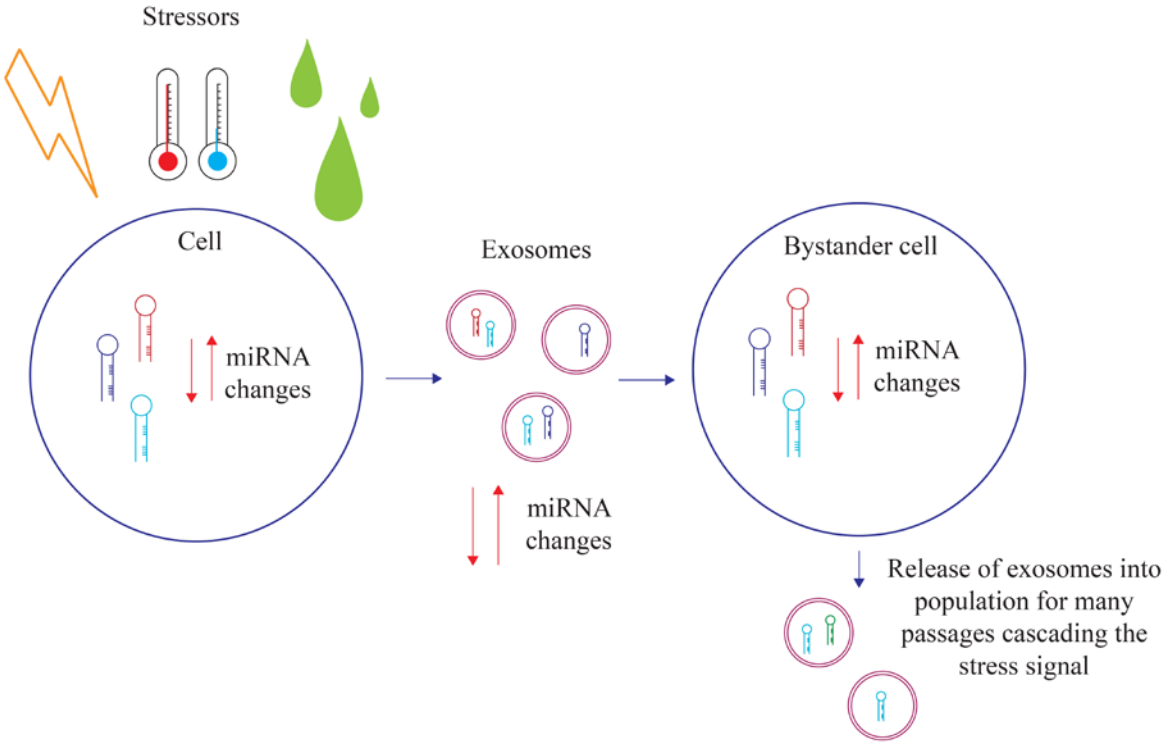

Figure 3.1. Modulation and transport of microRNAs following stress to the cell. *Stress to the cell can lead to changes in microRNA modulation and in turn to the microRNA levels in EVs released from those cells. Target cells subject to bystander microRNA modulation release further EVs that continue to influence the cell population.*

Bioinformatical studies have also previously been performed on the microRNAs shown to be involved in radiation response and also the mRNA targets of those microRNAs using the bioinformatics tool Cytoscape to identify novel pathways involved in radiation response (Lhakhang & Chaudhry, 2012). The results were complex, with single microRNAs targeting several target genes, in addition to mRNAs that are targeted by a multitude of microRNAs. Well established radiation-induced pathways such as the MAPK signalling pathway, focal adhesion and the TGF-ß signalling pathway featured. All of these have been previously reported in response to ionizing radiation (Dent et al., 2003; Ishikawa et al., 2006; Sandfort et al., 2007), however previously unidentified pathways including proliferation related pathways were also presented by the study, demonstrating the value of such meta-analyses.

The aforementioned analysis (Lhakhang & Chaudhry, 2012) was however limited to those microRNAs that were deregulated in 5 or more cell lines following IR, limiting the scope of the study. Furthermore it was demonstrated in a meta-analysis that the *let-7* family may play an important role in the radiation response (Dickey, Zemp, Martin, et al., 2011), This study however only focused on a small number of specific studies and so was not an exhaustive comparison. In order to study in-depth the role of microRNAs in the stress response the miRStress database was

manually curated to bring together the published data to produce lists of deregulated microRNAs under different conditions of stress (Jacobs et al., 2013).

In this chapter investigation of the general stress response, as well as the general radiation response and more specifically the X-ray response have been reported and reflect the role of the miRStress tool in providing valuable insights into stress responses of the cell. This is the first time that all of the published data have been brought together on microRNA stress responses and will aim to elucidate novel microRNA candidates in response to stress, in particular radiation.

3.2. Materials and methods

3.2.1. Study selection

The search term 'microRNA' was entered into PubMed (http://www.ncbi.nlm.nih.gov/pubmed/) to obtain a list of all microRNA publications to date. The entire history of microRNA publication abstracts (> 20,000 publications) were manually inspected to identify abstracts mentioning differential regulation of microRNAs following any stress to cells, for example radiation, hypoxia or heat stress. If the abstract did not specifically mention the use of a stressor followed by microRNA measurement then it was not included. Reports of treatments related to biological stresses, such as disease, infection with viruses or bacteria, or treatment with biological macromolecules such as hormones and peptides were not included in the database. Combination treatments were also excluded. Only values reported as statistically significant were included. The database contains a total of 7,663 microRNA entries from 315 papers. Details from each paper were manually curated into the database spreadsheet including the cell type, stressor conditions, quantification methods and microRNA species that were deregulated.

3.2.2. Database construction

The miRStress database is available for interrogation via a downloadable standalone module from the SourceForge website (https://sourceforge.net/projects/mirstress/). The miRStress download utilises a Python module for interrogation (written by Dr. Mark Poolman and Findlay Copley). A Tkinter python module was used to produce the graphical user interface that forms the standalone module that can be interrogated by the user (written by Findlay Copley). The database is also searchable offline.

Data can be accessed by selecting a field to search (PMID, Authors, Title, Year etc.) and then typing a search term into the module (Figure 3.3). The search term must be typed exactly as it appears in the database. It is possible to right click the search term box to obtain a list of available search terms. Results in the window can then be printed to a *.txt* file or have further filters applied to refine the microRNA list. The term 'total' reports the total number of entries of that microRNA in different papers in the database, 'up/down' indicates the direction of deregulation of the selected microRNA and 'NR' indicates that the direction of deregulation was not reported in the paper.

3.2.3. Radiation microRNA validation

For radiation stress the top twenty microRNAs deregulated in response to all modes of radiation were selected and named 'radiation microRNAs'. A list of twenty 'control microRNAs' was also produced by randomly selecting twenty microRNAs that only appeared once in the radiation list, to represent microRNAs that were unlikely to play a true role in radiation response (Figure 3.2). For X-ray only analysis the same procedure was applied, only for X-ray entries.

For each of the individual radiation and control microRNAs a list of high confidence targets were identified using the online microRNA binding-site prediction tool miRwalk (http://www.umm.uni-heidelberg.de/apps/zmf/mirwalk). miRwalk compares the results of various microRNA-target prediction algorithms. Genes that were predicted to be targeted by at least six of the algorithms were selected for further analysis. The lists of mRNA targets for each microRNA were then converted into Entrez IDs and entered into the DAVID functional annotation tool (http://david.abcc.ncifcrf. gov/home.jsp). This produced a list of KEGG pathways for each microRNA. KEGG pathways with a value of $p < 0.05$ for that microRNA were made into a list and termed 'predicted pathways'. All of the predicted pathways for all of the microRNAs in the radiation group were pooled together, and all of the predicted pathways for all of the control microRNAs were also pooled. Unique counts for each pathway were then established for the radiation microRNAs and the control microRNAs. Cancer pathways and disease pathways were removed from the lists. If a given KEGG pathway was then 'predicted' to be targeted by at least three radiation microRNAs and at least 50% fewer control microRNAs then it was used in the analysis.

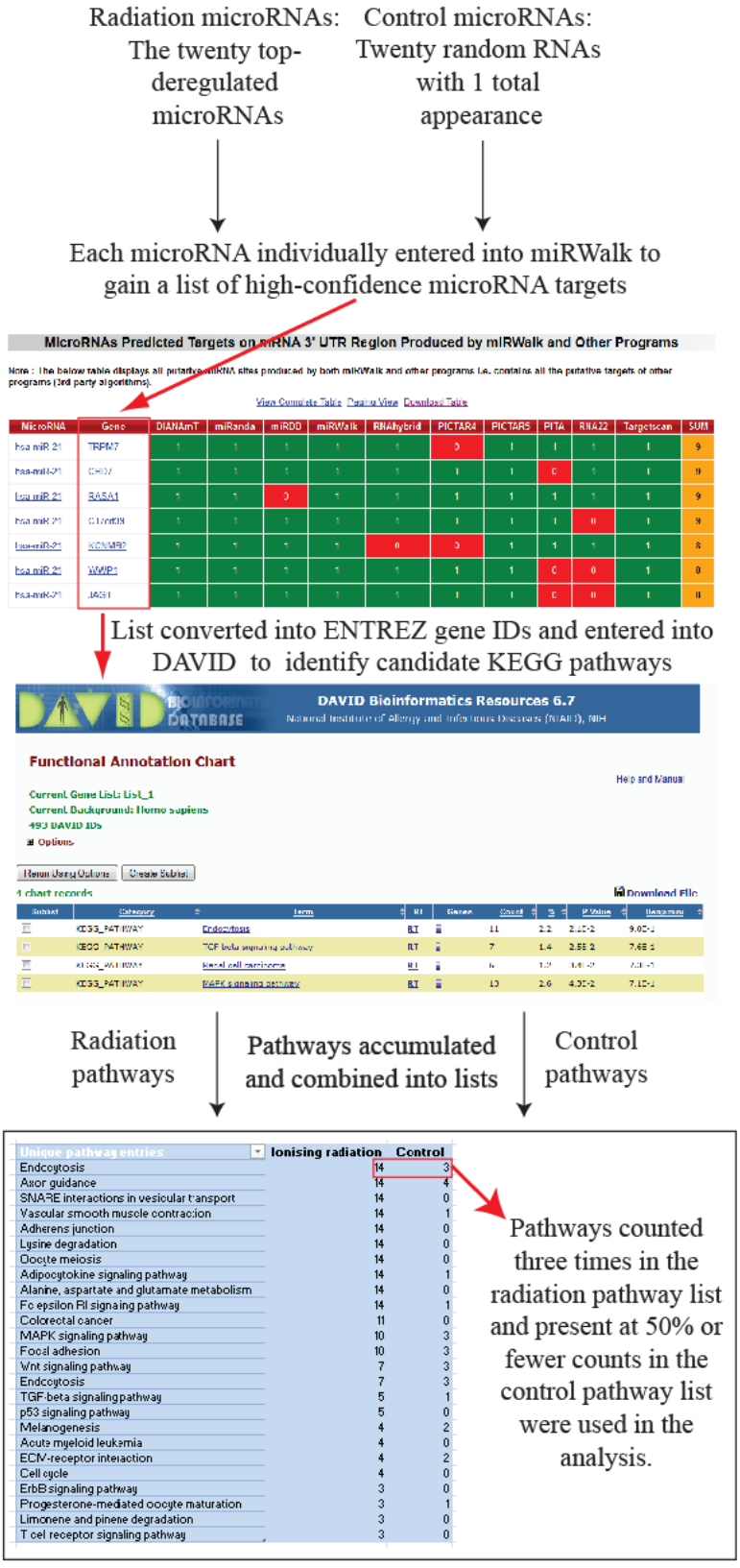

Unique pathway entries	Ionising radiation	Control
Endocytosis	14	3
Axon guidance	14	4
SNARE interactions in vesicular transport	14	0
Vascular smooth muscle contraction	14	1
Adherens junction	14	0
Lysine degradation	14	0
Oocyte meiosis	14	0
Adipocytokine signaling pathway	14	1
Alanine, aspartate and glutamate metabolism	14	0
Fc epsilon RI signaling pathway	14	1
Colorectal cancer	11	0
MAPK signaling pathway	10	3
Focal adhesion	10	3
Wnt signaling pathway	7	3
Endocytosis	7	3
TGF-beta signaling pathway	5	1
p53 signaling pathway	5	0
Melanogenesis	4	2
Acute myeloid leukemia	4	0
ECM-receptor interaction	4	2
Cell cycle	4	0
ErbB signaling pathway	3	0
Progesterone-mediated oocyte maturation	3	1
Limonene and pinene degradation	3	0
T cell receptor signaling pathway	3	0

Figure 3.2. Flow diagram demonstrating allocation of 'radiation' and 'control' microRNA and pathway lists. *Lists of microRNAs from the miRStress database proceed through the analysis pipeline to produce lists of predicted pathways linked to those microRNAs.*

3.2.4. miRStress database validation

In order to further validate the database, eighteen expression microarray datasets documenting mRNA changes following ionizing radiation treatment were obtained from Gene Expression Omnibus (http://www.ncbi.nlm.nih.gov/geo/) by Dr. Ryan Pink. Datasets were individually imported into Genespring 12.5 (Agilent Technologies) and normalised using 'Robust Multi-array Average'. Each dataset was then normalised to the median value for that dataset. Genes whose expression was altered by at least 2-fold in irradiated compared to control samples were imported into DAVID Bioinformatics Resource 6.7. This allowed identification of KEGG pathways that were significantly enriched in each of the eighteen radiation datasets.

In addition, SF5 (surviving fraction of cells following a 5 Gray dose of γ-rays) data were obtained for each cell line in the NCI-60 panel from previously published results (Patnaik et al., 2012). Levels of microRNA expression for each cell line were obtained from the E-MTAB-327 dataset. Pearson correlations were obtained between each microRNA and the SF5 data across the panel of cell lines. For comparison of different microRNAs the magnitude of Pearson correlation values was obtained by converting any negative values into positives.

3.2.5. Receiver operating characteristic (ROC) analysis

The ROC analysis was performed using SPSS (v19, IBM). In each test the list of high-confidence microRNAs for radiation stress was compared to an equivalent number of control microRNAs (that only appeared once in miRStress for that given stress). The number of appearances in the miRStress database was used as the test variable. A dichotomous output of whether the microRNA was a 'true positive' or not was used as the state variable. A microRNA was defined as a true positive if that microRNA had previously been shown to be functionally involved in the stress response, either by being involved in a defined stress response pathway or by affecting resistance (to the given stress) when manipulated as per the literature.

3.3. Results

3.3.1. The miRStress database

The miRStress database is a database of microRNA changes in response to many different forms of stress. The database can be manipulated to produce lists of deregulated microRNAs, and the frequency and direction in which they are deregulated. A comprehensive meta-analysis of the literature has not previously been performed on all microRNA responses of cells to stress. The data were taken from a wide variety of studies that documented changes using different models and cell lines, also using a variety of different techniques; therefore a tool collating all of this information makes the study of the cellular response to stress more manageable. By studying cell-wide stress-induced changes it is then possible to make inferences about new microRNA candidates and pathways involved in stress responses on a general or more specific treatment level, especially where the literature is not detailed in a particular area.

The database contains entries from over 300 papers, and contains more than 7500 individual entries across a variety of stress-types from chemical, to radiation, to heat stress, but excluding disease states and naturally occurring biological molecules.

The database is interrogated via the miRStress standalone module downloadable from (https://sourceforge.net/projects/mirstress) (Figure 3.3). The data can be browsed by selecting one of a number of variables and then entering a search term into the search box. Lists of deregulated microRNAs for the variable will be returned and document the total number of cases of deregulation, the number of times the microRNA was up or down-regulated, and also any cases in which the direction was not recorded (denoted by NR).

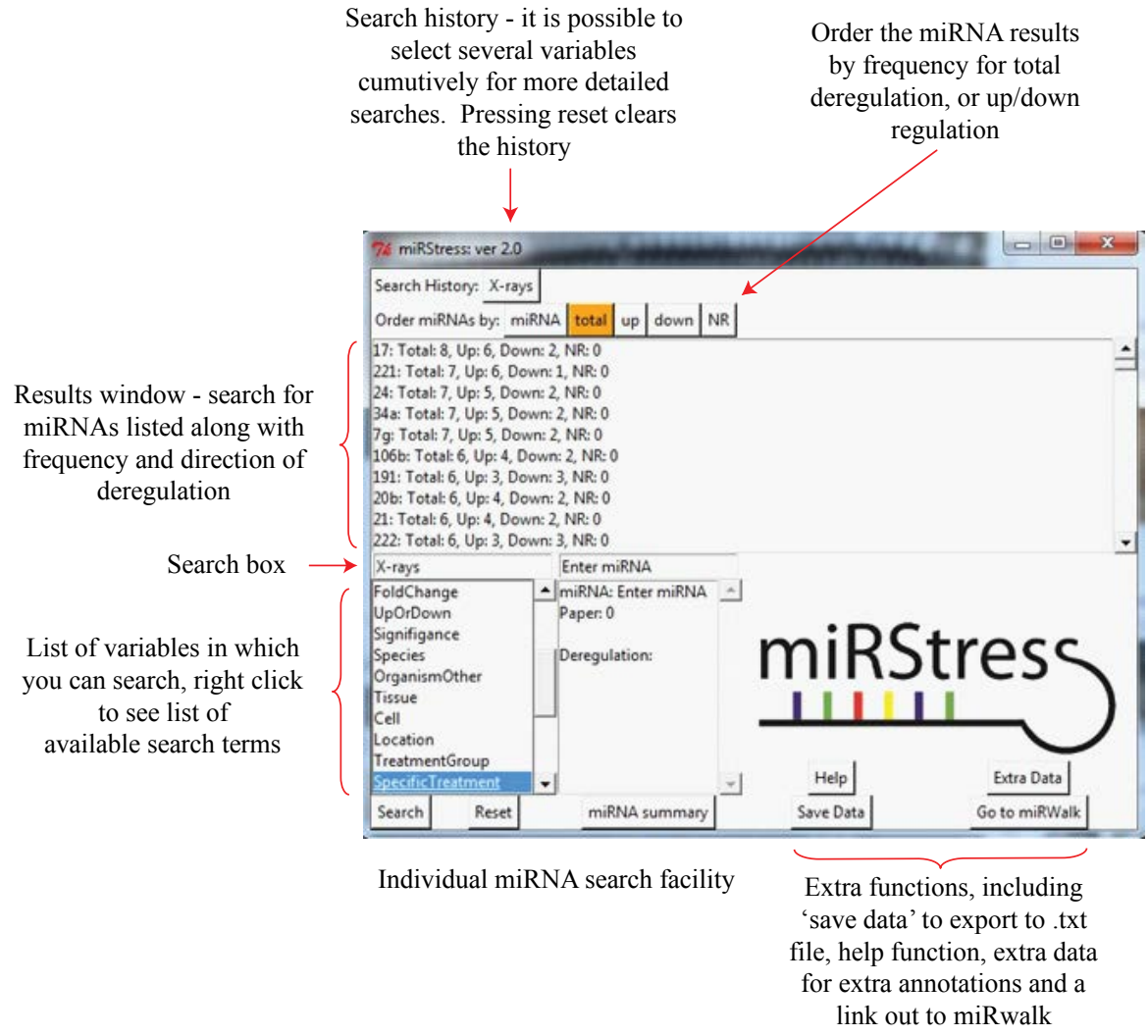

Figure 3.3. The miRStress standalone module. *The downloadable module can be used to filter and extract microRNA data from the miRStress database.*

3.3.2. Characterising the general stress response using the miRStress database

To characterise the microRNA response to general cellular stress – that is the microRNA response to all of the stresses recorded in the database – the standalone module was used to return a list of the ten most deregulated microRNAs across the database (Table 3.1). The top results included miR-21 and miR-34a that are well reported in the literature as playing a role in genotoxic and cardiac stress response (Mendell & Loson, 2013). This demonstrates that these results can be used to help establish common microRNAs in the general stress response and general stress pathways may then be determined.

Table 3.1. MiRStress-generated list of the most frequently deregulated microRNAs across all stress types. *NR = Not recorded – direction of deregulation was unknown for the deregulation event.*

microRNA	Up	Down	NR	Sum	% Upregulated	% Downregulated
21	68	25	1	94	72.3	26.6
210	72	10	1	83	86.7	12
34a	49	14	0	63	77.8	22.2
17	24	37	1	62	38.7	59.7
16	35	23	1	59	59.3	39
125b	30	25	1	56	53.6	44.6
26a	25	27	1	53	47.2	50.9
20a	19	27	1	47	40.4	57.4
155	33	14	0	47	70.2	29.8
29a	25	20	1	46	54.3	43.5

3.3.3. Characterising the general radiation stress response using the miRStress database

Alongside hypoxia, radiation stress entries represented a significant proportion of the literature base for the database. In order to better understand the radiation induced bystander effect, radiation stress has been further analysed for this chapter. The miRStress database documents data for many different types of radiation stress. For the purposes of the database the term 'radiation treatment' was used, referring to all forms of intentional experimental radiation exposure. The overall radiation treatment group can be divided into 'specific treatments' including X-rays, γ-rays and α-particle radiation. As of the date of publication in June 2013, the first release of the database contained entries for radiation from 56 different papers, with 304 individual microRNA species deregulated following radiation stress.

3.3.4. MicroRNAs deregulated during the general radiation stress response

To characterise the 'general' radiation response of cells – that is the response of cells or tissues to all types of radiation at all doses - the miRStress database was interrogated using the search term 'radiation'. The top twenty microRNA results returned were selected for analysis (Table 3.2). The top results for deregulation included miR-21, miR-34a and several members of the *let* family. As for many of the other microRNAs in the top twenty list, these have previously been shown to play a functional role in response to radiation (Chaudhry et al., 2013; Mert et al., 2012). Several microRNAs not previously associated with radiation response were also identified in the list, for example, miR-106a, miR-15b and miR-19b.

In order to test that the results from the database reflected actual changes in microRNA expression and were not purely coincidental, twenty 'control' microRNAs were also selected that only appeared once in the radiation microRNA list. These were not likely to play a significant role in radiation response. Overall the data demonstrates that miRStress can help in identifying novel candidates involved in the general radiation response by identifying consistently deregulated microRNAs across all of the published data and amongst overrepresented microRNAs.

Table 3.2. MiRStress-generated list of the top twenty deregulated microRNAs following radiation treatment. *NR = Not recorded – the direction of deregulation was unknown for the deregulation event.*

microRNA	Up	Down	NR	Sum	% Upregulated	% Downregulated
21	11	6	1	18	61.1	33.3
34a	11	6	0	17	64.7	35.3
16	10	5	1	16	62.5	31.3
17	8	6	1	15	53.3	40.0
let-7b	5	9	1	15	33.3	60.0
let-7g	9	5	0	14	64.3	35.7
let-7a	5	8	1	14	35.7	57.1
let-7f	6	7	0	13	46.2	53.8
19b	6	5	1	12	50.0	41.7
let-7d	4	6	2	12	33.3	50.0
let-7c	7	5	0	12	58.3	41.7
125b	5	6	1	12	41.7	50.0
143	4	5	2	11	36.4	45.5
24	8	3	0	11	72.7	27.3
20a	4	6	1	11	36.4	54.5
15b	4	5	2	11	36.4	45.5
106a	3	6	1	10	30.0	60.0
106b	4	5	1	10	40.0	50.0
let-7e	4	6	0	10	40.0	60.0
221	8	2	0	10	80.0	20.0

3.3.5. Predicted radiation pathways in the general radiation response

To assess whether the microRNA lists corresponded to actual radiation response events in the cell, KEGG pathway analysis was performed to search for pathways associated with the lists of miRNAs. In order to obtain the list of predicted KEGG pathways each of the twenty 'radiation' and 'control' microRNAs previously established was entered into miRwalk and the high confidence

targets entered to DAVID. The criteria for radiation-related pathways was that the pathway appeared at least three times in the radiation microRNA list and at an incidence of 50% or below in the corresponding control microRNA list.

As seen in (Table 3.3) the MAPK signalling pathway was the top pathway reported, targeted by sixteen microRNAs followed by pathways such as focal adhesion and TGF-ß signalling. These predicted pathways appear consistent with what might be expected for the radiation response.

Table 3.3. Top six pathways predicted with high confidence to play a role in radiation response. *Using KEGG pathway analysis the top twenty deregulated radiation/control microRNAs were used to create lists of high confidence targets to identify pathways involved in the radiation response.*

Name of KEGG pathway	Number of radiation microRNAs predicted to target the pathway	Number of control microRNAs that are predicted to target the pathway
MAPK signalling pathway	16	4
Focal adhesion	12	6
Endocytosis	11	4
Axon guidance	9	5
TGF-β signalling pathway	8	3
ECM-receptor interaction	7	0

3.3.6. Validation of the miRStress database results

In order to ensure that the predicted microRNA lists and pathway results obtained were representative of the microRNAs deregulated following stress responses, steps were taken to validate the database. To confirm that the predicted pathways do indeed reflect changes in mRNA expression following irradiation, eighteen microarray datasets were downloaded and the genes for real mRNA changes analysed using DAVID as in the radiation analysis. The results for this were then compared to the predicated pathways from the previous analysis. Results showed that the radiation predicted pathways appeared on average 4.2 times in the list of actual mRNA radiation pathways, compared to 1.5 times for the control predicted pathway (Figure 3.4a). This is a significant difference ($p = 0.002$), confirming that the predicted radiation pathways reflect the radiation pathways that have been shown experimentally reported as affected following irradiation.

Further validation of the biological relevance of the radiation microRNA data was performed using NCI-60 datasets, from a panel of 60 tumour cell lines used in anticancer drug screening (Shoemaker, 2006), and then testing using Pearson correlations (Figure 3.4b). The SF5 (surviving fraction of cells after a 5 Gy dose of radiation) value for each cell line and levels of microRNA expression in the E-MTAB-327 dataset (Patnaik et al., 2012) were used and Pearson correlations used to establish relationships within the data. The results showed that the Pearson correlation for the radiation microRNAs was significantly higher than the average for the control microRNAs (t

test, p = 0.017). A coefficient of determination (R^2) test was also performed and showed that the average R^2 value was three times higher than for the control microRNAs, demonstrating that the radiation microRNAs were more likely to correlate with sensitivity than the control microRNAs. This suggests that the microRNAs identified by miRStress are indeed biologically relevant and not random sampling artefacts.

A receiver operating characteristic (ROC) curve analysis was also performed to check that miRStress was identifying microRNAs genuinely associated with the radiation response. By coding the number of times that a microRNA appeared in the radiation or control microRNA list with a binary input referencing whether the microRNA has been shown to cause a functional change in the literature, it was possible to determine whether the tool was a true test. The area under the curve (AUC) value was 0.857, indicating a test of good sensitivity and specificity. In conclusion the results support that the miRStress database is both a sensitive and specific tool, able to produce lists of biologically functional microRNAs and their corresponding mRNA targets.

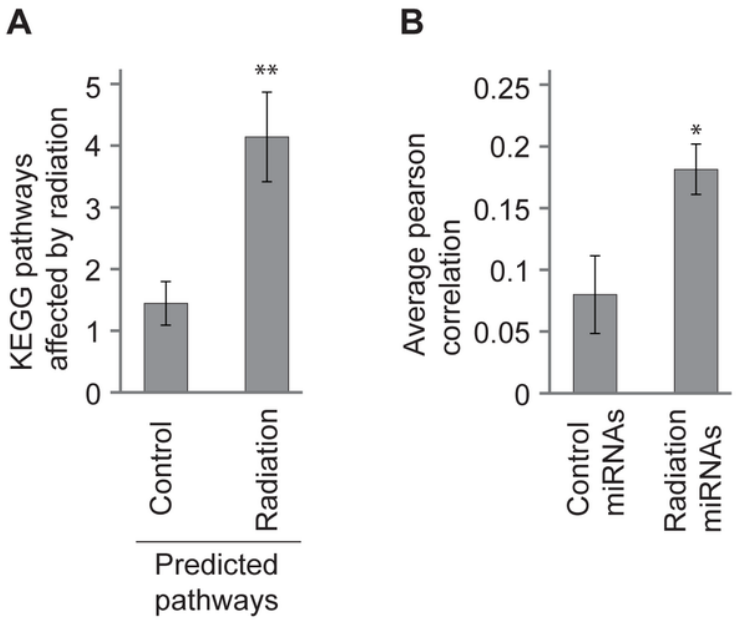

Figure 3.4. Radiation-responsive microRNAs predicted by miRStress are biologically relevant. *A: The average frequency with which the miRStress predicted control or radiation pathways appears in the observed pathways from the microarray dataset analysis is shown. Error bars = SEM. B: MiRStress predicted radiation and control microRNAs used in part A were used to test for correlations between SF5 and microRNA levels across the NCI-60 panel. The radiation microRNAs have a significantly higher correlation with radiosensitivity compared to the control microRNAs (t test, p < 0.02). Magnitude of Pearson correlations values were created by converting negative values into positive values. Error bars = SEM.*

3.3.7. MicroRNAs deregulated following X-ray irradiation

In order to establish whether the response to ionizing radiation in the form of X-rays was similar to that of the general radiation response, analysis was performed to obtain a list of microRNAs deregulated following X-ray irradiation and their associated predicted pathways. A total of 22 papers were found documenting the deregulation of microRNAs following exposure to X-rays at varying doses and varying time points out of the 56 radiation papers in the database (Table 3.4). The most deregulated microRNAs included *let-7g* (Chaudhry, 2014), miR-221 (Rao et al., 2011) and miR-24 (Meng et al., 2015). Many of the microRNAs in the list had been shown to play a functional role in radiation response; however novel candidates such as miR-191, miR-29b, miR-156 and miR-206 had not been documented at the time of publication. The top five deregulated X-ray microRNAs were also more frequently upregulated than downregulated, with only miR-148b upregulated in 100% of cases. Consequently, the list contains both established and novel RNA candidates involved in the X-ray response.

Table 3.4. MiRStress-generated list of the top twenty deregulated microRNAs deregulated following X-rays. *NR = The direction of deregulation was not recorded in the paper.*

microRNA	Up	Down	NR	Sum	% Upregulated	% Downregulated
17	6	2	0	8	75	25
221	6	1	0	7	85	14
24	5	2	0	7	71	29
34a	5	2	0	7	71	29
Let-7g	5	2	0	7	71	29
106b	4	2	0	6	66	34
191	3	3	0	6	50	50
20b	4	2	0	6	66	34
21	4	2	0	6	66	34
222	3	3	0	6	50	50
29b	3	3	0	6	50	50
Let-7a	2	4	0	6	33	67
Let-7b	2	4	0	6	33	67
106a	3	2	0	5	60	40
148b	5	0	0	5	100	0
15a	4	1	0	5	80	20
15b	2	3	0	5	40	60
16	4	1	0	5	80	20
194	4	1	0	5	80	20
206	3	2	0	5	60	40

3.3.8. Predicted pathways in the X-ray response

The top twenty X-ray induced microRNAs and twenty randomly selected control microRNAs were used to produce a list of KEGG pathways as previously described for the general radiation response (Table 3.3), this time for X-ray response only. The results showed that a number of pathways were deregulated following X-ray exposure, including endocytosis, the TGF-β signalling pathway and the MAPK signalling pathway as found in the general radiation response (Table 3.5). Other pathways not found in the general radiation response included SNARE interactions and the adherens junction was at the top of the list, suggesting pathways potentially unique to the X-ray response.

Consequently the top predicted pathways following X-irradiation differed from those pathways found for the general radiation response. A comparison of the top six pathways for each group demonstrated notable differences as only two of the top six pathways for the radiation response were found in the X-ray predicted pathway list. The remaining pathways in the general radiation response list were found in the X-ray predicted pathway list, but lower down in the results, suggesting that the X-ray radiation response is distinct from the general radiation response, or that more study is required to elucidate the pathways involved in the X-ray response. An increased number of publications would also diversify the dataset leading to discovery of new microRNAs and their associated pathways.

Table 3.5 Top KEGG pathways predicted with high confidence to be deregulated in the X-ray response. *Using KEGG pathway analysis the top twenty deregulated X-ray/control microRNAs were used to create lists of high confidence targets to identify pathways involved in the X-ray response.*

KEGG pathway	X-ray microRNAs	Control microRNAs
Endocytosis	14	3
Axon guidance	14	4
SNARE interactions in vesicular transport	14	0
Vascular smooth muscle contraction	14	1
Adherens junction	14	0
Lysine degradation	14	0
Oocyte meiosis	14	0
Adipocytokine signalling pathway	14	1
Alanine, aspartate and glutamate metabolism	14	0
Fc epsilon RI signalling pathway	14	1
MAPK signalling pathway	10	3
Focal adhesion	10	3
Wnt signalling pathway	7	3
TGF-beta signalling pathway	5	1
p53 signalling pathway	5	0
Melanogenesis	4	2
Acute myeloid leukaemia	4	0
ECM-receptor interaction	4	2
Cell cycle	4	0
ErbB signalling pathway	3	0
Progesterone-mediated oocyte maturation	3	1
Limonene and pinene degradation	3	0
T cell receptor signalling pathway	3	0

3.3.9. Comparison of the general radiation response and the X-ray response to radiation

A comparison of the general radiation and the X-ray specific microRNA response was carried out to establish common and unique microRNAs deregulated following the two groups of radiation stress and to offer clues as to novel candidates involved in response to the different modes of radiation. Overall the general radiation and X-ray response results contained similarities as expected as they are derived from the same dataset, but also notable differences. The top twenty microRNAs deregulated following X-ray exposure contained twelve of the top twenty microRNAs in the list for the general radiation response, including miR-21, miR-34a, miR-17 and *let-7g*. Consequently, eight of the top twenty deregulated microRNAs following general radiation exposure were not present in this list suggesting distinct responses of X-ray irradiated cells (Figure 3.5). Eight microRNAs were unique to X-ray stress. These included miR-222, miR-15a and miR-206 that have not previously been reported as functionally involved in radiation response. Consequently, in this chapter novel microRNA candidates have potentially been identified and suggest that the cellular response is different for different modes of radiation.

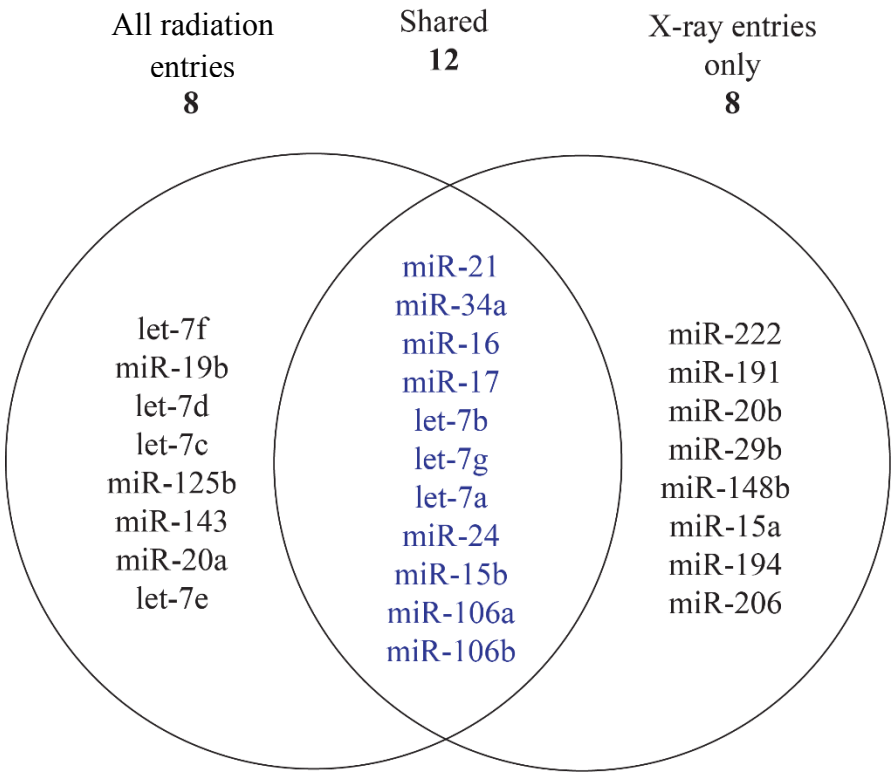

Figure 3.5. Overlap of microRNAs involved in the general radiation response and the X-ray response. *The general radiation response and X-ray response microRNAs predicted using the miRStress database*

shared twelve common microRNA candidates and had eight unique candidates each.

3.4. Discussion

Many studies have been published documenting deregulated microRNA expression in cells and tissues following various conditions of stress. The studies are however disparate and contain data from a wide variety of experimental conditions and models. There is also a certain levels of bias in these studies towards more 'popularised' microRNAs. Consequently, the miRStress database was created so that the data could be studied as a whole. Compiling all of the significant published data into one searchable resource enables a cell and organism-wide approach to the study of the eukaryotic stress response so that new inferences may be more effectively made.

One key aim of the database construction was to establish novel candidate RNAs and pathways involved in the radiation response. The miRStress database made it possible to address this aim effectively, and, as shown, productively. Due to the different effects of different radiation types upon cells, each microRNA response is likely to be individual to an extent; however it is possible that a characteristic radiation response of cells may exist. Consequently a 'general' radiation response analysis was performed to construct a list of the top deregulated microRNAs across all radiation modes. Some attempts have been previously made to draw together some of the published information on radiation (Dickey et al., 2011; Lhakhang & Chaudhry, 2012), however these were not inclusive of all the published radiation data and therefore only offer partial insights into the data as a whole.

3.4.1. Stress and the general radiation response

The microRNA lists generated for the general radiation response reported a number of microRNAs that have been well documented in the literature as anticipated, as well as a number of microRNAs that may be considered as novel candidates. The top twenty deregulated microRNAs included miR-21, miR-34a and miR-16. These microRNAs have not only been extensively reported in the literature, but also documented as functional following radiation exposure. It has been demonstrated *in vivo* that miR-21 increases significantly in the serum of women receiving ionizing radiotherapy for breast cancer and that it could be used as a biomarker for those having received ionizing radiation (Halimi et al., 2014). Furthermore, the role of the tumour suppressor p53 in genotoxic stress response is well documented and has been shown to form a feedback loop with miR-34a and *SIRT1*, an NAD-dependent lysine deacetylase, to modulate p53 responses that may in turn play a role in microRNA maturation and expression (Herbert et al., 2014). This study demonstrated that in p53-mutant keratinocyte cells, mature miR-34a levels were reduced and that SIRT removal resulted in lower pri-miR-34a levels. In combination, this led to failed microRNA maturation of miR-34a, and also miR-16, another p53 regulated microRNA. This demonstrates that

not only do these RNAs become deregulated following stress, but they may also be linked in a complex signalling network via other pathways in response to radiation stress on a functional level.

Many of the microRNAs reported for the general radiation response have been shown to play roles in the radiation response of cells. Members of the *let-7* family were also found in the general radiation response list and are well documented in the radiation response. It was shown in TK1 and WTK1 cells that following ionizing radiation exposure of 0.5 Gy and 2 Gy, eight of the *let* family were deregulated, being up regulated in TK6 cells but down regulated in WTK1 cells (Chaudhry et al., 2010). Furthermore, *let-7a* and *let-7b* were shown to be down regulated following ionizing radiation (Saleh et al., 2011) via a p53 dependent mechanism with p53 or ATM null colon cancer cells and knockdown mice not exhibiting down regulation of these microRNAs and the same effect was observed in knockdown mice. Despite being reported as deregulated in cells following ionizing radiation, *let-7* family members remained at normal levels in bystander cells (Chaudhry & Omaruddin, 2012). Interestingly, the top microRNAs deregulated following radiation response were similar to those found in an overall list of the top ten deregulated microRNAs found in response to all stresses in the database (Table 3.1). This is consistent with the fact that the radiation response is likely to be linked in to the overall stress response of the cell and that is reflected in the miRStress database.

The potential novel candidate microRNAs for the general radiation response in the list not reported at the time of publication in any of the radiation literature included miR-15b, miR-19b and miR-106a. Recently, however, miR-19b has been identified as playing a role in radiation response (Leung et al., 2014). Whilst being over-expressed in breast cancer, it was significantly down-regulated following a single dose of ionizing radiation. Leung et al. also reported that the miR-17-92 cluster plays a role in radiation signalling pathways in cancer cells, with several of the miR-17-92 cluster appearing in the general radiation top twenty list (miR-17,-19b and 20a). This demonstrates the utility of the miRStress database in identifying novel radiation microRNA candidates and that miR-15b and miR-106a remain as novel candidates in the radiation response that could be specifically tested functionally.

Pathway analysis was also performed on the microRNA lists to produce pathways known to be involved in the general radiation response. The MAPK pathway was the top-deregulated pathway in the general radiation response. As reported in the literature, the MAPK complex superfamily of pathways is extensively involved in radiation response (Dent et al., 2003). Cellular responses to radiation may also lead to self-stimulation of cells via their own signalling mechanism through members of the MAPK family, causing cytosolic events to reoccur in the affected cells (Valerie et al., 2007). These events may play a role in conditioning the cell in preparation for future radiation exposures. Other top pathways included the TGF-ß signalling pathway, extensively linked to both the direct (Lhakhang & Chaudhry, 2012) and indirect (Chai et al., 2013) effects of radiation. In terms of indirect radiation effects, including phenomena such as the bystander effect, TGF-ß and

TGFBR1expression was shown to be upregulated in non-targeted lung tissue following lower abdominal radiation to mice (Chai et al., 2013). Specifically, up regulation of the TGFBR1 receptor was significantly increased. This is known to be linked to COX-2 expression – a key component in the non-targeted response of radiation such as the bystander effect (Zhou et al., 2005). This reflects the fact that the radiation response pathways revealed by the database may also offer clues to pathways involved in the non-targeted effects of radiation also. Understanding new pathways may also help to identify other candidate microRNAs within those pathways.

3.4.2. Stress and the X-ray response

A separate analysis of the X-ray radiation entries exclusively was performed to compliment the experiments in this thesis. The X-ray papers made up twenty two of the fifty six papers on radiation in the database, therefore it is likely that the microRNAs deregulated in these papers reflect at least in part the general radiation response but also give a flavour of the X-ray response specifically. Many of the microRNAs in the top twenty were similar to that of the general radiation response, however there were differences. The top microRNAs were miR-17, miR-221 and miR-24, with miR-21 and miR-34a appearing notably further down the rankings than for the general radiation response, suggesting that other microRNAs play a more prominent role in X-ray response. MiR-17 has been shown to negatively regulate the *ATG7* pathway involved in cellular survival and death (Comincini et al., 2013). Furthermore, sensitization of cells to radiation is anticipated to be an adaptation of cells to survive future assaults, miR-221 binding with antagomirs has been shown to sensitize cells by up-regulating *PTEN* expression (Xue et al., 2013) and also via the p27 pathway in glioblastoma cells (Gillies & Lorimer, 2007). Overall this suggests a role of microRNAs in cell survival following X-ray assault. Several novel candidates for the X-ray response different to those found for the general radiation response were also identified, including miR-191, miR-29b, miR-156 and miR-206. The fact that all of these novel candidates are different to those found for the general radiation response suggests that the X-ray response is indeed characteristic.

For the X-ray analysis, the predicted pathways profile was also somewhat different to the general radiation response (Table 3.3). The top six deregulated pathways were very different to those of the general response, only including two from the general radiation response list. Interestingly, 'SNARE interactions in vesicular transport' was one of the top pathways reported for X-ray response. It is known that SNARE processes play a role in the release of EVs from cells (Südhof & Rothman, 2009). EVs have been shown to be released in response to radiation (Arscott et al., 2013) and to play a role in the radiation induced bystander effect (Al-Mayah et al., 2012; Jella et al., 2014). It is possible, therefore, that the release of EVs or vesicles from cells may play a role in cellular response to X-rays.

3.4.3. Important considerations in the identification of novel microRNAs

A potential reason for some of the novel microRNA candidates suggested in this work not having yet been tested functionally may be due to the fact that they are not amongst the traditionally well-studied microRNAs. Such bias in the microRNAs reported might also be explained by the use of specific primers in qPCR studies or the type of chip used for microarrays that hold different microRNA combinations and species. Older microarray systems may have also contained fewer genes. The more open platforms including RNA Seq and high-throughput PCR have likely more recently given undiscovered candidates the opportunity to appear in the lists produced by the database. Indeed it is also important to note that microarray platform results have been shown to differ from RNA sequencing results, for example, and that the comparison of results from the two platforms must be carefully monitored (Marioni et al., 2008; Mortazavi et al., 2008).

There are advantages and disadvantages of using different technologies to study gene expression. In qPCR studies single primers are often used as they can sensitively detect their target of interest. Alternatively, microarray has the ability to probe a large number of genes simultaneously, but at a lower level of sensitivity and often at greater cost. Consequently the miRStress database aims to combine the data from such different platforms. It is also important to note however, that even though the database is unlikely to provide 'false positives' it cannot be said that because a microRNA is not returned by the database that it is definitely not involved in the radiation response. Only data from further study of the microRNAs deregulated following radiation response can produce this information to identify 'false negatives'.

Compiling all of the published data into the miRStress database has enabled a wider, cellular-level approach for investigation of both well-established and novel microRNAs involved in the stress response. From the lists of deregulated microRNAs for each stress, mRNA targets for individual microRNAs were used to identify pathways related to stress responses. Studying the published data as a whole carries importance as at face value the literature is dominated by common microRNAs. These microRNAs are well characterised and have been shown to play lead roles in the stress response based upon previous publications. This bias can cause less obvious, but still important, functional microRNAs to be missed or discounted as they have not been prominently reported. Such lesser-known microRNAs might be consistently deregulated in the microRNA lists across the literature but have not been further characterised. The ROC analysis and Pearson correlations used to validate the miRstress database support that it produces lists of biologically relevant radiation microRNAs and consequently to the other stresses in the database.

Regarding specific phenomenon such as the bystander effect a cell-wide view of microRNAs deregulated in response to radiation is valuable, as the amount of data related to radiation assault, microRNAs and bystander effect is still relatively small. Facilitating a meta-analysis of the data can therefore offer clues as to which microRNAs might be viable candidate molecules for the bystander

effect. Experimental analysis may then be performed on these candidates as opposed to blind testing for novel microRNA candidates.

3.5. Conclusion

In conclusion, the responses of the two different radiation analyses suggest that the general response and the X-ray response share similarities, but however also exhibit notable differences. Each group reported eight unique microRNAs that were not present in the other group's list. For the general radiation response, pathways such as the MAPK pathway and TGF-ß signalling pathway were amongst the top pathways changed. Indeed, both pathways have been shown to play roles in general radiation response in the literature. The role of the MAPK and TGF-ß signalling pathways in radiation response of breast cancer cells has recently been reported alongside the presentation that members of the miR-19b family were deregulated in response to radiation (Leung et al., 2014). As miR-19b was one of the novel radiation candidates presented by the miRStress database it can be postulated that the other radiation microRNA candidates may come to light as functional in the radiation response of cells and supports that care should be taken to screen lesser-known microRNAs in future studies.

Taken together, the analysis and validation of the miRStress database suggests that the database produces lists of microRNAs that are both sensitive and specific, and also that the lists produced are of biological relevance. The microRNAs deregulated and pathways involved may also be different between different modes of radiation and future work will aim to establish common and unique changes following radiation exposure that will improve our understanding of the radiation response.

Chapter 4

Extracellular vesicles, RNase and the bystander effect

Chapter 4 Extracellular vesicles, RNase and the Bystander Effect

4.1. Introduction

The bystander effect is a well-established phenomenon; however the exact mechanism or combination of molecules responsible for the observed DNA damage have yet to be identified. In initial studies of BE, the induction of chromosomal damage was observed in mouse bone marrow stem cells following α-particle irradiation (Kadhim et al., 1992; Lorimore et al., 1998; Bowler et al., 2006). Media transfer between irradiated and unirradiated cells has been shown to mediate DNA damage in recipient cells (Mothersill & Seymour, 1997). The candidate mediators of bystander effect were consequently believed to be the types of molecules released into the extracellular environment by cells, for example cytokines or ROS (Havaki et al., 2014). However, recently EVs have been suggested to play a role in bystander effect (Al-Mayah et al., 2012). EVs are a component of cell media that are of interest in intracellular communication but had not previously been documented as potential bystander effect candidate messengers in irradiated cell media. Owing to their small size, EVs easily evade filtration steps normally incorporated into media transfer protocols.

Characterisation of populations of EVs from different sources under different biological conditions is important for better understanding their mechanism of action in health and disease. EVs are characterised by a variety of methods, including sizing, surface protein marker determination and electron microscopy (Vlassov et al., 2012). A number of technologies and protocols have been gradually developed as the study of EVs presents individual challenges owing, in particular, to their small size and lengthy extraction procedures. In addition to their various biological functions, various mRNA and microRNA species have been demonstrated in EVs from human and mouse cell lines shown to contain biologically functional forms of mRNA and microRNA via *in vitro* translation experiments (Valadi et al., 2007). RNAs in irradiated cells, in particular microRNAs, have been shown to be differentially modulated in directly irradiated and bystander cells, therefore it is postulated that they may play a role in radiation response (Chaudhry & Omaruddin, 2012). The radiation-induced microRNA transcriptional landscape in directly irradiated cells has also been characterised by RNA deep sequencing (Chaudhry et al., 2013) and, furthermore, a distinctive interactome exists between the gene targets of these deregulated microRNAs (Lhakhang & Chaudhry, 2012).

The first study to implicate EVs in radiation response demonstrated that EVs derived from breast cancer cells irradiated with X-rays mediated the bystander effect (Al-Mayah et al., 2012). Interestingly, RNase treatment of the EVs abrogated the observed bystander effect, suggesting that an RNA molecule in association with EVs may play a role in the radiation response of cells and their subsequent bystander signalling to surrounding cells. The uptake of EVs has also been shown to be increased following radiation whereby EVs released from irradiated cells bind to CD29/CD81

complexes that have co-localised on the recipient cell surface (Hazawa et al., 2014). This in turn results in increased cellular uptake of EVs following radiation stress and may play a key role in influencing populations of cells in the radiation response and during bystander effect.

In this chapter, to better understand the role of EVs and their cargo in radiation response and bystander effect, MCF7 cell EVs released from both unirradiated and irradiated cells have been studied with the aim of better understanding their release, morphology and ability to induce bystander effect in recipient cells.

4.2. Materials and methods

MCF7 cell culture was performed as previously described in section 2.1 and assay methods performed as previously published (Al-Mayah et al., 2012).

4.2.1. Media collection from irradiated and unirradiated cells

For radiation experiments MCF7 cells were seeded at approximately 2.1 $x10^6$ for a T75 flask and 4.5 $x10^6$ for a T175 flask. Directly prior to irradiation, cleared media was placed onto cells that were ~ 70% confluent. Cells were irradiated at the Gray Institute for Radiation, Oncology and Biology (University of Oxford), using a Siemens Stabiliplan X-ray machine (Siemens, Munich, Germany) delivering a total dose of 2 Gy. Sham-irradiated flasks were taken to the radiation facility but the flasks were not exposed to X-rays. Conditioned media was then removed at either four or eight hours post irradiation, centrifuged at 200 x g for five minutes to remove cellular debris and the supernatant filtered through 0.22 µm filters blocked with 0.1% BSA/PBS solution (Sigma, A4919; Sigma, D8662) and applied to fresh cells at ~70% confluency or stored at 4°C for further processing. Directly irradiated cells were fed with fresh complete media and both directly irradiated and bystander cells assayed at 24 hours post treatment by alkaline comet assay or an alternative end-point.

4.2.2. Sucrose density gradient centrifugation of EVs

The buoyant density of EVs was tested using sucrose gradient ultracentrifugation. EV pellets were resuspended in 1.8 mL 2.5 M sucrose (S0389, Sigma) in 20 mM HEPES (H3537, Sigma). A stepwise sucrose gradient was produced by overlaying eight individual fractions of 0.25–2 M sucrose solutions in individual steps carefully on top of the EV sample in ultracentrifuge tubes (Beckman, 344061). The samples were ultracentrifuged at 120,000 x g at 4˚C for 17 hours overnight. The fractions were then removed in 1.8 mL fractions and then resuspended in 20 mM HEPES. These fractions were centrifuged again at 120,000 x g for one hour and the extracellular vesicle pellets resuspended in 50 µl PBS and further analysed using electron microscopy.

4.2.3. Transmission Electron Microscopy (TEM) of extracellular vesicle samples

For TEM grid preparation an aliquot of extracellular vesicle sample was combined 1:1 with freshly made 4% PFA (Sigma, 158127) and chilled for 15 minutes on ice. The samples were then placed as a single drop onto a strip of Parafilm (VWR, 52858). Carbon-formvar coated copper grids, 200 mesh (F077, TAAB), were placed dull-side down onto the extracellular vesicle/PFA drop and left to incubate for 30-45 minutes at room temperature. Grids were then sequentially placed sample-side down onto three 30 µl drops of 0.22 µm filtered ultrapure water for one minute each and the side of the grids carefully touched to a filter paper between each drop to remove excess solution. Grids were then placed sample-side down onto a 30 µl drop of 2% (w/v) aqueous uranyl acetate for two minutes. The grids were touched to the filter paper once more and left to air dry sample-side up

for one hour. Grids were stored in a grid box for analysis using a Hitachi H7650 transmission electron microscope (TEM) at 120 kV. For the sizing experiments, EVs were sized using the count function in the AMT software (Advanced Microscopy Techniques, Massachusetts, USA) and the lists of sizes compared (n = 100 per replicate).

4.2.4. Nanoparticle Tracking Analysis (NTA) using the NanoSight NS500

In order to quantify and size EVs, use of the NanoSight NS500 (NanoSight, Malvern Instruments) was kindly facilitated by Dr Chris Gardiner at the Nuffield Department of Obstetrics and Gynaecology, John Radcliffe Hospital (University of Oxford). The NanoSight was calibrated using 5% (v/v) silica microspheres, 0.10 μm (colloidal) (Polysciences, Warrington, PA), diluted 1 in 100,000 to give a concentration of 5.29 x 10^8/ml prior to each day of use. Extracellular vesicle samples resuspended in PBS were loaded onto the machine and typically diluted 1:20 to 1:50 to ensure that the extracellular vesicle concentration was within the recommended range (1×10^8-8×10^8 particles/ml) of the instrument for accurate results (Dragovic et al., 2011). The exported results were adjusted to take into account the dilution of the sample. Background PBS readings were also performed prior to analysis to identify any contaminating particulate matter that might be mistaken as vesicles. Five technical replicates in the form of five 30 second videos were recorded for each biological replicate and the analysis performed with the NanoSight v2.3 software (NanoSight, Malvern Instruments). Excel spreadsheets of combined results and all other files produced were stored on an external hard drive and Student's t-tests performed on the data.

4.3. Results

4.3.1. Bystander response in non-irradiated cells following media transfer from directly irradiated cells

In order to establish the effects of 2 Gy X-ray irradiation on MCF7 cells, directly irradiated cells were assayed for DNA damage using the alkaline comet assay. Results showed that direct irradiation with 2 Gy X-rays had the ability to induce statistically significant DNA damage (Figure 4.1A). BE is traditionally studied using a media transfer model, with direct transfer of media using flasks, or via trans-well systems (Butterworth et al., 2013). As previously described, media transfer from directly irradiated MCF7 cells causes bystander response in recipient cells (Al-Mayah et al., 2015; Al-Mayah et al., 2012). Media from irradiated cells induced statistically significantly higher levels of DNA damage than media transferred from unirradiated control cells (Figure 4.1A). These results demonstrate that the bystander effect is mediated by conditioned media taken from 2 Gy irradiated cells at four hours post-irradiation.

4.3.2. Extracellular vesicle transfer and the bystander effect

It has been demonstrated that it is the EV fraction of the media from irradiated cells that has the ability to mediate bystander effect (Al-Mayah et al., 2012; Jella et al., 2014). In order to discern the fraction of the media responsible for mediating the bystander effect, MCF7 cells were irradiated with 2 Gy X-rays, the media was harvested and separated into an extracellular vesicle fraction and a supernatant fraction by ultracentrifugation. The EV fraction of the media taken from the irradiated media was able to significantly induce DNA damage in recipient cells compared to unirradiated control cells, however the supernatant fraction was not (Figure 4.1B). Overall, this confirmed that the factor responsible for mediating bystander effect can be found in the extracellular vesicle fraction of the cell media.

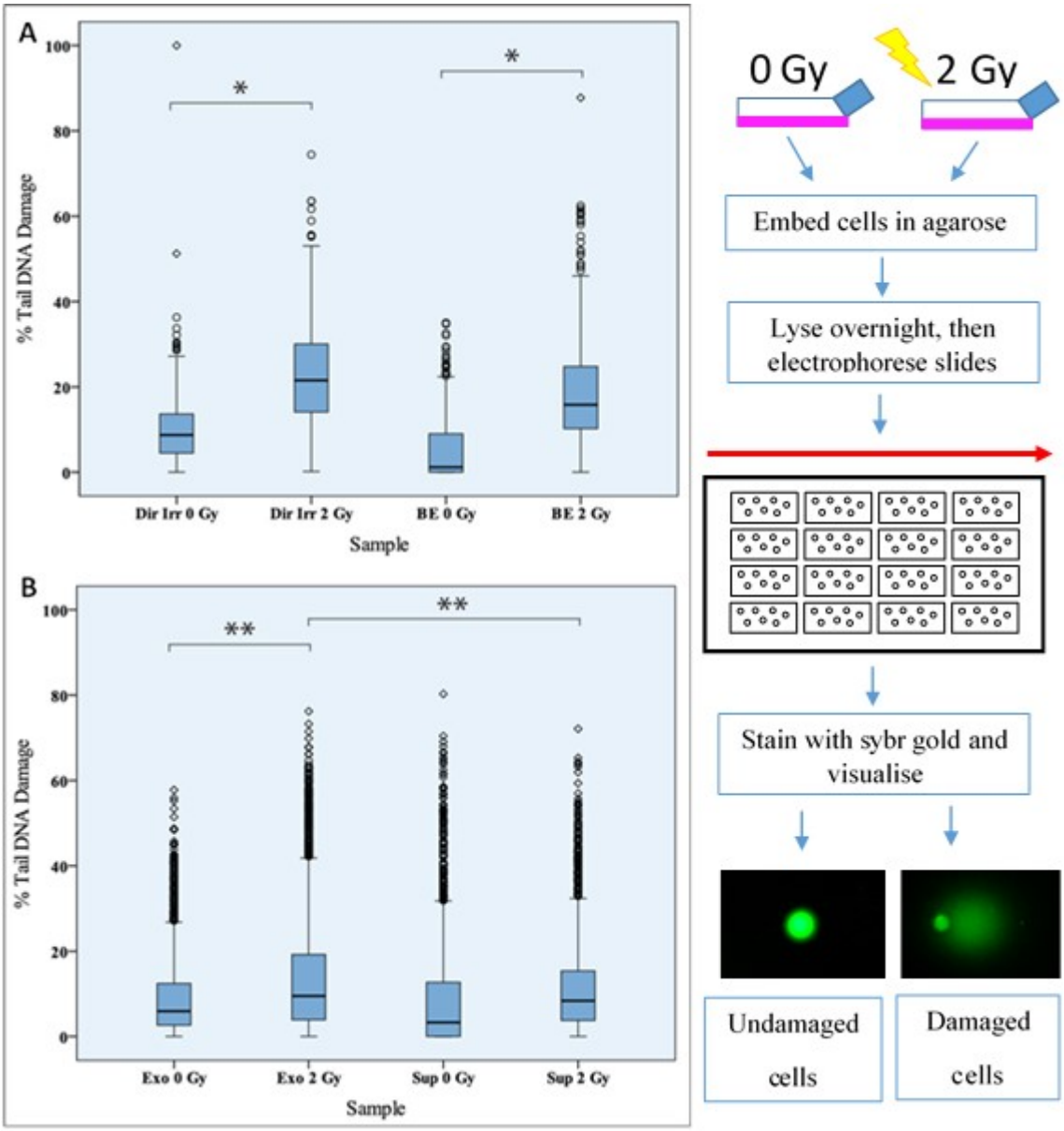

Figure 4.1. Irradiated cell media and EVs mediate bystander effect. A: *DNA damage is induced in 2 Gy directly irradiated cells and media transfer from irradiated cells causes a significant induction in DNA damage in bystander recipients compared to control media. Two biological replicates, n = 400.* **B:** *EVs taken from 2 Gy irradiated cells significantly increase DNA damage in MCF7 cells compared to EVs from 0 Gy cells. Supernatant from irradiated cells does not induce DNA damage in bystander cells (p = 0.44). Supernatant from 2 Gy irradiated cells induced significantly less DNA damage than 2 Gy EVs. Three biological replicates, n = 400. Dir Irr = directly irradiated. BE = Bystander Effect. Exo = exosome/EV. Sup = supernatant. Mann-Whitney test, *p < 0.05, **p<0.01. Circles represent 'outliers' more than 1.5 box lengths from a hinge of the plot and diamonds represent 'extreme values' that are more than three box lengths out.*

4.3.3. Effects of RNase on levels of MCF7 EV RNA

To establish how RNase A treatment affects the RNA content of EVs, RNase treatment of MCF7 EVs was performed and the RNA contents measured using the Agilent 2100 Bioanalyzer. Results showed that when non-lysed EVs were treated with RNase there was a drop in EV RNA concentration of 27% compared to complete RNA isolation from MCF7 EVs with no RNase treatment (Figure 4.2). When the RNA was extracted from EVs and then RNase treated, there was a drop in the EV RNA concentration of 41% compared to the control. Taken together, these results suggest that some RNA is found associated on the outside of the extracellular vesicle, but also that a portion of RNA is protected internally.

4.3.4. RNase treatment of irradiated cell EVs abrogates the bystander effect

In order to confirm that an RNA molecule is involved in the bystander effect, control and irradiated cell EVs were treated with RNase prior to transfer to recipient cells. Results showed that RNase treatment of 2 Gy EVs abrogated their ability to mediate bystander effect as previously observed (Al-Mayah et al., 2012) (Figure 4.3).

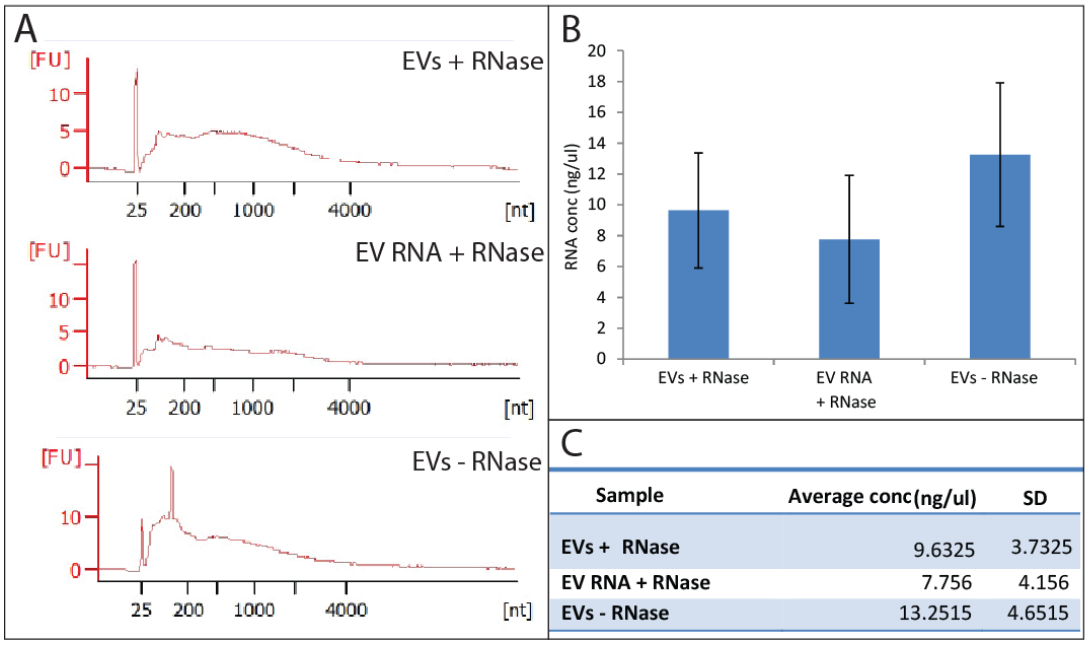

Figure 4.2. RNase treatment of EVs affects EV RNA contents. A: *RNase treatment of intact EVs (EVs + RNase) or RNA extracted from EVs (EV RNA + RNase) causes degradation of the RNA compared to the control (EVs – RNase).* **B:** *RNase treatment of EVs and EV RNA results in a drop in the concentration of RNA compared to control EV RNA.* **C:** *The concentrations of EV RNA samples treated with RNase. Two biological replicates. All RNA quantified using the Agilent 2100 Bioanalyzer Pico kit. Normal FCS used to supplement media. Error bars = SEM.*

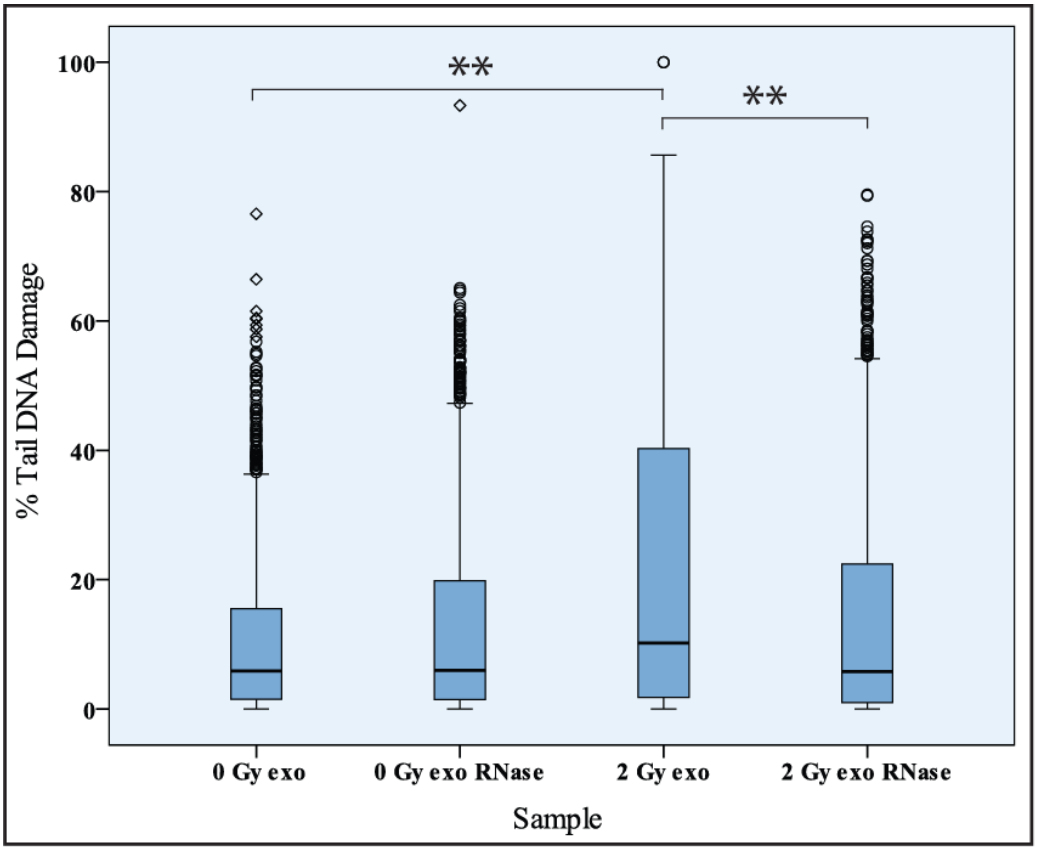

Figure 4.3. RNase treatment abrogates EV mediated DNA damage. *RNase treatment of 2 Gy EVs resulted in a significant decrease in their ability to cause DNA damage in MCF7 bystander cells. Four biological replicates, n = 400. Mann-Whitney test, ** $p < 0.01$. Circles represent 'outliers' that are more than 1.5 box lengths from a hinge of the plot and diamonds represent 'extreme values' that are more than three box lengths out.*

4.4. Characterisation of EVs

4.4.1. Cleared media and extracellular vesicle extractions

Cell media contains bovine EVs from the FCS that is used to supplement it, therefore in order to establish their levels in the media used in these experiments nanoparticle tracking analysis (NTA) was used to quantify the number of particles in the media supplemented with various types of FCS. These included normal FCS used to supplement cell media, in-house single- or double- cleared FCS and cleared FCS purchased from Systems Biosciences. Results showed that both the single and double cleared FCS types contained reduced numbers of particles compared to normal, unprocessed FCS. The SBI FCS contained the fewest particles (Figure 4.4). As the results only demonstrated a small decrease in particle content in double cleared FCS or SBI FCS compared to single cleared FCS, the single cleared FCS was used in future experiments as it required the least resources to produce and most closely reflected protocols suggested in the literature (Shelke et al., 2014).

4.5. Characterisation of radiation-induced EVs

4.5.1. Transmission electron microscopy (TEM) of radiation EVs

Owing to the small size of EVs, electron microscopy in combination with negative staining is used to visualise EVs in a sample. With the aim of confirming EV presence and size following 2 Gy X-ray exposure of cells, electron microscopy of radiation EVs and control EVs was performed (Figure 4.5). The results showed that the EVs from both 0 Gy and 2 Gy treated cells were within the expected size range of approximately 20-120 nm in diameter and appeared visually similar. Some cup-shaped vesicles were also present, likely to be artefacts from the fixation process. Overall the EVs in the images were as expected as per the literature (Raposo et al., 1996).

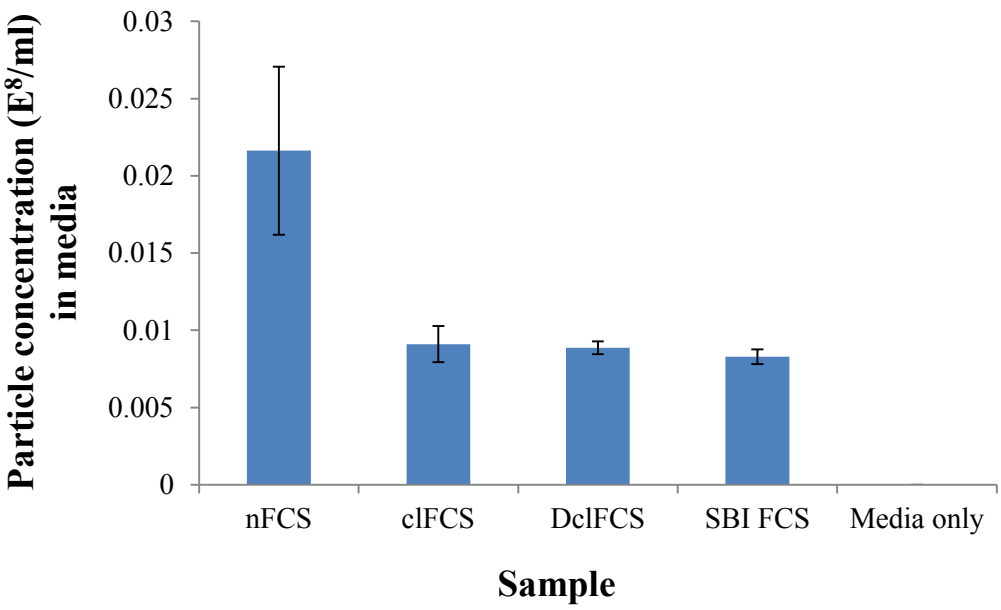

Figure 4.4. The concentration of particles differs between different types of FCS. *Concentrations reported as though supplemented in media* ***(percentage used to supplement media)****; nFCS = normal FCS* ***(10%)****, clFCS = cleared FCS* ***(5%)****, DclFCS = double-cleared FCS* ***(5%)****, SBI FCS = cleared FCS from SBI* ***(5%)****, media only = basal DMEM Hams-F12 media not supplemented with FCS. Error bars = SD. Two to three biological replicates for each sample.*

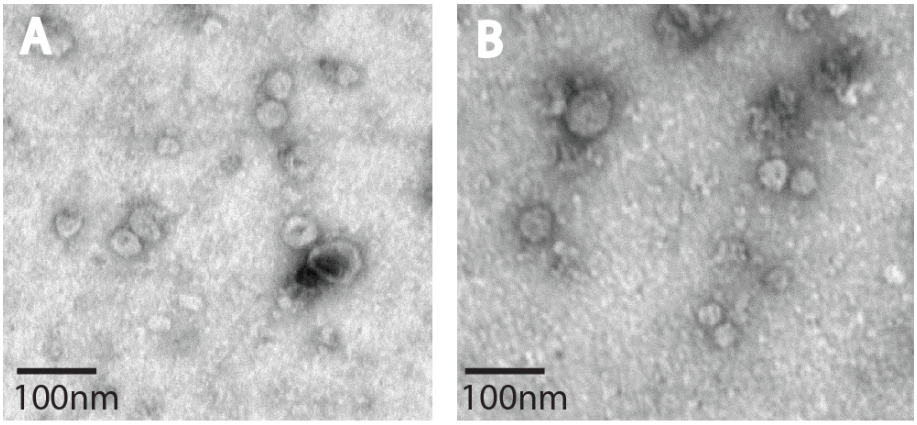

Figure 4.5. EVs from 0 Gy and 2 Gy irradiated MCF7 cells. *Both 0 Gy and 2 Gy irradiated MCF7 cells release EVs that appear as described in the literature (Raposo et al., 1996).* **A:** *0 Gy EVs.* **B:** *2 Gy EVs. Magnification 15000 x, 100 kV.*

4.5.2. Sucrose density gradient centrifugation of radiation EVs

To establish the buoyant density of the EVs released from MCF7 cells and thus that the ultracentrifugation extraction method used in this study was suitable for extracting EVs sucrose density gradient centrifugation was performed. After spinning overnight through a step-wise sucrose gradient individual fractions were manually taken from the tube, corresponding to the volume of the original fractions layered on top of each other. Consequently the densities reported in figure 4.6 are estimated, not accurately measured. Results demonstrated that the density of the most heavily populated fraction of sucrose (fraction 3) recovered following centrifugation was approximately 1.11-1.13 g/ml (Figure 4.6A). Furthermore, the extracellular vesicle size per sucrose gradient fraction and number of EVs found in each fraction were counted. The number of particles per frame also suggested a peak in fraction three (~1.1 g/ml). Overall these results suggest that as the size of the EVs increased the density of the EVs also increased as expected (Figure 4.6B) and furthermore that the preparations contain vesicles with the characteristics of EVs and not larger vesicles or apoptotic bodies.

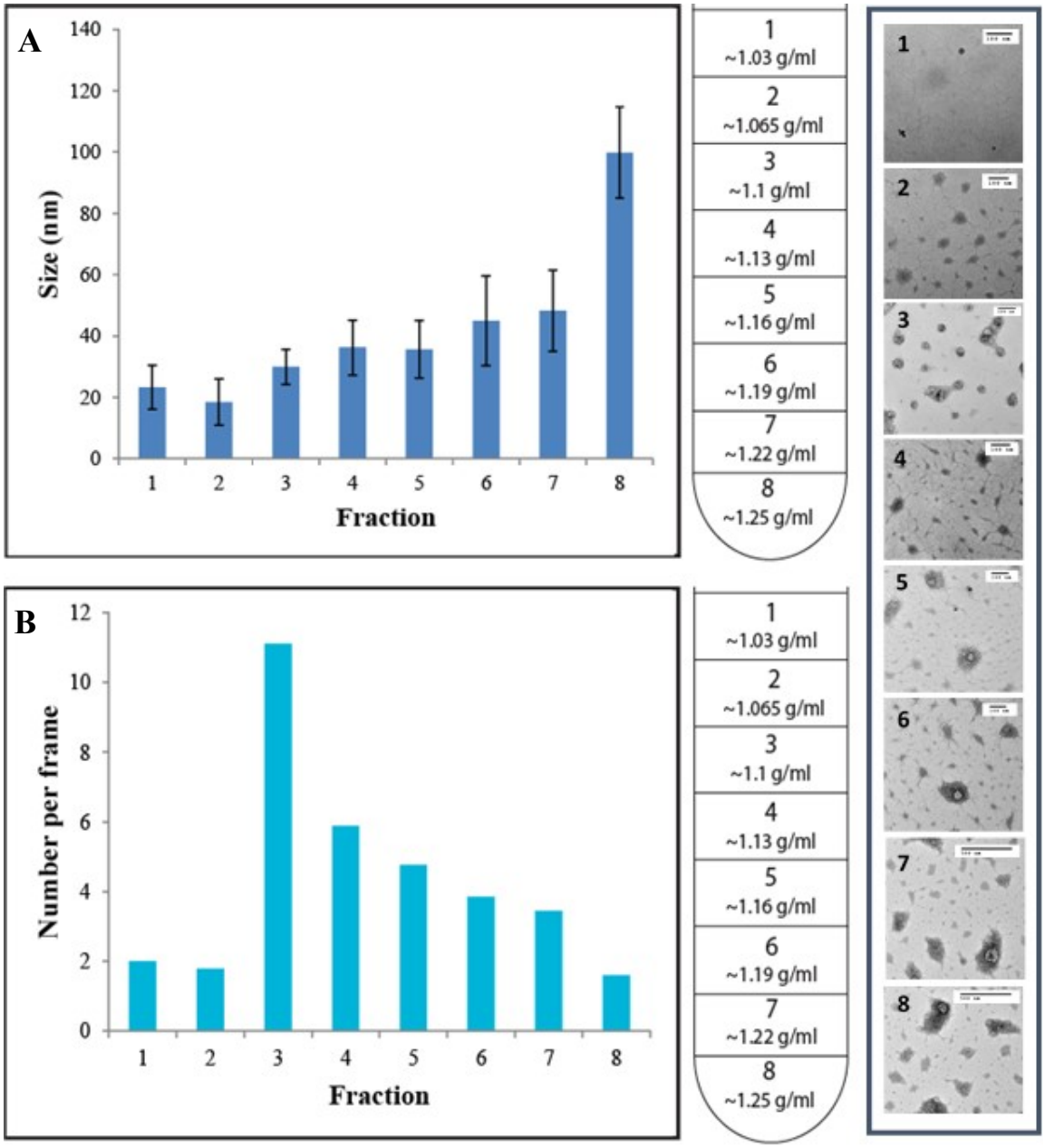

Figure 4.6. Sucrose gradient centrifugation of normal MCF7 EVs. A: *As the sucrose fraction density increased, the size of the EVs increased. Two biological replicates, n = 100.* **B**: *Upon manually counting the number of particles per frame using the electron microscope, fraction three contained the most EVs. Single replicate. Example TEM images of each fraction included in right hand panel. Magnification 15000 x, 100 kV.*

4.6. Novel characteristics of radiation EVs

4.6.1. Irradiated cells release higher levels of EVs than unirradiated cells

To better understand the release of EVs from irradiated MCF7 cells, cells were irradiated with 2 Gy X-rays and the EVs extracted from the cell media at eight hours post irradiation. Samples were analysed using the NanoSight NS500 to quantify the EVs in each preparation (Figure 4.7). Results demonstrated that the 2 Gy extracellular vesicle samples showed a marked, but not significant, increase in extracellular vesicle release. EVs from 0 Gy irradiated cells released on average 0.037 x 10^8 particles/ml MCF7 conditioned media, with EVs from 2 Gy irradiated cells released over two-fold the concentrations of the 2 Gy EVs, averaging at 0.082 x 10^8 particles/ml MCF7 conditioned media. Overall, this demonstrates an increase in extracellular vesicle release from irradiated cells, as seen in the literature (Jella et al., 2014; Al-Mayah et al., 2012).

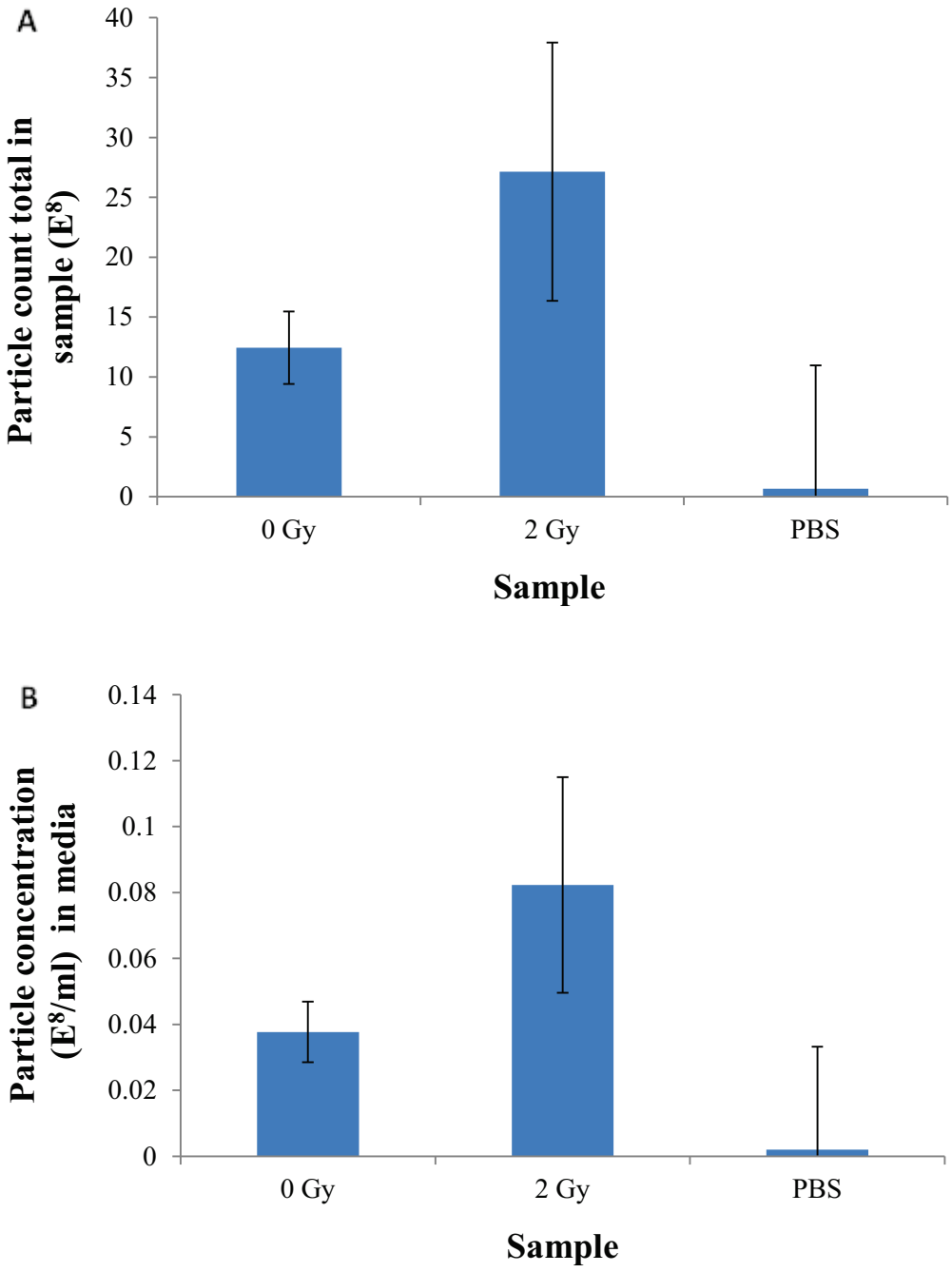

Figure 4.7. EV release increases in MCF7 cells irradiated at 2 Gy X-ray as measured using NTA. *Extracellular vesicle release following 0 Gy or 2 Gy irradiation.* **A***: Total particle number in EV preparations. Three biological replicates, error bars SEM (p = 0.4)* **B***: EV concentration per original sample media. Three biological replicates, error bars SEM (p = 0.4).*

4.6.2. Irradiated MCF7 cells may release smaller EVs than unirradiated MCF7 cells

In order to establish the size of typical MCF7 derived radiation EVs, NTA sizing was performed and electron microscopy images of 0 Gy and 2 Gy cell EVs were analysed. According to the NTA analysis there was no significant difference in EV size between 0 Gy and 2 Gy samples (Figure 4.8A). Contrarily, according to the TEM analysis the size profiles of the EVs released from 0 Gy cells versus 2 Gy irradiated cells were different. Across three biological replicates it became apparent that the EVs released from cells treated with 2 Gy X-rays were significantly smaller than 0 Gy cell EVs (Figure 4.8B) (t test, $p < 0.01$). The EVs released from 2 Gy irradiated cells were on average 22.5% smaller than the EVs taken from 0 Gy irradiated cells. Both types of EVs showed a peak at around 30-40 nm but 2 Gy EVs were more than twice as abundant at the 40 nm size (Figure 4.9). It is possible that the smaller size of the 2 Gy EVs reported by TEM may be due to changes in the adherent properties of the two different EV samples to the TEM grids, resulting in more of the smaller vesicles adhering to the grids and not being lost during washing steps. Overall the increase in extracellular vesicle concentration and potential decrease in extracellular vesicle size following 2 Gy X-irradiation of MCF7 cells reflect novel characteristics of EVs released from irradiated cells, however further work will aim to characterise EVs released from different cell lines and under different conditions of irradiation.

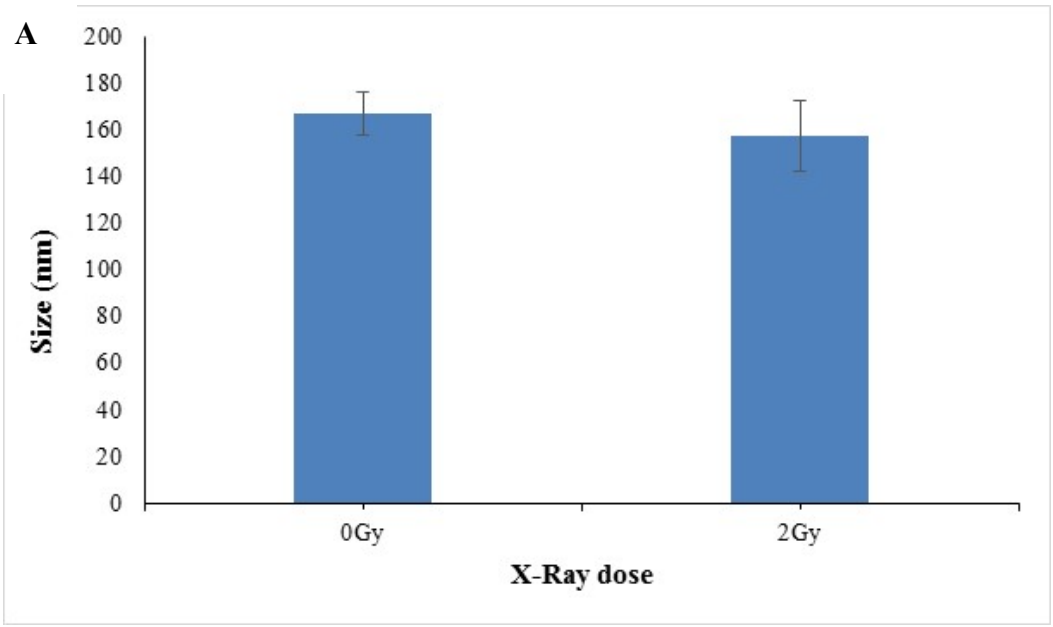

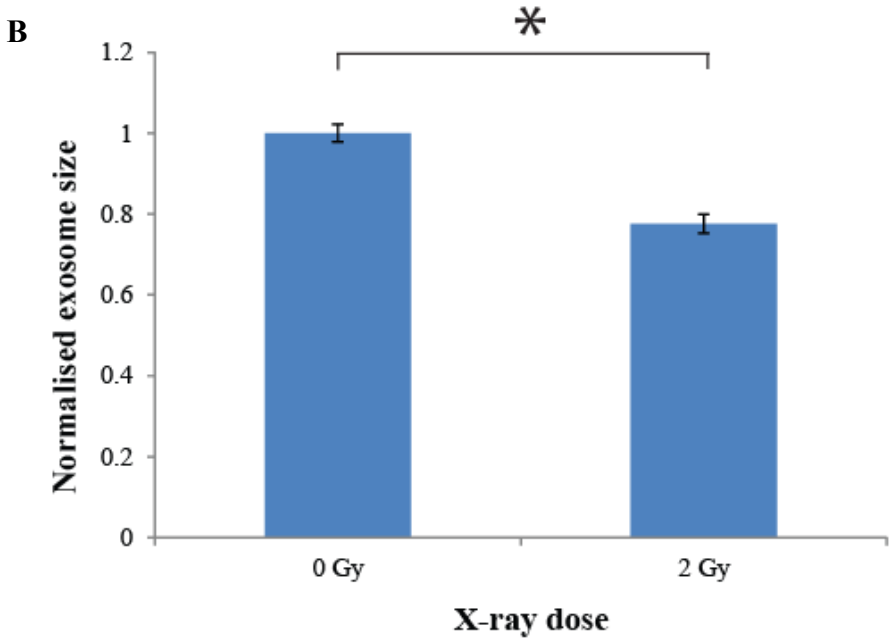

Figure 4.8. EV sizes from 0 Gy versus 2 Gy irradiated cells. A: *EV size (nm) as reported by NTA. No significant change in size was reported.* B: *Normalised EV size was measured by measuring individual EV size (nm) on TEM images. The size of 2 Gy EVs was 22.5% lower (t test, $p < 0.01$) than EVs from 0 Gy cells. Three biological replicates, n = 100. Error bars SD.*

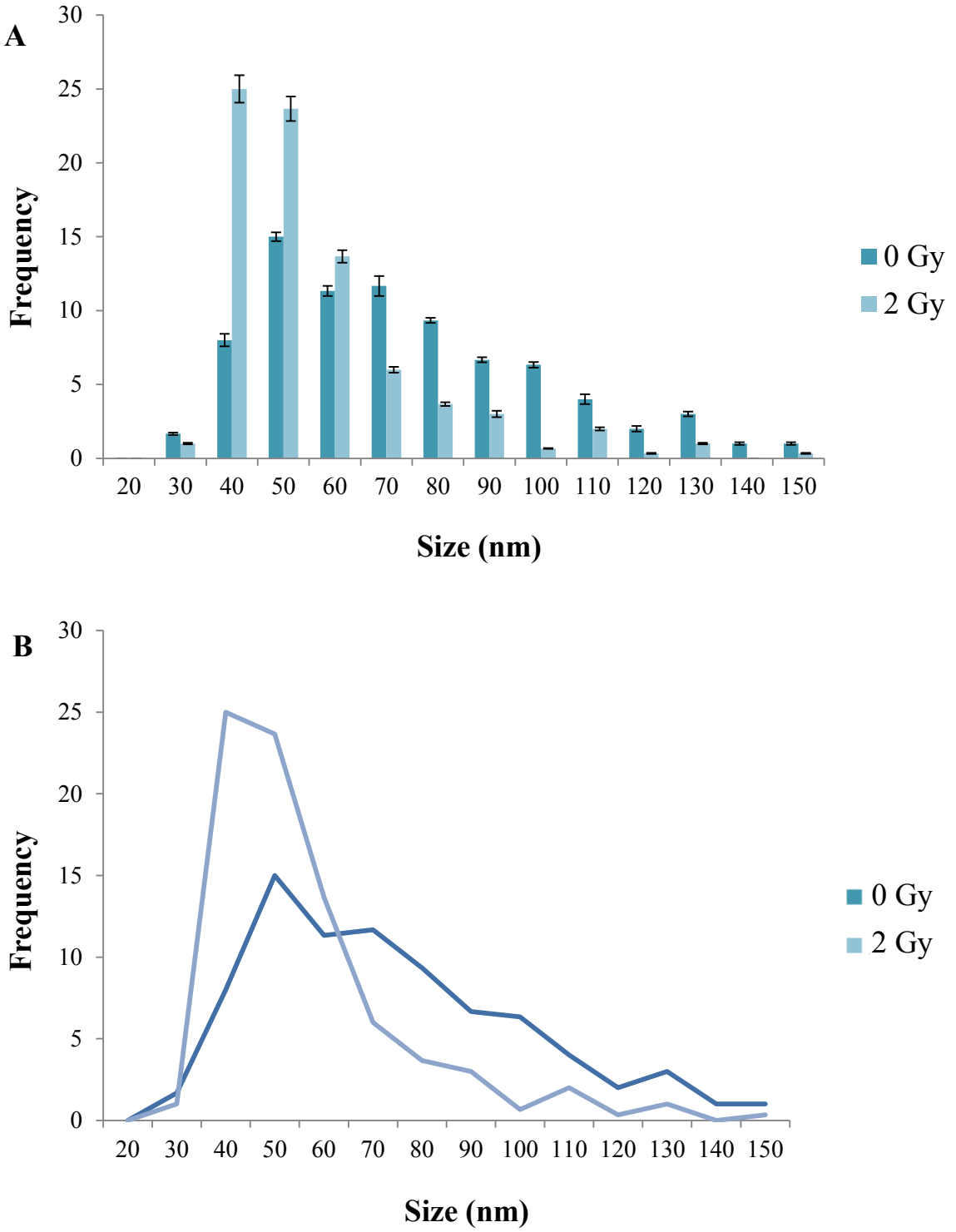

Figure 4.9. Irradiated cell EVs show a different size distribution to unirradiated cell EVs. A*: Bar chart showing 0 Gy vs 2 Gy EV size distribution. Three biological replicates, n = 75-100. Error bars SEM.* **B***: Line graph representation of data in (A) reveals a peak for 2 Gy EVs and a shallower distribution for 0 Gy EVs.*

4.6.3. An increased dose of unirradiated MCF7 EVs does not increase DNA damage in recipient cells

It is possible that BE is observed due to an increase in EV release to surrounding cells. To discount this idea, an increasing amount of EVs from unirradiated MCF7 cells were applied to fresh recipients. Results demonstrated that up to a four-fold increase in the amount of EVs applied did not induce DNA damage in recipient cells (Figure 4.10), therefore suggesting that DNA damage response following exposure to EVs is not purely quantitative and that a qualitative change is also required.

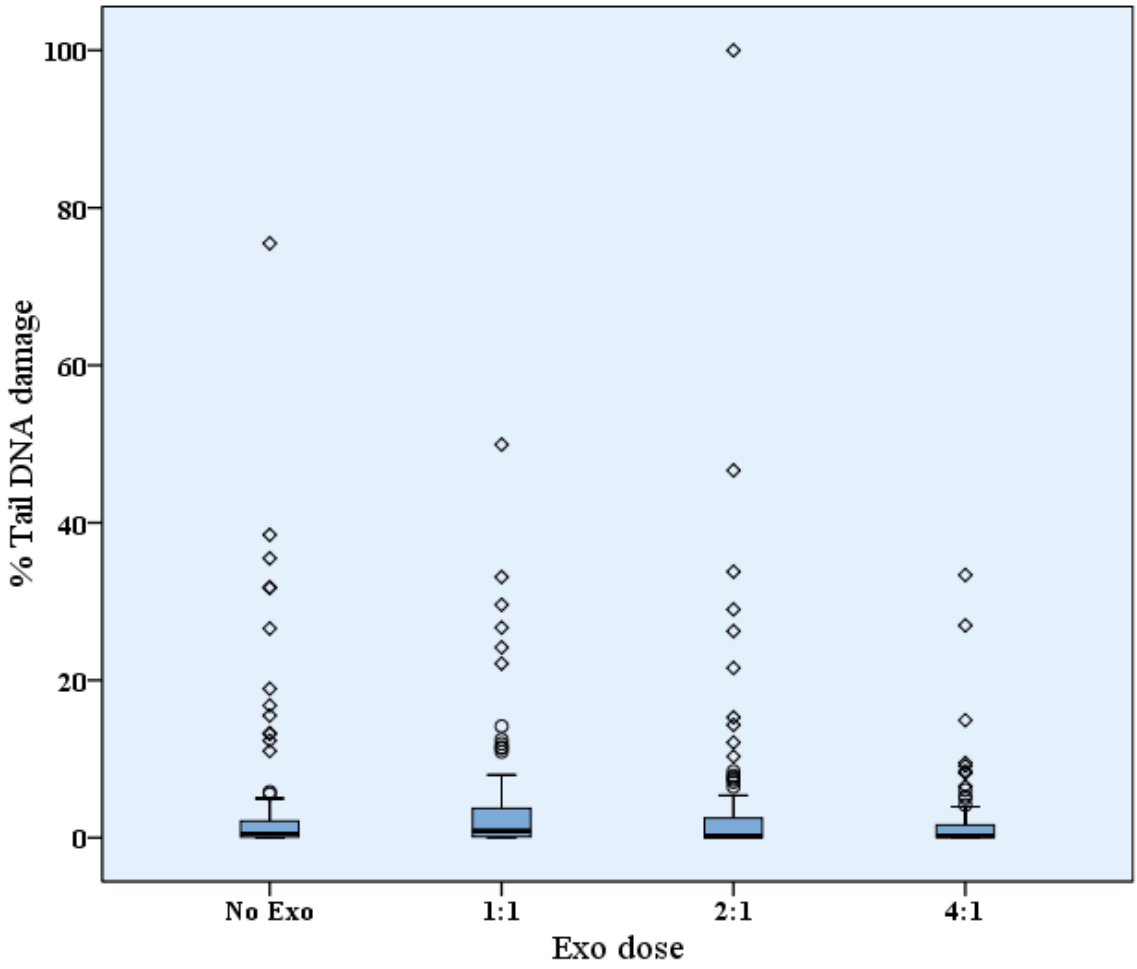

Figure 4.10. **Increasing EV dose does not induce DNA damage in recipient cells.** *Addition of increasing proportions of EVs from normal MCF7 cells does not induce significant DNA damage in recipient MCF7 cells. Two biological replicates, n = 100. Circles represent outliers, diamonds represent extreme outliers.*

4.7. Discussion

Characterisation of EVs released from cells under different conditions is important in developing a better understanding of their biological effects. The results in this chapter suggest that radiation EVs released from MCF7 breast cancer cells in response to 2 Gy X-rays are able to mediate bystander effect and have some different properties to those released from unirradiated cells.

4.7.1. The Bystander Effect and EVs

Since the beginning of this project, other studies have emerged documenting the role of EVs and RNA in radiation response. It has been established that EVs are released in higher concentrations in response to radiation (Jella et al., 2014; Al-Mayah et al., 2015) and also that EVs derived from irradiated cells harbour specific mRNA contents (Arscott et al., 2013). The timing of extracellular vesicle extraction from the media of irradiated cells may also play an important role in the RNA content of these EVs. It is known that following irradiation, the DNA damage response is able to start rapidly repairing some single strand DNA lesions and EVs have been shown to be released as soon as 20 minutes post stress (Koumangoye et al., 2011). Consequently EVs may play a role in the response to radiation assault in cells and their contents may reflect this response at particular timings post irradiation.

The extracellular vesicle fraction of the cell media has been shown in this chapter to carry the signal responsible for the bystander effect. It is therefore possible that some of the more classic bystander effect mediator candidates such as cytokines and ROS are released from cells in association with EVs, as has been demonstrated in HIV-1 infection where cytokines are shuttled between cells within vesicles (Konadu et al., 2014). In turn, RNase treatments as a method of depleting RNA found in EV preparations have been demonstrated in this chapter to abrogate bystander effect. RNase treatments were previously shown to have the same effect (Al-Mayah et al., 2012; Al-Mayah et al., 2015), however in what manner RNase affects EV RNA has yet to be fully determined. It would be expected that RNase treatment of an extracellular vesicle without any other direct lysis of the microvesicles would only act to remove RNA from the outside of the vesicle, as found in previous studies (Cheng et al., 2014). In this chapter it has been shown that RNase treatment of EVs does not completely deplete RNA, whether RNase treatment of whole EVs or extracted EV RNA is assayed. This may be due to the fact that proteinase treatment has not been used in association with the RNase treatment (Hill et al., 2013; Al-Mayah et al., 2015). Consequently, bystander effect could be mediated by both an RNA molecule and any combination of the more classic bystander candidates, or alternatively the bystander effector may be different under different conditions of radiation or when released from different cell types.

The concept that bystander effect may be mediated by RNA is supported by the fact that evidence exists demonstrating RNA deregulation in cells in response to irradiation (Chaudhry et al., 2013) and also in bystander cells (Chaudhry & Omaruddin, 2012). Furthermore, long non-coding RNAs

and snoRNAs are believed to be changed in cells in response to radiation (Chaudhry, 2013), suggesting a complex biological response involving various levels of regulation by RNAs and also other levels of genetic regulation for example epigenetic regulation (Ilnytskyy et al., 2009).

4.7.2. Bovine EVs and extracellular vesicle extractions

It is important to ensure that the purity of a given population of vesicles is measurable in any given experiment to establish, for example, contaminating protein content (Webber & Clayton, 2013). This is particularly key in the case of profiling EVs as there is often already limited biological material available to study, hence contaminants need to be avoided. One such contaminant in EV preparations can be bovine EVs from the growth serum that supplements the media and from which EVs are extracted. Bovine serum may contaminate extracellular vesicle samples by introducing bovine proteins or RNAs that might interfere with proteomics studies or sequencing experiments. Furthermore, when quantifying EVs by BCA assay or NTA, bovine EVs may constitute a portion of the extracellular vesicle sample, therefore leading to an overestimation of actual desired EV protein or concentration of a sample. Fluorescent labels may also be used in conjunction with the NanoSight to ensure that only EVs of interest are studied, however the production of fluorescent EVs adds to an extraction and quantification process already hindered by the small size and often limited concentration of EVs. It is possible to omit bovine EVs completely by growing cells with media not supplemented with serum for 48 hours prior to extraction; however this may lead to some serum starvation effects and therefore results in unwanted biological changes during the course of an experiment (Fader et al., 2008). This is shown to not be the case for some particular cell lines, however a less disruptive option is to supplement the media that the cells are grown in with a bovine-extracellular vesicle depleted FCS directly prior to experimentation (Eitan et al., 2015) that has been shown to contain reduced bovine EVs with some decrease in cell growth but not additional DNA damage.

4.7.3. Extracellular vesicles released in response to radiation are characteristic

Extracellular vesicle release has previously been shown to increase following ionizing radiation treatment to cancer cells (Jella et al., 2014), where increasing doses of γ-rays resulted in increases in extracellular vesicle concentration. Indeed, extracellular vesicle release has also been shown to be increased following other stressors including heat stress (Clayton et al., 2005) and exposure to anticancer drugs (Lv et al., 2012), consistent with an active role of EVs in intercellular communication following stress. Hypoxia has also been shown to increase extracellular vesicle release (Salomon et al., 2013; King et al., 2012) and EVs released from cells subjected to hypoxia have displayed distinct RNA and protein content (de Jong et al., 2012) with a slight reduction in the size of the vesicles, albeit not a significant reduction. This again supports that the stress response may be qualitative and not necessarily quantitative.

In this chapter it has also been shown for the first time that EVs released from 2 Gy cells were significantly smaller than EVs released from unirradiated cells. Other qualities characteristic of EVs were also reported, including TEM analysis and sucrose gradient centrifugation. It is possible that this might be due to a rapid *de novo* formation of the extracellular vesicle in response to stress, or that specific stress EVs are sequestered in the cell ready to be released in response to stressful stimuli. Methods of extracellular vesicle characterisation are constantly developing, with the development of nanoscale technologies, in particular, being the driving force of extracellular vesicle quantification and sizing. The original method of EV quantification, measurements of 'μg protein', may not reflect actual EV protein in the ultracentrifugation approach to extracellular vesicle extraction (Sverdlov, 2012). It is postulated that some small molecules and lipoproteins of a similar density to EVs are spun down along with the EVs in a sample during centrifugation. The question of EV quantification is complicated by the nanoscale nature of EVs. The two traditional methods of EV quantification include measurements of 'total μg protein' as measured by the BCA assay or by nanoparticle tracking analysis. Use of the NanoSight to perform this method simultaneously allows quantification and vesicle sizing using principles of light scatter and Brownian motion (Gercel-Taylor et al., 2012).

In this chapter nanoparticle tracking analysis of EVs released from irradiated cells demonstrated an increase in extracellular vesicle release following irradiation, potentially reflecting an increase in signalling to surrounding cells and propagation of the bystander effect. It would be interesting to study the origin of such EVs and to test if they are synthesised *de novo* or are alternatively stored in the cell ready to be released in response to stress. Alternatively a study has suggested that measuring extracellular vesicle release following irradiation using the qNano instrument from Izon supported the data in this chapter that extracellular vesicle release is increased in MCF7 cells following irradiation (Al-Mayah et al., 2015). However the study also suggested that the size of EVs was not significantly changed in response to 2 Gy irradiation, with 0 Gy EVs reported at 82.6 nm and 2 Gy EVs at 86.5 nm. This is potentially due to the different methods of size measurement employed, however when measured using the NanoSight there was also no change in extracellular vesicle size reported for the samples used in this chapter (data not shown). Use of the NanoSight in itself does have its own limitations, for example particulate matter may be refractive particles that are not EVs but are misinterpreted as such. This may reflect limitations in the instruments as individual EVs here were sized from electron microscopy images which could be argued to be more accurate, conversely it could be argued that the fixation process of the EVs may contribute to the sizing differences. Despite this fact all samples were treated in the same way and the observation was documented across three biological replicates, therefore advances in sizing technology may help to elucidate sizing better in the future.

4.7.4. Dose-dependent increase in EVs does not induce DNA damage

In order to address the point that the effect of EVs upon recipient cells might be quantitative and simply due to the increase in EVs released, not their contents, an experiment was conducted whereby increasing proportions of EVs were placed onto normal MCF7 cells. Results demonstrated that there was no dose-dependent increase in DNA damage when more EVs were placed onto cells and therefore that the EVs released by cells do not mediate effects quantitatively, but qualitatively.

4.8. Conclusions

The results in this chapter demonstrate that EVs released from unirradiated MCF7 and X-ray irradiated MCF7 cells have some different characteristics. An increase in extracellular vesicle release in combination with a smaller size following irradiation suggests differential modulation and therefore potentially a functional role of them in radiation response. Furthermore the morphology and density of the EVs suggests that a smaller vesicle type is present in the ultra-centrifuged preparations. Here it was also confirmed that it is the extracellular vesicle fraction of the supernatant that conveys the bystander effect.

The exact content and mechanism of EVs involved radiation response and bystander effect have yet to be fully elucidated and the controversy regarding EV nomenclature will also shape how the exact populations of vesicles are termed and classified. The work in this chapter has helped to better understand the release of EVs from breast cancer cells treated with ionizing radiation. Further characterisation and molecular profiling of these EVs will also help to establish their role in radiation response and the bystander effect, ultimately leading to increased understanding of the general mechanisms and levels of regulation involved in the radiation response. The results in the next chapter aim to enrich this knowledge and provide an insight into the RNA content of the extracellular vesicle potentially responsible, at least in part, for the bystander effect.

Chapter 5

The RNA composition of MCF7 cells and their EVs following X-ray exposure

Chapter 5 The RNA composition of MCF7 cells and their EVs following X-ray exposure

5.1. Introduction

Extracellular vesicle biology has become an area of intense research interest in part due to the realisation that they carry functional RNAs, including mRNAs and microRNAs, able to exert phenotypic effects upon recipient cells (Ratajczak et al., 2006; Valadi et al., 2007). Furthermore, these small vesicles were shown to shuttle functional RNAs between a variety of cell types including glioblastoma cells and also in the blood (Skog et al., 2008; Hunter et al., 2008). The term exosomal shuttle RNA (esRNA) has consequently been employed to refer to functional RNA that is specifically transferred between cells via EVs (Lotvall & Valadi, 2007).

EVs are considered an ideal vehicle for RNA signalling between cells as they have the ability to protect their contents from the extracellular milieu (Keller et al., 2011; Klibi et al., 2015) and have been shown to contain a variety of RNA species including mRNAs and microRNAs (Valadi et al., 2007; Ratajczak et al., 2006). Following stress, the mRNA contents of EVs has been shown to change, with radiation leading to upregulation of mRNAs such as Il-6 and Il-11, shown to be involved in radiation response and also mRNAs involved in cell migration such as *IGFBP2* (Arscott et al., 2013). Other stress types including hypoxia and TNF-α stress have been shown to differentially modulate the mRNA levels of EVs (de Jong et al., 2012). Under conditions of hypoxia, three mRNAs were significantly deregulated as reported by microarray *NDRG1*, *CIRBP* and *BNIP3*. TNF-α stress led to more changes including the mRNAs for *IL-8* and *NFKB1* (de Jong et al., 2012), both of which are known to be implicated in radiation response of directly irradiated and bystander cells (Hei et al., 2008; Zhou et al., 2008). Furthermore another study demonstrated the mRNA contents of EVs was altered in response to oxidative stress (Eldh et al., 2010) where it was shown that pre-treating cells with these EVs led to a resistance to stress in recipient cells. However this function was diminished following UV exposure of the EVs that is known to prevent RNA function. Therefore the RNA contents appeared to be responsible for mediating the protective effect. This highlights the potentially important role of EVs in association with RNAs in the cellular stress response.

EVs have been shown to contain microRNA contents that partially reflect the cell of origin (Ekstrom et al., 2012) but it is also postulated that RNAs might be selectively loaded into EVs (Guduric-Fuchs et al., 2012; Crescitelli et al., 2013). The method by which microRNAs are selectively loaded has been suggested as via short microRNA motifs (Villarroya-Beltri et al., 2013). It has also been confirmed that the microRNAs reported in EVs are not simply loaded into the vesicles along with their target mRNA transcripts (Gibbings et al., 2009). MicroRNA processing machinery such as the RISC complex involved in the processing of EVs has not only been shown to be associated with the endosomal pathway and MVBs (Lee et al., 2009), but also

Dicer has been identified as contained in EVs and was able to process precursor microRNAs into functional mature RNAs *en route* to recipient cells (Melo et al., 2015).

As well as mRNAs and microRNAs, other non-coding RNA species have been shown to be present in EVs (Nolte-'t Hoen et al., 2012). Long non-coding RNAs found in EVs include *HOTAIR* (Gezer et al., 2014) and the non-coding RNAs *TUC339*, involved in tumour growth and adhesion, and *linc-ROR*, a non-coding RNA expressed in response to stress (Takahashi et al., 2014; Kogure et al., 2013). Studies have aimed to demonstrate that the RNA contents of EVs are functional, including approaches that use fluorescent reporters in cells to demonstrate that RNAs do indeed reach their targets and induce translation (Mittelbrunn et al., 2011; Montecalvo et al., 2012). It is also known that RNAs exist in circulation complexed with other biological molecules such as Ago2 and HDLs (Arroyo et al., 2011; Vickers et al., 2011; Turchinovich et al., 2011) and, as such, the mode of action of RNA associated with EVs is a pertinent question.

The emergence of next-generation sequencing as a more readily available and affordable technique has led to an increase in the number of EV RNA studies published in recent years (Bellingham et al., 2012; Miranda et al., 2014; Ogawa et al., 2013). Owing to relatively low RNA levels in EVs reported to date, RNA sequencing can offer a deeper insight into the different RNA species contained within them in comparison to traditional DNA methods such as microarray ('t Hoen et al., 2008). To this end guidelines have been produced by the International Society for Extracellular Vesicles (ISEV) suggesting best practice for EV RNA sample collection and analysis as more studies are published in this area (Hill et al., 2013; Witwer et al., 2013). This will allow for easier comparison and facilitate more reliable meta-analysis of such data.

Several studies have reported differential RNA modulation in cells in response to irradiation. In early irradiation studies, gene changes suggesting a role of the cytoskeleton in radiation response (Woloschak et al., 1990). Furthermore, mRNA changes have been observed in 3D tissue models (Mezentsev & Amundson, 2011), demonstrating that certain genes were present at higher levels following particular doses of radiation. The link between mRNA and microRNA deregulation has also been discussed, with a negative correlation between mRNA and microRNA expression following irradiation of the rat lung (Xie et al., 2014). MicroRNAs have been shown to be deregulated using both microarray and next generation sequencing approaches (Chaudhry & Omaruddin, 2012; Chaudhry et al., 2013; Dickey et al., 2011). As well as traditional RNA species, small non-coding RNA species were also found to be differentially regulated in both directly irradiated and bystander cells (Chaudhry, 2014).

Limited literature exists to date to document the roles of RNA in EVs released from irradiated cells. Since the beginning of this project, it has been demonstrated that EVs released from irradiated U87MG cells contain different RNA contents to those released from unirradiated cells (Arscott et al., 2013). To this end, the aim of this chapter is to characterise the RNA contents of

EVs released from irradiated MCF7 breast cancer cells in an effort to better understand the role of EV RNA in radiation-induced bystander effect.

5.2. Materials and methods

5.2.1. Sample processing and library preparation of RNA Seq and miRNA Seq samples

RNA samples were extracted as per section 2.6.1 and libraries prepared and multiplexed as per Figure 5.1 by Liverpool Centre for Genomic Research.

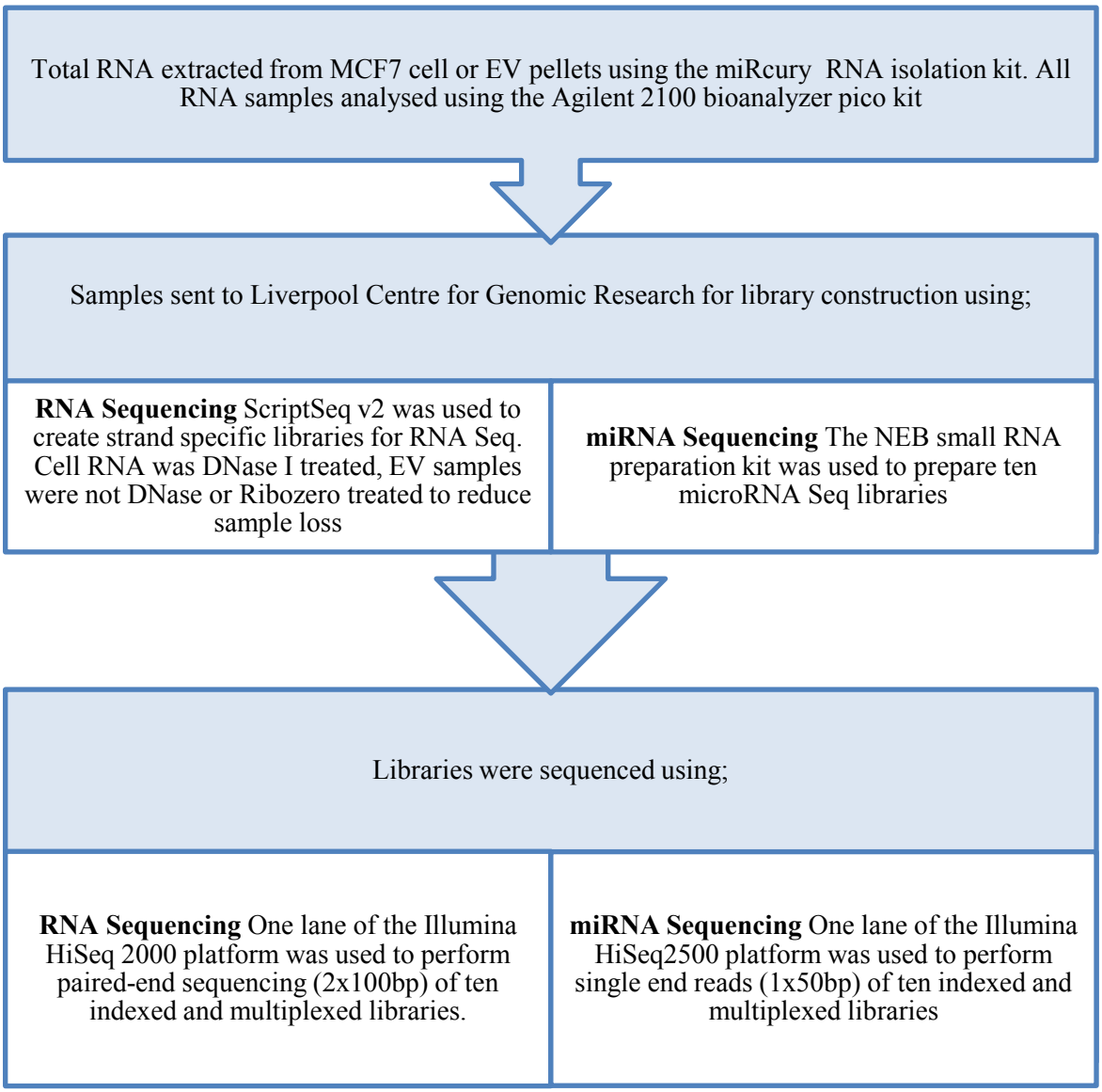

Figure 5.1. Workflow detailing RNA extraction, individual sample library preparation and platforms used to perform RNA sequencing. *RNA samples were extracted from MCF7 cells or EVs and separate libraries prepared for either RNA Seq or miRNA Seq. Libraries were then sequenced as detailed.*

5.2.2. RNA Sequencing analysis

5.2.3. Galaxy Project

RNA Sequencing analysis was performed using the online usegalaxy.org instance of the Galaxy Project that contains a suite of tools used for RNA Seq analysis in a user friendly web interface (Giardine et al., 2005; Blankenberg et al., 2010; Goecks et al., 2010). A protocol was adapted for use with the Tuxedo suite of tools (Trapnell et al., 2012) in Galaxy to establish differentially expressed (DE) genes. Raw FASTQ files from Liverpool Genomic Centre were uploaded via FTP server to the usegalaxy.org instance and workflows performed as documented in this chapter. The names of the programs used within the Galaxy interface and the R environment are highlighted in **bold** for clarity.

5.2.4. Alignment to the genome

Forward and reverse FASTQ files for each sample library were aligned to the hg19 version of the human genome using **Tophat for Illumina** and the FR-SECONDSTRAND option due to the library preparation method used. The resultant BAM files for each sample were checked for percentage alignment to the genome using **flagstat** in Galaxy.

The **Cufflinks** program was then used to assemble transcripts in the individual BAM files and annotated them using the **hg19 iGenome** downloaded from **Data Library** in Galaxy. **Cuffmerge** was then run for all 'assembled transcript' files from **Cufflinks** to create a single merged annotation file for all samples.

5.2.5. Differential gene expression analysis using Cuffdiff

The **Cuffdiff** program, part of the Tuxedo package (Trapnell et al., 2012), was used to generate differential gene analysis directly from the files produced in the Galaxy environment by taking the **Cuffmerge** dataset created above and all of the individual **Tophat for Illumina** 'accepted_hit' files for each sample and entering them into the program as per the groups of samples and replicates (Figure 5.2). The outputs for the differential gene expression analysis and also isoform analysis were exported into Excel for further processing.

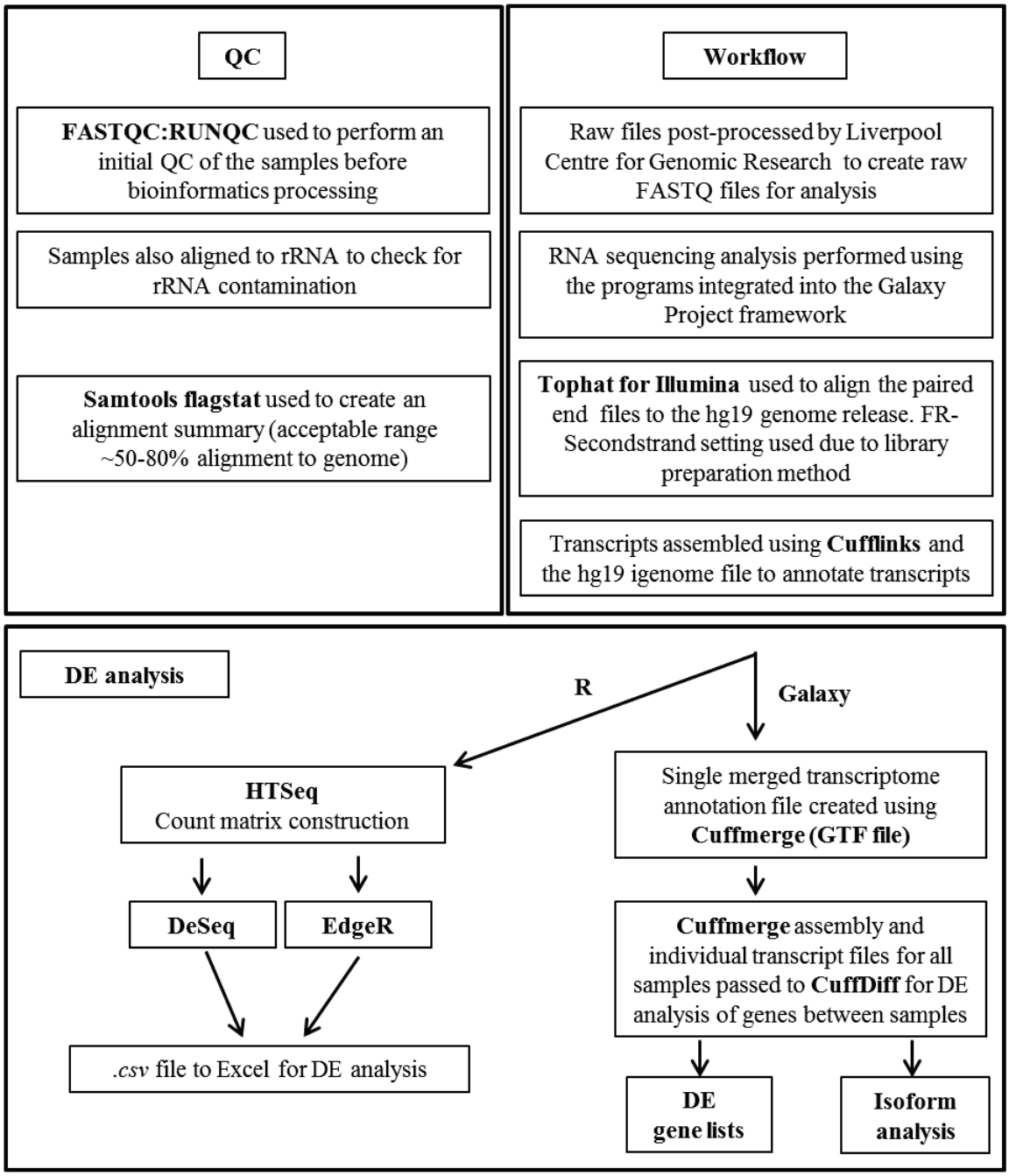

Figure 5.2. Differential gene analysis workflow for RNA Seq samples. *The FASTQ files were passed into Galaxy to produce BAM files that were then further processed to establish DE genes in Galaxy or passed to the R packages* ***DEseq*** *or* ***EdgeR*** *for DE analysis using alternative algorithms.*

5.2.6. Differential gene expression using the R environment

R v3.0.1 was used to perform DE analysis using the BAM files from the **Tophat for Illumina** alignment in Galaxy.

5.2.7. CummerBund in R

The **CummerBund** package for R was used to take the resultant files from the **Cuffdiff** output in Galaxy to visualise the data in scatterplots and was downloaded from the Bioconductor website (http://bioconductor.org/packages/release/bioc/html/cummeRbund).

5.2.8. Count matrix construction using HTSeq-count

Count matrices were constructed for the datasets to be used for differential expression analysis in the R environment. The HTSeq Python Package was installed from (http://www-huber.embl.de/HTSeq/doc/install.html#install) via the Python Package Index (PyPI) onto a Linux machine running Biomint Debian 64-bit.

BAM files were saved onto the Linux machine via FTP client and **SAMtools** (Li et al., 2009) was used to sort the BAM files by gene name using the command (samtools sort –n (file name)). The **HTseq-count** feature was then run on the command line and the resultant .txt files saved to a new directory using the command (htseq-count –f bam –r pos –s yes RR10E_SORTED.bam hg19.gtf > /SORTED/RR10E.txt). The hg19 file was held in the same directory as the sorted BAM files. Individual *.txt* files were then arranged into a count table in Excel with the first column as the gene ID and the following columns for each of the samples. The count table was then saved as a *.csv* file for reading into the R environment and used for differential expression using the **DESeq** or a .txt file for the **EdgeR** Bioconductor packages.

5.2.9. DeSeq

The **DESeq** R package, v1.12.1 (Anders & Huber, 2010), was downloaded from the Bioconductor website (http://bioconductor.org/packages). The **DESeq** library was opened at the beginning of each programming session and the relevant count matrix was read into the R environment and genes with low cumulative read count of 10 were filtered out. Factors were assigned to each sample condition and a CountDataSet produced for the samples as the key data structure for the differential analysis to be calculated from. The effective library size and dispersion were then calculated for each library and differential expression then calculated and the files exported to Excel for further filtering and observation.

5.2.10. EdgeR

The **EdgeR** Bioconductor package (Robinson et al., 2009), v3.2.4 was downloaded from the Bioconductor website (http://bioconductor.org/packages/release/bioc/html/edgeR.html). The **EdgeR** library was loaded into the R environment at the beginning of each R session and the relevant count matrix was read into the R environment to create the edgeR object. Low read counts were then filtered out at the cutoff level of 1 read per million. Common and tagwise dispersions were then calculated and the differential expressions between the desired samples calculated and datasheets exported to Excel for further analysis.

5.2.11. miRNA Sequencing analysis

Galaxy was used to align the miRNA FASTQ files to all known human rRNA Sequences from the UCSC file browser (http://genome.ucsc.edu/cgi-bin/hgTables) to establish the level of rRNA contamination. Unaligned rRNA reads were then carried forward into the next analysis. The original FASTQ files were then converted to FASTA format using the **FASTQ to FASTA** tool in Galaxy and imported into the UEA sRNA workbench (Stocks et al., 2012). Samples were filtered and rRNA/tRNA sequences removed. The filtered files were entered into the **miRProf** tool within the workbench, with default parameters. Samples were then aligned to miRbase release 21 (www.mirbase.org) and normalized to the number of genome matching reads. Excel was then used to construct a count matrix from the ´normalized count´ output *.csv* files and the matrix interrogated in **DESeq** and **EdgeR** (Figure 5.3).

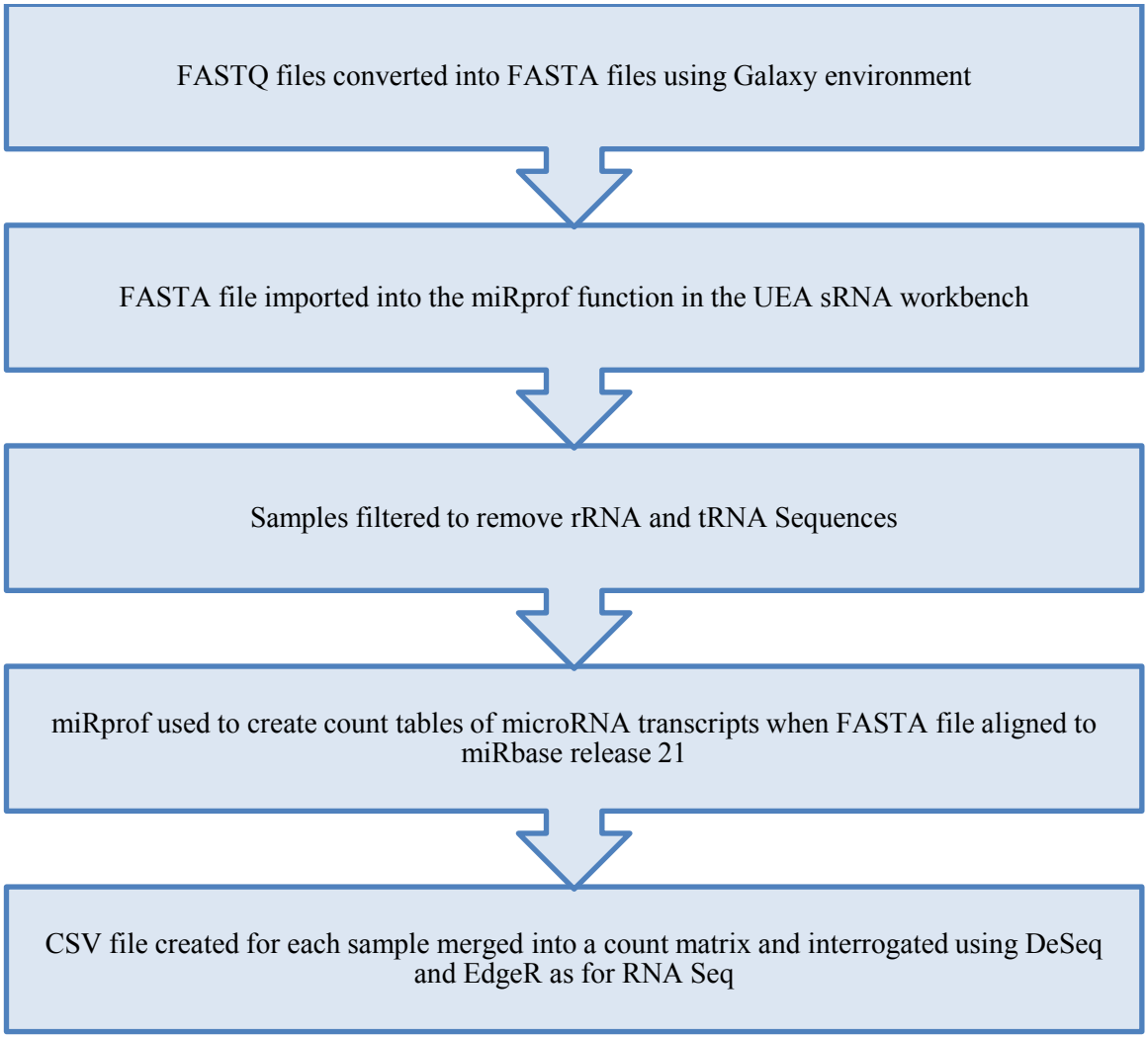

Figure 5.3. miRNA Seq workflow using the UEA sRNA workbench. *The FASTQ files supplied from the RNA sequencing were converted into FASTA files for analysis in the UEA sRNA workbench. Samples were aligned to miRbase release 21 and DE genes analysed using* ***DeSeq*** *and* ***EdgeR****.*

5.2.12. Ribosomal RNA content analysis of all samples

In order to establish the rRNA contents of the samples all FASTQ files were aligned to all known human rRNA Sequences in Galaxy using a FASTA file of rRNA Sequences obtained from the UCSC genome browser (http://genome.ucsc.edu/cgi-bin/hgTables) (Figure 5.4). Results were reported as percentage mapped reads or percentage of total reads.

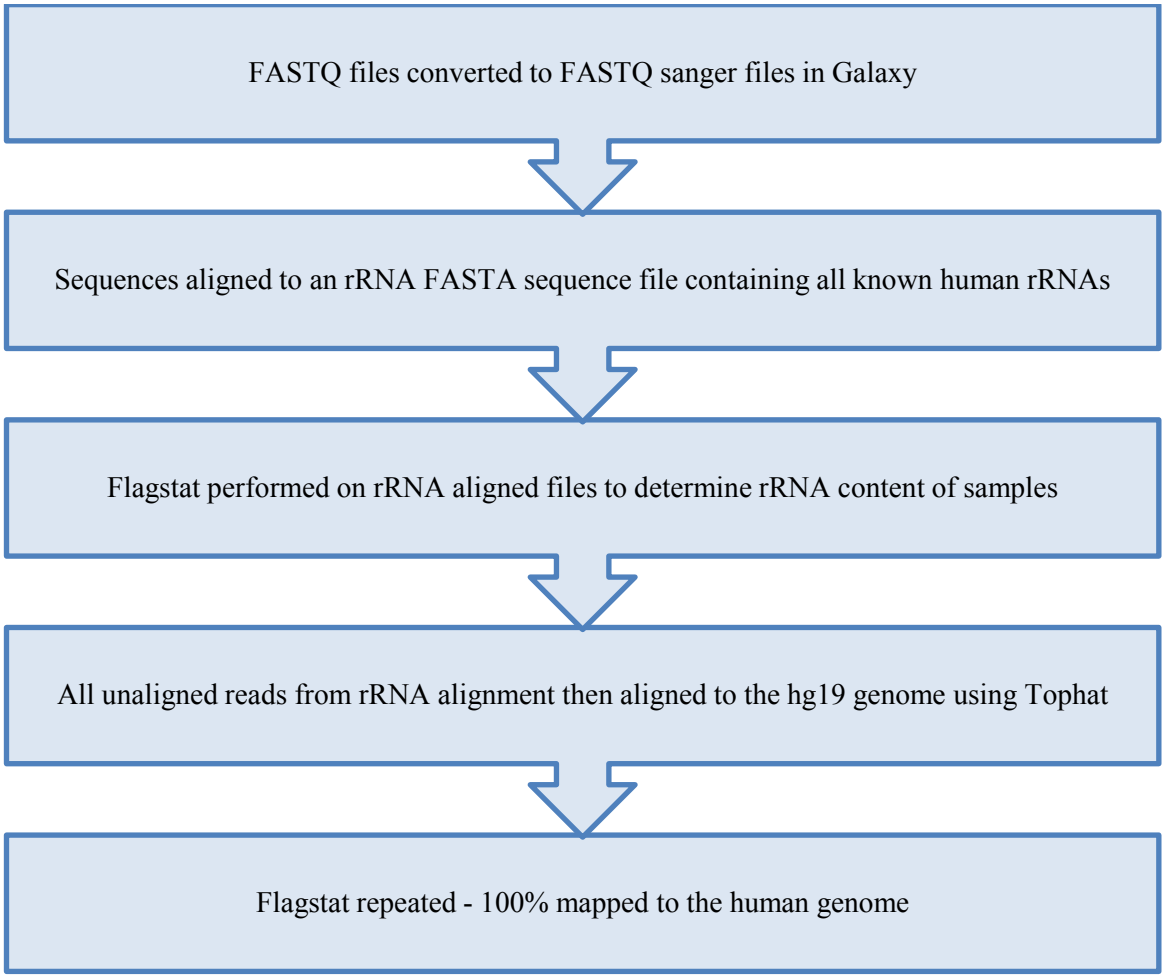

Figure 5.4. Ribosomal RNA Seq workflow to remove rRNA prior to RNA Seq analysis. *To establish the proportion of rRNA reads all samples were aligned to a file containing all known rRNA sequences in Galaxy and flagstat used to measure their % mapping to the samples.*

5.3. Results

In order to characterise the RNA contents of MCF7 cells and the RNA content of their EVs, RNA was harvested from unirradiated or 2 Gy X-ray irradiated MCF7 parent cells and EVs released from the cells (Figure 5.5). RNA was assigned a code to keep track of samples generated (Table 5.1). Samples collected in radiation round 2 (data not shown) were discarded due to ribosomal RNA contamination in the extracellular vesicle RNA samples.

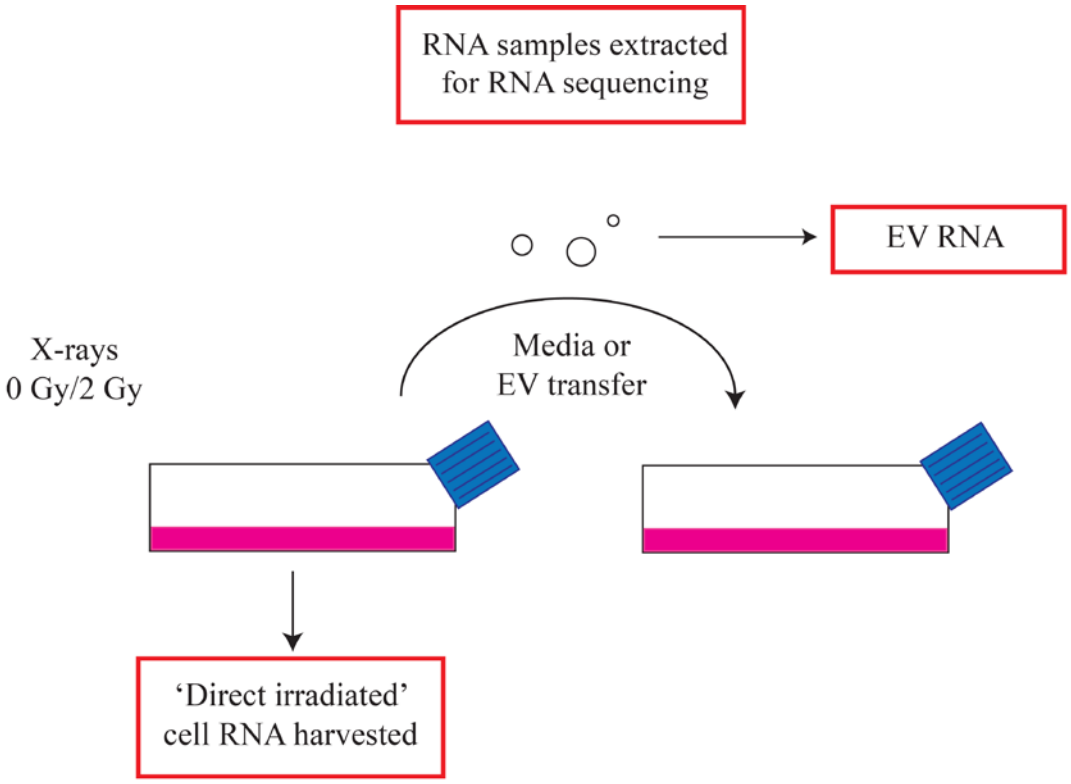

Figure 5.5. Representation of the samples created and used for RNA Sequencing analysis. *RNA extracted from samples in red boxes.*

Table 5.1. **RNA samples collected for radiation RNA Sequencing.** *Parental and EV RNAs were assigned a code based on the biological replicate (radiation round), X-ray dose and RNA source.*

Sample abbreviation	Radiation round	X-ray dose	RNA source
RR10P	Radiation round 1	0 Gy	Parent cell
RR12P	Radiation round 1	2 Gy	Parent cell
RR10E	Radiation round 1	0 Gy	Extracellular vesicle
RR12E	Radiation round 1	2 Gy	Extracellular vesicle
RR30P	Radiation round 3	0 Gy	Parent cell
RR32P	Radiation round 3	2 Gy	Parent cell
RR30E	Radiation round 3	0 Gy	Extracellular vesicle
RR32E	Radiation round 3	2 Gy	Extracellular vesicle
RR40P	Radiation round 4	0 Gy	Parent cell
RR42P	Radiation round 4	2 Gy	Parent cell
RR40E	Radiation round 4	0 Gy	Extracellular vesicle
RR42E	Radiation round 4	2 Gy	Extracellular vesicle

5.3.1. RNA profiles of irradiated MCF7 cells

Differential modulation of several species of RNA has been demonstrated following ionizing radiation (Chaudhry & Omaruddin, 2012; Chaudhry, 2013). In order to establish the RNA profiles of unirradiated and irradiated MCF7 breast cancer cells, total RNA was extracted from MCF7 cells for RNA sequencing. Three biological replicates were performed and analysed on the Agilent 2100 Bioanalyzer to check RNA quality (Figure 5.6). Results demonstrated that good quality cellular RNA was extracted from irradiated and unirradiated cell samples with and RNA integrity number (RIN - score of 10 indicates purest RNA) values of 8.2-9.2. There were no notable differences in size or composition of cellular RNA between irradiated and unirradiated cell RNAs. These results suggest that the cellular RNA samples are not degraded and were of a good RNA quality therefore suitable for use in the RNA-Sequencing experiments.

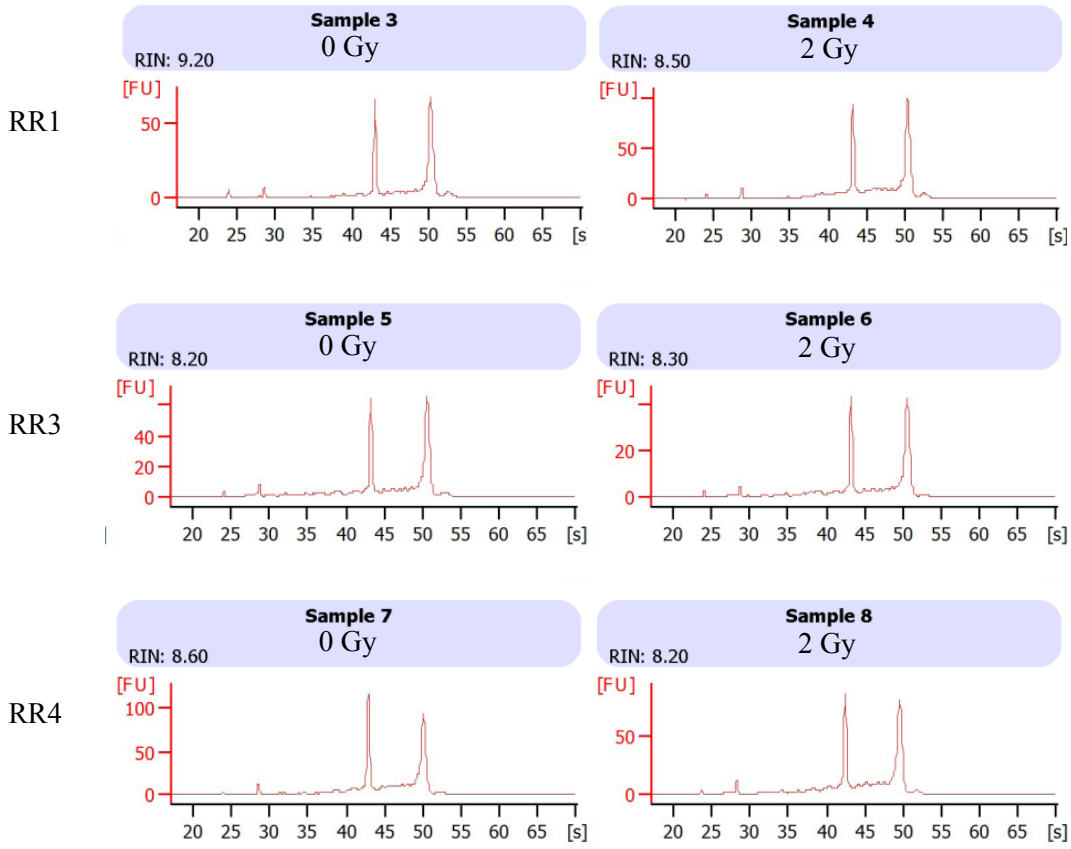

Figure 5.6. Bioanalyzer profiles of unirradiated and irradiated MCF7 cell total RNA. *Profiles of the three biological replicates of cellular RNA used for RNA and miRNA Sequencing (RR1, RR3 and RR4).*

5.3.2. RNA profile of EVs released from MCF7 cells

RNA molecules in association with EVs have been suggested to be responsible for bystander effect (Al-Mayah et al., 2012; Al-Mayah et al., 2015). Consequently, in order to assess the RNA profile of normal MCF7 and irradiated cell EVs media from unirradiated or irradiated cells was conditioned for eight hours post irradiation and the total RNA extracted (Figure 5.7). Results demonstrated a variety of RNA species of different sizes within the EV RNA samples. Both irradiated and unirradiated extracellular vesicle RNA samples demonstrated a peak at around 80-100 nucleotides in all samples that then steadily decreased to a maximum size of approximately 2000 nucleotides for samples RR1 and RR4 and around 4000 nucleotides for sample RR3. Overall the presence of 18S/28S appeared negligible in A and C, with low levels apparent in sample B. The plots demonstrate that there a variety of RNA species present in the RNA from irradiated and unirradiated MCF7 EVs. The typical yield of RNA also varied between the replicates and results can be seen in Table 5.2.

A ladder picture was used to determine approximate RNA sizes as the ladder had run incorrectly on the Bioanalyzer and no further original sample was available for re-analysis. Following analysis of the RNA samples extracted they were carried forward into RNA sequencing.

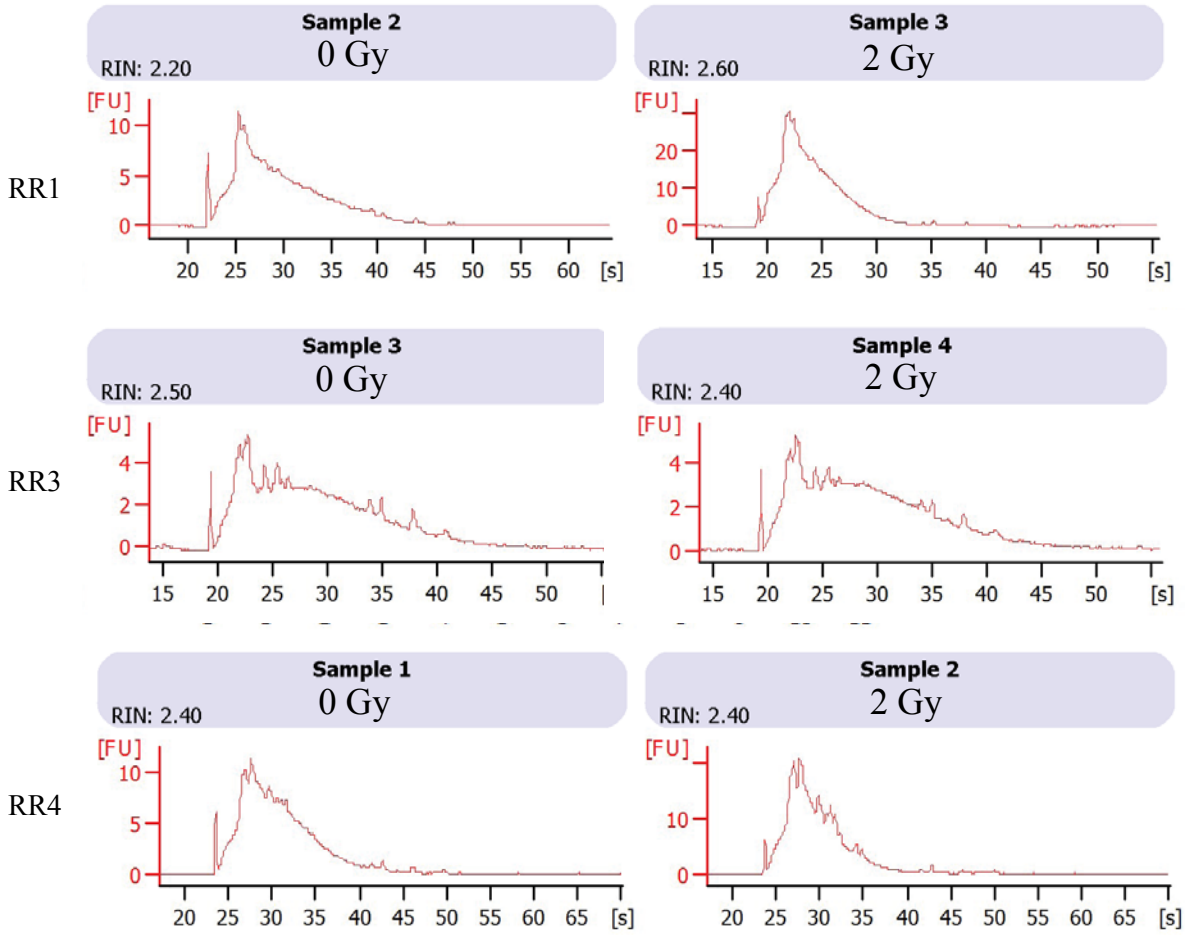

Figure 5.7. Bioanalyzer profiles of total EV RNA. *Bioanalyzer profiles of the three biological replicates of EV RNA used for RNA and miRNA Sequencing (RR1, RR3 and RR4). Each EV RNA sample was harvested from 11 x T175 flasks of MCF7 cell media conditioned for 8 hours each.*

Table 5.2. EV RNA yield from MCF7 cells. *Three biological replicates. Bold = total RNA (ng).*

Sample	0 Gy EV RNA ng/µl **(total)**	2 Gy EV RNA ng/µl **(total)**
RR1	12.7 **(635)**	11.9 **(595)**
RR3	8.7 **(435)**	9.1 **(455)**
RR4	14.4 **(720)**	21.9 **(1095)**

5.3.3. miRNA Sequencing analysis

5.3.4. Small RNA sample libraries for MCF7 cell and EVs samples

In order to test the microRNA changes in cells and EVs following irradiation, miRNA Seq libraries were constructed for sequencing and subsequent DE analysis. For each of the samples the library depth was greater than 8 million reads per library (Figure 5.8). As depths greater than 5 million are not believed to improve microRNA coverage this depth is therefore considered as more than sufficient (Metpally et al., 2013). Most of the reads were trimmed to between 20 and 30 bp as part of post-processing QC and for each library less than 500,000 reads were discarded due to poor quality.

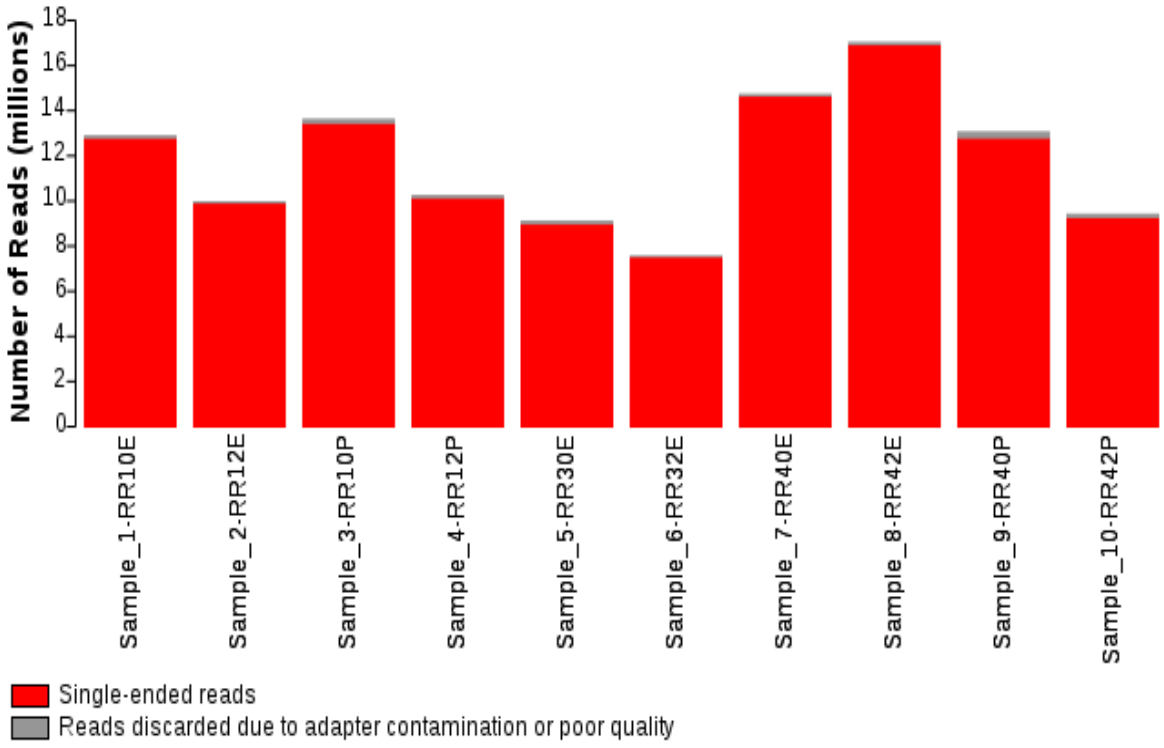

Figure 5.8. Number of reads obtained for miRNA Seq libraries. *Single ended read counts are reported. Reads that were discarded due to poor quality scores or matching adaptor sequences are shown in grey.*

5.3.5. Ribosomal RNA content of miRNA Seq samples

Prior to alignment of the miRNA Seq data to identify microRNA candidates in the radiation response the FASTQ files for each sample were aligned to all known human rRNA sequences so that only sequences that did not align to rRNA could be carried forward in the analysis (Figure 5.9). Results demonstrated high levels of ribosomal RNA present in all of the EV samples, at up to

90% ribosomal RNA. This reflects the fact that for miRNA Seq none of the EV RNA samples were treated to remove ribosomal RNA prior library preparation. This was due to the fact that very low RNA yields were obtained for the EV RNA preparations, possibly due to the short media conditioning time used to capture the bystander effect signal. The cell RNA samples were however much lower in rRNA. For the purpose of the future analysis only the reads that had not aligned to ribosomal RNA were carried forward to analysis in miRprof to identify microRNA candidates differentially regulated between samples.

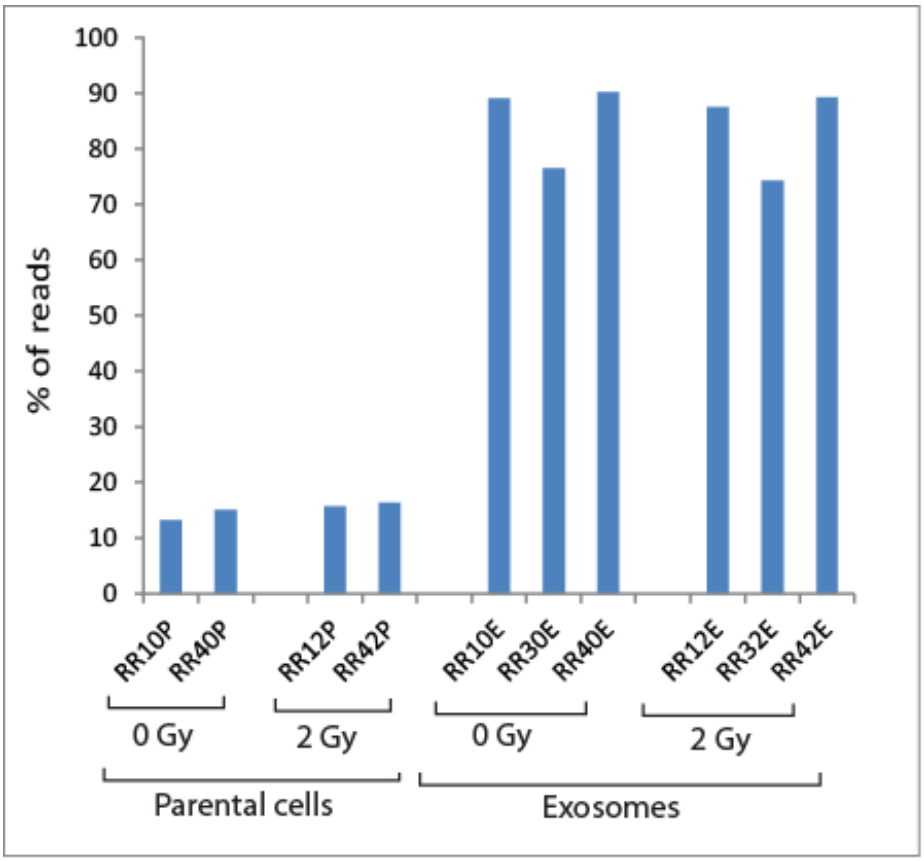

Figure 5.9. The percentage of reads in each sample aligning to human rRNA sequences in the miRNA Seq samples. *Parental cell samples showed levels of around 10-20% rRNA content, whereas EV RNA was higher at 70-90%.*

5.3.6. Correlations between MCF7 cell and extracellular vesicle microRNA content

In order to identify differences or similarities in the microRNA content of sham or irradiated MCF7 cells and their EVs, scatter plots were created using the normalised counts exported from **DeSeq** (Figure 5.10). Results demonstrated that between 0 Gy and 2 Gy EVs or between 0 Gy and 2 Gy cells, microRNA profiles were similar and positive with Spearman's rank values of 0.88 and 0.86 respectively. The correlation between 2 Gy parent cells and their EVs was also positive at a value of 0.71. Interestingly, the correlation between 0 Gy cells and their EVs was still positive, but to a

lesser degree at 0.26. These data taken together may reflect the fact that microRNAs are selectively loaded into EVs following irradiation.

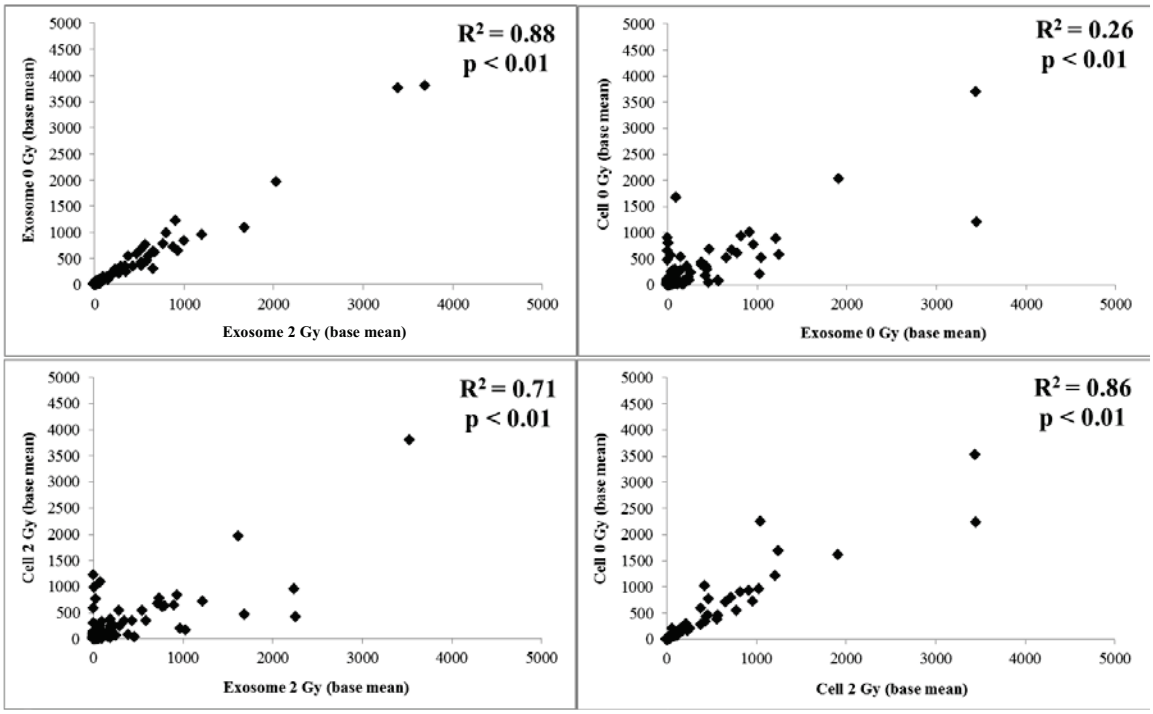

Figure 5.10. Scatterplots showing relationships between cell and EV microRNA in miRNA Seq samples. *Spearman's rank correlations on dataset from **DESeq**, p values from t test.*

5.4. MicroRNA deregulation in response to ionizing radiation

5.4.1. MicroRNA deregulation in directly irradiated and unirradiated cells

In order to test the changes in microRNA deregulation between directly irradiated and unirradiated cells, samples were passed through the miRNA Seq workflow (Figure 5.3). Results demonstrated that for **DeSeq** there were no significantly deregulated microRNAs between 0 Gy and 2 Gy cells. For **EdgeR** a small number of microRNAs were differentially regulated between the 0 Gy and 2 Gy cells including miR-148, miR-19 and miR-188 (Table 5.4). These results suggest that there are few changes in miRNAs in directly irradiated cells in response to radiation in the samples generated, potentially due to the presence of the rRNA.

Table 5.4. The differential regulation of microRNAs between 0 Gy and 2 Gy irradiated cells. *As reported by **edgeR**, cut-off value $p < 0.05$.*

miRNA	Fold change	P value
mir148	3.314	0.009
mir155	3.098	0.039
mir489	0.386	0.046
mir363	0.330	0.036
mir19	0.319	0.025
mir542	0.287	0.034
mir4661	0.276	0.039
mir3188	0.244	0.048
mir6859	0.182	0.007
mir188	0.135	0.006
mir1237	0.129	0.021
mir2276	0.119	0.003
mir5010	0.115	0.012
mir6716	0.100	0.005

5.4.2. MicroRNA deregulation between parent cells and their EVs

In order to test the hypothesis that selective loading occurs in EVs from their parent cells, comparisons were made between unirradiated and irradiated parent cells and the EVs derived from them. When initially tested using **DeSeq** and **EdgeR**, there were no significantly deregulated microRNAs between 0 Gy and 2 Gy EVs as for the parent cell/extracellular vesicle comparisons. In order to identify groups of microRNAs deregulated between 0 Gy and 2 Gy EVs a different approach was taken to establish differences between microRNAs in unirradiated or directly irradiated cells.

The comparison for 0 Gy and 2 Gy cells and their EVs was used to find significantly deregulated genes between parent cells and EVs (Figure 5.11). These lists were then compared; the microRNAs unique to the list of differences between 2 Gy cells and EVs were marked as green and considered as microRNAs enriched in response to 2 Gy irradiation. Results demonstrated a number of microRNAs common to both 0 Gy and 2 Gy EVs (when compared to their parent cells), however there were microRNAs reported only as present in the 2 Gy EVs, including mir-100 and mir-223. This may point to a small population of microRNAs selectively incorporated into 2 Gy EVs.

	Fold change	
miRNA	miRNAs sig. dereg. between 0 Gy cells and 0 Gy exosomes	miRNAs sig. dereg. between 2 Gy cells and 2 Gy exosomes
mir100	1402	Inf
mir127	350.85	Inf
mir142	Inf	Inf
mir144	Inf	Inf
mir150	Inf	Inf
mir223	Inf	Inf
mir369	NA	Inf
mir379	NA	Inf
mir381	Inf	Inf
mir382	NA	Inf
mir409	Inf	Inf
mir412	Inf	Inf
mir432	Inf	Inf
mir433	Inf	Inf
mir451	NA	Inf
mir495	Inf	Inf
mir543	NA	Inf
mir143	NA	2198.13
mir493	519.97	723.34
mir122	NA	581.03
mir411	259.11	522.86
mir7704	2563.1	436.73
mir486	192.05	161.88
mir199	217.27	66.58
mir10	NA	36.68
mir1	NA	27.79
mir126	NA	14.93
mir139	NA	10.91
mir155	NA	7.99
mir149	NA	0.20
mir375	0.1939	0.20
mir744	NA	0.19
mir125	NA	0.16
mir615	NA	0.08
mir1180	0.0918	0.06
mir1307	0.1136	0.06
mir941	NA	0.04

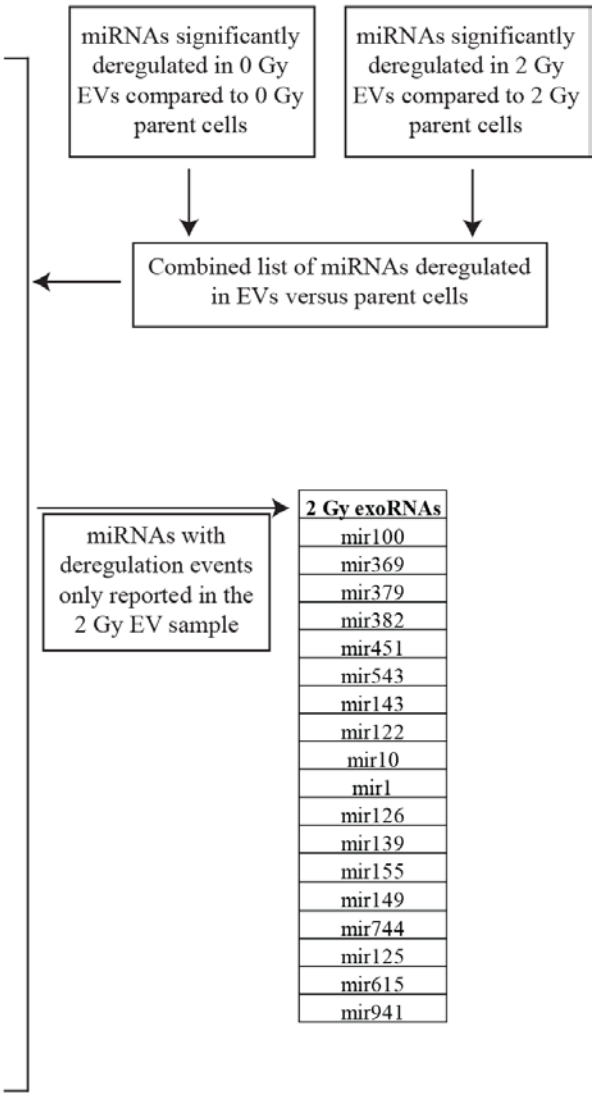

Figure 5.11. Table of microRNAs significantly different between 0 Gy and 2 Gy cells and EVs. *Clear rows indicate microRNAs reported by both the 0 Gy and 2 Gy analyses. Green rows indicate microRNAs unique to the 2 Gy analysis. NA signifies no deregulation event for that particular miRNA in the 0 Gy EVs.* ***Deseq*** *results used.*

5.4.3. RNA Sequencing of MCF7 cell RNA and EV RNA following X-rays

5.4.4. RNA Sequencing analysis

The RNA Sequencing workflow was carried out in the Galaxy interface environment on the samples mentioned previously in this chapter (Figure 5.2). This part of the sequencing was intended to analyse the mRNAs, their isoforms and some non-coding RNA species.

5.4.5. RNA Sequencing libraries for MCF7 cell and extracellular vesicle samples

As for the miRNA Seq, libraries were constructed for the RNA-Seq samples to investigate mRNA and long non-coding RNA changes. For each of the libraries constructed by Liverpool Centre for Genomic Research reads were reported for each sample following a sample QC removing low quality reads (Figure 5.12). It has been reported by the ENCODE consortium that for differential expression analysis of paired-end reads 25-30 million reads is recommended for differential expression analysis (http://genome.ucsc.edu/ENCODE/protocols/dataStandards/ENCODE_RNA Seq_Standards_V1.0.pdf). The proportion of singlet reads and reads discarded due to poor quality was also small at less than a million reads discarded per sample. Consequently, the number of reads per sample library in the pool was of a similar read depth and sufficient depth for the purposes of differential expression.

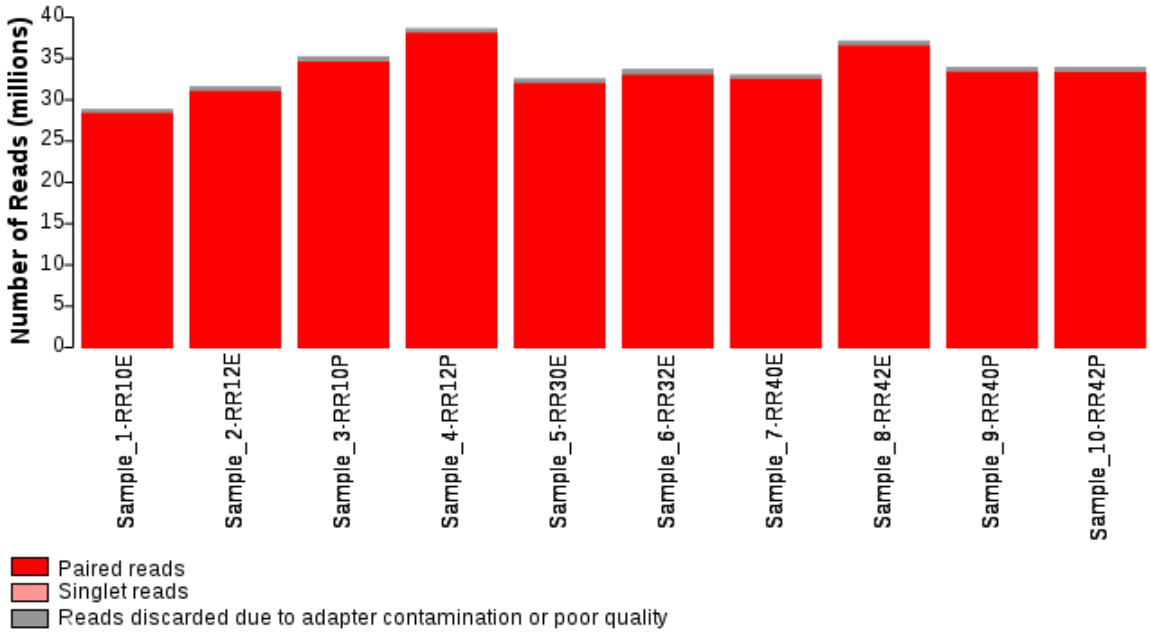

Figure 5.12 Number of reads obtained for RNA Seq libraries. *Bars show reads that were successfully paired (paired reads), reads that did not pair (singlet reads) and poor quality reads or adapter sequences (reads discarded).*

5.4.6. Ribosomal RNA contents of RNA Sequencing samples

Some EV preparations have been shown to contain differing amounts of ribosomal RNA (Jenjaroenpun et al., 2013). Therefore, the rRNA content of the libraries was established by aligning all reads to all known human rRNA sequences (Figure 5.12). Results showed that each of the samples contained small amounts of rRNA and also that the majority of the reads for each sample library aligned to the hg19 human gene file release. Ribosomal RNA pre-clearing was only performed on cell, not extracellular vesicle samples. Bioinformatic removal of rRNA sequences from the samples was not performed as the rRNA content was minimal. As a result of the

alignment of most reads to the genome and the minimal rRNA contamination, RNA sequencing analysis was then continued to identify differentially regulated RNAs.

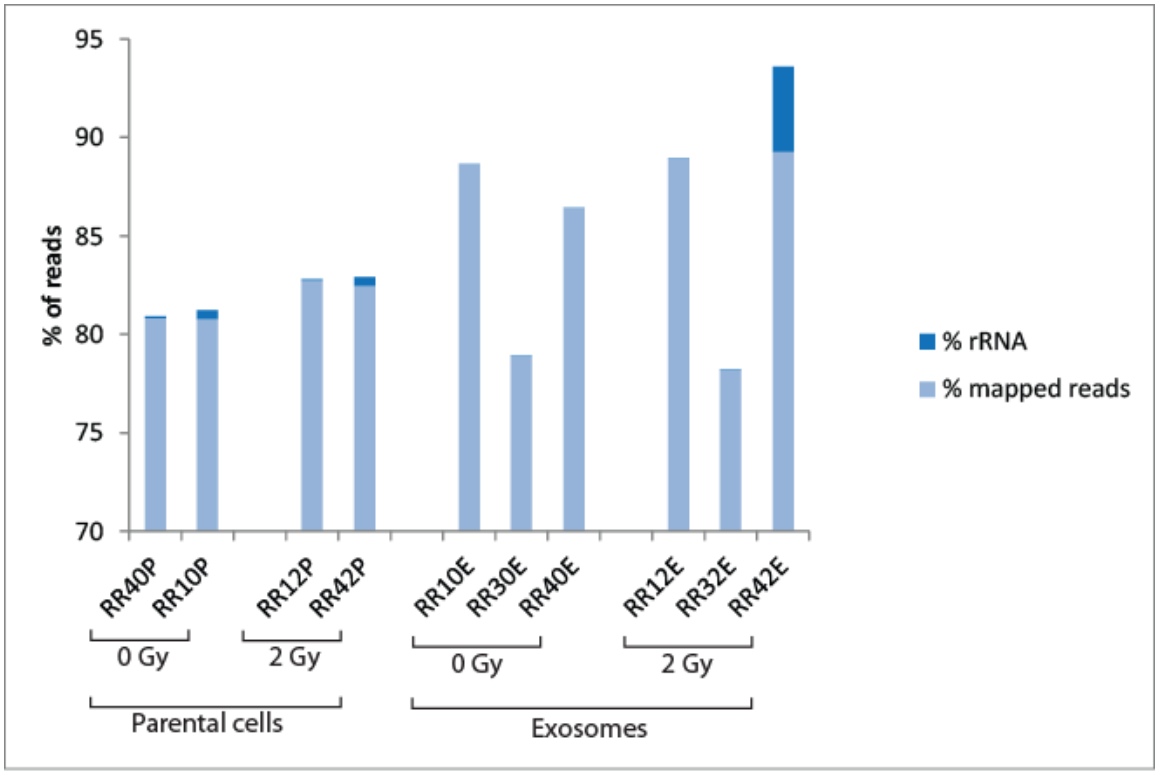

Figure 5.13. The percentage of reads mapped to the hg19 release of the human genome and the percentage of reads aligned to all known human rRNA sequences. *For parental and EV samples the percentage alignment to the genome was performed as well as to rRNA sequences.*

5.4.7. Differential Gene Analysis of sequenced libraries

Following library preparation and quality control the files were analysed for differential gene expression between cell and extracellular vesicle samples (Figure 5.2). Three different programs; **Cuffdiff, EdgeR** and **DeSeq** were used to analyse differential gene expression to establish a list of high confidence RNA targets involved in radiation response.

5.4.8. Correlations of MCF7 cell and EV RNA contents

In order to establish whether the RNA contents of sham or irradiated MCF7 cells and EVs reflected or differed from each other the Cummerbund suite in R was used to produce scatter plots and Spearman's rank values calculated to report how closely the RNA profiles of cells and EVs compared (Figure 5.14). Results demonstrated that unirradiated and irradiated MCF7 cells had similar RNA profiles with a Spearman's rank value of 0.97, as did EVs from both 0 Gy and 2 Gy irradiated cells with a correlation value of 0.96. Conversely the parent cell RNA profile of both

unirradiated and irradiated cells appeared different than that of their respective EVs, with unirradiated cells compared to their EVs at 0.58 and irradiated cells compared to their EVs at 0.63. These results suggest a potential loading of selective RNAs into EVs as opposed to EVs simply reflecting their cell of origin.

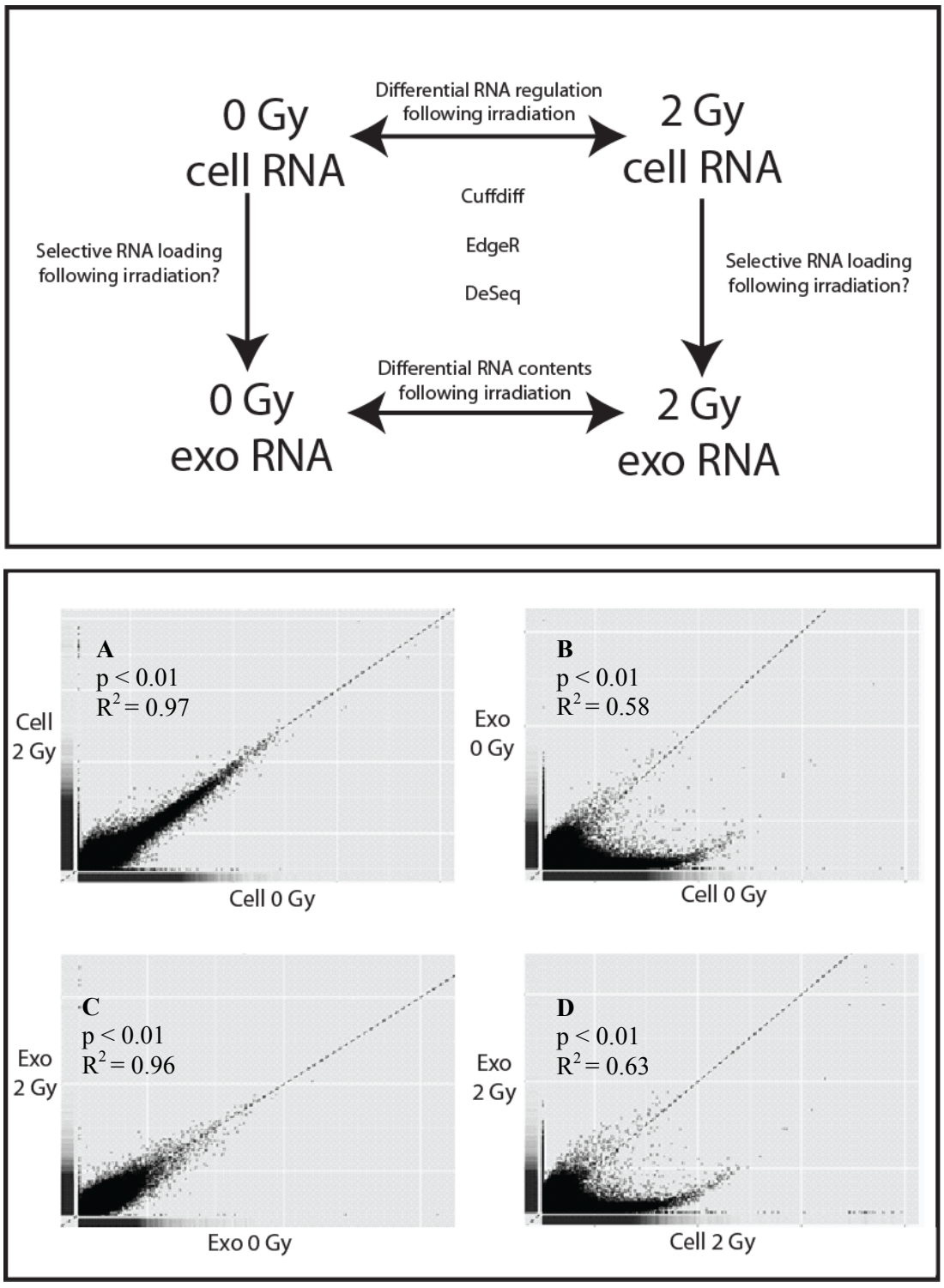

Figure 5.14. Correlations between parent cells and EVs released from those cells. A*: 0 Gy versus 2 Gy cells.* **B***: Unirradiated cells versus their EVs. C: Unirradiated cell EVs versus 2 Gy irradiated cell EVs. D: Irradiated cell RNA versus irradiated cell EVs. Scatter plots in log10 FPKM values for each of the samples produced in CummeRbund. Two biological replicates for cell samples and three biological*

replicates for EV samples. Spearman's rank correlations and t test.

5.4.9. Differential gene analysis of 0 Gy vs 2 Gy parental cell RNA

In order to test for RNA changes between 0 Gy and 2 Gy irradiated cells, differential expression analysis was performed firstly using the Cuffdiff program. Analysis of all significantly deregulated genes between 0 Gy and 2 Gy cells with a p value of less than p = 0.05 produced a list of 1581 RNAs. The ten most significantly upregulated and ten most significantly downregulated RNAs were explored (Table 5.3). Results demonstrated for the upregulated RNAs, many small nucleolar RNAs including *SNORA31* and *SNORA74A*. Furthermore genes including *SOX14*, *GALNTL6* and miR-622 were present in the list. Down regulated genes including *RAD51* and *ANP32B* were reported as well as miR-4426. Taken together, these results suggest that a variety of RNA species are significantly deregulated in response to cellular irradiation.

Table 5.3. Differentially regulated genes between 0 Gy and 2 Gy irradiated cells. *Cuffdiff analysis, $p < 0.05$.*

gene	p-value	Fold change	Direction
ABHD11-AS1	0.00	Inf	UP
SNORA31	0.00	Inf	UP
LOC388946	0.00	Inf	UP
SNORA74A	0.01	Inf	UP
SNORA50	0.01	Inf	UP
C3orf38	0.02	Inf	UP
SOX14	0.03	Inf	UP
SNORA21	0.03	Inf	UP
MIR622	0.04	Inf	UP
GALNTL6	0.03	3.63	UP
MIR4426,RPS27A	0.00	0.13	DOWN
NUDC	0.00	0.14	DOWN
RPS16	0.00	0.14	DOWN
MYBL2	0.00	0.16	DOWN
RAD51	0.00	0.17	DOWN
ANP32B	0.00	0.18	DOWN
FAM127C	0.00	0.19	DOWN
DCTPP1	0.00	0.19	DOWN
UTP3	0.00	0.21	DOWN

RAB13	0.00	0.21	DOWN

5.4.10. KEGG pathway analysis of parental cell analysis

Using the list of 1581 differentially regulated RNAs from the **Cuffdiff** analysis, KEGG pathway analysis was performed to identify pathways involved in the radiation response of directly irradiated cells. DNA replication and repair, cell cycle and the MAPK pathway featured. These pathways reflect some of the cellular processes implicated in irradiation and the bystander response (Dickey et al., 2012; Dent et al., 2003) and consequently show that the RNA Seq has produced RNA candidates relevant to the radiation response. Furthermore there were some similarities upon comparison with the data generated from miRStress in chapter 3. For the general radiation response only the MAPK pathway was present (Table 3.3). However, in the KEGG pathways for the specific X-ray response (Table 3.5), the adherens junction, cell cycle and MAPK signalling pathway were shared with this KEGG analysis. Overall, this shows that the miRStress search and the RNA Seq have identified some similar pathways involved in radiation response. It is possible that the differences between these lists are due to the fact that a comparison between the miRNA response and the RNA response have been compared.

Table 5.4. KEGG pathway analysis of DE genes between 0 Gy and 2 Gy RNA Seq samples. Cut-off value $p < 0.05$.

KEGG Term	P-Value
Cell cycle	0.000011
Spliceosome	0.00001
DNA replication	0.000012
Adherens junction	0.0025
MAPK signalling pathway	0.015
Circadian rhythm	0.019
Base excision repair	0.024
Notch signalling pathway	0.041

5.4.11. Differential gene analysis of 0 Gy vs 2 Gy EVs

Amalgamation of results from **DeSeq**, **EdgeR** and **Cuffdiff** resulted in a list of high confidence targets of 0 Gy EVs vs 2 Gy EVs. Criteria for an RNA being considered a high confidence target included being significantly different between two of the three algorithms used (Table 5.5). The mir-17-92HG cluster was an exception but was also selected as it was so highly upregulated in the

Cuffdiff program. Results demonstrated that a number of mRNAs and some non-coding RNAs were significantly upregulated in 2 Gy EVs compared to 0 Gy EVs. Candidates consistently significantly deregulated between algorithms included *NET1*, *ACTB*, *MALAT1*, *RPS4X*, *TMSB4X* and *EEF2*. The genes *ANP32B*, NCL were all upregulated in at least two algorithms with the *miR1792HG* cluster showing the highest deregulation but only reported in the **Cuffdiff** list. Furthermore, the fold change values were generally similar between the **EdgeR** and **DeSeq** algorithms, reflecting that they both work using a similar algorithm in the R environment.

Table 5.5. Top deregulated genes for RNA sequencing results for 0 Gy vs 2 Gy EVs from three different DE algorithms. *Irradiated cell EVs demonstrated upregulation of a number of genes. Some of these genes were highly upregulated, for example the miR17-92 HG cluster, whereas others were consistently deregulated between the three algorithms* ***DeSeq****,* ***EdgeR*** *and* ***Cuffdiff****. Inf = infinite, na = not available.*

	Cuffdiff		DeSeq		EdgeR	
Gene	**Fold change**	**P val**	**Fold change**	**P val**	**Fold change**	**P val**
NET1	6.7	0.000	3.6	0.006	3.6	0.000
ANP32B	6.1	0.001	6.7	0.141	6.6	0.000
NCL	3.8	0.004	2.2	0.104	2.2	0.001
MIR17,MIR17HG, -18A, -19A, -19B1 -20A, -92A1	122.2	0.005	na	na	na	na
RPL32,SNORA7A	18.4	0.021	1.4	0.516	1.4	0.262
HSP90AA1	2.2	0.024	1.9	0.123	1.9	0.002
ACTB	2.4	0.027	2.1	0.000	2.1	0.001
RNU11	inf	0.037	inf	0.278	64.6	0.000
MALAT1	2.1	0.039	2.0	0.051	2.0	0.000
RPS4X	2.4	0.044	2.0	0.007	2.0	0.008
TMSB4X	2.4	0.049	2.2	0.000	2.2	0.002
EEF2	2.1	0.050	2.0	0.000	2.0	0.003
KRT8	2.3	0.126	1.9	0.000	1.9	0.003

5.4.12. Differential regulation of RNAs in EVs

As it was observed that the genes in 2 Gy EVs were generally upregulated, their direction of deregulation in the parent cells was checked to test if the RNAs were being selectively upregulated in EVs. Of the top 40 deregulated genes in EVs as per the Cuffdiff analysis, 95% of those were

reduced in directly irradiated cells (Figure 5.15). This suggests a selective loading of the RNAs from 2 Gy irradiated cells into their EVs.

As the miR-17-92 host gene cluster was upregulated greater than 100-fold in the CuffDiff analysis (Table 5.5), the percentage of up or downregulated entries for the individual members of the cluster were compared to two commonly deregulated microRNAs in the database, miR-21 and miR-34a. Results demonstrated that miR-21 and miR-34a were increased in response to stress, however the members of the miR-17-92 cluster were significantly downregulated in comparison (Figure 5.16).

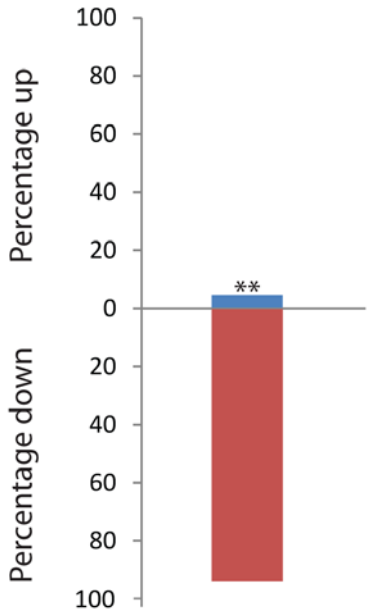

Figure 5.15. The top forty deregulated EV RNAs are upregulated in 2 Gy EVs but reduced in 2 Gy parent cells. *The top EV RNAs were all upregulated with 95% downregulated in parent cells. **p < 0.01, t test.*

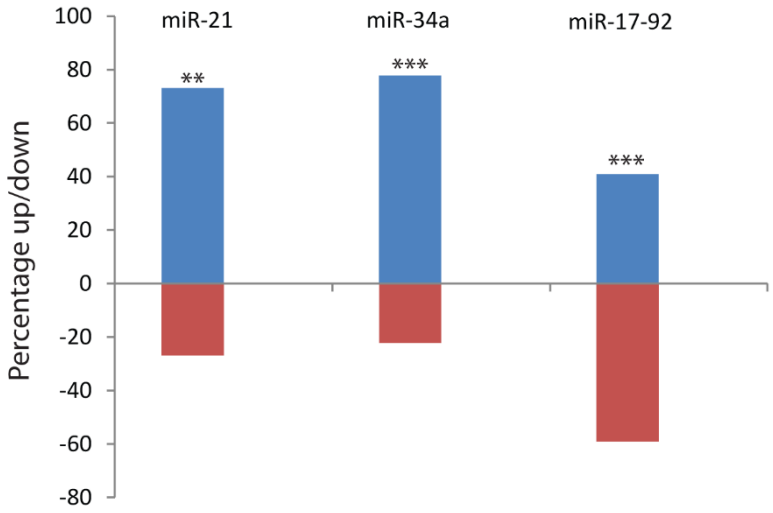

Figure 5.16. MicroRNAs commonly deregulated in the stress response are typically upregulated in cells. *As reported by the miRStress database, two of the most commonly deregulated miRNAs in the general stress response, miR-21 and miR-34a, were upregulated. Conversely members of the miR17-92 host gene cluster reported as upregulated by >100-fold in EVs were downregulated. **p<0.05, ***p<0.01, t test.*

5.4.13. Quantitative PCR analysis of cell and EV RNA samples

Based upon the results for the RNA sequencing and some literature searching, a number of candidates were selected for further analysis. In order to validate the results obtained by RNA Seq qPCR was performed to test the direction of regulation (Table 5.6).

Table 5.6. **Candidate genes for further study following RNA Seq analysis.** *Based upon the RNA Seq results the following genes were selected for quantitative qPCR validation.*

Candidate	Examples of functions reported by the literature
ANP32B	Anti-apoptosis/caspase-3 inhibitor (Shen et al., 2010) Chromatin regulation (Munemasa et al., 2008) RNA translocation (Chemnitz et al., 2009)
EEF2	mRNA elongation (Kaul et al., 2011)
Mir-17-92 cluster	Ageing (Bates et al., 2009) Oncogenesis (Volinia et al., 2006)
NET1	Invasive tumor phenotype (Lahiff et al., 2013) Mitosis regulator/GI (Menon et al., 2013)
MALAT1	Metastasis (Hu et al., 2015)
HSP90AA1	Cell motility (McCready et al., 2010)
RPS4X	40S ribosomal subunit (Watanabe et al., 1991)
NCL	Double strand break repair (Kobayashi et al., 2012) Protein trafficking during stress (Nalabothula et al., 2010)

5.4.14. qPCR of direct irradiated cells

In order to validate the RNA sequencing results and confirm the direction of gene deregulation in directly irradiated cells, qPCR was performed on the radiation RNA samples. When compared to the selected housekeeping genes, the levels of *EEF2*, *miR-17-92*, *HSP90AA1*, *NET1* and NCL reflected a slight downregulation for most genes, whereas an upregulation was observed for *MALAT1*, *ANP32B* and *RPS4X* (Figure 5.17). These results demonstrate that some of the RNA-Seq changes were reflected in the cellular RNA content as per qPCR, however the changes were not

significant. It is possible that the RNA sequencing provides a more sensitive analysis of RNA deregulation.

5.4.15. qPCR of EV RNA samples

In order to validate the EV RNA gene changes reported by the RNA Seq the same procedure was carried out for EV RNA (Figure 5.18). Results demonstrated some differences when compared to the two housekeeping genes. For B2M comparison most of the genes were slightly upregulated, excluding *NET1* and NCL. However, when compared to UBC these genes were not downregulated. *MALAT1* and *ANP32B* were upregulated compared to both genes. In conclusion, these results suggest that the qPCR results do support a slight trend of upregulation of the selected genes in 2 Gy EVs, however these were not significant. New RNA samples were generated to supplement the EV RNA used for qPCR, therefore it is possible that biological variation has attenuated the qPCR results.

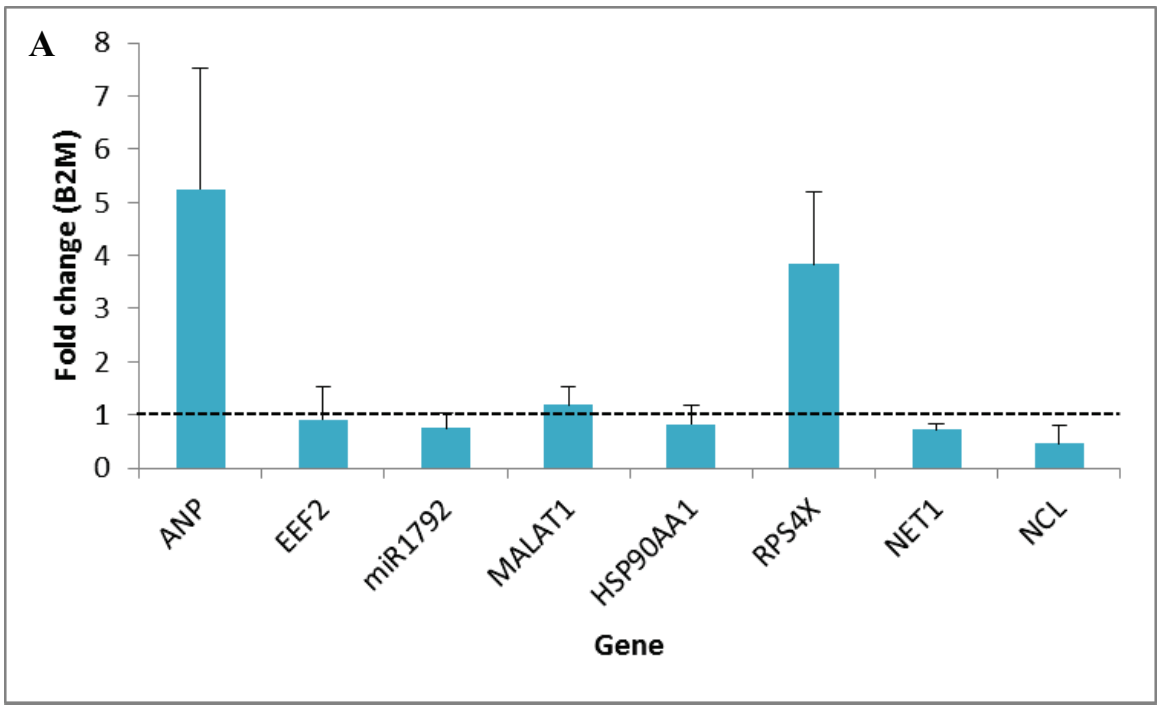

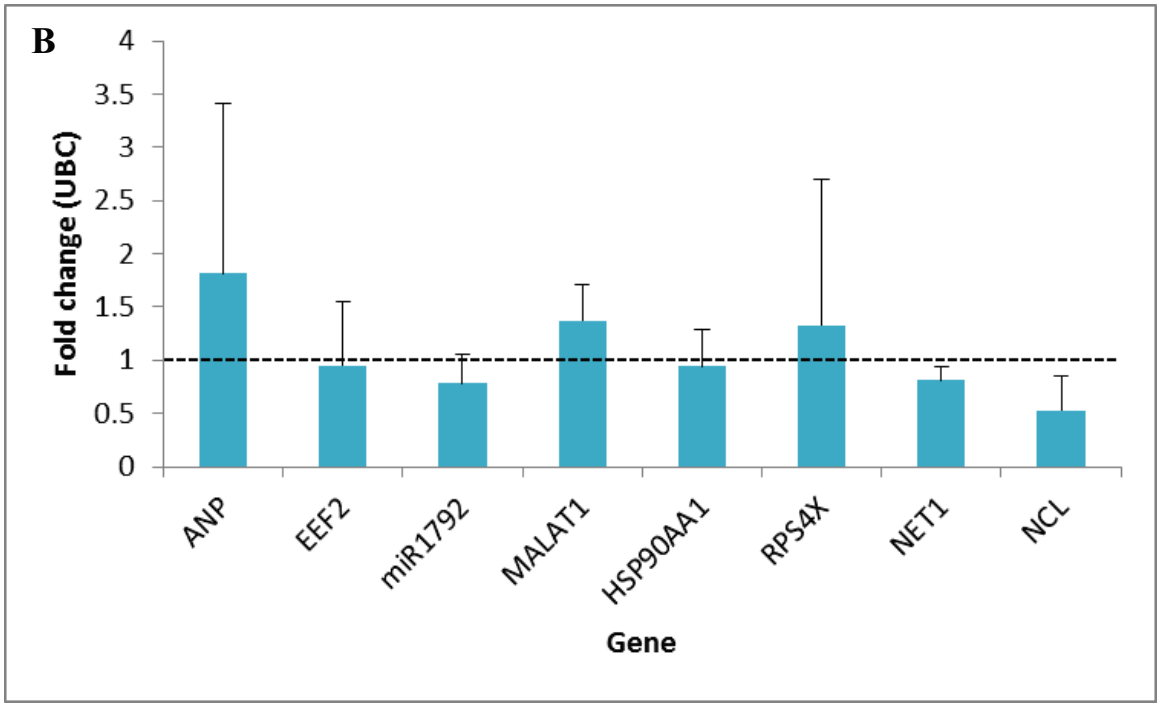

Figure 5.17. Quantitative PCR analysis of RNA Seq candidate genes in directly irradiated parent cell RNA. *Fold change for each gene corrected to housekeeping gene indicated* **(A: B2M, B: UBC)** *is reported. Four biological replicates. Error bars SEM.*

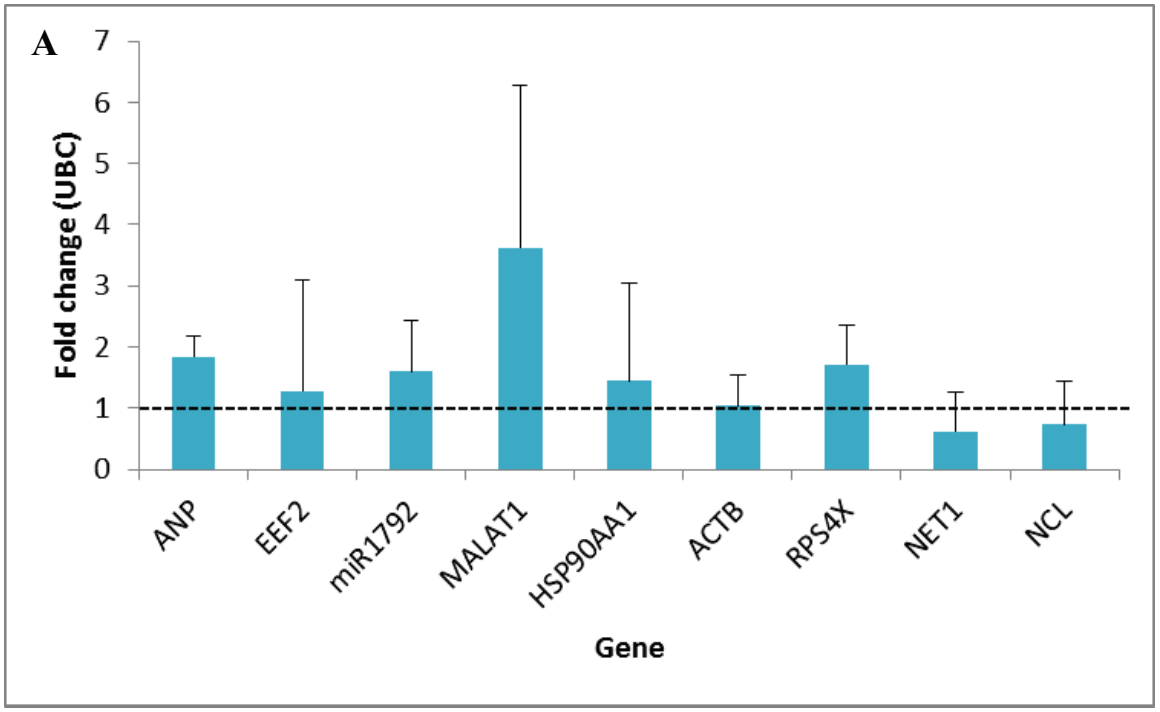

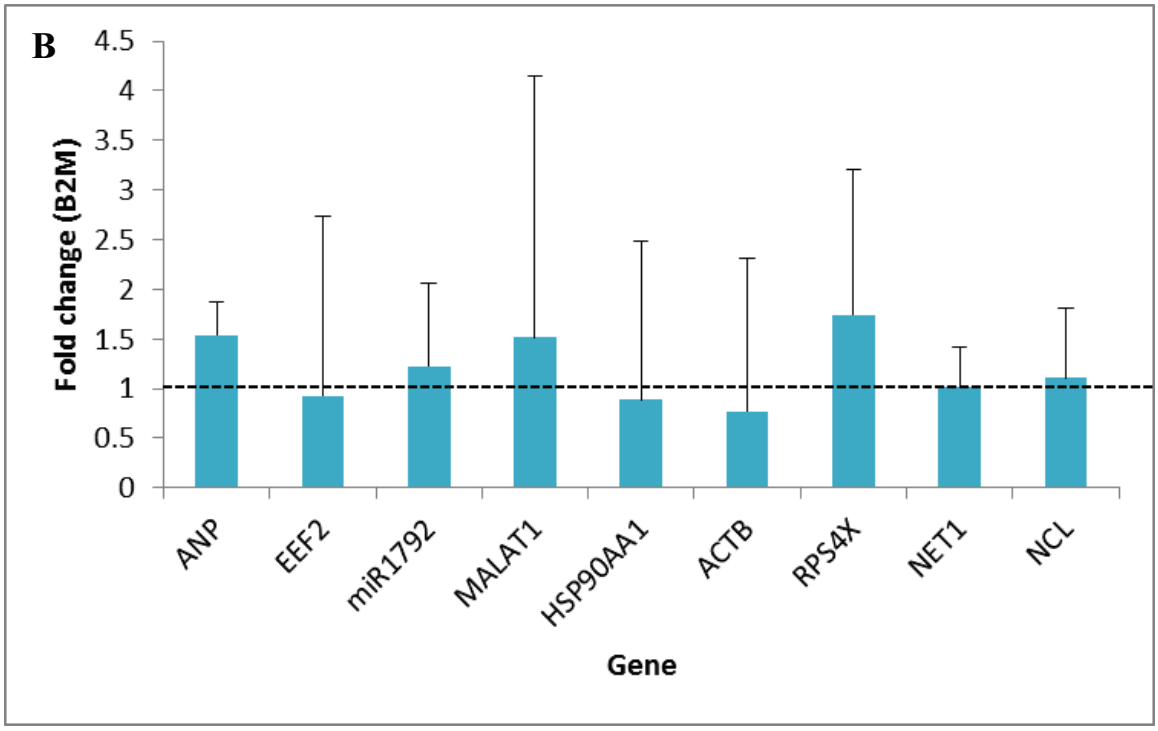

Figure 5.18. Quantitative PCR analysis of RNA Seq candidate genes in EV RNA samples. *Fold change for each gene corrected to housekeeping gene indicated (UBC/B2M) is reported. Four biological replicates. Error bars SEM.*

5.5. Discussion

The study of differential RNA regulation in response to X-rays is important in developing a better understanding the biological effects of radiation and also the general stress response. RNA deregulation has been documented in both directly irradiated and bystander cells (Chaudhry & Omaruddin, 2012) and EVs derived from irradiated cells (Arscott et al., 2013). To this end, the work in this chapter aimed to characterise the RNA contents of X-irradiated MCF7 cells and the EVs released from them in an attempt to identify novel RNA candidates involved in the bystander effect.

5.5.1. RNA contents of irradiated MCF7 cells and their EVs

EVs have been documented as containing predominantly small RNAs less than 200 nt in length (Batagov et al., 2011), but also to contain functional mRNAs (Valadi et al., 2007) and long noncoding RNAs (Takahashi et al., 2014; Kogure et al., 2013) that are present in low levels in parent cells but at higher levels in EVs (Gezer et al., 2014). EVs released from oxidatively stressed cells were able to confer a protective effect upon recipient cells that was lost when the EVs were treated with UV to deactivate RNA prior to transfer (Eldh et al., 2010) suggesting that the RNA

component is playing an important role in the stress response. It has been hypothesised that the mRNA load of EVs may be that of 3'UTR fragments acting in a more regulatory role in recipient cells rather than in a protein translation capacity (Batagov & Kurochkin, 2013). The Bioanalyzer plots in this chapter are consistent with the literature that suggests EVs contain a distinct profile of mainly mRNAs and microRNAs (Ekstrom et al., 2012), with no dominant 18S or 28S as normally found in total cell RNA.

Several of the candidate genes have played roles in cellular communication that could plausibly be linked to radiation DNA damage response and BE. Although originally suggested as a diagnostic lung cancer marker (Ji et al., 2003) and identified as upregulated in a wide variety of cancers (Han et al., 2015; Zheng et al., 2014; Gutschner et al., 2013), *MALAT1* levels have been shown to increase in the ionizing radiation response of cells (Chaudhry, 2014). As it has also been implicated in cell cycle arrest and DSB formation (Tripathi et al., 2013) it is interesting that *MALAT1* levels were significantly increased in the 2 Gy EVs and further work will aim to elucidate the possible involvement of *MALAT1* in the radiation response. Additionally *ANP32B* is believed to be cleaved by caspase-3 acting as a negative regulator of apoptosis (Shen et al., 2010), another potentially interesting interaction with the bystander effect as it has been postulated that caspase inhibitors may be used as part of targeting apoptosis pathways for using in radiation and cancer therapies (Ghobrial et al., 2005). *Nucleolin* has also been implicated in the response of cells to DSBs, facilitating their repair via the MDC1-realed pathway and also the ATM response known to be implicated ionizing radiation (Kobayashi et al., 2012). Finally, the microRNAs of the miR-17-92 cluster have been implicated in the radiation response (Leung et al., 2014). Consequently the genes identified as differentially expressed following radiation have been implicated in radiation response and therefore reflect that the analysis has identified plausible radiation response candidates.

5.5.2. MicroRNA contents of radiation EVs

The current understanding of the extent of the role of microRNAs in radiation response is that they are directly modulated following radiation but may not be the primary signalling molecule involved in the transmission of the bystander effect. Evidence includes that the knockdown of Dicer in cells was not able to completely abrogate the bystander effect (Dickey et al., 2011). The impact of microRNAs should however not be underestimated as full Dicer knockdown cell-lines are non-viable (Cummins & Velculescu, 2006), therefore a more complete depletion of microRNAs might indeed prevent the bystander effect from being observed. Furthermore, not all microRNAs are Dicer dependent (Cheloufi et al., 2010).

Some deregulation of microRNAs in directly irradiated cells was observed. The microRNAs deregulated are not those typically associated with the radiation response and it is possible that the rRNA levels in the miRNA seq samples reduced the read depth and therefore subtle changes in microRNAs have been concealed. The fact that there were also no significantly deregulated microRNAs between 0 Gy and 2 Gy EVs in the analysis in this chapter is interesting, as is the fact

that there were relatively few deregulated between parent cells as previously mentioned. MicroRNA enrichment of the samples using ribosome depletion protocols might increase the detail of microRNA deregulation observed (O'Neil et al., 2001). In the future, generation of more EV RNA should be focused upon to permit ribosomal RNA depletions and still have enough RNA for sequencing. The subtractive version of analysis, however, demonstrated some differences in the relative microRNA cargo of EVs released from 2 Gy irradiated cells, suggesting that the data may require different manipulation to uncover groups of deregulated microRNAs. It is important to note also that microRNAs have also been identified in the circulation independent of vesicles, for example complexed with carriers such as Argonaute2 (Arroyo et al., 2011) and also in association with high density lipoproteins (Vickers et al., 2011). The contributions of such sources of microRNA are important during, for example, quantification of EVs samples. Further work will ascertain the exact proportions of the extracellular vesicle sample that these external microRNA components comprise.

5.5.3. Ribosomal RNA in EV preparations

Originally, ribosomal RNA was reported as absent from EV preparations, but as our understanding of EV RNA has increased it has been demonstrated more recently that some EV preparations do indeed contain notable levels of rRNA, despite using established extracellular vesicle isolation procedures (Jenjaroenpun et al., 2013; Miranda et al., 2014; Huang et al., 2013). As the first studies using next generation sequencing for EV RNA analysis have emerged it is possible that the RNA contents of these vesicles is more accurately reported. In the case of ribosomal RNA presence it may be argued that non-vesicular matter is present in the vesicle preparation, however until protocols are standardised and vesicle classification and nomenclature agreed by the international community it will be important to analyse the evidence presented by each study based upon its own merit.

5.5.4. Technical aspects of EV RNA extraction and RNA sequencing technologies

RNA Seq is considered as an advantageous method of RNA detection, not least because transcript number is not reported by microarray technologies ('t Hoen et al., 2008). However many analyses revealing important information on EV RNA contents have been performed on EV-like vesicles using microarray technology (Noerholm et al., 2012; Skog et al., 2008). Several comparisons of RNA Seq technology and microarray approaches have been performed (Marioni et al., 2008; Garber et al., 2011; Mortazavi et al., 2008). One of the main issues to overcome is the diversity between biological replicates that cannot fit a Poisson distribution as previously thought, resulting in the development of negative binomial models to reduce the elevated rate of false positives (Trapnell et al., 2012; Anders & Huber, 2010). The Benjamini-Hochberg correction has been developed as a statistical correction to address the issue of false rate discovery (Benjamini & Hochberg, 1995).

There are many programs available for differential expression analysis of RNA Seq data and comparison of many of the available programs has been made (Seyednasrollah et al., 2013), however conclusions suggest that no one pipeline will be suitable under all circumstances. In this chapter, three algorithms were adopted for differential expression analysis, two adopting the negative binomial model – **EdgeR** (Robinson et al., 2009) and **DeSeq** (Anders & Huber, 2010). **Cuffdiff** works at the transcript level to align individual transcripts to the genome and then perfom DE analysis (Trapnell et al., 2012). **Cuffdiff** itself has been suggested to be a superior DE algorithm (Trapnell et al., 2013). However three algorithms were used here in an attempt to identify high confidence targets across them.

Importance has been placed upon the method of RNA extraction used for EV RNA studies (Eldh et al., 2012) and by comparing some of the commonly used EV RNA extraction methods as it is believed that the lipid composition of EVs may play a role in RNA extraction (Laulagnier et al., 2004). Different RNA extraction methods may also produce different yields of RNA (Eldh et al., 2012) and indeed the amount of microRNA found in preparations requires further investigation, with some studies reporting less than one microRNA per extracellular vesicle (Chevillet et al., 2014). This work has attempted to characterise RNAs in EVs involved in the radiation response and although numerous mRNA changes were identified, few, if any, miRNA changes were discovered. This is consistent with previous work (Arscott et al., 2013) and future work will test the hypothesis that miRNA changes in EVs are minimal or below the limit of detection in some cases.

5.6. Conclusion

In conclusion, the results in this chapter have revealed RNAs involved in the radiation response in parent cells and EVs derived from unirradiated and irradiated cells, suggesting that these RNAs might play a functional role in the bystander effect.

EV RNA has been traditionally studied using qPCR and microarray technology, however more recently next generation RNA sequencing studies have aimed to more sensitively explore the RNA contents of the EVs (Nolte-'t Hoen et al., 2012; Jenjaroenpun et al., 2013; Bellingham et al., 2012) and report, as previously mentioned, the presence of mRNAs and a variety of small RNAs and some long-coding RNAs. In this chapter, the RNA Seq results reporting not only mRNAs including the anti-apoptotic protein *ANP32B* and *NET1* guanine nucleotide regulatory protein, but also the long non-coding RNA *MALAT1* and the microRNA-17-92 host gene cluster. The work in the next chapter aims to functionally test these RNAs

Chapter 6

Functional study of candidate genes identified by RNA sequencing

Chapter 6 Functional study of candidate genes identified by RNA sequencing

6.1. Introduction

The study of individual gene deregulation in response to stress such as ionizing radiation is important as it facilitates pathway modelling and other bioinformatic processes such as GO term analysis. The knockdown of genes using RNAi facilitates the study of gene knockdown in a variety of living systems (Agrawal et al., 2003) and is derived from study of the natural system that protects against retrotransposons and viral genetic threats harmful to the host organism (Hammond et al., 2001). Consequently, siRNAs or shRNAs can be developed to knock down desired genes to then observe changes in cell phenotype.

Few studies document gene knockdown and the radiation induced bystander effect. Recently it was shown that overexpression of the *SIRT1* gene had the ability to prevent ROS production following γ-irradiation, whereas its knockdown permitted accumulation of ROS (Xie et al., 2015). Upregulation of *c-myc* by *SIRT1* appeared to mediate this process that was also amplified by hypoxia, suggesting that multiple stresses may act to amplify DNA damage effects. In another study, COX-2 knockdown in irradiated HeLa cells overexpressing connexin26 junctions reduced bystander effect but resulted in increased micronuclei formation in bystander cell progeny (Zhao et al., 2014). COX-2 knockdown also affected connexin-MAPKKK interaction at the plasma membrane, known to play a significant role in bystander signalling, demonstrating that a single gene knockdown has the ability affect several key pathways of the bystander response. TGF-ß knockdown has also been shown to cause changes in bystander signalling (Temme & Bauer, 2012) and EVs have also been shown to have the capacity to shuttle siRNA between cells following electroporation of the EVs (Alvarez-Erviti et al., 2011). Knockdown of key proteins involved in the DNA damage response, DNA-PKcs, has also been shown to induce mutation formation in directly irradiated p53 mutant cells, but not in wild-type or p53 null cells (Zhang et al., 2008). P53 status, however, did not change observed increased mutagenesis in the bystander cells. The differences in response between directly irradiated and bystander cells suggests different pathway modulation within directly irradiated and bystander cells (Zhang et al., 2008).

Gene knockdown has also been shown to be able to change the biological functions or release of EVs from cells. Knockdown of *nSMase1* and *nSMase2* involved in the neutral sphingomyelinase pathway has been shown to reduce extracellular vesicle release and be necessary for packaging of prions into EVs (Guo et al., 2015). Furthermore knockdown of *WNT-4* abrogated the ability of EVs derived from human umbilical cord mesenchymal cells to accelerate wound healing (Zhang et al., 2014). These EVs were no longer able to cause skin cell proliferation or *ß-catenin* activation

following infliction of a burn wound demonstrating a potent role of extracellular vesicle cargoes in intercellular communication.

In addition to the functional role of their cargo, the details of extracellular vesicle uptake have yet to be fully elucidated (Mulcahy et al., 2014), however, a variety of routes have been documented and heparin treatment, for example, has been shown to prevent phenotypic changes in cells (Franzen et al., 2014; Barrès et al., 2010). Cellular uptake of radiation EVs has been shown to increase due to localisation of CD29 and CD81 on the cell surface, with knockdown of CD29 preventing radiation extracellular vesicle uptake (Hazawa et al., 2014), however there are no studies published demonstrating that knockdown of RNAs in EVs can affect modulation of the bystander effect. The work in this chapter therefore aims to test the functional significance of the RNA Seq candidates obtained in the previous chapter by performing knockdown of the candidates and will identify genes that play functional roles in the radiation response of MCF7 cells and the bystander effect.

6.2. Materials and methods

6.2.1. siRNA transfections

For knockdown of MCF7 cells, cells were seeded into 6-well plates at 0.3 x 10^6 cells/well and incubated overnight. The following day cells were transfected with RNA Seq candidate siRNAs or negative control siRNA (Table 6.1) at 25 nM per well using 6.6 µl per well DharmaFECT 1 reagent (Fisher, 11846654) as per manufacturer's recommendations for MCF7 cells. Cells were incubated for 48 hours and harvested for use in the alkaline comet or nuclear fragmentation assay, or for RNA extraction and qPCR to verify knockdown level.

Table 6.1. siRNAs purchased for use in knockdown experiments.

Gene	Company	Product number
NET1	Qiagen	SI02662086
ANP32B	Qiagen	SI02655380
NCL	Qiagen	SI02654925
HSP90AA1	Qiagen	SI02635024
MALAT1	Sigma	SASI_Hs02_00377093
Universal Negative Control #1	Sigma	SIC001

6.2.2. MTT cell viability assay

For the MTT cell viability assay, MCF7 cells were plated at 1 x 10^6 cells in 96-well plates per well 24 hours prior to siRNA transfection using 25 nM siRNA. Cells were then allowed to recover for a further 48 or 72 hours before 40 mg/ml MTT reagent (Sigma, M5655) was added to the media and incubated at 37°C, 5% CO_2, for 4 hours in the incubator. The media and MTT reagent were then removed carefully from wells to avoid crystal aspiration and 100 µl MTT solvent (4 nM HCl, 0.1% IPEGAL in isopropanol) added to each well. Plates were read on an absorbance plate reader at 595 nm with a reference filter of 620 nm and statistics calculated using the Student's t test.

6.2.3. Nuclear fragmentation assay

Cells were pelleted, washed with PBS and fixed with 3:1 methanol:acetic acid fixative dropwise to resuspend the pellet and incubated at room temperature for 15 minutes. Fixed cells were dropped onto microscope slides and air-dried for 30 minutes. Slides were mounted in the dark using 30 µl prolong gold antifade mountant with DAPI (Invitrogen, P36931) using a coverslip. Slides were left to cure for 24 hours and two hundred cells were counted per slide and analysed using a fluorescent filter at 365 nm. The Chi-squared test of independence was used for statistical analysis.

6.2.4. Alternative comet assay analysis

Due to a technical problem with the Komet v5.5 software detailed in the Materials and methods chapter (section 2.4), an alternative analysis software was used for the comet assay in this chapter as follows.

Individual pictures of the individual slides were taken and saved onto an external harddrive. Casplab software was downloaded (http://casplab.com/download) and the picture series for each sample loaded into the Casplab program. At least 100 comets were scored per slide and the Excel sheet recorded for each set of pictures saved. The percentage tail DNA damage for each sample was then processed as before using SPSS for the Mann-Whitney statistic (section 2.4). Due to the large amount of comet slides produced in this experiment, several electrophoresis runs were performed with controls and are indicated on graphs.

6.3. Results

6.3.1. siRNA mediated knockdown of candidate genes in MCF7 cells

In order to study the functional effects of siRNA mediated knockdown of the candidate genes upregulated in 2 Gy EVs (Table 5.6), single siRNAs were purchased and transfected into MCF7 cells (Table 6.1). Unirradiated MCF7 cells were first transfected to test the level of knockdown prior to radiation experiments. Results demonstrated that all siRNAs caused knockdown of the desired gene as assayed using qPCR (Figure 6.1). Results demonstrated that all siRNAs induced > 50% knockdown, signifying that the siRNAs selected were suitable for the knockdown of the candidate genes in MCF7 cells.

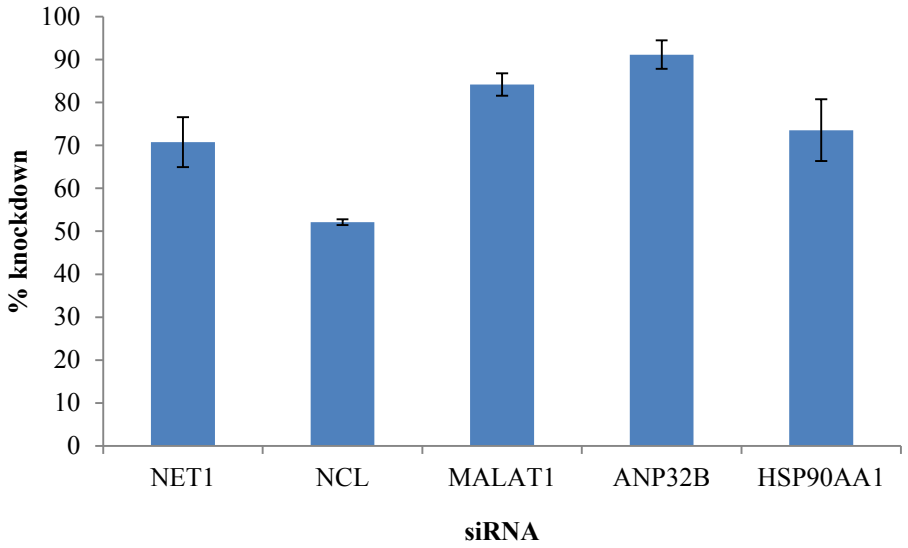

Figure 6.1. Knockdown of genes using single siRNAs resulted in 50-90% knockdown efficiency. *25 nM siRNA transfected into MCF7 cells and assayed by qPCR at 48 hours post transfection. Two to three biological replicates. *p<0.05, error bars SD.*

6.3.2. Effect of siRNA transfection on cell viability

In order to test cell viability following transfection, cells were transfected with the siRNAs and assayed at forty-eight to seventy-two hours post transfection. Results demonstrated that two days post transfection there was a significant drop in cell viability of around 40% for all siRNAs when compared to the untreated growth control (Figure 6.2). Three days post transfection, a significant increase in cell viability was observed for all siRNAs, except for the *NET1* and NEG (negative control) siRNAs. This observation suggests that cell regrowth is occurring at 72 hours post transfection.

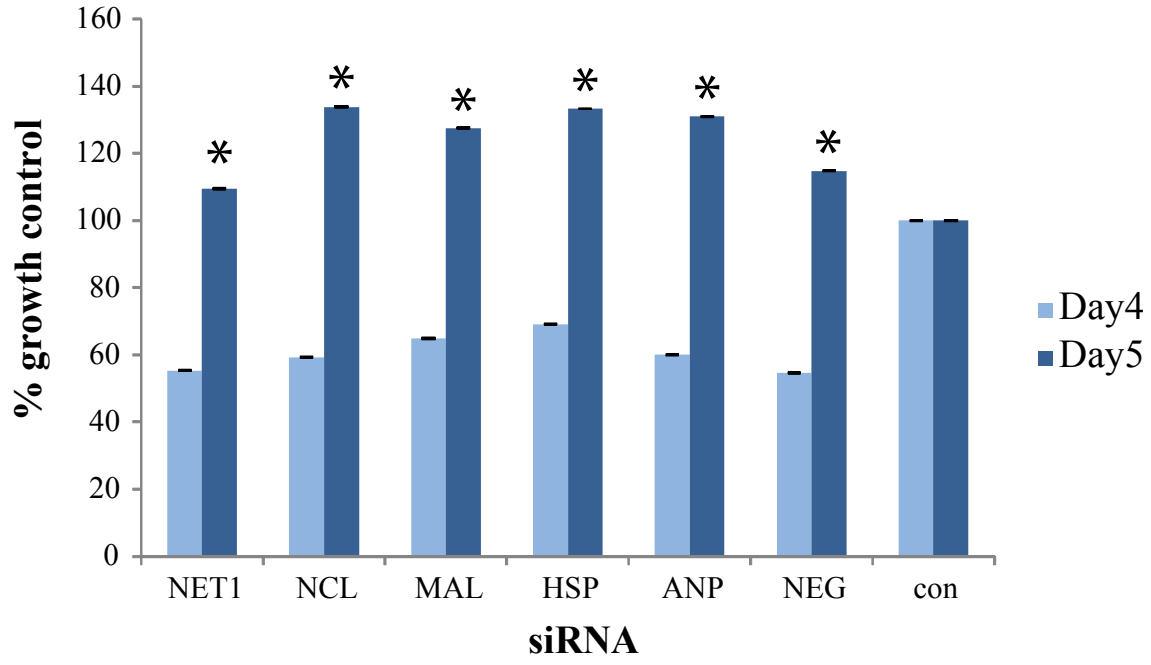

Figure 6.2. Viability of cells following siRNA transfection at 48 or 72 hours post transfection. *MTT assay, values reported as % of the untreated growth control. Eight biological replicates, *p<0.05, t test. Error bars = SD.*

6.3.3. Knockdown of RNA Seq candidate genes reduces DNA damage in MCF7 cells

In order to test the effect of siRNA transfection on DNA damage levels in MCF7 cells, siRNA knockdown was performed and DNA damage measured using the comet assay. Knockdown of *HSP90AA1*, *MALAT1* and *NET1* knockdown significantly reduced levels of DNA damage compared to the negative control. Knockdown of NCL and *ANP32B* however did not result in any significant difference in DNA damage compared to the negative siRNA control (Figure 6.3). Taken together these results suggest that knockdown of three genes affects DNA damage response in normal cells. Consequently this might be due to a direct effect of knocking down those particular genes on the DNA response of the cell.

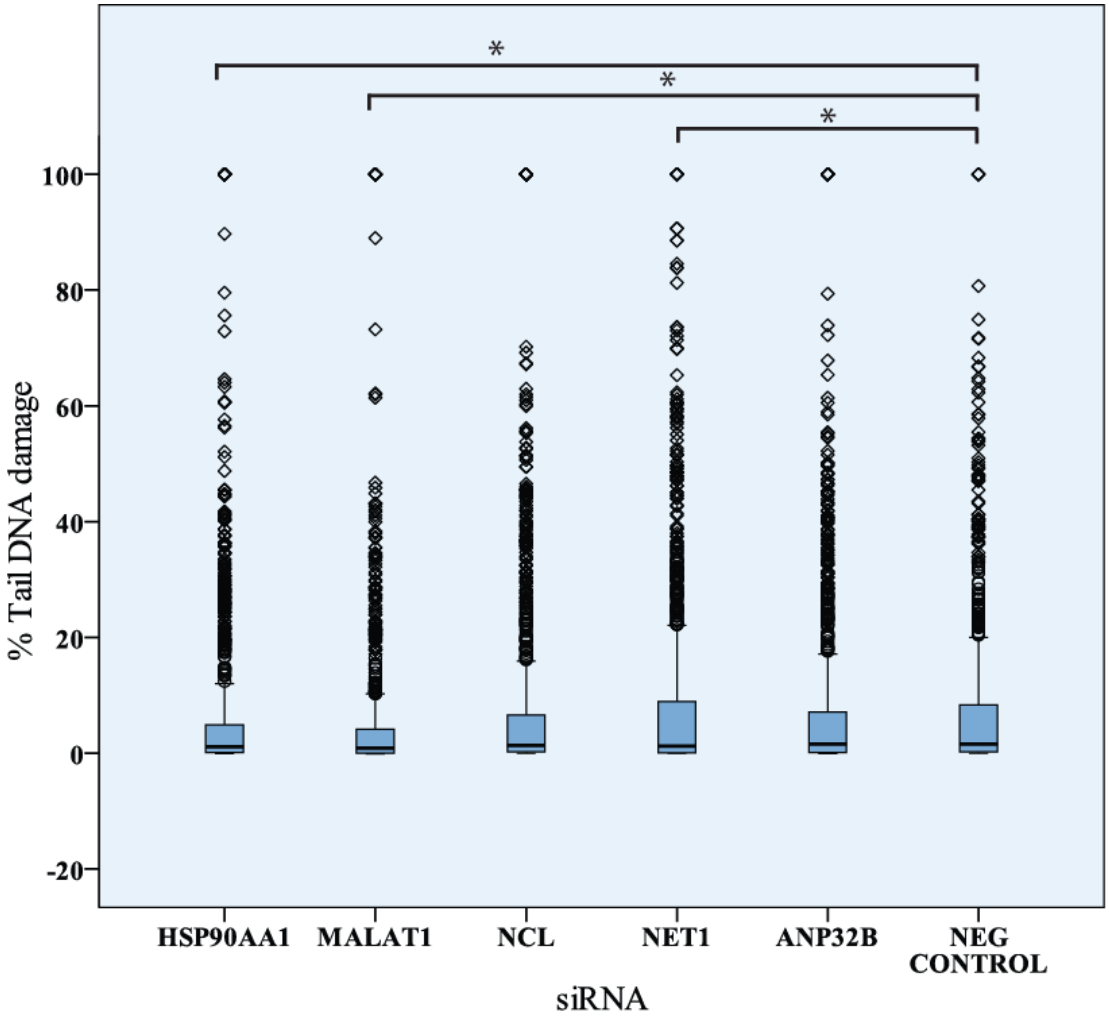

Figure 6.3. Effect of siRNA knockdown on DNA damage in unirradiated MCF7 cells. *Three biological replicates. NCl vs NEG (p=0.494). ANP vs NEG (p=0.143). Mann-Whitney test. (n = 200). Circles represent outliers and diamonds represent extreme outliers. *p<0.05.*

6.3.4. Knockdown of apoptosis related genes results in increased levels of apoptosis in MCF7 cells.

Following the above knockdown of the candidate genes in MCF7 cells, the DAPI nuclear fragmentation assay was used to investigate levels of apoptosis in the transfected MCF7 cells, in particular following knockdown of apoptosis associated genes *ANP32B* and *NET1*. Results demonstrated that the majority of the genes induced apoptosis in siRNA transfected cells compared to the negative control. *NET1* siRNA transfection demonstrated the most substantial increase in apoptosis induction, followed by *ANP32B*. Results were not significant, however compared to the negative control a trend is apparent (Figure 6.4). Taken together these results suggest that the siRNAs are able to knock down the genes in MCF7 cells and that this process has some effects on apoptosis and DNA damage induction of the cells. Consequently the siRNAs were carried forward for use in the next part of this chapter.

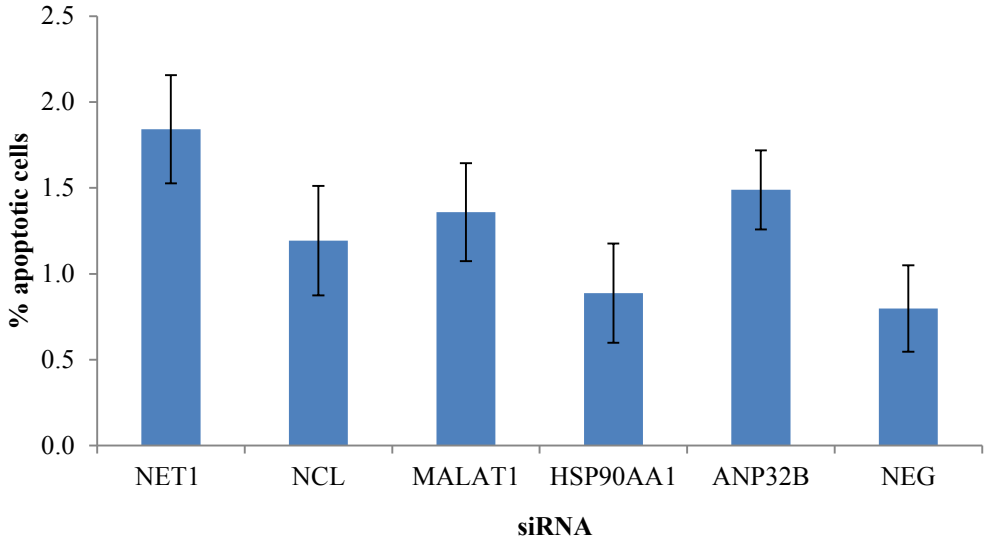

Figure 6.4 Percentage of apoptotic MCF7 cells following siRNA transfection. *Cells were transfected with the siRNAs and assayed for apoptosis. Three biological replicates. Chi-squared test of independence, n = 200.*

6.3.5. Knockdown of candidate genes in directly irradiated cells

In order to test the effects of knockdown of the candidate genes on DNA damage response in directly irradiated cells, MCF7 cells were transfected with siRNAs, irradiated and then assayed for DNA damage using the alkaline comet assay. In electrophoresis run 1 (Figure 6.4). *NET1* demonstrated the traditional induction in DNA damage following 2 Gy irradiation as per the comet assay, however in the NCL knockdown cells there was no significant induction of DNA damage in response to 2 Gy X-rays, suggesting that knockdown of NCL specifically prevents DNA damage in response to 2 Gy irradiation. In run 2 for *ANP32B* and *MALAT1* the normal significant increase in DNA damage following 2 Gy irradiation occurred (Figure 6.6). The *MALAT1* 0 Gy and 2 Gy damage results appeared very similar but were significantly different as per the Mann-Whitney test. For run 3 HSP90AA1 demonstrated a significant induction in DNA damage in response to radiation (Figure 6.7). The control and negative scrambled siRNA worked for all runs with all showing a significant increase in DNA damage following X-ray exposure. Altogether these results suggest that the majority of the gene candidates do not appear to have a significant role in the DNA damage response of directly irradiated cells and so the recipient cells were also assayed for changes in DNA damage.

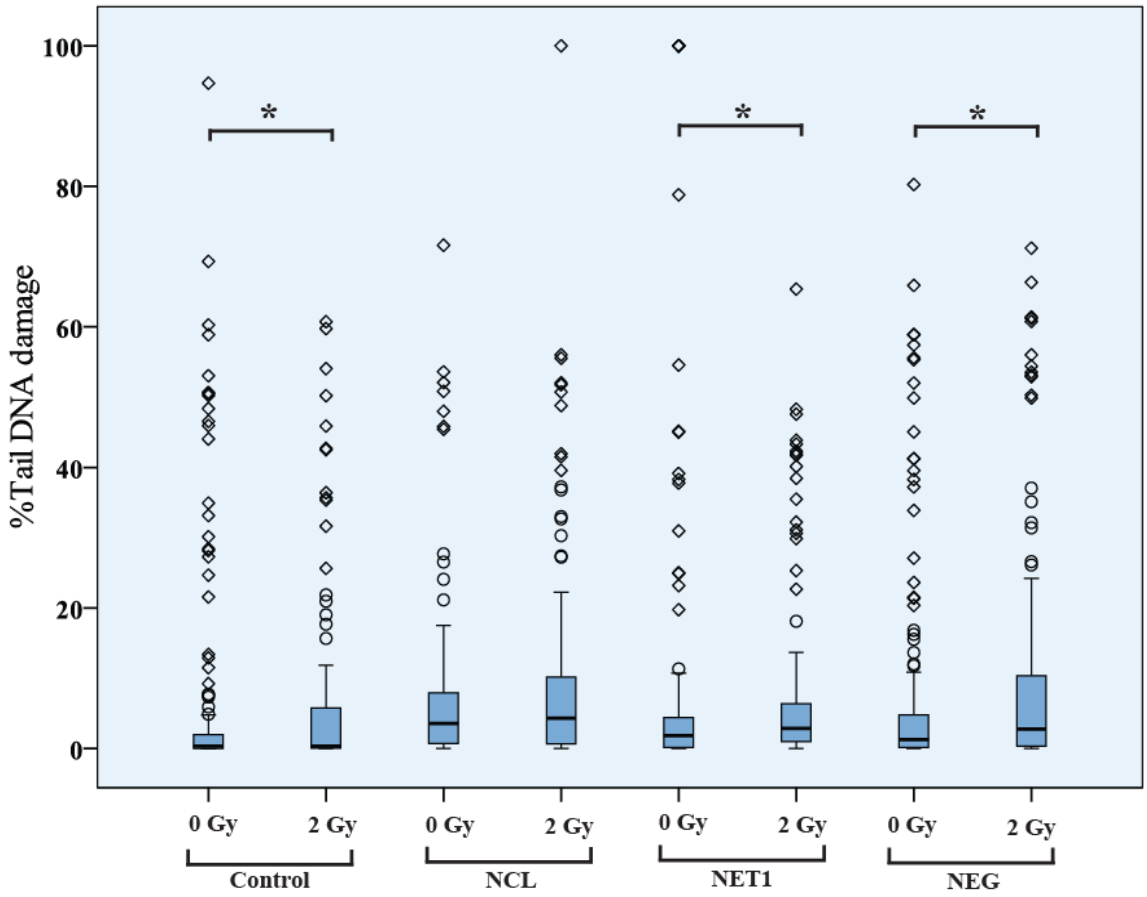

Figure 6.5. Effect of siRNA knockdown on DNA damage in directly irradiated cells (Run 1). *Control sample refers to no siRNA knockdown. NCL, NET1 and NEG refer to siRNA knockdown. Mann-Whitney test, *p <0.05. Three biological replicates (n = 100-200).*

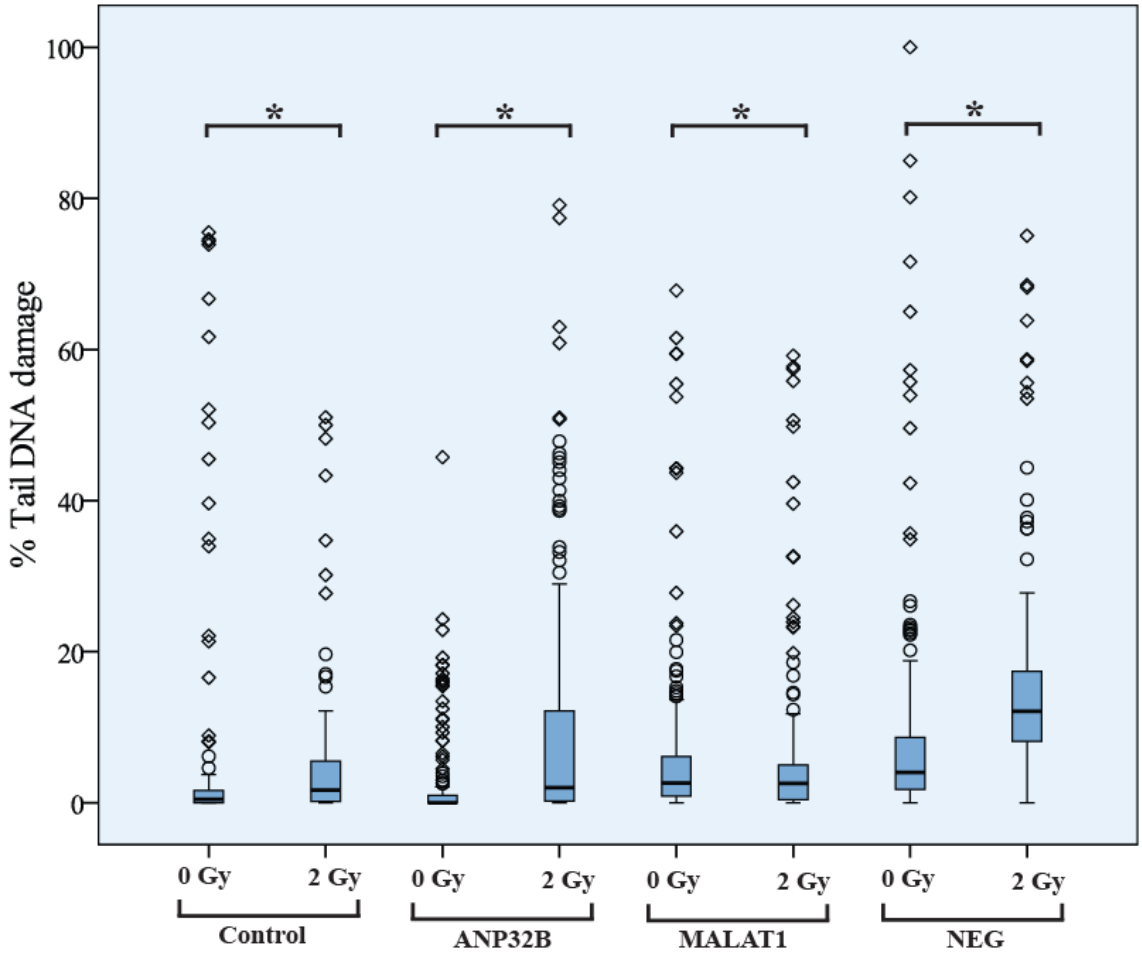

Figure 6.6. Effect of gene knockdown on DNA damage in directly irradiated cells (Run 2). *Control sample refers to no siRNA knockdown. ANP32B, MALAT1 and NEG refer to siRNA knockdown. Mann-Whitney test, *p <0.05. Three biological replicates (n = 100-200).*

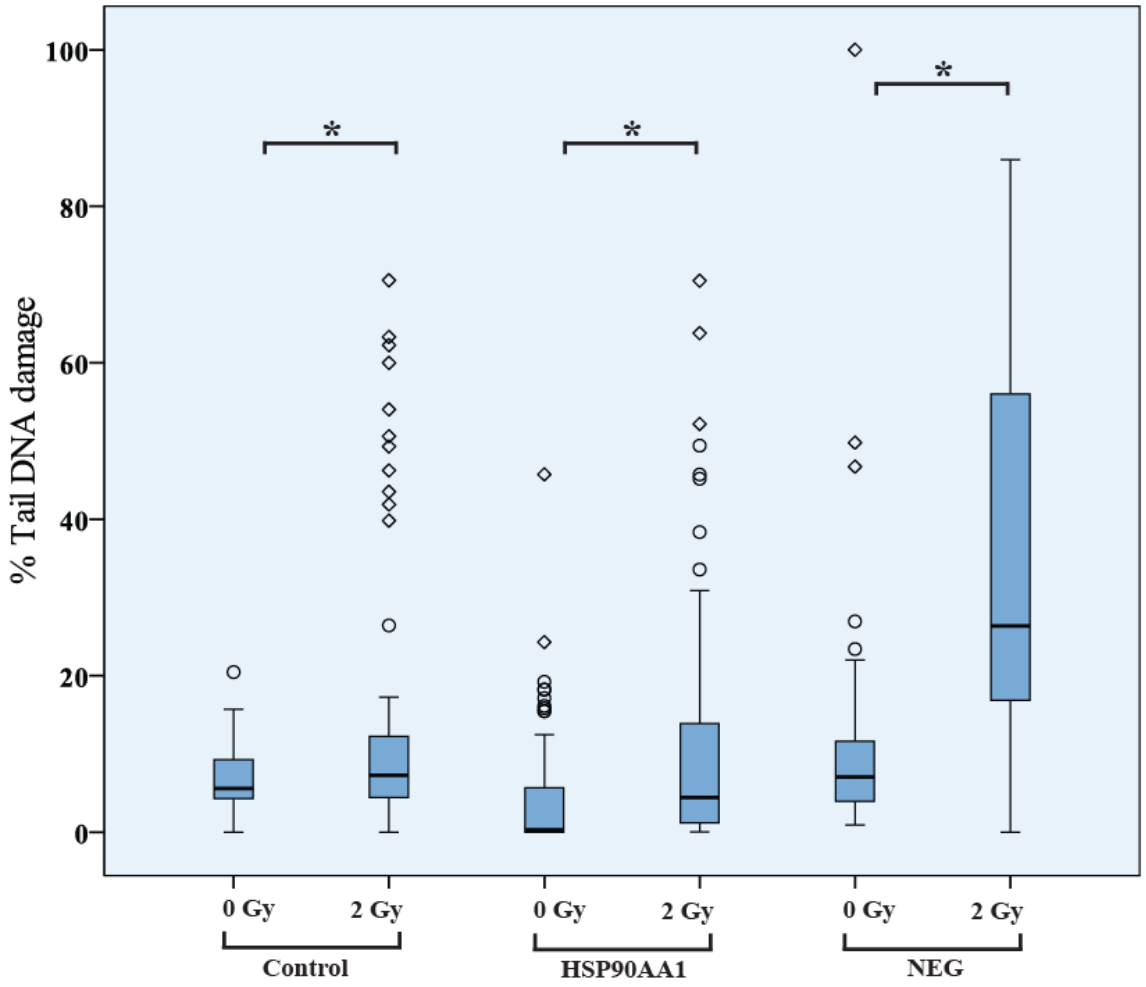

Figure 6.7. Effect of gene knockdown on DNA damage in directly irradiated cells (Run 3). *Control sample refers to no siRNA knockdown. HSP90AA1 and NEG refer to siRNA knockdown. Mann-Whitney test, *p <0.05. Three biological replicates (n = 100-200).*

6.3.6. Knockdown of genes in directly irradiated cells and apoptosis

In order to test the effect of gene knockdown on apoptosis in directly irradiated cells, the nuclear fragmentation assay was performed on the same samples as for the comet assay (Figure 6.8). In 2 Gy directly irradiated cells there was an increase in apoptosis for the control sample, however not significant. For the negative control siRNA there was a significant increase in apoptosis in response to 2 Gy X-rays. For the *MALAT1*, *HSP90AA1*, NCL and *NET1* siRNAs there was an increase in apoptosis, however not a significant induction. For *ANP32B* knockdown there was a marked reduction in apoptosis following 2 Gy radiation. *ANP32B* is an anti-apoptotic protein; therefore the knockout would be expected to permit higher amounts of apoptosis to occur. These results together suggest that the apoptotic response to radiation is perhaps different to the DNA damage response to radiation.

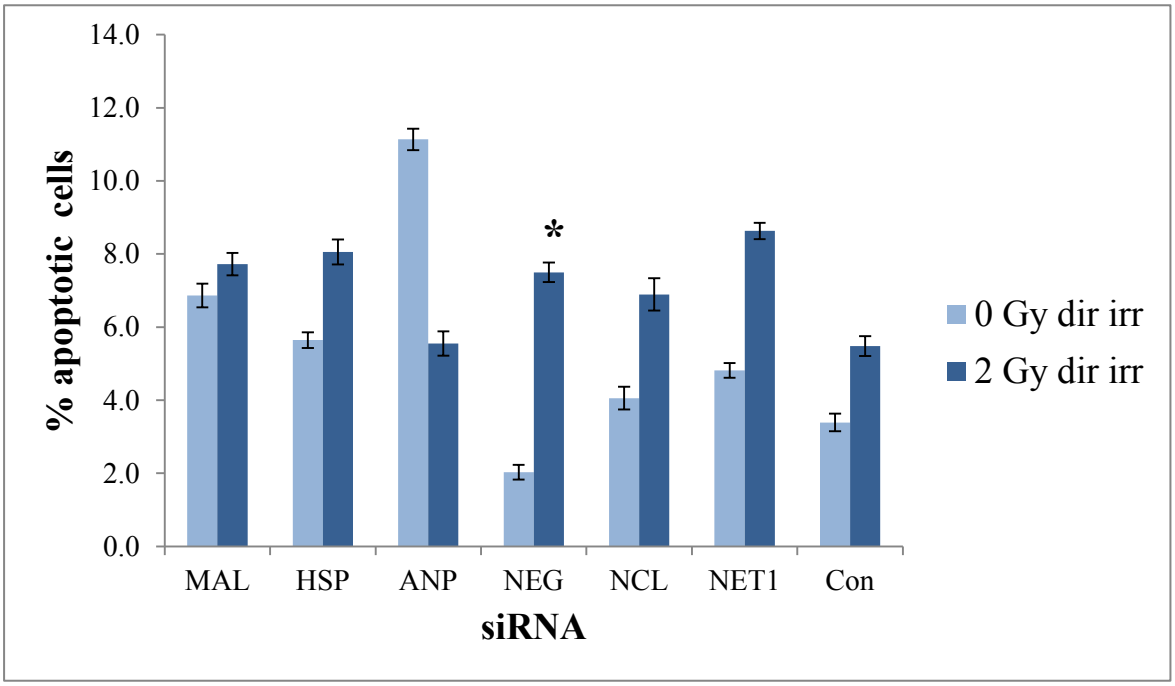

Figure 6.8. Effect of siRNA knockdown on apoptosis in directly irradiated cells. *Three biological replicates. Chi-squared test of independence, n = 100. Error bars = SEM. *p<0.05.*

6.3.7. Effect of direct irradiated MCF7 cell knockdown on bystander induction in recipient cells

In order to test the ability of the directly irradiated knockdown cells to induce bystander effects in recipient cells following media transfer, the media was taken from the above cells 4 hours post irradiation, filtered and placed onto recipient cells for 24 hours. Results demonstrated that transmission of DNA damage via media transfer in classic bystander effect was disrupted. For run 4, classic bystander response was observed for media from *NET1* and NEG knockdown cells, with an increase in DNA damage in response to media from 2 Gy irradiated cells (Figure 6.9). For *MALAT1* there was no significant damage induced between the unirradiated and irradiated cells, suggesting that MALAT1 knockdown prevents bystander induction in recipient cells. The control for run 4 showed a significant down-regulation of DNA damage in the 2 Gy cells. This might be attributed to problems with the 0 Gy control slides as the level of DNA damage observed is not normally seen even in 2 Gy irradiated cells. In run 5 *ANP32B* and NCL knockdown induced a statistically significant drop in DNA damage in response to 2 Gy X-rays (Figure 6.10). These results suggest that the knockdown of the genes identified in the RNA Seq analysis has caused a functional change in the bystander recipient cells, whereby the normal DNA damage responses observed are changed. Following *HSP90AA1* knockdown there was no longer a significant increase in DNA damage in response to 2 Gy irradiation.

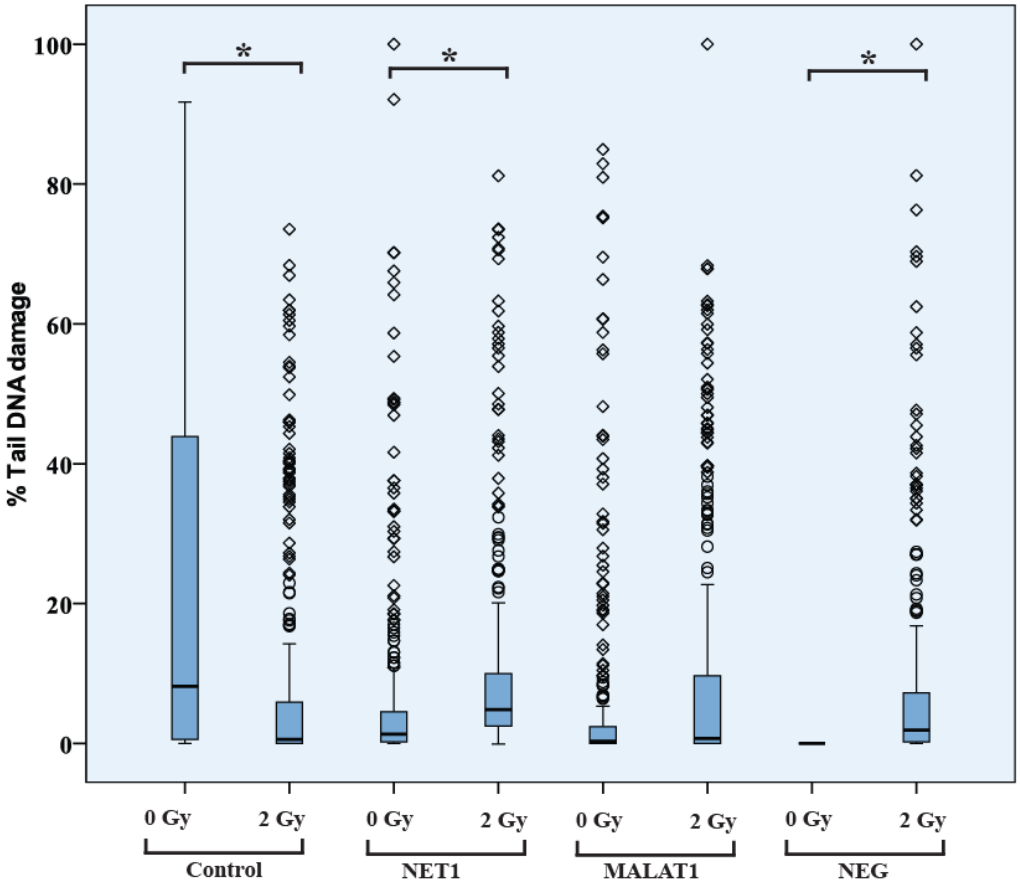

Figure 6.9. Effect of gene knockdown on DNA damage in bystander recipient cells (Run 4). *Three biological replicates. Mann-Whitney test, *p <0.05, (n = 200). Circles represent outliers and diamonds represent extreme outliers.*

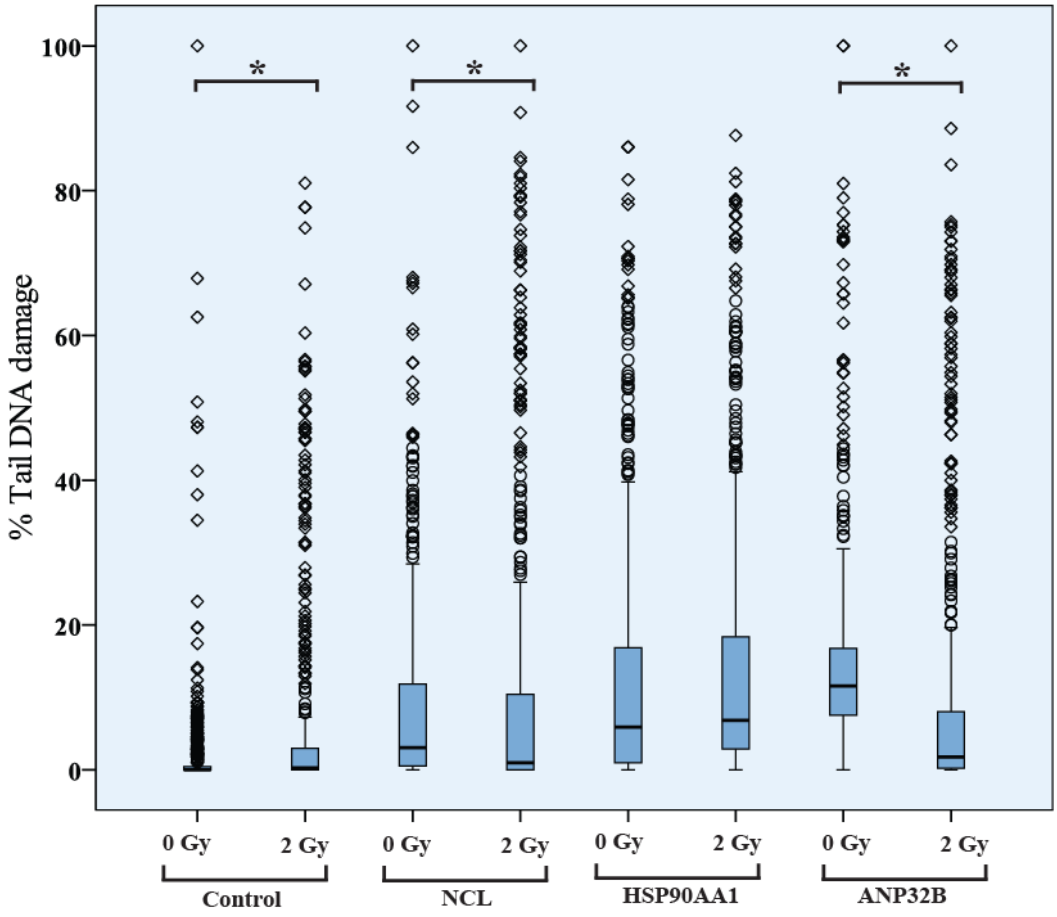

Figure 6.10. Effect of gene knockdown on DNA damage in bystander recipient cells (Run 5). *Three biological replicates. Mann-Whitney test, *p <0.05, (n = 200). Circles represent outliers and diamonds represent extreme outliers.*

6.4. Discussion

The results in this chapter have tested the functional significance of the RNA Seq candidate genes in chapter 5, namely by measuring the effect of their knockdown on DNA damage and apoptosis induction in cells. Knockdown of many of the genes resulted in changes in the DNA damage response in both directly irradiated and bystander cells, suggesting that the RNA Seq analysis produced candidates that do play functional roles in the radiation response. Further study of these genes will help to better understand their role in radiation response and the bystander effect.

In this chapter siRNA knockdown of the selected RNA Seq candidates was performed producing a knockdown of 50–90% in unirradiated MCF7 cells (Figure 6.1). This suggested that the siRNAs were suitable for use in preliminary knockdown experiments.

6.4.1. Effect of *NET1* knockdown

NET1 knockdown did not affect DNA damage induction in irradiated cells nor in the bystander cells despite the literature reporting a role for *NET1* in the radiation response. Knockdown of *NET1* has been shown to increase RhoB activity and also JNK pathway activation, leading to cell death in response to ionizing radiation (Srougi & Burridge, 2011). Furthermore, the Rho GTPases, known to be controlled by *NET1,* have been shown to play a role in activation of the ATM pathway known to be involved in bystander response (Burdak-Rothkamm et al., 2008; Oh & Frost, 2014). It is possible that different doses or time points would induce changes in *NET1* modulation, or alternatively that it is not deregulated in MCF7 cells or may not be involved in the bystander effect. *NET1* knockdown did not affect apoptosis induction in directly irradiated cells, suggesting that is also does not cause apoptosis in response to 2 Gy X-rays.

6.4.2. Effect of *HSP90AA1* knockdown

In directly irradiated cells, knockdown of *HSP90AA1* had no effect on DNA damage levels, however knockdown abrogated the ability of the cell media to induce significant DNA damage in recipient cells, suggesting that it may be involved in DNA damage induction. *HSP90* is key in the anti-apoptotic response and has been shown to be upregulated in a wide variety of cancers (Whitesell & Lindquist, 2005) and its knockdown has also been shown to inhibit breast tumour growth by ErbB (Schulz et al., 2012). Interestingly *HSP90α* has also been shown to be released from cells on EVs, playing a role in the increase of cell motility in invasive cells (McCready et al., 2010). There was no notable effect on apoptosis in directly irradiated cells following knockdown.

6.4.3. Effect of *ANP32B* knockdown

Knockdown of *ANP32B* had no effect upon DNA damage in directly irradiated cells, however, like NCL knockdown, the transfer of media from *ANP32B* knockdown cells resulted in lower levels of DNA damage observed in bystander cells, suggesting that *ANP32B* is required for DNA damage induction in recipient cells. Furthermore *ANP32B* knockdown led to a marked, but not significant,

reduction in apoptosis in directly irradiated cells. It might be expected that knocking down an anti-apoptotic protein might induce damage to the cell, however *ANP32B* has been shown to affect apoptosis via caspase-3 apoptotic response (Shen et al., 2010), therefore further work would be required to understand the response observed.

6.4.4. Effect of NCL knockdown

Unlike the other genes NCL knockdown resulted in changes in the DNA damage response in both directly irradiated and bystander cells. NCL knockdown in directly irradiated cells prevented DNA damage formation, suggesting that it plays a role in DNA damage induction following irradiation. NCL plays an important role in the stability of mRNAs, for example *BCL-2* and is a protein abundant in the nucleolus of the cell (Srivastava et al., 1999). It has also been suggested that it plays a role in processing pri to pre-microRNA for mir-15a and mir-16 (Pickering et al., 2011) and in the maturation mir-21 (Pichiorri et al., 2013). Interestingly, mir-16 was identified as one of the top deregulated microRNAs following radiation exposure and in the general stress response as per the miRStress database (Table 3.2). Furthermore mir-21 is the top deregulated microRNA in response to general stress and radiation stress (Jacobs et al., 2013). This suggests that there may be interaction between microRNAs and the candidate genes in radiation response and the bystander effect. Following media transfer from NCL knockdown cells, a significant drop in the levels of DNA damage was observed in bystander cells suggesting a protective effect of NCL knockdown in recipient cells.

Taken together this might suggest that preventing NCL transfer from directly irradiated to recipient cells prevents DNA damage. Indeed it has been shown that Nucleolin interrupts nucleosome disruption that facilitates DSB repair (Goldstein et al., 2013) and also NCL knockdown has also been shown to prevent mechanisms by the cell that are in place to prevent stress-induced cell death (Wang et al., 2014).

6.4.5. Effect of *MALAT1* knockdown

No significant effect on DNA damage was observed following *MALAT1* knockdown in directly irradiated cells although visually the DNA damage levels appeared very similar between 0 Gy and 2 Gy irradiated cells. *MALAT1* knockdown abrogated the ability of the cell media to induce significant DNA damage suggesting that it normally plays a role in DNA damage induction in bystander cells. *MALAT1* has been shown to be induced in directly irradiated cells (Chaudhry, 2013) and despite the work described here demonstrating that it does not have an immediately obvious effect on apoptosis in directly irradiated cells, it has been shown to be reduced in cells undergoing apoptosis in response to genotoxic assault (Özgür et al., 2013).

MALAT1 (also known as *NEAT1*) was one of the first long non-coding RNAs to be discovered (Ji et al., 2003) and is highly conserved across mammalian species (Bernard et al., 2010). Its mechanism of action includes cleavage of its 3' –end to produce a small mascRNA fragment that

moves to the nucleus while the longer transcript is retained in the nucleus in nuclear speckles (Wilusz et al., 2008). Due to its upregulation in a wide variety of cancers it has been reported as a biomarker of malignancy and has been shown to be implicated in metastasis and cell proliferation (Hu et al., 2015; Tripathi et al., 2013; Lin et al., 2007). Despite its association with a number of important cellular processes *MALAT1* is not required for pre- or post-natal development in mice (Zhang et al., 2012). This suggests that *MALAT1* may work under conditions of stress, whereby an organism or cell experiencing normal conditions does not require it, however that under conditions of stress, it is deregulated and is important in the cellular response to external stressors.

6.5. Conclusions

Knockdown of genes believed to play a role in the radiation response and induction of BE in association with EVs has not yet been reported in the literature. The results reported in this chapter tested whether candidates produced by RNA sequencing analysis play a functional role in radiation response in directly irradiated and bystander cells. Results identified that genes such as NCL and *MALAT1* do indeed appear to play a functional role in DNA damage induction in directly irradiated and bystander recipient cells. Results also suggest that the apoptotic response does not mirror the DNA damage response of cells and that further work is required in this area. Future work is required focusing on the action of these genes using different approaches such as overexpression vectors and EV transfer experiments. Investigation of the interplay between the RNA and miRNA response to radiation would also be of value.

Chapter 7

Discussion

Chapter 7 Discussion

Our current understanding of the role of EVs in the radiation induced bystander effect is still limited. Studies have identified their role in the mediation of bystander damage (Al-Mayah et al., 2015; Al-Mayah et al., 2012; Jella et al., 2014). Despite the exciting discovery of these EVs in radiation response, further characterisation of their size, morphology, cargo and release is still required. As EVs have also been shown to lose their ability to mediate bystander effect following RNase treatment (Al-Mayah et al., 2012; Al-Mayah et al., 2015), a key question is what type of RNA species are involved in the transmission of the observed bystander effect? Furthermore, the mode of action of these RNAs and their targets in recipient cells would help to elucidate the components of the bystander effect mechanism.

Regarding EVs, we now know that they are involved in intercellular communication for a wide variety of biological processes and that they contain a characteristic RNA cargo, particularly under different conditions of stress (de Jong et al., 2012; Eldh et al., 2010). Developments in technology are leading to new extraction and quantification protocols required for the study of EVs. Further work is also required on the standardisation and validation of these procedures so that we can better understand EV release and function. Additionally, as more studies emerge documenting the use of next-generation sequencing technology to study EV RNA, our understanding of the species loaded into EVs will expand.

Regarding the radiation induced bystander effect, it is well accepted that media from irradiated cells has the ability to induce a variety of biological damage effects such as apoptosis, chromosomal damage and mutations in recipient cells that have not been irradiated (Kadhim et al., 2013). Candidate molecules have been relatively well characterised as various cytokines and reactive oxygen species, DNA damage response of bystander cells is also similar to that of directly irradiated cells, but with some nuances. How genomic instability develops in the progeny of the irradiated and bystander cells also requires further investigation to clarify which mechanisms are involved.

Based upon the above knowledge, this study was set up to identify candidate mRNAs and non-coding RNAs released from MCF7 cells in EVs in response to ionizing radiation. Further to this, the RNA candidates could then be functionally tested to begin to establish their role in DNA damage induction and bystander effect in recipient cells. Thus the key aims were proposed;

1. To identify novel microRNA candidates involved in the radiation response by performing a meta-analysis of the literature

2. To confirm that bystander effect was mediated by EVs using media transfer and extracellular vesicle/supernatant transfer experiments.

3. To characterise the vesicles released from directly irradiated cells, including sizing, quantification, morphology and density.

4. To extract and characterise EV RNA from the vesicles using RNA Seq and microRNA Seq to identify novel mRNA and microRNA candidates by comparing EVs released from 0 Gy and 2 Gy irradiated MCF7 cells.

5. To functionally test the role of the candidate RNAs in mediation of bystander effect by knocking out the RNAs identified and testing DNA damage and apoptosis levels.

The experiments described in this thesis aimed to address the above questions using a variety of approaches. A 2 Gy dose of radiation was used in the experiments as it is the typical therapeutic dose for radiotherapy, consequently its use would help to address the effects of BE applicable to the clinical setting. The benefits of the bystander effect have been cited as causing apoptosis and DNA damage leading to cell death in bystander cells in the irradiated volume, therefore preventing the accumulation of mutations and formation of malignancies, but not affecting unirradiated cells (Abdelrazzak et al., 2011). However, if mutations accumulate in unirradiated cells genomic instability can ensue in both directly irradiated, bystander cells and their progeny, up to 12 passages post irradiation (Al-Mayah et al., 2012).

The miRStress database analysis and the miRNA sequencing performed aimed to address the identification of novel microRNAs involved in the radiation response by two different approaches. The results in chapter three utilised a meta-analysis produced using the miRStress database to identify novel microRNA signatures involved in stress responses (Jacobs et al., 2013). Both established microRNA signatures and novel microRNAs not reported as functional in the literature were reported by the analysis. The miRstress database was also validated and shown to be accurate at predicting novel microRNAs. Study of the general stress response and the radiation response of cells are naturally interlinked and despite the different nature of the DNA damage caused by different agents there are likely to be similarities and crossovers in the responses. The miRstress database reflected this, with many of the top microRNAs involved in the general stress response present in the top twenty deregulated microRNAs in response to radiation. The database was also able to facilitate a more specific analysis of all of the microRNA deregulation in response to X-rays that identified some microRNAs that appeared specific to the X-ray response in comparison for all radiation responses together, demonstrating the utility of the database in comparison of individual and general stress responses. Further screens will be required in the study of radiation induced microRNAs, however the miRstress database can provide a starting point for analysis. Indeed a study released after publication of the miRStress meta-analysis confirmed that one of the putative candidates identified by the database had been shown to play functional role in cells in response to radiation (Leung et al., 2014). Consequently the value of the database is that it allows identification of candidates from across the literature that can then be tested functionally.

The experimental approach to microRNA deregulation in stress response came from the miRNA Seq analysis reported in chapter six. Total RNA was extracted from cells and EVs. Bioanalyzer profiles suggested the presence of microRNAs in the samples and the sizes of the RNAs in the extracellular vesicle samples reflected that of the literature, with a predominance of small RNAs present. MicroRNA sequencing was performed and differential expression of microRNAs between samples was compared. Some differences in microRNA composition between unirradiated and irradiated cells were reported, however there were no significant changes in microRNA contents between EVs derived from unirradiated and irradiated cells by miRprof analysis. This was an unexpected result, however other studies have demonstrated similar results, with numerous mRNA changes, but no notable microRNA changes between treated and untreated EVs (Arscott et al., 2013). High ribosomal RNA content is also likely to have concealed some of the deregulated microRNA transcripts as the sample was not as enriched in microRNA as desired. Whether EVs contain ribosomal RNA is an area of interest as originally they were shown to have minimal rRNA compared to the levels in the parent cells (Valadi et al., 2007) or compared to larger microvesicles or apoptotic bodies (Crescitelli et al., 2013). It is possible that the presence of dead cells is likely to contribute to rRNA in EV samples (Miranda et al., 2010), however with the advent of next-generation sequencing some studies report a larger rRNA component in extracellular vesicle preparations than previously expected (Jenjaroenpun et al., 2013; Miranda et al., 2014).

Overall, microRNAs predicted to be involved in radiation response were identified by miRStress and miRNA Seq, but their interaction with EVs is not yet clear. Further work would help to elucidate how microRNAs are packaged into EVs and whether their transport between cells via EVs is involved in the bystander effect. Furthermore, it has been suggested that microRNAs are present at as little as one transcript per hundred EVs, therefore further characterisation of the microRNA content of EVs is generally required (Chevillet et al., 2014). Selective loading of microRNAs into EVs has been suggested following with a drop in microRNA level in directly damaged podocytes but a significant increase in EVs, supporting the idea that miRNAs may be selectively loaded into EVs under different stressed conditions (Ichii et al., 2014). MicroRNAs have also been shown to contain zip-code like sequences that are believed to mediate their movement into EVs (Bolukbasi et al., 2012). Consequently, the selective packaging of microRNAs into EVs is indeed plausible and would support the concept that microRNAs are directed to surrounding cells in the mediation of stress responses.

The results in chapter two confirmed that the extracellular vesicle fraction of the media taken from 2 Gy irradiated cells had the ability to induce bystander effect in recipient cells as in previous studies (Al-Mayah et al., 2015; Al-Mayah et al., 2012; Jella et al., 2014). Furthermore, it was demonstrated that the EVs released from the 2 Gy cells had specific characteristic properties. Firstly there was a greater than two-fold increase in the number of EVs released from the 2 Gy cells, as previously demonstrated (Jella et al., 2014; Lehmann et al., 2008). This suggests that there is an active response of extracellular vesicle release in response to ionizing radiation, suggesting a

potential deliberate removal of material from the cell or intentional signalling to surrounding cells. Treatment of cells with calcium has also been shown to increase the excretion of EVs from cells (Savina et al., 2003) and as previously mentioned rapid calcium influxes have been documented as part of the bystander response (Azzam et al., 2002). Conditioned media from irradiated cells causes calcium influx in bystander recipient cells and EVs from directly irradiated cells also induce calcium influx in the bystanders (Jella et al., 2014). A number of different inhibitors have been used to study the action of candidate molecules in BE (Table 7.1) and demonstrate that different mechanisms are modulated by different types of bystander mediator as reported using different endpoints. The traditional bystander mediators in table 7.1 are better characterised than the newly implicated EVs. Consequently mechanisms traditionally studied as part of the bystander effect may tie in with EV biogenesis or release that we now know plays a role in radiation response and the bystander effect (Al-Mayah et al., 2015; Al-Mayah et al., 2012; Jella et al., 2014; Arscott et al., 2013). The association of the established bystander mediators such as ROS and cytokines with the EV pellet from the irradiated cell media may be an example of this interaction.

Table 7.1. Inhibitors of a variety of candidate molecules have been used to study BE. *Inhibition of different bystander candidate molecules affects different mechanisms associated with bystander responses.*

Bystander mediator	Inhibitor	Effect upon BE induction	Reference
ROS	N-acetyl cysteine (NAC)	Prevention of growth arrest	(Macip et al., 2002)
Cytokines i.e. TNF-α	Anti-sense oligonucleotides	Reduction in radiation-induced apoptosis	(Zhang et al., 2008)
Mitochondria	DNA depletion	Reduced γ-H2AX induction	(Chen et al., 2008)
Gap-junctions	Lindane/Octanol	Reduced p53 modulation/reduced mutagenesis	(Zhou et al., 2001; Azzam et al., 1998)
COX-2	NS-398	Reduced DNA damage	(Zhou et al., 2005)
Calcium	Calcicludine	Prevention of micronuclei induction	(Shao et al., 2006)
Extracellular vesicles	RNase A	Abrogation of DNA damage mediation via an RNA-dependent mechanism	(Al-Mayah et al., 2012)

Investigation of the biogenesis of EVs released from 2 Gy irradiated cells compared to normal EVs would help discern whether they are produced *de novo* or stored in cells ready to be released in response to stress. Indeed our knowledge of the biogenesis of EVs under different conditions is still relatively undeveloped. Linked to the increased concentration of EVs released in this thesis was a

statistically significant decrease in the size of the EVs from the 2 Gy irradiated cells. The vesicle sizing was performed by manual directly sizing of EVs on TEM images and calculating the average size. NanoSight measurements showed no change in size between 0 Gy and 2 Gy vesicles (data not shown), however the capacity of technology to size EVs accurately is arguably still under development and a manual method is time consuming but allows individual particle analysis. Furthermore, the heterogeneity of the contents of the vesicles cannot be accounted for by sizing or visualisation alone.

The different RNA species reported here in 2 Gy EVs along with the increase in EV release following 2 Gy irradiation and also dose-dependent increases in EV release previously reported (Jella et al., 2014) all pose the question of whether irradiated cell EVs act in a quantitative or a qualitative way to induce their effect in recipient cells. To address the question of whether EVs exert their functions in a qualitative or a quantitative manner an increasing dose of EVs was added to MCF7 cells. An increase in the amount of normal EVs applied to fresh cells produced no significant increase in DNA damage with increasing extracellular vesicle quantity (Figure 4.10). This suggests that the increase in release of EVs alone did not lead to DNA damage effects in recipient cells and that a qualitative aspect must be involved in the EV's ability to mediate bystander effect. This is reflected by the RNA Seq reported changes in composition between irradiated and unirradiated cells and their EVs and the fact that the knockdown of some of the genes altered the bystander response in recipient cells.

The key aim of the project was to identify novel mRNA and miRNA candidates involved in the radiation response in order to test their functional role in BE. The current knowledge of the contents of EVs released from irradiated cells is limited as previously stated. Amongst the significantly upregulated RNAs identified by the RNA Seq analysis mRNAs such as *NET1* and *ANP32B*, the non-coding RNA *MALAT1* and also the *mir-17-92* host gene cluster were identified. Consistent with the results presented here, it is possible that *MALAT1* acts only under conditions of stress, or that it is used in intercellular communication following stress to a cell. In the case of the *miR-17-92* host gene cluster for example it has been demonstrated that EVs are able to shuttle long unprocessed miRNA transcripts to recipient cells and to process them *en route* (Chevillet et al., 2014) and this is a possibility in the mediation of bystander effect. Known as an oncogenic transcript the combined actions of the daughter miRNAs may have very interesting effects in the recipient cells.

This variety of RNA species reported by the RNA Seq suggests that EVs contain a mix of smaller RNAs. Another interesting finding was the correlations of the RNAs between the parent cells and their EVs, and also between the 0 Gy and 2 Gy EVs. Strong correlations were observed between irradiated and unirradiated cells and between irradiated and unirradiated EVs. The correlations between cells and their EVs however was weaker, potentially signifying a selective loading of

RNA contents into EVs and therefore hinting towards an intended priming of EVs for use in particular functions.

In order to test the functional significance of some of the genes reported by the RNA Seq selected genes were knocked down based upon the qPCR validation analysis and DNA damage and nuclear fragmentation assays demonstrated that knockdown had a functional effect. To this end *ANP32B*, *NET1*, NCL, *MALAT1* and *HSP90AA1* were used for knockdown in directly irradiated cells. Knockdown of one of the genes, NCL prevented the induction of DNA damage in directly irradiated cells, with the other genes having no effect on the directly irradiated cells. In bystander cells, a more varied response was observed. *NET1* knockdown in directly irradiated cells had no effect on the induction of significant DNA damage in recipient cells. NCL knockdown and *ANP32B* knockdown resulted in the media from the irradiated cells inducing significantly lower levels of DNA damage. This suggests that knockdown of these genes has a protective effect on bystander recipient cells, or that they play a role in DNA damage induction in recipient cells. *HSP90AA1* and *MALAT1* knockdown resulted in there being no significant induction in DNA damage in cells receiving media from 2 Gy irradiated cells. This suggests that they also contribute to bystander effect but that they were not as strongly involved as NCL and *ANP32B* that reduced DNA damage in recipient cells.

These intriguing results prompt further questions and repeats of these experiments using multiple siRNAs and EV transfer specifically would lead to a better understanding of how these RNAs are being shuttled between cells in a functional way. The DNA damage response to knockdown of some of the genes appears to be complex (Table 7.2Table 7.2). Naturally, these cellular responses are complex and as the bystander response is undoubtedly multifaceted, the study of soluble factors such as cytokines and proteins in combination with the RNA cargo of the EVs released from irradiated cells can only help to better our understanding of these effects. Here knockdown was only performed in the directly irradiated cells, to test whether it might affect loading of genes implicated in BE into the EVs. Complementary approaches, including overexpression of these genes, would confirm their participation. In addition, the knockdown of these genes in recipient cells would elucidate whether the delivery of the RNAs alone was sufficient to mediate bystander effect. Gap junction communication has also been shown to play an important role in the transfer of BE mediators between cells. Gap-junctional inhibitors would allow testing to understand whether BE is being mediated solely via EV release or also in combination with gap junction communication of ROS for example.

		MCF-7 wild type	NET1	NCL	ANP	HSP	MAL	NEG
Direct irradiated	DNA damage sig. increased with 2 Gy X-rays?	✔	✔	**X**	✔	✔	✔	✔
	Direction of change	↑	↑	↑	↑	↑	↑	↑
		MCF-7	**NET1**	**NCL**	**ANP**	**HSP**	**MAL**	**NEG**

Table 7.2. Overview of knockdown effect on DNA damage in directly irradiated and recipient cells. *Ticks indicate the expected DNA damage increase was observed, 'X' indicates that a significant upregulation was not observed. Direction of DNA damage deregulation indicated by arrows.*

		wild type						
Classic bystander	DNA damage sig. increased with 2 Gy media transfer?	✔	✔	**X**	**X**	**X**	**X**	✔
	Direction of change	↑	↑	↓	↓	↑	↑	↑

In addition to the identification of the candidate genes, the role that RNase treatment can play in the abrogation of the bystander effect requires further attention. RNase treatments can be used to remove assumed non-EV associated RNAs from preparations, however it is possible that the functional RNA is not only held in the lumen of the extracellular vesicle, but may also be found outside of the vesicles, integrated into the EV membrane. Some groups have used RNase to demonstrate when an RNA is necessary for the functional activity of the EVs (Deregibus et al., 2007).

Altogether, the results in this thesis have characterised EVs released in the radiation response of cell to ionizing radiation. This is the first study to investigate the effects of knockdown of candidate genes in directly irradiated cells and show that knockdown has the ability to change the response of directly irradiated cells to ionising radiation and also their ability to induce BE via EV transfer. These results suggest that increased numbers of EVs are released from cells exposed to ionizing radiation and that they not only carry different RNA species but that some of these species are involved in the mediation of bystander effect as their knockdown changes their ability to induce DNA damage.

Conclusions and future directions

These findings propose that EVs released from MCF7 cells directly irradiated with a 2 Gy X-ray dose have different characteristics and RNA contents compared to those released from unirradiated cells. Furthermore, the RNA species found released in EVs were varied and were significantly upregulated in the EVs compared to the parent cells where they were downregulated, suggesting selective loading and a functional role for them in the mediation of bystander effect. Knockdown of the RNAs identified altered the ability of the irradiated cell media to cause DNA damage in recipient cells.

The overall results from this study have significantly contributed to the previous study of the role of EVs in BE and the radiation response and set foundations for future investigation. Overexpression of the genes identified and testing of extracellular vesicle transfer following

knockdown of these genes would offer a more complete view of how the extracellular vesicle fraction of the media is involved in bystander signalling. How these RNAs are exported from cells associated with EVs will also be interesting and investigation of their combination with other bystander candidates would provide an insight into how these different factors can contribute to such potent effects in surrounding cells.

Chapter 8 References

Abdelrazzak, A.B., Stevens, D.L., Bauer, G., O'Neill, P. & Hill, M.A. (2011). The role of radiation quality in the stimulation of intercellular induction of apoptosis in transformed cells at very low doses. *Radiation Research*, 176(**3**), p.346–355.

Agrawal, N., Dasaradhi, P.V.N., Mohmmed, A., Malhotra, P., Bhatnagar, R.K. & Mukherjee, S.K. (2003). RNA Interference: Biology, Mechanism, and Applications. *Microbiology and Molecular Biology Reviews*, 67(**4**), p.657–685.

Al-Mayah, A.H.J., Bright, S., Chapman, K., Irons, S., Luo, P., Carter, D.R.F., Goodwin, E. & Kadhim, M.A. (2015). The non-targeted effects of radiation are perpetuated by exosomes. *Mutation Research/Fundamental and Molecular Mechanisms of Mutagenesis*, 772, p.38–45.

Al-Mayah, A.H.J., Irons, S.L., Pink, R.C., Carter, D.R.F. & Kadhim, M.A. (2012). Possible role of exosomes containing RNA in mediating nontargeted effect of ionizing radiation. *Radiation Research*, 545(**5**), p.539–545.

Al-Nedawi, K., Meehan, B., Micallef, J., Lhotak, V., May, L., Guha, A. & Rak, J. (2008). Intercellular transfer of the oncogenic receptor EGFRvIII by microvesicles derived from tumour cells. *Nature Cell Biology*, 10(**5**), p.619–624.

Alvarez-Erviti, L., Seow, Y., Yin, H., Betts, C., Lakhal, S. & Wood, M. (2011). Delivery of siRNA to the mouse brain by systemic injection of targeted exosomes. *Nature Biotechnology*, 29(**4**), p.341–345.

Anders, S. & Huber, W. (2010). Differential expression analysis for sequence count data. *Genome Biology*, 11(**10**), p.R106. doi: 10.1186/gb–2010–11–10–r106.

Arroyo, J.D., Chevillet, J.R., Kroh, E.M., Ruf, I.K., Pritchard, C.C., Gibson, D.F., Mitchell, P.S., Bennett, C.F., Pogosova-Agadjanyan, E.L., Stirewalt, D.L., Tait, J.F. & Tewari, M. (2011). Argonaute2 complexes carry a population of circulating microRNAs independent of vesicles in human plasma. *Proceedings of the National Academy of Sciences of the United States of America*, 108(**12**), p.5003–5008.

Arscott, W.T., Tandle, A.T., Zhao, S., Shabason, J.E., Gordon, I.K., Schlaff, C.D., Zhang, G., Tofilon, P.J. & Camphausen, K.A. (2013). Ionizing radiation and glioblastoma exosomes: Implications in tumor biology and cell migration. *Translational Oncology*, 6(**6**), p.638–648.

Aziz, K., Nowsheen, S., Pantelias, G., Iliakis, G., Gorgoulis, V.G. & Georgakilas, A.G. (2012). Targeting DNA damage and repair: Embracing the pharmacological era for successful cancer therapy. *Pharmacology & Therapeutics*, 133(**3**), p.334–350.

Azzam, E., de Toledo, S. & Little, J. (2004). Stress signaling from irradiated to non-irradiated cells. *Current Cancer Drug Targets*, 4(**1**), p.53–64.

Azzam, E.I., de Toledo, S.M., Gooding, T. & Little, J.B. (1998). Intercellular communication is involved in the bystander regulation of gene expression in human cells exposed to very low fluences of alpha particles. *Radiation Research*, 150(**5**), p.497–504.

Azzam, E.I., de Toledo, S.M. & Little, J.B. (2003). Oxidative metabolism, gap junctions and the ionizing radiation-induced bystander effect. *Oncogene*, 22(**45**), p.7050–7057.

Azzam, E.I., de Toledo, S.M. & Spitz, D.R. (2002). Oxidative metabolism modulates signal transduction and micronucleus formation in bystander cells from α-particle-irradiated normal human fibroblast cultures. *Cancer Research*, 62(**19**), p.5436–5442.

Bailey, S.M. & Bedford, J.S. (2006). Studies on chromosome aberration induction: What can they tell us about DNA repair? *DNA Repair*, 5(**9-10**), p.1171–1181.

Barrès, C., Blanc, L., Bette-Bobillo, P., André, S., Mamoun, R., Gabius, H.J. & Vidal, M. (2010). Galectin-5 is bound onto the surface of rat reticulocyte exosomes and modulates vesicle uptake by macrophages. *Blood*, 115(**3**), p.696–705.

Bartel, D.P. (2004). MicroRNAs: Genomics, biogenesis, mechanism, and function. *Cell*, 116(**2**), p.281–297.

Bartel, D.P. (2009). MicroRNAs: Target recognition and regulatory functions. *Cell*, 136(**2**), p.215–233.

Batagov, A.O. & Kurochkin, I. V. (2013). Exosomes secreted by human cells transport largely mRNA fragments that are enriched in the 3'-untranslated regions. *Biology direct*, 8(**12**), p.doi: 10.1186/1745–6150–8–12.

Batagov, A.O., Kuznetsov, V.A. & Kurochkin, I. V. (2011). Identification of nucleotide patterns enriched in secreted RNAs as putative cis-acting elements targeting them to exosome nano-vesicles. *BMC genomics*, 12(**Suppl 3**), p.S18 doi: 10.1186/1471–2164–12–S3–S18.

Bates, D.J., Liang, R., Li, N. & Wang, E. (2009). The impact of noncoding RNA on the biochemical and molecular mechanisms of aging. *Biochimica et Biophysica Acta*, 1790(**10**), p.970–979.

Bellingham, S.A., Coleman, B.M. & Hill, A.F. (2012). Small RNA deep sequencing reveals a distinct miRNA signature released in exosomes from prion-infected neuronal cells. *Nucleic Acids Research*, 40(**21**), p.10937–10949.

Beltran, M., Puig, I., Peña, C., García, J.M., Alvarez, A.B., Peña, R., Bonilla, F. & de Herreros, A.G. (2008). A natural antisense transcript regulates Zeb2/Sip1 gene expression during Snail1-induced epithelial-mesenchymal transition. *Genes & Development*, 22(**6**), p.756–769.

Benjamini, Y. & Hochberg, Y. (1995). Controlling the false discovery rate : A practical and powerful approach to multiple testing. *Journal of the Royal Statistical Society*, 57(**1**), p.289–300.

Bentwich, I., Avniel, A., Karov, Y., Aharonov, R., Gilad, S., Barad, O., Barzilai, A., Einat, P., Einav, U., Meiri, E., Sharon, E., Spector, Y. & Bentwich, Z. (2005). Identification of hundreds of conserved and nonconserved human microRNAs. *Nature Genetics*, 37(**7**), p.766–770.

Bernard, D., Prasanth, K. V, Tripathi, V., Colasse, S., Nakamura, T., Xuan, Z., Zhang, M.Q., Sedel, F., Jourdren, L., Coulpier, F., Triller, A., Spector, D.L. & Bessis, A. (2010). A long nuclear-retained non-coding RNA regulates synaptogenesis by modulating gene expression. *The EMBO Journal*, 29(**18**), p.3082–3093.

Blankenberg, D., von Kuster, G., Coraror, N., Ananda, G., Lazarus, R., Mangan, M., Nekrutenko, A. & Taylor, J. (2010). Galaxy, a web-based genome analysis tool for experimentalists. *Current Protocols in Molecular Biology*, 89:19.10:1.

Bobrie, A., Colombo, M., Krumeich, S., Raposo, G. & Théry, C. (2012). Diverse subpopulations of vesicles secreted by different intracellular mechanisms are present in exosome preparations obtained by differential ultracentrifugation. *Journal of Extracellular Vesicles*, 1, p.18397 doi: 10.3402/jev.v1i0.18397.

Bobrie, A., Colombo, M., Raposo, G. & Théry, C. (2011). Exosome secretion: Molecular mechanisms and roles in immune responses. *Traffic*, 12(**12**), p.1659–1668.

Bolukbasi, M.F., Mizrak, A., Ozdener, G.B., Madlener, S., Ströbel, T., Erkan, E.P., Fan, J.B., Breakefield, X.O. & Saydam, O. (2012). miR-1289 and "zipcode"-like sequences enrich mRNAs in microvesicles. *Molecular Therapy-Nucleic Acids*, 1(**2**), p.e10 doi: 10.1038/mtna.2011.2.

Bowler, D.A., Moore, S.R., Macdonald, D.A., Smyth, S.H., Clapham, P. & Kadhim, M.A. (2006). Bystander-mediated genomic instability after high LET radiation in murine primary haemopoietic stem cells. *Mutation Research*, 597(**1-2**), p.50–61.

Bryant, P.E. (2004). Repair and chromosomal damage. *Radiotherapy and Oncology*, 72(**3**), p.251–256.

Bryant, P.E. & Iliakis, G. (1984). Possible correlations between cell killing, chromosome damage and DNA repair after X-irradiation. *Nucleic Acids Symposium Series*, (**13**), p.291–308.

Buitenhuis, W., Fritschi, L., Thomson, A., Glass, D., Heyworth, J. & Peters, S. (2013). Occupational exposure to ionizing radiation and risk of breast cancer in western Australia. *Journal of Occupational and Environmental Medicine*, 55(**12**), p.1431–1435.

Burdak-Rothkamm, S. & Prise, K.M. (2009). New molecular targets in radiotherapy: DNA damage signalling and repair in targeted and non-targeted cells. *European Journal of Pharmacology*, 625(**1–3**), p.151–155.

Burdak-Rothkamm, S., Rothkamm, K. & Prise, K.M. (2008). ATM acts downstream of ATR in the DNA damage response signaling of bystander cells. *Cancer Research*, 68(**17**), p.7059–7065.

Burdak-Rothkamm, S., Short, S.C., Folkard, M., Rothkamm, K. & Prise, K.M. (2007). ATR-dependent radiation-induced γH2AX foci in bystander primary human astrocytes and glioma cells. *Oncogene*, 26(**7**), p.993–1002.

Butterworth, K.T., McMahon, S.J., Hounsell, A.R., O'Sullivan, J.M. & Prise, K.M. (2013). Bystander signalling: Exploring clinical relevance through new approaches and new models. *Clinical Oncology*, 25(**10**), p.586–592.

Calin, G.A., Sevignani, C., Dumitru, C.D., Hyslop, T., Noch, E., Yendamuri, S., Shimizu, M., Rattan, S., Bullrich, F., Negrini, M. & Croce, C.M. (2004). Human microRNA genes are frequently located at fragile sites and genomic regions involved in cancers. *Proceedings of the National Academy of Sciences of the United States of America*, 101(**9**), p.2999–3004.

Chai, Y., Lam, R.K.K., Calaf, G.M., Zhou, H., Amundson, S. & Hei, T.K. (2013). Radiation-induced non-targeted response *in vivo*: role of the TGFβ-TGFBR1-COX-2 signalling pathway. *British Journal of Cancer*, 108(**5**), p.1106–1112.

Chaudhry, M.A. (2013). Expression pattern of small nucleolar RNA host genes and long non-coding RNA in X-rays-treated lymphoblastoid cells. *International Journal of Molecular Sciences*, 14(**5**), p.9099–9110.

Chaudhry, M.A. (2014). Small nucleolar RNA host genes and long non-coding RNA responses in directly irradiated and bystander cells. *Cancer Biotherapy & Radiopharmaceuticals*, 29(**3**), p.135–141.

Chaudhry, M.A., Kreger, B. & Omaruddin, R.A. (2010). Transcriptional modulation of micro-RNA in human cells differing in radiation sensitivity. *International Journal of Radiation Biology*, 86(**7**), p.569–583.

Chaudhry, M.A. & Omaruddin, R.A. (2012). Differential regulation of MicroRNA expression in irradiated and bystander cells. *Molecular Biology*, 46(**4**), p.569–578.

Chaudhry, M.A., Omaruddin, R.A., Brumbaugh, C.D., Tariq, M.A. & Pourmand, N. (2013). Identification of radiation-induced microRNA transcriptome by next-generation massively parallel sequencing. *Journal of Radiation Research*, 54(**5**), p.808–822.

Cheloufi, S., Santos, C.O.D., Chong, M.M.W. & Hannon, G.J. (2010). A Dicer-independent miRNA biogenesis pathway that requires Ago catalysis. *Nature*, 465(**7298**), p.584–589.

Chemnitz, J., Pieper, D., Grüttner, C. & Hauber, J. (2009). Phosphorylation of the HuR ligand APRIL by casein kinase 2 regulates CD83 expression. *European Journal of Immunology*, 39(**1**), p.267–279.

Chen, S., Zhao, Y., Han, W., Zhao, G., Zhu, L., Wang, J., Bao, L., Jiang, E., Xu, A., Hei, T.K., Yu, Z. & Wu, L. (2008). Mitochondria-dependent signalling pathway are involved in the early process of radiation-induced bystander effects. *British Journal of Cancer*, 98(**11**), p.1839–44.

Cheng, L., Sharples, R.A., Scicluna, B.J. & Hill, A.F. (2014). Exosomes provide a protective and enriched source of miRNA for biomarker profiling compared to intracellular and cell-free blood. *Journal of Extracellular Vesicles*, 3, p.23743 doi: 10.3402/jev.v3.23743.

Cheruvanky, A., Zhou, H., Pisitkun, T., Kopp, J.B., Knepper, M.A., Yuen, P.S.T. & Star, R.A. (2008). Rapid isolation of urinary EV biomarkers using a nanomembrane ultrafiltration concentrator. *American Journal of Physiology. Renal Physiology*, 292(**5**), p.1657–1661.

Chevillet, J.R., Kang, Q., Ruf, I.K., Briggs, H.A., Vojtech, L.N., Hughes, S.M., Cheng, H.H., Arroyo, J.D., Meredith, E.K., Gallichotte, E.N., Pogosova-Agadjanyan, E.L., Morrissey, C., Stirewalt, D.L., Hladik, F., Yu, E.Y., Higano, C.S. & Tewari, M. (2014). Quantitative and stoichiometric analysis of the microRNA content of exosomes. *Proceedings of the National Academy of Sciences of the United States of America*, 111(**41**), p.14888–14893.

Clayton, A., Mitchell, J.P., Court, J., Mason, M.D. & Tabi, Z. (2007). Human tumor-derived exosomes selectively impair lymphocyte responses to interleukin-2. *Cancer Research*, 67(**15**), p.7458–7466.

Clayton, A., Turkes, A., Navabi, H., Mason, M.D. & Tabi, Z. (2005). Induction of heat shock proteins in B-cell exosomes. *Journal of Cell Science*, 118(**16**), p.3631–3638.

Comincini, S., Allavena, G., Palumbo, S., Morini, M., Durando, F., Angeletti, F., Pirtoli, L. & Miracco, C. (2013). microRNA-17 regulates the expression of ATG7 and modulates the autophagy process, improving the sensitivity to temozolomide and low-dose ionizing radiation treatments in human glioblastoma cells. *Cancer Biology & Therapy*, 14(**7**), p.574–586.

Conde-vancells, J., Rodriguez-suarez, E., Embade, N. & Gil, D. (2009). Characterisation and comprehensive proteome profiling of exosomes secreted by hepatocytes. *Journal of Proteomics*, 7(**12**), p.5157–5166.

Crescitelli, R., Lässer, C., Szabó, T.G., Kittel, A., Eldh, M., Dianzani, I., Buzás, E.I. & Lötvall, J. (2013). Distinct RNA profiles in subpopulations of extracellular vesicles: apoptotic bodies, microvesicles and exosomes. *Journal of Extracellular Vesicles*, 2, p.20677 doi: 10.3402/jev.v2i0.20677.

Cui, W., Ma, J., Wang, Y. & Biswal, S. (2011). Plasma miRNA as biomarkers for assessment of total-body radiation exposure dosimetry. *PloS one*, 6(**8**), p.e22988 doi: 10.1371/journal.pone.0022988.

Cummins, J.M. & Velculescu, V.E. (2006). Implications of micro-RNA profiling for cancer diagnosis. *Oncogene*, 25(**46**), p.6220–6227.

Darby, S.C., Mcgale, P., Taylor, C.W. & Peto, R. (2005). Long-term mortality from heart disease and lung cancer after radiotherapy for early breast cancer: prospective cohort study of about 300 000 women in US SEER cancer registries. *The Lancet Oncology*, 6(**8**), p.557–565.

Dent, P., Yacoub, A., Fisher, P.B., Hagan, M.P. & Grant, S. (2003). MAPK pathways in radiation responses. *Oncogene*, 22(**37**), p.5885–5896.

Deregibus, M.C., Cantaluppi, V., Calogero, R., Lo Iacono, M., Tetta, C., Biancone, L., Bruno, S., Bussolati, B. & Camussi, G. (2007). Endothelial progenitor cell derived microvesicles activate an angiogenic program in endothelial cells by a horizontal transfer of mRNA. *Blood*, 110(**7**), p.2440–2448.

Deutsch, M., Land, S.R., Begovic, M., Wieand, H.S., Wolmark, N. & Fisher, B. (2003). The incidence of lung carcinoma after surgery for breast carcinoma with and without postoperative radiotherapy. *Cancer*, 98(**7**), p.1362–1368.

Dickey, J.S., Baird, B.J., Redon, C.E., Avdoshina, V., Palchik, G., Wu, J., Kondratyev, A., Bonner, W.M. & Martin, O.A. (2012). Susceptibility to bystander DNA damage is influenced by replication and transcriptional activity. *Nucleic Acids Research*, 40(**20**), p.10274–10286.

Dickey, J.S., Baird, B.J., Redon, C.E., Sokolov, M. V, Sedelnikova, O. a & Bonner, W.M. (2009). Intercellular communication of cellular stress monitored by γ-H2AX induction. *Carcinogenesis*, 30(**10**), p.1686–1695.

Dickey, J.S., Zemp, F.J., Altamirano, A., Sedelnikova, O.A., Bonner, W.M. & Kovalchuk, O. (2011). H2AX phosphorylation in response to DNA double-strand break formation during bystander signalling: effect of microRNA knockdown. *Radiation Protection Dosimetry*, 143(**2-4**), p.264–269.

Dickey, J.S., Zemp, F.J., Martin, O.A. & Kovalchuk, O. (2011). The role of miRNA in the direct and indirect effects of ionizing radiation. *Radiation and Environmental Biophysics*, 50(**4**), p.491–499.

Dragovic, R.A., Gardiner, C., Brooks, A.S., Tannetta, D.S., Ferguson, D.J.P., Hole, P., Carr, B., Redman, C.W.G., Harris, A.L., Dobson, P.J., Harrison, P. & Sargent, I.L. (2011). Sizing and phenotyping of cellular vesicles using Nanoparticle Tracking Analysis. *Nanomedicine*, 7(**6**), p.780–788.

Eitan, E., Zhang, S., Witwer, K.W. & Mattson, M.P. (2015). Extracellular vesicle–depleted fetal bovine and human sera have reduced capacity to support cell growth. *Journal of Extracellular Vesicles*, 4, p.26373 doi: 10.3402/jev.v4.26373.

Ekstrom, K., Valadi, H., Sjo, M., Malmha, C., Bossios, A. & Eldh, M. (2012). Characterization of mRNA and microRNA in human mast cell-derived exosomes and their transfer to other mast

cells and blood CD34 progenitor cells. *Journal of Extracellular Vesicles*, 1, p.18389 doi:103402/jev.v1i0.18389.

Eldh, M., Ekström, K., Valadi, H., Sjöstrand, M., Olsson, B., Jernås, M. & Lötvall, J. (2010). Exosomes communicate protective messages during oxidative stress; possible role of EV shuttle RNA. *PloS one*, 5(**12**), p.e15353 doi: 10.1371/journal.pone.0015353.

Eldh, M., Lötvall, J., Malmhäll, C. & Ekström, K. (2012). Importance of RNA isolation methods for analysis of EV RNA: Evaluation of different methods. *Molecular Immunology*, 50(**4**), p.278–286.

Escola, J.M., Kleijmeer, M.J., Stoorvogel, W., Griffith, J.M., Yoshie, O. & Geuze, H.J. (1998). Selective enrichment of tetraspan proteins on the internal vesicles of multivesicular endosomes and on exosomes secreted by human B-lymphocytes. *Journal of Biological Chemistry*, 273(**32**), p.20121–20127.

Escrevente, C., Keller, S., Altevogt, P. & Costa, J. (2011). Interaction and uptake of exosomes by ovarian cancer cells. *BMC cancer*, 11(**1**), p.108 doi: 10.1186/1471–2407–11–108.

Fabbri, M., Garzon, R., Cimmino, A., Liu, Z., Zanesi, N., Callegari, E., Liu, S., Alder, H., Costinean, S., Fernandez-Cymering, C., Volinia, S., Guler, G., Morrison, C.D., Chan, K.K., Marcucci, G., Calin, G.A., Huebner, K. & Croce, C.M. (2007). MicroRNA-29 family reverts aberrant methylation in lung cancer by targeting DNA methyltransferases 3A and 3B. *Proceedings of the National Academy of Sciences of the United States of America*, 104(**40**), p.15805–15810.

Fader, C.M., Sánchez, D., Furlán, M. & Colombo, M.I. (2008). Induction of autophagy promotes fusion of multivesicular bodies with autophagic vacuoles in K562 cells. *Traffic*, 9(**2**), p.230–250.

Feng, J., Bi, C., Clark, B.S., Mady, R., Shah, P. & Kohtz, J.D. (2006). The Evf-2 noncoding RNA is transcribed from the Dlx-5/6 ultraconserved region and functions as a Dlx-2 transcriptional coactivator. *Genes and Development*, 1(**20**), p.1470–1484.

Franzen, C.A., Simms, P.E., Van Huis, A.F., Foreman, K.E., Kuo, P.C. & Gupta, G.N. (2014). Characterization of uptake and internalization of exosomes by bladder cancer cells. *BioMed Research International*, 2014, p.619829 doi: 10.1155/2014/619829.

Fulda, S., Gorman, A.M., Hori, O. & Samali, A. (2010). Cellular stress responses: cell survival and cell death. *International Journal of Cell Biology*, 2010, p.214074 doi: 10.1155/2010/214074.

Garber, M., Grabherr, M.G., Guttman, M. & Trapnell, C. (2011). Computational methods for transcriptome annotation and quantification using RNA-seq. *Nature Methods*, 8(**6**), p.469–477.

Gardiner, C., Ferreira, Y.J., Dragovic, R.A., Redman, C.W.G. & Sargent, I.L. (2013). Extracellular vesicle sizing and enumeration by nanoparticle tracking analysis. *Journal of Extracellular Vesicles*, 2, 19671 doi: 10.3402/jev.v2i0.19671.

Gardiner, C., Shaw, M., Hole, P., Smith, J., Tannetta, D., Redman, C.W. & Sargent, I.L. (2014). Measurement of refractive index by nanoparticle tracking analysis reveals heterogeneity in extracellular vesicles. *Journal of Extracellular Vesicles*, 1, p.25361 doi: 10.3402/jev.v3.25361.

Gercel-Taylor, C., Atay, S., Tullis, R.H., Kesimer, M. & Taylor, D.D. (2012). Nanoparticle analysis of circulating cell-derived vesicles in ovarian cancer patients. *Analytical Biochemistry*, 428(**1**), p.44–53.

Gezer, U., Özgür, E., Cetinkaya, M., Isin, M. & Dalay, N. (2014). Long non-coding RNAs with low expression levels in cells are enriched in secreted exosomes. *Cell Biology International*, 38(**9**), p.1076–1079.

Ghobrial, I.M., Witzig, T.E. & Adjei, A.A. (2005). Targeting apoptosis pathways in cancer therapy. *CA: a cancer journal for clinicians*, 55(**3**), p.178–194.

Giardine, B., Riemer, C., Hardison, R.C., Burhans, R., Elnitski, L., Shah, P., Zhang, Y., Blankenberg, D., Albert, I., Taylor, J., Miller, W., Kent, W.J. & Nekrutenko, A. (2005). Galaxy: a platform for interactive large-scale genome analysis. *Genome Research*, 15(**10**), p.1451–1455.

Gibbings, D.J., Ciaudo, C., Erhardt, M. & Voinnet, O. (2009). Multivesicular bodies associate with components of miRNA effector complexes and modulate miRNA activity. *Nature Cell Biology*, 11(**9**), p.1143–1149.

Gillies, J.K. & Lorimer, I.A.J. (2007). Regulation of p27Kip1 by miRNA 221/222 in glioblastoma. *Cell Cycle*, 6(**16**), p.2005–2009.

Ginger, M.R., Shore, A.N., Contreras, A., Rijnkels, M., Miller, J., Gonzalez-Rimbau, M.F. & Rosen, J.M. (2006). A noncoding RNA is a potential marker of cell fate during mammary gland development. *Proceedings of the National Academy of Sciences of the United States of America*, 103(**15**), p.5781–5786.

Goecks, J., Nekrutenko, A. & Taylor, J. (2010). Galaxy: a comprehensive approach for supporting accessible, reproducible, and transparent computational research in the life sciences. *Genome Biology*, 11(**8**), pp.R86. doi: 10.1186/gb–2010–11–8–r86.

Goldstein, M., Derheimer, F.A., Tait-Mulder, J. & Kastan, M.B. (2013). Nucleolin mediates nucleosome disruption critical for DNA double-strand break repair. *Proceedings of the National Academy of Sciences of the United States of America*, 110(**42**), p.16874–16879.

Goodhead, D.T. (1994). Initial events in the cellular effects of ionizing radiations: Clustered damage in DNA. *International Journal of Radiation Biology*, 65(**1**), p.7–17.

Gorgoulis, V.G., Zacharatos, P., Kotsinas, A., Kletsas, D., Mariatos, G., Zoumpourlis, V., Ryan, K.M., Kittas, C. & Papavassiliou, A.G. (2003). p53 activates ICAM-1 (CD54) expression in an NF-kB-independent manner. *The EMBO Journal*, 22(**7**), p.1567–1578.

Gould, G.W. & Lippincott-Schwartz, J. (2013). New roles for endosomes: from vesicular carriers to multi-purpose platforms. *Nature Reviews Molecular Cell Biology*, 10(**4**), p.287–292.

Gould, S.J. (2013). As we wait: coping with an imperfect nomenclature for extracellular vesicles. *Journal of Extracellular Vesicles*, 1, p.20389 doi:10.3402/jev.v2i0.20839.

Guduric-Fuchs, J., O'Connor, A., Camp, B., O'Neill, C.L., Medina, R.J. & Simpson, D. a. (2012). Selective extracellular vesicle-mediated export of an overlapping set of microRNAs from multiple cell types. *BMC Genomics*, 13(**1**), p.357.

Guo, B.B., Bellingham, S.A. & Hill, A.F. (2015). The neutral sphingomyelinase pathway regulates packaging of the prion protein into exosomes. *Journal of Biological Chemistry*, 290(**6**), p.3455–3467.

Gutschner, T., Hämmerle, M. & Diederichs, S. (2013). MALAT1 - a paradigm for long noncoding RNA function in cancer. *Journal of Molecular Medicine*, 91(**7**), p.791–801.

Halazonetis, T.D., Gorgoulis, V.G. & Bartek, J. (2008). An oncogene-induced DNA damage model for cancer development. *Science*, 319(**5868**), p.1352–1355.

Halimi, M., Parsian, H., Asghari, S.M., Sariri, R., Moslemi, D., Yeganeh, F. & Zabihi, E. (2014). Clinical translation of human microRNA 21 as a potential biomarker for exposure to ionizing radiation. *Translational Research : the Journal of Laboratory and Clinical Medicine*, 163(**6**), p.578–584.

Hall, E.J. & Giaccia, A.J. (2012). *Radiobiology for the Radiologist* 7th ed., Philadelphia (PA): Lippincott, Williams and Wilkins. pp.1-567.

Hamada, N., Matsumoto, H., Hara, T. & Kobayashi, Y. (2007). Intercellular and intracellular signaling pathways mediating ionizing radiation-induced bystander effects. *Journal of Radiation Research*, 48(**2**), p.87–95.

Hammond, S.M., Caudy, A.A. & Hannon, G.J. (2001). Post-transcriptional gene silencing by double-stranded RNA. *Nature Reviews Genetics*, 2(**2**), p.110–119.

Han, Y., Liu, Y., Nie, L., Gui, Y. & Cai, Z. (2015). Inducing cell proliferation inhibition, apoptosis, and motility reduction by silencing long noncoding ribonucleic acid metastasis-associated lung adenocarcinoma transcript 1 in urothelial carcinoma of the bladder. *Urology*, 81(**1**), p.209.e1–209.e7.

Harding, C., Heuser, J. & Stahl, P. (1983). Receptor-mediated endocytosis of transferrin and recycling of the transferrin receptor in rat reticulocytes biochemical approaches to transferrin. *The Journal of Cell Biology*, 97(**2**), p.329–339.

Harrow, J., Frankish, A., Gonzalez, J.M., Tapanari, E., Diekhans, M., Kokocinski, F., Aken, B.L., Barrell, D., Zadissa, A., Searle, S., Barnes, I., Bignell, A., Boychenko, V., Hunt, T., Kay, M., Mukherjee, G., Rajan, J., … Hubbard, T.J. (2012). GENCODE: the reference human genome annotation for The ENCODE Project. *Genome Research*, 22(**9**), p.1760–1774.

Havaki, S., Kotsinas, A., Chronopoulos, E., Kletsas, D., Georgakilas, A. & Gorgoulis, V.G. (2014). The role of oxidative DNA damage in radiation induced bystander effect. *Cancer Letters*, 356(**1**), p.43–51.

Hazawa, M., Tomiyama, K., Saotome-Nakamura, A., Obara, C., Yasuda, T., Gotoh, T., Tanaka, I., Yakumaru, H., Ishihara, H. & Tajima, K. (2014). Radiation increases the cellular uptake of exosomes through CD29/CD81 complex formation. *Biochemical and Biophysical Research Communications*, 446(**4**), p.1165–1171.

He, L., He, X., Lim, L.P., de Stanchina, E., Xuan, Z., Liang, Y., Xue, W., Zender, L., Magnus, J., Ridzon, D., Jackson, A.L., Linsley, P.S., Chen, C., Lowe, S.W., Cleary, M.A. & Hannon, G.J. (2007). A microRNA component of the p53 tumour suppressor network. *Nature*, 447(**7148**), p.1130–1134.

Hei, T.K., Zhou, H., Ivanov, V.N., Hong, M., Lieberman, H.B., Brenner, D.J., Amundson, S.A. & Geard, C.R. (2008). Mechanism of radiation-induced bystander effects: a unifying model. *Journal of Pharmacy and Pharmacology*, 60(**8**), p.943–950.

Herbert, K.J., Cook, A.L. & Snow, E.T. (2014). SIRT1 modulates miRNA processing defects in p53-mutated human keratinocytes. *Journal of Dermatological Science*, 74(**2**), p.142–149.

Hill, A.F., Pegtel, D.M., Lambertz, U., Leonardi, T., O'Driscoll, L., Pluchino, S., Ter-Ovanesyan, D. & Nolte-'t Hoen, E.N.M. (2013). ISEV position paper: extracellular vesicle RNA analysis and bioinformatics. *Journal of Extracellular Vesicles*, 2, p.22859 doi: 10.3402/jev.v2i0.22859.

Hu, L., Wu, Y., Tan, D., Meng, H., Wang, K., Bai, Y. & Yang, K. (2015). Up-regulation of long noncoding RNA MALAT1 contributes to proliferation and metastasis in esophageal squamous cell carcinoma. *Journal of Experimental & Clinical Cancer Research:CR*, 34(**1**), p.7 doi:10.1186/s13046–015–0123–z.

Huang, X., Yuan, T., Tschannen, M., Sun, Z., Jacob, H., Du, M., Liang, M., Dittmar, R.L., Liu, Y., Liang, M., Kohli, M., Thibodeau, S.N., Boardman, L. & Wang, L. (2013). Characterization of human plasma-derived EV RNAs by deep sequencing. *BMC Genomics*, 14(**319**), p.1–14.

Hunter, M.P., Ismail, N., Zhang, X., Aguda, B.D., Lee, E.J., Yu, L., Xiao, T., Schafer, J., Lee, M.-L.T., Schmittgen, T.D., Nana-Sinkam, S.P., Jarjoura, D. & Marsh, C.B. (2008). Detection of microRNA expression in human peripheral blood microvesicles. *PloS one*, 3(**11**), p.e3694 doi: 10.1371/journal.pone.0003694.

Ichii, O., Otsuka-Kanazawa, S., Horino, T., Kimura, J., Nakamura, T., Matsumoto, M., Toi, M. & Kon, Y. (2014). Decreased miR-26a expression correlates with the progression of podocyte injury in autoimmune glomerulonephritis. *PLoS one*, 9(**10**), p.e110383 doi:10.1371/journal.pone.0110383.

Ilnytskyy, Y., Koturbash, I. & Kovalchuk, O. (2009). Radiation-induced bystander effects *in vivo* are epigenetically regulated in a tissue-specific manner. *Environmental and Molecular Mutagenesis*, 50(**2**), p.105–113.

Ishikawa, K., Ishii, H. & Saito, T. (2006). DNA damage-dependent cell cycle checkpoints and genomic stability. *DNA and Cell Biology*, 25(**7**), p.406–411.

Jacobs, L.A., Bewicke-Copley, F., Poolman, M.G., Pink, R.C., Mulcahy, L.A., Baker, I., Beaman, E.-M., Brooks, T., Caley, D.P., Cowling, W., Currie, J.M.S., Horsburgh, J., Kenehan, L., Keyes, E., Leite, D., Massa, D., McDermott-Rouse, A., Samuel, P., Wood, H., Kadhim, M. A. & Carter, D.R.F. (2013). Meta-analysis using a novel database, miRStress, reveals miRNAs that are frequently associated with the radiation and hypoxia stress-responses. *PloS one*, 8(**11**), p.e80844 doi: 10.1371/journal.pone.0080844.

Janowska-Wieczorek, A., Wysoczynski, M., Kijowski, J., Marquez-Curtis, L., Machalinski, B., Ratajczak, J. & Ratajczak, M.Z. (2005). Microvesicles derived from activated platelets induce metastasis and angiogenesis in lung cancer. *International Journal of Cancer.*, 113(**5**), p.752–760.

Jella, K., Rani, S., O'Driscoll, L., McClean, B., Byrne, H. & Lyng, F. (2014). Exosomes are involved in mediating radiation induced bystander signaling in human keratinocyte cells. *Radiation Research*, 181(**2**), p.138–145.

Jen, K.Y. & Cheung, V.G. (2003). Transcriptional response of lymphoblastoid cells to ionizing radiation. *Genome Research*, 13(**9**), p.2092–2100.

Jenjaroenpun, P., Kremenska, Y., Nair, V.M., Kremenskoy, M., Joseph, B. & Kurochkin, I. V. (2013). Characterization of RNA in exosomes secreted by human breast cancer cell lines using next-generation sequencing. *PeerJ*, 1, p.e201 doi: 10.7717/peerj.201.

Ji, P., Diederichs, S., Wang, W., Böing, S., Metzger, R., Schneider, P.M., Tidow, N., Brandt, B., Buerger, H., Bulk, E., Thomas, M., Berdel, W.E., Serve, H. & Müller-Tidow, C. (2003). MALAT-1, a novel noncoding RNA, and thymosin beta4 predict metastasis and survival in early-stage non-small cell lung cancer. *Oncogene*, 22(**39**), p.8031–8041.

Jiang, Y., Chen, X., Tian, W., Yin, X., Wang, J. & Yang, H. (2014). The role of TGF-ß1-miR-21-ROS pathway in bystander responses induced by irradiated non-small-cell lung cancer cells. *British Journal of Cancer*, 111(**4**), p.772–780.

Johnstone, R.M., Adam, M., Hammonds, J.R. & Turbide, C. (1987). Vesicle formation during reticulocyte maturation. *The Journal of Biological Chemistry*, 262(**1**), p.9412–9420.

De Jong, O.G., Verhaar, M.C., Chen, Y., Vader, P., Gremmels, H., Posthuma, G., Schiffelers, R.M., Gucek, M. & van Balkom, B.W.M. (2012). Cellular stress conditions are reflected in the protein and RNA content of endothelial cell-derived exosomes. *Journal of Extracellular Vesicles*, 1, p.18396 doi: 10.3402/jev.v1i0.18396.

Kadhim, M.A., Macdonald, D.A., Goodhead, D.T., Lorimore, S.A., Marsden, S.J. & Wright, E.G. (1992). Transmission of chromosomal instability after plutonium α-particle irradiation. *Nature*, 355(**6362**), p.738–740.

Kadhim, M.A., Salomaa, S., Wright, E., Hildebrandt, Belyakov, O., Prise, K. & Little, M. (2013). Non-targeted effects of ionising radiation -Implications for low dose risk. *Mutation Research*, 752(**2**), p.84–98.

Kalanxhi, E. & Dahle, J. (2011). Genome-wide microarray analysis of human fibroblasts in response to γ radiation and the radiation-induced bystander effect. *Radiation Research*, 177(**1**), p.35–43.

Kalra, H., Simpson, R.J., Ji, H., Aikawa, E., Altevogt, P., Askenase, P., Bond, V.C., Borràs, F.E., Breakefield, X., Budnik, V., Buzas, E., Camussi, G., Clayton, A., Cocucci, E., Falcon-Perez, J.M., Gabrielsson, S., Gho, Y.S., … Mathivanan, S. (2012). Vesiclepedia: a compendium for extracellular vesicles with continuous community annotation. *PLoS Biology*, 10(**12**), p.e1001450 doi: 10.1371/journal.pbio.1001450.

Kaul, G., Pattan, G. & Rafeequi, T. (2011). Eukaryotic elongation factor-2 (eEF2): its regulation and peptide chain elongation. *Cell Biochemistry and Function*, 29(**3**), p.227–234.

Kawaji, H., Nakamura, M., Takahashi, Y., Sandelin, A., Katayama, S., Fukuda, S., Daub, C.O., Kai, C., Kawai, J., Yasuda, J., Carninci, P. & Hayashizaki, Y. (2008). Hidden layers of human small RNAs. *BMC Genomics*, 10(**9**), p.157 doi: 10.1186/1471–2164–9–157.

Keller, S., Ridinger, J., Rupp, A.-K., Janssen, J.W.G. & Altevogt, P. (2011). Body fluid derived exosomes as a novel template for clinical diagnostics. *Journal of translational medicine*, 9(**1**), p.86 doi: 10.1186/1479–5876–9–86.

Khanna, K.K. & Jackson, S.P. (2001). DNA double-strand breaks: signaling, repair and the cancer connection. *Nature Genetics*, 27(**3**), p.247–254.

Kharaziha, P., Ceder, S., Li, Q. & Panaretakis, T. (2012). Tumor cell-derived exosomes: A message in a bottle. *Biochimica et Biophysica Acta - Reviews on Cancer*, 1826(**1**), p.103–111.

Kim, D.-K., Kang, B., Kim, O.Y., Choi, D.-S., Lee, J., Kim, S.R., Go, G., Yoon, Y.J., Kim, J.H., Jang, S.C., Park, K.-S., Choi, E.-J., Kim, K.P., Desiderio, D.M., Kim, Y.-K., Lötvall, J., Hwang, D. & Gho, Y.S. (2013). EVpedia: an integrated database of high-throughput data for systemic analyses of extracellular vesicles. *Journal of Extracellular Vesicles*, 2, p.20384 doi: 10.3402/jev.v2i0.20384.

King, H.W., Michael, M.Z. & Gleadle, J.M. (2012). Hypoxic enhancement of exosome release by breast cancer cells. *BMC cancer*, 12(**421**), p.doi: 10.1186/1471–2407–12–421.

Klibi, J., Niki, T., Riedel, A., Pioche-durieu, C., Souquere, S., Rubinstein, E., Moulec, S. Le, Hirashima, M., Guemira, F., Adhikary, D., Mautner, J. & Busson, P. (2015). Blood diffusion and Th1-suppressive effects of galectin-9-containing exosomes released by Epstein-Barr virus-infected nasopharyngeal carcinoma cells. *Immunobiology*, 113(**9**), p.1957–1967.

Kobayashi, J., Fujimoto, H., Sato, J., Hayashi, I., Burma, S., Matsuura, S., Chen, D.J. & Komatsu, K. (2012). Nucleolin participates in DNA double-strand break-induced damage response through MDC1-dependent pathway. *PLoS one*, 7(**11**), p0049245 doi: 10.1371.

Kogure, T., Yan, I.K., Lin, W.-L. & Patel, T. (2013). Extracellular vesicle-mediated transfer of a novel long noncoding RNA TUC339: A mechanism of intercellular signaling in human hepatocellular cancer. *Genes & Cancer*, 4(**7-8**), p.261–272.

Konadu, K.A., Chu, J., Huang, M.B., Amancha, P.K., Armstrong, W., Powell, M.D., Villinger, F. & Bond, V.C. (2014). Association of cytokines with exosomes in the plasma of HIV-1–seropositive individuals. *Journal of Infectious Diseases*, p.doi: 10.1093/infdis/jiu676.

Kosaka, N., Iguchi, H., Yoshioka, Y., Takeshita, F., Matsuki, Y. & Ochiya, T. (2010). Secretory mechanisms and intercellular transfer of microRNAs in living cells. *The Journal of Biological Chemistry*, 285(**23**), p.17442–17452.

Koturbash, I., Boyko, A., Rodriguez-Juarez, R., McDonald, R.J., Tryndyak, V.P., Kovalchuk, I., Pogribny, I.P. & Kovalchuk, O. (2007). Role of epigenetic effectors in maintenance of the long-term persistent bystander effect in spleen *in vivo*. *Carcinogenesis*, 28(**8**), p.1831–1838.

Koturbash, I., Zemp, F.J., Kutanzi, K., Luzhna, L., Loree, J., Kolb, B. & Kovalchuk, O. (2008). Sex-specific microRNAome deregulation in the shielded bystander spleen of cranially exposed mice. *Cell Cycle*, 7(**11**), p.1658–1667.

Koumangoye, R.B., Sakwe, A.M., Goodwin, J.S., Patel, T. & Ochieng, J. (2011). Detachment of breast tumor cells induces rapid secretion of exosomes which subsequently mediate cellular adhesion and spreading. *PloS one*, 6(**9**), p.e24234 doi: 10.1371/journal.pone.0024234.

Kovalchuk, O., Zemp, F.J., Filkowski, J.N., Altamirano, A.M., Dickey, J.S., Jenkins-Baker, G., Marino, S.A., Brenner, D.J., Bonner, W.M. & Sedelnikova, O.A. (2010). microRNAome changes in bystander three-dimensional human tissue models suggest priming of apoptotic pathways. *Carcinogenesis*, 31(**10**), p.1882–1888.

Lahiff, C., Cotter, E., Casey, R., Doran, P., Pidgeon, G., Reynolds, J., Macmathuna, P. & Murray, D. (2013). Expression of neuroepithelial transforming gene 1 is enhanced in oesophageal cancer and mediates an invasive tumour cell phenotype. *Journal of Experimental Clinical Cancer Research*, 32(**1**), p.55 doi: 10.1186/1756–9966–32–55.

Lancaster, G.I. & Febbraio, M.A. (2005). Mechanisms of stress-induced cellular HSP72 release: implications for exercise-induced increases in extracellular HSP72. *Exercise Immunology Review*, 11, p.46–52.

Laulagnier, K., Motta, C., Hamdi, S., Roy, S., Fauvelle, F., Pageaux, J.-F., Kobayashi, T., Salles, J.-P., Perret, B., Bonnerot, C. & Record, M. (2004). Mast cell- and dendritic cell-derived exosomes display a specific lipid composition and an unusual membrane organization. *The Biochemical Journal*, 380(**1**), p.161–171.

Lee, R.C., Feinbaum, R.L. & Ambros, V. (1993). The *C. elegans* heterochronic gene lin-4 encodes small RNAs with antisense complementarity to lin-14. *Cell*, 75(**5**), p.843–854.

Lee, Y.S., Pressman, S., Andress, A.P., Kim, K., White, J.L., Cassidy, J.J., Li, X., Lubell, K., Lim, D.H., Cho, I.S., Nakahara, K., Preall, J.B., Bellare, P., Sontheimer, E.J. & Carthew, R.W. (2009). Silencing by small RNAs is linked to endosomal trafficking. *Nature Cell Biology*, 11(**9**), p.1150–1156.

Lehmann, B.D., Paine, M.S., Brooks, A.M., McCubrey, J.A., Renegar, R.H., Wang, R. & Terrian, D.M. (2008). Senescence-associated exosome release from human prostate cancer cells. *Cancer Research*, 68(**19**), p.7864–7871.

Lehnert, B.E. & Goodwin, E.H. (1997). Extracellular factor(s) following exposure to α particles can cause sister chromatid exchanges in normal human cells. *Cancer Research*, 57(**11**), p.2164–2171.

Lespagnol, A., Duflaut, D., Beekman, C., Blanc, L., Fiucci, G., Marine, J.-C., Vidal, M., Amson, R. & Telerman, A. (2008). Exosome secretion, including the DNA damage-induced p53-dependent secretory pathway, is severely compromised in TSAP6/Steap3-null mice. *Cell Death and Differentiation*, 15(**11**), p.1723–1733.

Leung, A.K.L. & Sharp, P.A. (2010). MicroRNA functions in stress responses. *Molecular Cell*, 40(**2**), p.205–215.

Leung, C., Chen, T., Li, S., Ho, M., Hu, L., Liu, W., Wu, T., Hsu, P., Chang, H. & Tsai, K. (2014). MicroRNA expression profiles in human breast cancer cells after multifraction and single-dose radiation treatment. *Oncology Reports*, 31(**5**), p.2147–2156.

Lhakhang, T.W. & Chaudhry, M.A. (2012). Interactome of radiation-induced microRNA-predicted target genes. *Comparative and Functional Genomics*, 2012, p.569731 doi:10.1155/2012/569731.

Li, H., Handsaker, B., Wysoker, A., Fennell, T., Ruan, J., Homer, N., Marth, G., Abecasis, G. & Durbin, R. (2009). The sequence alignment/map format and SAMtools. *Bioinformatics*, 25(**16**), p.2078–2079.

Lin, R., Maeda, S., Liu, C., Karin, M. & Edgington, T.S. (2007). A large noncoding RNA is a marker for murine hepatocellular carcinomas and a spectrum of human carcinomas. *Oncogene*, 26(**6**), p.851–858.

Lliakis, G. (1991). The role of DNA double strand breaks in ionizing radiation-induced killing of eukaryotic cells. *BioEssays*, 13(**12**), p.641–648.

Lorimore, S.A., Kadhim, M.A., Pocock, D.A., Papworth, D., Stevens, D.L., Goodhead, D.T. & Wright, E.G. (1998). Chromosomal instability in the descendants of unirradiated surviving cells after α-particle irradiation. *Proceedings of the National Academy of Sciences of the United States of America*, 95(**10**), p.5730–5733.

Lotvall, J. & Valadi, H. (2007). Cell to cell signalling via exosomes through esRNA. *Cell Adhesion & Migration*, 1(**3**), p.156–158.

Lv, L.-H., Wan, Y.-L., Lin, Y., Zhang, W., Yang, M., Li, G.-L., Lin, H.-M., Shang, C.-Z., Chen, Y.-J. & Min, J. (2012). Anticancer drugs cause release of exosomes with heat shock proteins from human hepatocellular carcinoma cells that elicit effective natural killer cell antitumor responses *in vitro*. *The Journal of Biological Chemistry*, 287(**19**), p.15874–15885.

Ma, L., Bajic, V.B. & Zhang, Z. (2013). On the classification of long non-coding RNAs. *RNA Biology*, 10(**6**), p.925–933.

Macip, S., Igarashi, M., Fang, L., Chen, A., Pan, Z.Q., Lee, S.W. & Aaronson, S.A. (2002). Inhibition of p21-mediated ROS accumulation can rescue p21-induced senescence. *EMBO Journal*, 21(**9**), p.2180–2188.

Marioni, J.C., Mason, C.E., Mane, S.M., Stephens, M. & Gilad, Y. (2008). Comparison with gene expression arrays RNA-seq: An assessment of technical reproducibility and comparison with gene expression arrays. *Genome Research*, 18(**9**), p.1509–1517.

Marshall, M., Gibson, J.A. & Holt, P.D. (1970). An analysis of the target theory of Lea with modern data. *International journal of radiation biology and related studies in physics, chemistry, and medicine*, 18(**2**), p.127–138.

Mathivanan, S., Fahner, C.J., Reid, G.E. & Simpson, R.J. (2012). ExoCarta 2012: Database of EV proteins, RNA and lipids. *Nucleic Acids Research*, 40 (Database Issue), p.1241–1244.

Mathivanan, S. & Simpson, R.J. (2009). ExoCarta: A compendium of EV proteins and RNA. *Proteomics*, 9(**21**), p.4997–5000.

Matsumoto, H., Hayashi, S., Hatashita, M., Ohnishi, K., Shioura, H., Ohtsubo, T., Kitai, R., Ohnishi, T. & Kano, E. (2001). Induction of radioresistance by a nitric oxide-mediated bystander effect. *Radiation Research*, 155(**3**), p.387–396.

McCready, J., Sims, J.D., Chan, D. & Jay, D.G. (2010). Secretion of extracellular hsp90α via exosomes increases cancer cell motility: a role for plasminogen activation. *BMC Cancer*, 10, p.294 doi:10.1186/1471–2407–10–294.

Melo, S.A., Sugimoto, H., O'Connell, J.T., Kato, N., Villanueva, A., Vidal, A., Qiu, L., Vitkin, E., Perelman, L.T., Melo, C.A., Lucci, A., Ivan, C., Calin, G.A. & Kalluri, R. (2015). Cancer exosomes perform cell-independent microRNA biogenesis and promote tumorigenesis. *Cancer Cell*, 26(**5**), p.707–721.

Mendell, J. & Loson, E. (2013). MicroRNAs in stress signaling and human disease. *Cell*, 148(**6**), p.1172–1187.

Meng, F., Henson, R., Lang, M., Wehbe, H., Maheshwari, S., Mendell, J.T., Jiang, J., Schmittgen, T.D. & Patel, T. (2015). Involvement of human micro-RNA in growth and response to chemotherapy in human cholangiocarcinoma cell lines. *Gastroenterology*, 130(**7**), p.2113–2129.

Menon, S., Oh, W., Carr, H.S. & Frost, J.A. (2013). Rho GTPase–independent regulation of mitotic progression by the RhoGEF Net1. *Molecular Biology of the Cell*, 24(**17**), p.2655–2667.

Mert, U., Ozgür, E., Tiryakioglu, D., Dalay, N. & Gezer, U. (2012). Induction of p53-inducible microRNA miR-34 by gamma radiation and bleomycin are different. *Frontiers in genetics*, 3(6), p.220 doi: 10.3389/fgene.2012.00220.

Metpally, R.P.R., Nasser, S., Courtright, A., Carlson, E., Ghaffari, L., Villa, S., Tembe, W. & Van Keuren-Jensen, K. (2013). Comparison of analysis tools for miRNA high throughput sequencing using nerve crush as a model. *Frontiers in Genetics*, 4, p.20 doi: 10.3389/fgene.2013.00020.

Mezentsev, A. & Amundson, S.A. (2011). Global gene expression responses to low- or high-dose radiation in a human three-dimensional tissue model. *Radiation Research*, 175(**6**), p.677–688.

Miranda, K.C., Bond, D.T., Levin, J.Z., Adiconis, X., Sivachenko, A., Russ, C., Brown, D., Nusbaum, C. & Russo, L.M. (2014). Massively parallel sequencing of human urinary exosome/microvesicle RNA reveals a predominance of non-coding RNA. *PloS one*, 9(**5**), p.e96094 10.1371/journal.pone.0096094.

Miranda, K.C., Bond, D.T., McKee, M., Skog, J., Paunescu, T.G., Da Silva, N., Brown, D. & Russo, L.M. (2010). Nucleic acids within urinary exosomes/microvesicles are potential biomarkers for renal disease. *Kidney International*, 78(**2**), p.191–199.

Mittelbrunn, M., Gutierrez-Vazquez, C., Villarroya-Beltri, C., Gonzalez, S., Sanchez-Cabo, F., Gonzalez, M.A., Bernad, A. & Sanchez-Madrid, F. (2011). Unidirectional transfer of microRNA-loaded exosomes from T cells to antigen-presenting cells. *Nature Communications*, 2, p.282.

Montecalvo, A., Larregina, A.T. & Morelli, A.E. (2013). Methods of analysis of dendritic cell-derived exosome-shuttle microRNA and its horizontal propagation between dendritic cells. *Methods in Molecular Biology*, 1024, p.19–40.

Montecalvo, A., Larregina, A.T., Shufesky, W.J., Beer Stolz, D., Sullivan, M.L.G., Karlsson, J.M., Baty, C.J., Gibson, G.A., Erdos, G., Wang, Z., Milosevic, J., Tkacheva, O.A., Divito, S.J., Jordan, R., Lyons-Weiler, J., Watkins, S.C. & Morelli, A.E. (2012). Mechanism of transfer of functional microRNAs between mouse dendritic cells via exosomes. *Blood*, 119(**3**), p.756–766.

Morel, Doussiere & Vignais. (1991). The superoxide-generating oxidase of phagocytic cells Physiological , molecular and pathological aspects. *European Journal Biochemistry*, 201(**3**), p.523–546.

Mortazavi, A., Williams, B.A., McCue, K., Schaeffer, L. & Wold, B. (2008). Mapping and quantifying mammalian transcriptomes by RNA-Seq. *Nature Methods*, 5(**7**), p.621–628.

Mothersill, C. & Seymour, C. (1997). Medium from irradiated human epithelial cells but not human fibroblasts reduces the clonogenic survival of unirradiated cells. *International Journal of Radiation Biology*, 71(**4**), p.421–427.

Mothersill, C. & Seymour, C. (2001). Radiation-induced bystander effects: Past history and future directions. *Radiation Research*, 155(**6**), p.759–767.

Mozdarani, H. & Bryant, P.E. (1987). The effect of 9-β-D-arabinofuranosyladenine on the formation of X-ray induced chromatid aberrations in X-irradiated G2 human cells. *Mutagenesis*, 2(**5**), p.371–374.

Mulcahy, L.A., Pink, R.C., Raul, D. & Carter, F. (2014). Routes and mechanisms of extracellular vesicle uptake. *Journal of Extracellular Vesicles*, 3, p.24641 doi: 10.3402/jev.v3.24641.

Munemasa, Y., Suzuki, T., Aizawa, K., Miyamoto, S., Imai, Y., Matsumura, T., Horikoshi, M. & Nagai, R. (2008). Promoter region-specific histone incorporation by the novel histone chaperone ANP32B and DNA-binding factor KLF5. *Molecular and Cellular Biology*, 28(**3**), p.1171–1181.

Nagasawa, H. & Little, J.B. (1992). Induction of Sister Chromatid Exchanges by Extremely Low Doses of α-Particles Advances in Brief Induction of Sister Chromatid Exchanges by Extremely Low Doses of α-Particles. *Cancer Research*, 52(**22**), p.6394–6396.

Nalabothula, N., Indig, F.E. & Carrier, F. (2010). The nucleolus takes control of protein trafficking under cellular stress. *Molecular and Cellular Pharmacology*, 2(**5**), p.203–212.

Narayanan, P.K., Goodwin, E.H. & Lehnert, B.E. (1997). α particles initiate biological production of superoxide anions and hydrogen peroxide in human cells. *Cancer Research*, 57(**18**), p.3963–3971.

Van Niel, G., Porto-Carreiro, I., Simoes, S. & Raposo, G. (2006). Exosomes: A common pathway for a specialized function. *Journal of Biochemistry*, 140(**1**), p.13–21.

Noerholm, M., Balaj, L., Limperg, T., Salehi, A., Zhu, L.D., Hochberg, F.H., Breakefield, X.O., Carter, B.S. & Skog, J. (2012). RNA expression patterns in serum microvesicles from patients with glioblastoma multiforme and controls. *BMC Cancer*, 12(**1**), p.22 doi: 10.1186/1471–2407–12–22.

Nolte-'t Hoen, E.N.M., Buermans, H.P.J., Waasdorp, M., Stoorvogel, W., Wauben, M.H.M. & 't Hoen, P.A.C. (2012). Deep sequencing of RNA from immune cell-derived vesicles uncovers the selective incorporation of small non-coding RNA biotypes with potential regulatory functions. *Nucleic Acids Research*, 40(**18**), p.9272–9285.

O'Neil, D., Glowatz, H. & Schlumpberger, M. (2001). Ribosomal RNA depletion for efficient use of RNA-Seq capacity. *Current Protocols in Molecular Biology*, 103:4.19.1.

Ogawa, Y., Taketomi, Y., Murakami, M., Tsujimoto, M. & Yanoshita, R. (2013). Small RNA transcriptomes of two types of exosomes in human whole saliva determined by next generation sequencing. *Biological & Pharmaceutical Bulletin*, 36(**1**), p.66–75.

Oh, W. & Frost, J.A. (2014). Rho GTPase independent regulation of ATM activation and cell survival by the RhoGEF Net1A. *Cell Cycle*, 13(**17**), p.2765–2772.

Özgür, E., Mert, U., Isin, M., Okutan, M., Dalay, N. & Gezer, U. (2013). Differential expression of long non-coding RNAs during genotoxic stress-induced apoptosis in HeLa and MCF-7 cells. *Clinical and Experimental Medicine*, 13(**2**), p.119–126.

Palma, J., Yaddanapudi, S.C., Pigati, L., Havens, M.A., Jeong, S., Weiner, G.A., Weimer, K.M.E., Stern, B., Hastings, M.L. & Duelli, D.M. (2012). MicroRNAs are exported from malignant cells in customized particles. *Nucleic Acids Research*, 40(**18**), p.9125–9138.

Parolini, I., Federici, C., Raggi, C., Lugini, L., Palleschi, S., De Milito, A., Coscia, C., Iessi, E., Logozzi, M., Molinari, A., Colone, M., Tatti, M., Sargiacomo, M. & Fais, S. (2009). Microenvironmental pH is a key factor for exosome traffic in tumor cells. *The Journal of Biological Chemistry*, 284(**49**), p.34211–34222.

Patnaik, S.K., Dahlgaard, J., Mazin, W., Kannisto, E., Jensen, T., Knudsen, S. & Yendamuri, S. (2012). Expression of microRNAs in the NCI-60 cancer cell-lines. *PloS one*, 7(**11**), p.e49918 doi:10.1371/journal.pone.0049918.

Pegtel, D.M., van de Garde, M.D.B. & Middeldorp, J.M. (2011). Viral miRNAs exploiting the endosomal-EV pathway for intercellular cross-talk and immune evasion. *Biochimica et Biophysica Acta*, 1809(**11-12**), p.715–721.

Perez-Hernandez, D., Gutiérrez-Vázquez, C., Jorge, I., López-Martín, S., Ursa, A., Sánchez-Madrid, F., Vázquez, J. & Yáñez-Mó, M. (2013). The intracellular interactome of tetraspanin-enriched microdomains reveals their function as sorting machineries toward exosomes. *Journal of Biological Chemistry*, 288(**17**), p.11649–11661.

Pichiorri, F., Palmieri, D., De Luca, L., Consiglio, J., You, J., Rocci, A., Talabere, T., Piovan, C., Lagana, A., Cascione, L., Guan, J., Gasparini, P., Balatti, V., Nuovo, G., Coppola, V., Hofmeister, C.C., Marcucci, G., Byrd, J.C., Volinia, S., Shapiro, C.L., Freitas, M.A., Croce, C.M. (2013). *In vivo* NCL targeting affects breast cancer aggressiveness through miRNA regulation. *The Journal of Experimental Medicine*, 210(**5**), p.951–968.

Pickering, B.F., Yu, D. & Van Dyke, M.W. (2011). Nucleolin protein interacts with microprocessor complex to affect biogenesis of microRNAs 15a and 16. *Journal of Biological Chemistry*, 286(**51**), p.44095–44103.

Prise, K.M. & Sullivan, J.M.O. (2010). Radiation-induced bystander signalling in cancer therapy. *Nature Reviews Cancer*, 9(**5**), p.351–360.

Qu, Y., Franchi, L., Nunez, G. & Dubyak, G.R. (2007). Nonclassical IL-1 Secretion Stimulated by P2X7 Receptors Is Dependent on Inflammasome Activation and Correlated with Exosome Release in Murine Macrophages. *The Journal of Immunology*, 179(**3**), p.1913–1925.

Rak, J. (2013). Extracellular vesicles - biomarkers and effectors of the cellular interactome in cancer. *Frontiers in Pharmacology*, 4, p.doi: 10.3389/fphar.2013.00021.

Rao, B.S.S., Upadhya, D. & Adiga, S.K. (2008). Protection of ionizing radiation-induced cytogenetic damage by hydroalcoholic extract of Cynodon dactylon in chinese hamster lung fibroblast cells and human peripheral blood lymphocytes. *Journal of Environmental Pathology, Toxicology and Oncology*, 27(**2**), p.101–112.

Rao, X., Di Leva, G., Li, M., Fang, F., Devlin, C., Hartman-Frey, C., Burow, M.E., Ivan, M., Croce, C.M. & Nephew, K.P. (2011). MicroRNA-221/222 confers breast cancer fulvestrant resistance by regulating multiple signaling pathways. *Oncogene*, 30(**9**), p.1082–1097.

Raposo, G. & Stoorvogel, W. (2013). Extracellular vesicles: exosomes, microvesicles, and friends. *The Journal of Cell Biology*, 200(**4**), p.373–383.

Raposo, G., Nijman, H.W., Stoorvogel, W., Leijendekker, R., Harding, C. V., Melief, C.J., & Geuze, H., J. (1996). B lymphocytes secrete antigen-presenting vesicles. *Journal Experimental Medicine*, 183(**3**), p.1161–1172.

Rashi-Elkeles, S., Elkon, R., Shavit, S., Lerenthal, Y., Linhart, C., Kupershtein, A., Amariglio, N., Rechavi, G., Shamir, R. & Shiloh, Y. (2011). Transcriptional modulation induced by ionizing radiation: p53 remains a central player. *Molecular Oncology*, 5(**4**), p.336–348.

Ratajczak, J., Miekus, K., Kucia, M., Zhang, J., Reca, R., Dvorak, P. & Ratajczak, M.Z. (2006). Embryonic stem cell-derived microvesicles reprogram hematopoietic progenitors: evidence for horizontal transfer of mRNA and protein delivery. *Leukemia*, 20(**5**), p.847–856.

Reeves, M.B., Davies, A.A., McSharry, B.P., Wilkinson, G.W. & Sinclair, J.H. (2007). Complex I binding by a virally encoded RNA regulates mitochondria-induced cell death. *Science*, 316(**5829**), p.1345–1348.

Reinhart, B.J., Slack, F.J., Basson, M., Pasquinelli, A.E., Bettinger, J.C., Rougvie, A.E., Horvitz, H.R. & Ruvkun, G. (2000). The 21-nucleotide let-7 RNA regulates developmental timing in *Caenorhabditis elegans*. *Nature*, 403(**6772**), p.901–906.

Rieger, K.E. & Chu, G. (2004). Portrait of transcriptional responses to ultraviolet and ionizing radiation in human cells. *Nucleic Acids Research*, 32(**16**), p.4786–4803.

Rinn, J.L., Kertesz, M., Wang, J.K., Squazzo, S.L., Xu, X., Brugmann, S.A., Goodnough, H., Helms, J.A., Farnham, P.J. & Chang, H.Y. (2007). Functional demarcation of active and silent chromatin domains in human HOX loci by non-coding RNAs. *Cell*, 129(**7**), p.1311–1323.

Rintala-Maki, N.D. & Sutherland, L.C. (2009). Identification and characterisation of a novel antisense non-coding RNA from the RBM5 gene locus. *Gene*, 445(**1–2**), p.7–16.

Robinson, M.D., McCarthy, D.J. & Smyth, G.K. (2009). edgeR: A Bioconductor package for differential expression analysis of digital gene expression data. *Bioinformatics*, 26(**1**), p.139–140.

Rudt, S. & Müller, R.H. (1993). *In vitro* phagocytosis assay of nano- and microparticles by chemiluminescence. III. Uptake of differently sized surface-modified particles, and its correlation to particle properties and *in vivo* distribution. *European Journal of Pharmaceutical Sciences*, 1(**1**), p.31–39.

Sakly, A., Gaspar, J.F., Kerkeni, E., Silva, S., Teixeira, J.P., Chaari, N. & Cheikh, H. Ben. (2012). Genotoxic damage in hospital workers exposed to ionizing radiation and metabolic gene polymorphisms. *Journal of Toxicology and Environmental Health*, 75(**13-15**), p.934–946.

Saleh, A.D., Savage, J.E., Cao, L., Soule, B.P., Ly, D., DeGraff, W., Harris, C.C., Mitchell, J.B. & Simone, N.L. (2011). Cellular stress induced alterations in microRNA let-7a and let-7b expression are dependent on p53. *PloS one*, 6(**10**), p.e24429 doi:10.1371/journal.pone.0024429.

Salomon, C., Kobayashi, M., Ashman, K., Sobrevia, L., Mitchell, M.D. & Rice, G.E. (2013). Hypoxia-induced changes in the bioactivity of cytotrophoblast-derived exosomes. *PLoS one*, 8(**11**), p.e79636 doi:10.1371/journal.pone.0079636.

Sandfort, V., Koch, U. & Cordes, N. (2007). Cell adhesion-mediated radioresistance revisited. *International Journal of Radiation Biology*, 83(**11-12**), p.727–732.

Savina, A., Furlán, M., Vidal, M. & Colombo, M.I. (2003). Exosome release is regulated by a calcium-dependent mechanism in K562 cells. *The Journal of Biological Chemistry*, 278(**22**), p.20083–20090.

Schulz, R., Marchenko, N.D., Holembowski, L., Fingerle-Rowson, G., Pesic, M., Zender, L., Dobbelstein, M. & Mol, U.M. (2012). Inhibiting the HSP90 chaperone destabilizes macrophage migration inhibitory factor and thereby inhibits breast tumor progression. *Journal of Experimental Medicine*, 209(**2**), p.275–289.

Segura, E., Guerin, C., Hogg, N., Amigorena, S. & Théry, C. (2007). CD8+ dendritic cells use LFA-1 to capture MHC-peptide complexes from exosomes *in vivo*. *The Journal of Immunology*, 179(**3**), p.1489–1496.

Seyednasrollah, F., Laiho, A. & Elo, L.L. (2013). Comparison of software packages for detecting differential expression in RNA-seq studies. *Briefings in Bioinformatics*, 16(**1**), p.59–70.

Seymour, C.B. & Mothersill, C. (1997). Delayed expression of lethal mutations and genomic instability in the progeny of human epithelial cells that survived in a bystander-killing environment. *Radiation Oncology Investigations*, 5(**3**), p.106–110.

Seymour, C.B., Mothersill, C. & Alper, T. (1986). High yields of lethal mutations in somatic mammalian cells that survive ionizing radiation. *International Journal of Radiation Biology*, 50(**1**), p.167–179.

Shahbazi-Gahrouei, D., Gholami, M. & Setayandeh, S. (2013). A review on natural background radiation. *Advanced Biomedical Research*, 2(**3**), p.65 doi: 10.4103/2277–9175.115821.

Shao, C., Lyng, F.M., Folkard, M. & Prise, K.M. (2006). Calcium fluxes modulate the radiation-induced bystander responses in targeted glioma and fibroblast cells. *Radiation Research*, 166(**3**), p.479–487.

Shelke, G. V, Lasser, C., Gho, Y.S. & Lotvall, J. (2014). Importance of exosome depletion protocols to eliminate functional and RNA-containing extracellular vesicles from fetal bovine serum. *Journal of Extracellular Vesicles*, 3, p.24783 doi: 10.3402/jev.v3.24783.

Shen, S.M., Yu, Y., Wu, Y.L., Cheng, J.K., Wang, L.S. & Chen, G.Q. (2010). Downregulation of ANP32B, a novel substrate of caspase-3, enhances caspase-3 activation and apoptosis induction in myeloid leukemic cells. *Carcinogenesis*, 31(**3**), p.419–426.

Shoemaker, R.H. (2006). The NCI60 human tumour cell line anticancer drug screen. *Nature Reviews Cancer*, 6(**10**), p.813–823.

Simone, N.L., Soule, B.P., Ly, D., Saleh, A.D., Savage, J.E., Degraff, W., Cook, J., Harris, C.C., Gius, D. & Mitchell, J.B. (2009). Ionizing radiation-induced oxidative stress alters miRNA expression. *PloS one*, 4(**7**), p.e6377 doi:10.1371/journal.pone.0006377.

Simpson, R.J., Kalra, H. & Mathivanan, S. (2012). ExoCarta as a resource for EV research. *Journal of Extracellular Vesicles*, 1, p.18374 doi: 10.3402/jev.v1i0.18374.

Skog, J., Wurdinger, T., van Rijn, S., Meijer, D.H., Gainche, L., Curry, W.T., Carter, B.S., Krichevsky, A.M. & Breakefield, X.O. (2008). Glioblastoma microvesicles transport RNA and proteins that promote tumour growth and provide diagnostic biomarkers. *Nature Cell Biology*, 10(**12**), p.1470–1476.

Smilenov, L.B., Hall, E.J., Bonner, W.M. & Sedelnikova, O.A. (2006). A microbeam study of DNA double-strand breaks in bystander primary human fibroblasts. *Radiation Protection Dosimetry*, 122(**1-4**), p.256–259.

Sokolov, M. V, Dickey, J.S., Bonner, W.M. & Martin, O.A. (2007). Gamma-H2AX in bystander cells: Not just a radiation-triggered event, a cellular response to stress mediated by intercellular communication. *Cell Cycle*, 6(**18**), p.2210–2212.

Song, S.J., Poliseno, L., Song, M.S., Ala, U., Webster, K., Ng, C., Beringer, G., Brikbak, N.J., Yuan, X., Cantley, L.C., Richardson, A.L. & Pandolfi, P.P. (2013). MicroRNA-antagonism regulates breast cancer stemness and metastasis via TET-family-dependent chromatin remodeling. *Cell*, 154(**2**), p.311–324.

Srivastava, M., Pollard, H.B. & Pollard, H.B. (1999). Molecular dissection of nucleolin's role in growth and cell proliferation: new insights. *The FASEB journal*, 13(**14**), p.1911–1922.

Srougi, M.C. & Burridge, K. (2011). The nuclear guanine nucleotide exchange factors Ect2 and Net1 regulate RhoB-mediated cell death after DNA damage. *PLoS one*, 6(**2**), p.e17108 doi:10.1371/journal.pone.0017108.

Staubach, S., Razawi, H. & Hanisch, F.-G. (2009). Proteomics of MUC1-containing lipid rafts from plasma membranes and exosomes of human breast carcinoma cells MCF-7. *Proteomics*, 9(**10**), p.2820–2835.

Stocks, M.B., Moxon, S., Mapleson, D., Woolfenden, H.C., Mohorianu, I., Folkes, L., Schwach, F., Dalmay, T. & Moulton, V. (2012). The UEA sRNA workbench: a suite of tools for analysing and visualizing next generation sequencing microRNA and small RNA datasets. *Bioinformatics*, 28(**15**), p.2059–2061.

Stoorvogel, W., Kleijmeer, M.J., Geuze, H.J. & Raposo, G. (2002). The biogenesis and functions of exosomes. *Traffic*, 3(**5**), p.321–330.

Stoorvogel, W., Strous, G.J., Geuze, H.J., Oorschot, V. & Schwartzt, A.L. (1991). Late endosomes derive from early endosomes by maturation. *Cell*, 65(**3**), p.417–427.

Subra, C., Grand, D., Laulagnier, K., Stella, A., Lambeau, G., Paillasse, M., De Medina, P., Monsarrat, B., Perret, B., Silvente-Poirot, S., Poirot, M. & Record, M. (2010). Exosomes account for vesicle-mediated transcellular transport of activatable phospholipases and prostaglandins. *Journal of Lipid Research*, 51(**8**), p.2105–2120.

Südhof, T.C. & Rothman, J.E. (2009). Membrane fusion: Grappling with SNARE and SM proteins. *Science*, 323(**5913**), p.474–477.

Svensson, K.J., Christianson, H.C., Wittrup, A., Bourseau-Guilmain, E., Lindqvist, E., Svensson, L.M., Morgelin, M. & Belting, M. (2013). Exosome uptake depends on ERK1/2-heat shock protein 27 signalling and lipid raft-mediated endocytosis negatively regulated by caveolin-1. *The Journal of Biological Chemistry*, 288(**24**), p.17713–17724.

Sverdlov, E.D. (2012). Amedeo Avogadro's cry: What is 1 μg of exosomes? *BioEssays : news and reviews in molecular, cellular and developmental biology*, 34(**10**), p.873–875.

't Hoen, P.A.C., Ariyurek, Y., Thygesen, H.H., Vreugdenhil, E., Vossen, R.H.A.M., de Menezes, R.X., Boer, J.M., van Ommen, G.J.B. & den Dunnen, J.T. (2008). Deep sequencing-based expression analysis shows major advances in robustness, resolution and inter-lab portability over five microarray platforms. *Nucleic Acids Research*, 36(**21**), p.e141. doi: 10.1093/nar/gkn705.

Takahashi, K., Yan, I.K., Kogure, T., Haga, H. & Patel, T. (2014). Extracellular vesicle-mediated transfer of long non-coding RNA ROR modulates chemosensitivity in human hepatocellular cancer. *FEBS open bio*, 4, p.458–467.

Tartier, L., Gilchrist, S., Burdak-Rothkamm, S., Folkard, M. & Prise, K.M. (2007). Cytoplasmic irradiation induces mitochondrial-dependent 53BP1 protein relocalization in irradiated and bystander cells. *Cancer Research*, 67(**12**), p.5872–5879.

Temme, J. & Bauer, G. (2012). Low-dose gamma irradiation enhances superoxide anion production by nonirradiated cells through TGF-β1-dependent bystander signaling. *Radiation Research*, 179(**4**), p.422–432.

Théry, C., Amigorena, S., Raposo, G. & Clayton, A. (2006). Isolation and characterization of exosomes from cell culture supernatants and biological fluids. *Current Protocols in Cell Biology*, 30:3.22:3.

Théry, C., Boussac, M., Veron, P., Ricciardi-Castagnoli, P., Raposo, G., Garin, J. & Amigorena, S. (2001). Proteomic analysis of dendritic cell-derived exosomes: A secreted subcellular compartment distinct from apoptotic vesicles. *The Journal of Immunology*, 166(**12**), p.7309–7318.

Théry, C., Regnault, A., Garin, J., Wolfers, J., Zitvogel, L., Ricciardi-Castagnoli, P., Raposo, G. & Amigorena, S. (1999). Molecular characterization of dendritic cell-derived exosomes. Selective accumulation of the heat shock protein hsc73. *The Journal of cell biology*, 147(**3**), p.599–610.

Tian, T., Wang, Y., Wang, H., Zhu, Z. & Xiao, Z. (2010). Visualizing of the cellular uptake and intracellular trafficking of exosomes by live-cell microscopy. *Journal of Cellular Biochemistry*, 111(**2**), p.488–496.

Tice, R.R., Agurell, E., Anderson, D., Burlinson, B., Hartmann, A., Kobayashi, H., Miyamae, Y., Rojas, E., Ryu, J.C. & Sasaki, Y.F. (2000). Single cell gel/Comet assay: Guidelines for *in*

vitro and *in vivo* genetic toxicology testing. *Environmental and Molecular Mutagenesis*, 35(**3**), p.206–221.

Trams, E.G., Lauter, C.J., Salem, J.N. & Heine, U. (1981). Exfoliation of membrane ecto-enzymes in the form of micro-vesicles. *Biochimica et Biophysica Acta*, 645(**1**), p.63–70.

Trapnell, C., Hendrickson, D.G., Sauvageau, M., Goff, L., Rinn, J.L. & Pachter, L. (2013). Differential analysis of gene regulation at transcript resolution with RNA-seq. *Nature Biotechnology*, 31(**1**), p.46–53.

Trapnell, C., Roberts, A., Goff, L., Pertea, G., Kim, D., Kelley, D.R., Pimentel, H., Salzberg, S.L., Rinn, J.L. & Pachter, L. (2012). Differential gene and transcript expression analysis of RNA-seq experiments with TopHat and Cufflinks. *Nature Protocols*, 7(**3**), p.562–578.

Tripathi, V., Shen, Z., Chakraborty, A., Giri, S., Freier, S.M., Wu, X., Zhang, Y., Gorospe, M., Prasanth, S.G., Lal, A. & Prasanth, K. V. (2013). Long noncoding RNA MALAT1 controls cell cycle progression by regulating the expression of oncogenic transcription factor B-MYB. *PLoS Genetics*, 9(**3**), p.e1003368. doi: 10.1371/journal.pgen.1003368.

Turchinovich, A., Weiz, L., Langheinz, A. & Burwinkel, B. (2011). Characterization of extracellular circulating microRNA. *Nucleic Acids Research*, 39(**16**), p.7223–7233.

Valadi, H., Ekstrom, K., Bossios, A., Sjostrand, M., Lee, J.J. & Lotvall, J.O. (2007). Exosome-mediated transfer of mRNAs and microRNAs is a novel mechanism of genetic exchange between cells. *Nature Cell Biology*, 9(**6**), p.654–659.

Valerie, K., Yacoub, A., Hagan, M.P., Curiel, D.T., Fisher, P.B., Grant, S. & Dent, P. (2007). Radiation-induced cell signaling: inside-out and outside-in. *Molecular Cancer Therapeutics*, 6(**3**), p.789–801.

Vickers, K.C., Palmisano, B.T., Shoucri, B.M., Shamburek, R.D. & Remaley, A.T. (2011). MicroRNAs are transported in plasma and delivered to recipient cells by high-density lipoproteins. *Nature Cell Biology*, 13(**4**), p.423–433.

Villarroya-Beltri, C., Gutiérrez-Vázquez, C., Sánchez-Cabo, F., Pérez-Hernández, D., Vázquez, J., Martin-Cofreces, N., Martinez-Herrera, D.J., Pascual-Montano, A., Mittelbrunn, M. & Sánchez-Madrid, F. (2013). Sumoylated hnRNPA2B1 controls the sorting of miRNAs into exosomes through binding to specific motifs. *Nature Communications*, 4, p.2980 doi: 10.1038/ncomms3980.

Vlassov, A. V., Magdaleno, S., Setterquist, R. & Conrad, R. (2012). Exosomes: Current knowledge of their composition, biological functions, and diagnostic and therapeutic potentials. *Biochimica et Biophysica Acta*, 1820(**7**), p.940–948.

Volinia, S., Calin, G.A., Liu, C.-G., Ambs, S., Cimmino, A., Petrocca, F., Visone, R., Iorio, M., Roldo, C., Ferracin, M., Prueitt, R.L., Yanaihara, N., Lanza, G., Scarpa, A., Vecchione, A., Negrini, M., Harris, C.C. & Croce, C.M. (2006). A microRNA expression signature of human solid tumors defines cancer gene targets. *Proceedings of the National Academy of Sciences of the United States of America*, 103(**7**), p.2257–2261.

Wang, J. & Cui, Q. (2012). Specific roles of microRNAs in their interactions with environmental factors. *Journal of Nucleic Acids*, 2012, p.978384 doi:10.1155/2012/978384.

Wang, J., Su, L., Chen, X., Li, P., Cai, Q., Yu, B., Liu, B., Wu, W. & Zhu, Z. (2014). MALAT1 promotes cell proliferation in gastric cancer by recruiting SF2/ASF. *Biomedicine & Pharmacotherapy*, 68(**5**), p.557–564.

Wang, K., Zhang, S., Weber, J., Baxter, D. & Galas, D.J. (2010). Export of microRNAs and microRNA-protective protein by mammalian cells. *Nucleic Acids Research*, 38(**20**), p.7248–7259.

Wang, W.-H., Childress, M.O. & Geahlen, R.L. (2014). Syk interacts with and phosphorylates nucleolin to stabilize Bcl-xL mRNA and promote cell survival. *Molecular and Cellular Biology*, 34(**20**), p.3788–3799.

Wang, X., Arai, S., Song, X., Reichart, D., Du, K., Tempst, P., Rosenfeld, M.G. & Glass, C.K. (2010). Induced ncRNAs allosterically modify RNA binding proteins in cis to inhibit transcription. *Nature*, 454(**7200**), p.126–130.

Ward, J.F. (1988). DNA damage produced by ionizing radiation in mammalian cells: identities, mechanisms of formation, and reparability. *Progress in Nucleic Acid Research and Molecular Biology*, 35, p.95–125.

Watanabe, M., Furuno, N., Goebl, M., Go, M., Miyauchi, K., Sekiguchi, T., Basilico, C. & Nishimito, T. (1991). Molecular cloning of the human gene, CCG2, that complements the BHK-derived temperature-sensitive cell cycle mutant tsBN63: identity of CCG2 with the human X chromosomal SCAR/RPS4X gene. *Journal of Cell Science*, 100(**1**), p.35–43.

Webber, J. & Clayton, A. (2013). How pure are your vesicles? *Journal of Extracellular Vesicles*, 2, p.19861 doi: 10.3402/jev.v2i0.19681.

Weilner, S., Schraml, E., Redl, H., Voglauer-Grillari, R. & Grillari, J. (2012). Secretion of microvesicular miRNAs in cellular and organismal aging. *Experimental Gerontology*, 48(**7**), p.626–633.

Whitesell, L. & Lindquist, S.L. (2005). HSP90 and the chaperoning of cancer. *Nature Reviews Cancer*, 5(**10**), p.761–772.

Wilusz, J.E., Freier, S.M. & Spector, D.L. (2008). 3' end processing of a long nuclear-retained noncoding RNA yields a tRNA-like cytoplasmic RNA. *Cell*, 135(**5**), p.919–932.

Witwer, K.W., Buzás, E.I., Bemis, L.T., Bora, A., Lässer, C., Lötvall, J., Nolte-'t Hoen, E.N., Piper, M.G., Sivaraman, S., Skog, J., Théry, C., Wauben, M.H. & Hochberg, F. (2013). Standardization of sample collection, isolation and analysis methods in extracellular vesicle research. *Journal of Extracellular Vesicles*, 2, p.20360 doi: 10.3402/jev.v2i0.20360.

Woloschak, G.E., Shearin-Jones, P. & Chang-Liu, C.-M. (1990). Effects of ionizing radiation on expression of genes encoding cytoskeletal elements: Kinetics and dose effects. *Molecular Carcinogenesis*, 3(**6**), p.374–378.

Wubbolts, R., Leckie, R.S., Veenhuizen, P.T.M., Schwarzmann, G., Möbius, W., Hoernschemeyer, J., Slot, J.-W., Geuze, H.J. & Stoorvogel, W. (2003). Proteomic and biochemical analyses of human B cell-derived exosomes. Potential implications for their function and multivesicular body formation. *The Journal of Biological Chemistry*, 278(**13**), p.10963–10972.

Xie, L., Zhou, J., Zhang, S., Chen, Q., Lai, R., Ding, W., Song, C., Meng, X. & Wu, J. (2014). Integrating microRNA and mRNA expression profiles in response to radiation-induced injury in rat lung. *Radiation Oncology*, 9, p.111 doi: 10.1186/1748–717X–9–111.

Xie, Y., Tu, W., Zhang, J., He, M., Ye, S., Dong, C. & Shao, C. (2015). SirT1 knockdown potentiates radiation-induced bystander effect through promoting c-Myc activity and thus facilitating ROS accumulation. *Mutation Research/Fundamental and Molecular Mechanisms of Mutagenesis*, 772, p.23–29.

Xue, Q., Sun, K., Deng, H.-J., Lei, S.-T., Dong, J.-Q. & Li, G.-X. (2013). Anti-miRNA-221 sensitizes human colorectal carcinoma cells to radiation by upregulating PTEN. *World Journal of Gastroenterology*, 19(**48**), p.9307–9317.

Yang, I.-P., Tsai, H.-L., Huang, C.-W., Huang, M.-Y., Hou, M.-F., Juo, S.-H.H. & Wang, J.-Y. (2013). The functional significance of microRNA-29c in patients with colorectal cancer: A potential circulating biomarker for predicting early relapse. *PloS one*, 8(**6**), p.e66842 doi:10.1371/journal.pone.0066842.

Yates, L.A., Norbury, C.J. & Gilbert, R.J.C. (2013). The long and short of microRNA. *Cell*, 153(**3**), p.516–519.

Yu, X., Harris, S.L. & Levine, A.J. (2006). The regulation of exosome secretion: a novel function of the p53 protein. *Cancer Research*, 66(**9**), p.4795–4801.

Zhang, B., Arun, G., Mao, Y.S., Lazar, Z., Hung, G., Bhattacharjee, G., Xiao, X., Booth, C.J., Zhang, C. & Spector, D.L. (2012). The lncRNA MALAT1 is dispensable for mouse development but its transcription plays a cis-regulatory role in the adult. *Cell Reports*, 2(**1**), p.111–123.

Zhang, B., Wang, M., Gong, A., Zhang, X., Wu, X., Zhu, Y., Shi, H., Wu, L., Zhu, W., Qian, H. & Xu, W. (2014). HucMSC-exosome mediated -Wnt4 signaling is required for cutaneous wound healing. *Stem Cells*, p.doi: 10.1002/stem.1771.

Zhang, H.-G., Liu, C., Su, K., Yu, S., Zhang, L., Zhang, S., Wang, J., Cao, X., Grizzle, W. & Kimberly, R.P. (2006). A membrane form of TNF-α presented by exosomes delays T cell activation-induced cell death. *The Journal of Immunology*, 176(**12**), p.7385–7393.

Zhang, M., Qian, J., Xing, X., Kong, F.-M., Zhao, L., Chen, M. & Lawrence, T.S. (2008). Inhibition of the tumor necrosis factor-α pathway is radioprotective for the lung. *Clinical cancer research : an official journal of the American Association for Cancer Research*, 14(**6**), p.1868–1876.

Zhang, Y., Zhou, J., Held, K.D., Redmond, R.W., Prise, K.M. & Liber, H.L. (2008). Deficiencies of double-strand break repair factors and effects on mutagenesis in directly γ-irradiated and medium-mediated bystander human lymphoblastoid cells. *Radiation Research*, 169(**2**), p.197–206.

Zhao, Y., de Toledo, S.M., Hu, G., Hei, T.K. & Azzam, E.I. (2014). Connexins and cyclooxygenase-2 crosstalk in the expression of radiation-induced bystander effects. *British Journal of Cancer*, 111(**1**), p.125–131.

Zheng, H.T., Shi, D., Zheng, H., Zhuo, C., Peng, J., Li, D., Xu, Y., Li, X., Cai, G. & Cai, S. (2014). High expression of lncRNA MALAT1 suggests a biomarker of poor prognosis in colorectal cancer. *Medical Oncology*, 31(**7**), p.3174–3181.

Zhou, H., Ivanov, V.N., Gillespie, J., Geard, C.R., Amundson, S.A., Brenner, D.J., Yu, Z., Lieberman, H.B. & Hei, T.K. (2005). Mechanism of radiation-induced bystander effect: role of the cyclooxygenase-2 signaling pathway. *Proceedings of the National Academy of Sciences of the United States of America*, 102(**41**), p.14641–14646.

Zhou, H., Ivanov, V.N., Lien, Y.-C., Davidson, M. & Hei, T.K. (2008). Mitochondrial function and nuclear factor-kappaB-mediated signaling in radiation-induced bystander effects. *Cancer Research*, 68(**7**), p.2233–2240.

Zhou, H., Suzuki, M., Randers-Pehrson, G., Vannais, D., Chen, G., Trosko, J.E., Waldren, C.A. & Hei, T.K. (2001). Radiation risk to low fluences of alpha particles may be greater than we

thought. *Proceedings of the National Academy of Sciences of the United States of America*, 98(**25**), p.14410–14415.

Zhou, Q., Li, M., Wang, X., Li, Q., Wang, T., Zhu, Q., Zhou, X., Wang, X., Gao, X. & Li, X. (2012). Immune-related microRNAs are abundant in breast milk exosomes. *International Journal of Biological Sciences*, 8(**1**), p.118–123.